Disentangling Disconnection and Unconsciousness: The Electrophysiological Signatures of Sensory Awareness and Conscious Experience During Anesthesia and Sleep

By

Cameron Patrick Casey

A dissertation submitted in partial fulfillment of the requirements for degree of

Doctor of Philosophy

(Neuroscience)

at the

UNIVERSITY OF WISCONSIN-MADISON

2023

Date of final oral examination: 12/14/2022

This dissertation is approved by the following members of the Final Oral Committee:

Robert A. Pearce, Professor, Department of Anesthesiology

Matthew I. Banks, Professor, Department of Anesthesiology

Barbara B. Bendlin, Professor, Department of Medicine

Ruth Y. Litovsky, Professor, Communication Sciences and Disorders

Yuri B. Saalmann, Associate Professor, Psychology

ACKNOWLEDGEMENTS

The work presented in this dissertation is the product of an enormous amount of collaborative work, both within the University of Wisconsin-Madison and beyond with international collaborators. Firstly, I would like to thank my original thesis advisor, Robert Sanders, who initiated the studies under which the data presented here were collected. Rob welcomed me into his lab, advised me when I needed help, treated me with respect, and even continued to fulfill this role from across the globe after moving to Australia. I would also like to express profound gratitude for my current thesis advisor, Robert (Bob) Pearce, who kindly stepped into this role when Rob left UW-Madison. Bob has been consistently supportive of me and provided me the space and resources to continue my research, as I had planned it, after transitioning into his lab.

I would also like to thank the rest of my advisory committee, Yuri Saalmann, Matthew Banks, Ruth Litovsky, and Barbara Bendlin. Your expertise and thoughtful feedback have been essential, not only to my progress on my dissertation work, but also to my development as a scientist in general. Your guidance has been instrumental to my success and I thank you each for the time and energy you have given me.

As I mentioned above, this dissertation would not have been possible without a great deal of collaboration. I would like to express my sincerest gratitude to the many research specialists and undergraduate research students who made the collection of these data possible. Zahra Farahbakhsh, Maggie Parker, Sean Tanabe, Andrew Mcintosh, and many others have dedicated huge amounts of time to collecting these data. The nature of these studies

required extreme flexibility, working both late at night and early in the morning, and the willingness of our lab-members to do so without complaint has been phenomenal. Without these collective efforts, this dissertation fundamentally could not have happened, so I thank you all profusely!

Finally, I cannot express enough thanks to my friends and family who have supported me throughout this process. A PhD is not a quick or easy undertaking. There have been numerous times during my graduate studies when I have felt exhausted, frustrated, or defeated, but was able to regroup and find the confidence to keep going because of all your love and support. Thank you to my loving partner, Kevin Dupuis, my parents, Anne Larson and Carlie Casey, and my siblings, Colin Casey and Jessie Chase. It means more than I can say that you have believed in me all these years.

With Gratitude,

Cameron

TABLE OF CONTENTS

ABSTRACT

Objective assessments of consciousness are of clear clinical utility but have had limited success so far. Developing methods that can distinguish between consciousness and unconsciousness requires collecting data that are representative of both states. However, attempts to do so have largely relied on clinical responsiveness scales to label which data come from a conscious subject vs an unconscious one. Using responsiveness data as a surrogate for consciousness is problematic as these qualities are dissociable. A positive response may be a reliable indicator of consciousness but lack of response is by no means a confirmation of unconsciousness. The goal of the current thesis work is to improve our methods of detecting consciousness and sensory awareness (connectedness). Here, commonly reported electrophysiological markers of "consciousness", derived based on assessments of responsiveness, were tested for their association with connectedness or consciousness *per se* using high density electroencephalography (HD-EEG) data collected, as part of the UNderstanding Consciousness Connectedness and Intra-Operative Unresponsiveness Study (UN-ConsCIOUS). First, frequency-based EEG measures were tested for associations with consciousness and connectedness in source reconstructed data collected during natural sleep, dexmedetomidine sedation, and propofol sedation, to identify anatomical correlates of these states. Secondly, putative measures of (un)consciousness from anesthesia literature were tested for specificity to consciousness or connectedness and for generalizability across pharmacological and non-pharmacological conditions. Lastly, auditory evoked potentials generated under dexmedetomidine sedation were analyzed to assess differences in hierarchical information processing in connected consciousness and disconnected consciousness. This body

of work provides evidence that the neural correlates of consciousness and connectedness show considerable overlap, however, states of disconnected consciousness and unconsciousness are still measurably distinct. These findings highlight the importance of distinguishing between disconnected consciousness and unconsciousness when the quality of consciousness *per se* is of interest, as conflating these phenomenologically and electrophysiologically distinct states may result in erroneous conclusions being drawn and ascribed to unconsciousness.

INTRODUCTION

Defining Consciousness and Connectedness

Consciousness is a phenomenon with which we are all familiar, yet it remains difficult to explicitly define. What is the essence of a conscious experience? Without a concrete definition of consciousness, any attempt at scientifically rigorous study of this phenomenon will not be possible. Current leaders in the field of consciousness science define consciousness as, "*what abandons us every night when we fall into dreamless sleep and returns the next morning when we wake up*[1]." That is, **to be conscious is to have a subjective experience**. In arriving at such a definition, we place the presence or absence of phenomenological experience at the heart of any discussion of consciousness. While our waking lives are dominated by conscious experiences related to the world around us, this needn't be the case. Dreams are also a type of subjective experience and therefore, by definition, a type of consciousness. However, rather than being related to the world around us, dreams are internally generated experiences divorced from sensory information related to one's surroundings. Based on the above definition, unconsciousness *per se* is only achieved when there is a complete absence of any sort of phenomenological experience.

To distinguish between states of consciousness that are related to the environment (as in wake) and those that are divorced from environmental information (as in dreaming), I will be using the language of "connectedness" throughout this dissertation. States of consciousness with environmental awareness are termed "connected consciousness" while those without environmental awareness are termed "disconnected consciousness"[2]. "Connection" here refers to whether or not a conscious experience is connected to the environment through the senses.

Consciousness and connectedness have been previously hypothesized to be regulated by two distinct primary neurotransmitter systems, namely cholinergic and noradrenergic activity, respectively[2]. Evidence in support of this hypothesis has been derived from the scientific literature of sleep and anesthesia.

Cortical levels of both acetylcholine (ACh) and noradrenaline (NA) are high during normal wake (connected consciousness)[3]. During rapid eye movement (REM) sleep, a state of disconnection with high rates of consciousness (77% of REM wakeup reports include dreams[4]) and electroencephalographic (EEG) activity similar to normal wake[5], NA neurons within the locus coeruleus (LC) become almost entirely silent[6,7] while basal forebrain (BF) ACh firing remains elevated[8–10]. During NREM, a state of disconnection with lower incidence rates of consciousness (34% of NREM wakeup reports include dreams and dreams tend to be less vivid[4]), ACh activity is lower than in wake or REM[3]. It has also been shown that optogenetic stimulation of BF ACh neurons results in EEG desynchronization and state transitions from NREM to REM or wake states, demonstrating a causal roles of BF ACh activity in facilitating these conscious states[11]. Pharmacological manipulation of the ACh system also alters conscious state during anesthesia. Under propofol anesthesia, scopolamine, a muscarinic ACh receptor antagonist, prevents dreaming[12], and physostigmine, a cholinesterase inhibitor, induces a return of consciousness[13]. Taken together, these findings strongly implicate BF ACh activity in regulating consciousness.

As stated above, NA activity is high during wake and low during NREM and REM sleep, i.e. NA activity correlates with connectedness[3]. This physiological correlation appears to be the result of LC NA activity causally regulating arousal/connectedness. Suppressing LC activity via

alpha2-receptor agonist administration reduces arousal and, at high enough doses, produces a state of sedation similar to sleep[14], while chemo- or optogenetic activation of the LC promotes wake[15,16]. LC firing has also been shown to causally influence sensory evoked awakenings from sleep[17]. Based on just these findings, one could argue that NA activity could simply be encoding arousal alone. However, additional work demonstrates that NA signaling from the LC is also critical to orienting of attention to external stimuli[18,19], a role that is at the heart of connectedness, and controls cortical signal to noise ratio[20]. It can also be seen that the LC encodes general state of arousal and orienting to external stimuli via distinct firing patterns, the former being encoded by tonic activity and the latter by phasic activity[17]. These findings suggest that NA activity from the LC plays a key role in mediating sensory connection to the environment.

Consciousness and connectedness are distinct and dissociable qualities. Consciousness refers the presence of subjective experience, and is associated with ACh activity from the BF, while connectedness refers to a state of receptiveness to external stimuli, such that external information is incorporated into one's conscious experience, and is associated with NA activity from the LC. A graphical depiction of this framework is presented in Fig 1. Within this dissertation, both of these qualities will be treated as dichotomous, i.e. a person is conscious or unconscious, connected or disconnected. However, it is worth noting that this is largely a methodological choice as opposed to a theoretical one. Categorizing our data in this manner allows for relatively straightforward contrasts to isolate the statistical effects of consciousness

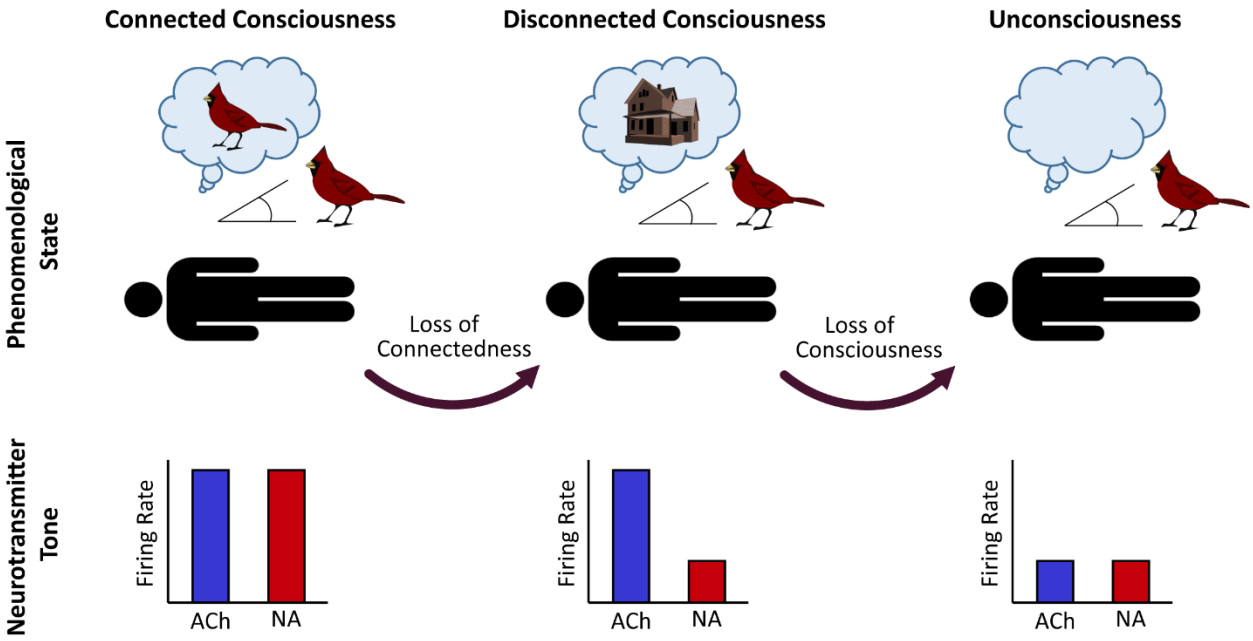

Figure 1. Graphical summary of connectedness and consciousness. (Top), Connected consciousness, disconnected consciousness, and unconsciousness as they are defined by their phenomenology. During connected consciousness, the individual sees a bird in the environment and has a conscious experience related to the bird. During disconnected consciousness, the bird is still present in the environment, however, information about the bird does not enter the figure's conscious experience. Instead, the figure is having a dream about a house. During unconsciousness, the figure has a complete absence of subjective experience. (Bottom) The levels of acetylcholine (ACh) and noradrenaline (NA) activity in each state. In connected consciousness, both ACh and NA activity is high. In disconnected consciousness, NA signaling drops but ACh activity remains elevated. In unconsciousness, both ACh and NA activity is low. Figure adapted from Sanders, Casey & Saalmann, 2021, BJA.

and connectedness. With that said, the nature of either consciousness or connectedness as discrete or continuous remain open questions.

Some theories of consciousness, such as integrated information theory (IIT)[1,21], make explicit claims about the continuous nature of consciousness[22]. Others assume continuity more implicitly, drawing on medical language of "level of consciousness" to describe certain states as more or less conscious[23,24]. However, these notions have also been challenged on the grounds

that if consciousness is defined based on the presence of a subjective experience, then one either has a subjective experience or doesn't have it, "it cannot come in degrees[25]." Similarly, sensory disconnection could be said to be binary, i.e. information is included into one's conscious experience or it isn't. On the other hand, there exist counter examples that do not easily fit as connected or disconnected. Multiple studies have reported external stimuli, presented while participants were asleep, becoming incorporated into participants' dreams[26–28]. However, the ability of these stimuli to incorporate into dream contents is inconsistent[29]. From these observations, one could argue that disconnection is a continuous quality and that some states are more disconnected than others. For example, a state of dreaming that includes some information from the outside world could be considered to be more connected than a dream where all external cues have been neglected. On the other hand, it is possible that the incorporation of sensory information into the dream occurred through a brief transient episode of connectedness, followed by a return to disconnection. In this latter case, sensory disconnection could still be a binary phenomenon.

I have included the above discourse on the nature of consciousness and connectedness to provide a broader context for these qualities and how they are being discussed within this academic field. Resolving these questions of consciousness/connectedness as continuous vs discrete is, however, beyond the scope of this dissertation. Instead, these qualities will be operationalized as dichotomous such that data labeled as "conscious" indicates the presence of subjective experience while "unconscious" indicates the absence of subjective experience. Similarly, data labeled as "connected" indicates awareness of the environment while "disconnected" will refer to absence of awareness of the environment.

Motivations for developing objective measures of connectedness and consciousness

Limited understanding of the nature and quantification of consciousness remains not only a fundamental and philosophical open question in neuroscience, but also a pragmatic challenge for clinical practice. 313 million surgical procedures are performed worldwide each year, with this figure expected to grow with increases in population and spread of medical coverage[30]. General anesthesia has become an essential component for surgery, making delicate and invasive procedures possible by preventing patient movement and disconnecting them from the trauma of the operation. This is, however, under ideal circumstances. While explicit recall of surgical awareness is quite low (0.1-0.2% of operations)[31–33] assessments of awareness made during operations indicate that incidence rates are significantly higher, estimated to occur in roughly 5% of operations and up to 11% in patients between the ages of 18 and 40[34,35]. Real time clinical information on patients' state of conscious awareness during an operation should make it possible for anesthesiologists to adjust drug administration in order to reduce or even eliminate incidences of intra-operative awareness. However, reliable means of doing so have yet to be developed[36] and the very drugs that have been administered to protect patients also render their ability to behaviorally respond, during instances of awareness, unreliable[37–39].

Beyond intraoperative awareness, our limited ability to objectively detect consciousness in the absence of motor response presents major challenges for diagnosis, treatment, and prognosis of disorders of consciousness (DoC). DoC may occur after severe brain injury resulting in disruption of the brain's arousal and awareness systems[40]. These disorders, which include minimally conscious states (MCS) and vegetative state (VS), place enormous emotional burden

on families and loved ones and often result in tremendous financial costs[41,42]. Clinical diagnosis for DoC relies almost entirely on behavioral responsiveness and have a disconcertingly high misdiagnosis rate (up to 40%)[43,44]. Incorrect diagnosis can result in incorrect treatment procedures and inaccurate medical advice for medical powers of attorney regarding care, prognosis, and end of life decisions. While this high misdiagnosis rate is unsettling, it is also to be expected given that responsiveness tests have no ability to discriminate between states of true unconsciousness and states of consciousness without perception of the environment, e.g. dreaming[2]. A patient may be experiencing a state of internal consciousness and never respond to a behavioral test because information about the test, and the outside world in general, is not being integrated into their conscious perceptions. Behavioral testing is even likely to fail in situations where a patient is conscious and aware of their environment; motor or executive dysfunction can easily lead to failure to respond when consciousness and external awareness are both present[37,45].

In addition to these pressing clinical use cases, the lack of objective measures of consciousness poses major constraints on our ability to study the phenomenon. If a researcher aims to study the effects of consciousness or unconsciousness within the brain, in the absence of quantitative measures of consciousness, researchers must either 1) rely on subjective reports given by study participants assessing their own mental state, or 2) rely on a behavioral proxy as an indirect readout of consciousness.

Both of the above noted approaches have limitations that merit discussion, but as will be seen in the following section, the majority of the work investigating neural correlates of consciousness through neuroimaging has been conducted using the second approach, i.e. using

behavioral responsiveness as an index of consciousness. However, as I have outlined in the prior discussion of intra-operative awareness and DoC, responsiveness is readily dissociable from consciousness. In the language of research validity, this means that responsiveness has poor construct validity as a measure of consciousness. Because of this, we are limited in the conclusions we can draw from such experiments as they pertain to consciousness *per se*. This point will be elaborated on within the next section.

The experiments included in Chapters 1-3, which make up the bulk of this dissertation, make use of the first method of assessing consciousness, i.e. direct subjective report. Though not without limitations, this method is currently the closest we can come to accessing the experiences of another person. A subjective report is the closest thing we have to ground truth of consciousness as a subjective experience (or lack of experience) is being explicitly communicated by the person having the experience. This makes the construct validity of the subjective report much higher than that of a behavioral proxy such as responsiveness. However, subjective reports are also subject to human error. Furthermore, to use subjective reports, we must constrain our experimental designs to situations in which reports can be given. In practice, this means studying verbal humans who are easily rousable.

Between responsiveness and subjective reports as measures of consciousness, we are limited in either our ability to draw specific conclusions about consciousness or our ability to study consciousness outside of a limited experimental context. A robust objective marker of consciousness would remove these limitations and allow researchers to make specific conclusions about consciousness with higher confidence and in a broader set of contexts. Such gains would likely accelerate progress within the field of consciousness science.

Prior attempts at objective measurements of consciousness

Due to the importance of accurate clinical assessment of awareness and consciousness, as well as the current limitations in studying consciousness empirically, it is clear why physicians and researchers alike would desire quantitative measures of consciousness that do not depend on behavioral response. In fact, many attempts have been made from the late 20th century to present[36,46–50]. Over the last few decades, efforts have been made to develop quantitative metrics of awareness for depth of anesthesia (DoA) monitoring. DoA monitors such as the bispectral index (BIS)[47], Narcotrend [46], and patient state index (PSI)[48] have been developed to predict patient responsiveness under anesthesia. These existing DoA monitoring methods have shown epidemiological value in reducing the amount of drug needed to achieve general anesthesia and speeding up recovery times after the operation[51–56]. Though useful, these methods remain far from perfect, often performing poorly when applied to 'non-standard' patients, e.g. young children or people with neurological conditions, as well as drugs that do not induce major slowing of the EEG, such as ketamine[36,57]. Even under standard conditions, studies have demonstrated that these tools lack the ability to effectively detect intraoperative awareness[58–60]. In addition, regardless of clinically utility, these metrics provide little scientific benefit, beyond serving as benchmarks, due to the proprietary nature of their calculation.

These limitations in DoA performance are not surprising when one considers how current monitors have been calibrated. The DoA monitors above[46–48] were all developed based on adult participants assessed using *responsiveness* scales, such as the Observer's Assessment of Alertness/Sedation Scale (OAA/S)[61]. These monitors have been designed to detect responsiveness from their inception, they have not been designed to detect connected

consciousness. At this point, it should be clear that responsiveness is not the same thing as connectedness or consciousness. It is therefore little surprise that they should fail in detecting connected consciousness when prompted to do so.

The need for objective monitoring of consciousness has provoked extensive research into the signatures of consciousness beyond the private sector DoA endeavors mentioned above[49,62,63]. Much of this work leverages anesthesia as a tool for influencing states of consciousness and connectedness[64–66]. The most prevalent paradigm within this body of work is to record neural activity from participants while administering some anesthetic. Participants will be instructed to periodically respond to some external stimulus, e.g. auditory tones or a researcher calling their names. Once participants stop responding when prompted, they are considered "unconscious". Their brain activity during this state of presumed unconsciousness can then be compared to the activity observed when they are awake (before and/or after anesthesia) to identify signatures of loss of consciousness. See[67–75] for example studies.

Attentive readers may have noted that the above paradigm is dependent on participant responsiveness as a read out of conscious state. The consequence of this dependence is that all such studies implementing this paradigm, or any similar paradigm that infers unconsciousness from unresponsiveness, will suffer from the limitations outlined in *Motivations for developing objective measurements of connectedness and consciousness*. That is, these studies cannot make strong claims about unconsciousness *per se* because the data collected may represent any combination of connected conscious, disconnected conscious, or unconscious states. These studies have been designed to detect correlates of unresponsiveness rather than unconsciousness. In order to improve upon these early attempts at monitoring consciousness,

an important step forward will be to move away from tracking responsiveness and instead track connectedness and consciousness, the core processes of clinical interest.

The bulk of this section has been focused on limitations in the existing research aimed at measuring consciousness. Understanding these limitations is key to understanding the motivations for the work presented in this dissertation. However, it is also important to note major strides that have been taken towards identifying signatures of consciousness *per se*. One promising method is the perturbational complexity index (PCI)[76]. This method, which involves monitoring the brain's response to a magnetic pulse delivered by transcranial magnetic stimulation (TMS), is meant to measure the degree of information differentiation and integration in the brain[76]. The PCI has proven effective at differentiating DoC, DoA, and sleep stages[76–79]. While further testing of the PCI against data that have been more explicitly coded based on connectedness and consciousness is warranted, the data thus far are quite promising and the European Academy of Neurology has recently recommended incorporating TMS-EEG within best practices for evaluating DoC[80]. The biggest limitation to PCI, at present, is that its dependence on TMS makes it economically challenging to scale up. In the context of DoC, which have relatively low prevalence rates[42,81–83], it may be possible for a single TMS-EEG system per hospital to keep up with patient demand. For DoA, however, the large volumes of surgical procedures happening every day would necessitate a TMS-EEG system be incorporated in every operating room. The cost of this would make implementation prohibitively expensive for many institutions. Limiting accessibility of DoA technology to affluent hospitals would only further exacerbate healthcare disparities along racial and socioeconomic lines[84,85]. Furthermore, it remains an open question as to how well PCI would work for detecting connected

consciousness under anesthesia distinct from disconnected consciousness, as the latter is acceptable during surgery but the former is not[2]. If the PCI is truly specific to consciousness, then it may make a poor DoA monitor as dreaming may produce false alarms when monitoring for intra-operative awareness. To overcome these limitations, it would be ideal to have separate measurements of connectedness and consciousness that also do not require TMS to calculate.

Lastly, an important experimental update in recent years has been the introduction of serial reports of subjective conscious state[4,86,87]. This paradigm allows researchers to explicitly identify a participant's mental state, during a brief recording period, as connected consciousness, disconnected consciousness, or unconsciousness. This information allows researchers to specifically isolate effects of connectedness and consciousness. This method has been previously applied to identify neural correlates of dreaming (disconnected conscious) compared to non-dreaming (unconscious) sleep[86]. The work I present in this dissertation is also built upon the serial report paradigm, which will be elaborated on in the next section.

The Understanding Consciousness Connectedness and Intra-Operative Unresponsiveness Study

In order to disentangle the constructs of connectedness and consciousness, the data and analyses in the following chapters have made use of data collected under the UNderstanding Consciousness Connectedness and Intra-Operative Unresponsiveness Study (UN-ConsCIOUS). To set the stage for these papers and illuminate how these data have been acquired, the overarching design of the study will be outlined here. Additional details related to the specific data being used for each analysis can be found within the corresponding chapter.

The UN-ConsCIOUS project was designed to track the electrophysiological signatures of consciousness and connectedness using high density electroencephalography (HD-EEG) in healthy volunteers. Study sessions were either sleep or sedation visits. During sleep visits, participants would come to the Wisconsin Psychiatry Institute and Clinics Sleep Center 2 hours prior to their normal bedtime and lasted until 8 AM the following morning or until the participant expressed a desire to get out of bed, whichever occurred first. Sedation visits started at 6 AM and lasted until clinical assessment by University of Wisconsin Hospital nursing staff deemed the participant fit to leave the hospital after the end of drug administration. During sedation visits, participants were administered one of three possible sedatives: dexmedetomidine, propofol, or ketamine. For any given study visit, regardless of sedation or sleep visit, a participant would be monitored using HD-EEG while resting, listening to auditory stimuli, or performing cognitive tests. At the end of each task or resting period, the participant would be approached by a member of the study team who would call their name to initiate a series of questions related to the participants state of connectedness and consciousness (examples of responses to these questions can be found in Appendix A). The answers to these questions were then used to assign each report as connected conscious, disconnected conscious, or unconscious. The data from the ketamine visits have not been incorporated into the analyses within this document due to amnestic properties of the drug compromising the validity of the subjective reports used to code conscious states throughout these analyses along with high rates of unresponsiveness at higher drug doses.

During sedation visits, sedatives were administered by a licensed anesthetist to progressively increasing doses throughout the duration of the visit. In doing so, participants

were biased into deeper states of sedation over time, allowing for more comprehensive sampling of behavioral and electrophysiological states than if a single steady state physiological drug concentration was targeted. Importantly, by collecting data across multiple drug steps of sedative and estimating the current plasma concentration of drug (Cp) using pharmacokinetic-pharmacodynamic (PKPD) modeling[88–90], we were able to estimate the covariance between Cp and the EEG separately from the covariance of conscious state and EEG. This allowed us to statistically control for non-specific drug effects within the statistics presented in the following chapters. By controlling for Cp and explicitly measuring mental state through verbal reports, these studies provide additional specificity for our results to connectedness and consciousness that has not been demonstrated by prior studies to date.

Electroencephalography: A Short Primer

All of the primary analyses within chapters 1-3 are based on EEG data collected through the UN-ConsCIOUS project. Therefore, I believe it is important that the reader have a degree of baseline understanding of how EEG signals are generated, recorded, and analyzed prior to reading the main body of this text. In order to facilitate this background knowledge, this section will serve as a short primer on EEG targeted at the general scientific audience.

EEG data are time varying electrical potentials recorded via electrodes placed on the scalp[91]. The recorded potentials may be a mixture of biological and environmental signals, however, the primary goal of such recordings is to detect brain generated activity. In the absence of contaminating artifacts, such as muscle activity or electrical noise, the EEG at any given electrode represents a summation of excitatory and inhibitory post-synaptic potentials (EPSP and IPSP) and, to a lesser extent, action potentials[91,92]. The primary drivers of such

potentials have been identified as pyramidal neurons within cortex, thanks to the consistent orientation of apical dendrites (perpendicular to the cortical surface) allowing for efficient summation of electric fields[92]. That said, comparisons of simultaneous EEG and intracranial recordings demonstrate that even neural activity generated by deep subcortical structures can be detected by EEG[93].

The electric fields generated by the brain can be recorded as electric potentials by placing electrodes on the scalp. EEG can be collected with as few as a single electrode (along with an electrical reference) or as many electrodes as surface area permits be placed on the head. In practice, the current state of the art for so called “high-density” recordings is to use a montage of 256 electrodes, sometimes referred to as “channels”. All of the HD-EEG recordings included within the following chapters made use of 256 channel gel electrode caps purchased from Electrical Geodesics, Inc. (EGI). The potentials observed on the scalp are passed through an amplifier which increases the amplitude of the signals while attenuating certain artifacts[94]. The amplified signals are then sampled to digitize the analogue signal into a computer usable recording.

Once the data are in hand, researchers must make many decisions regarding how those data will be analyzed. One key consideration is the degree of anatomical specificity necessary to address the research question. Due to the distal arrangement of electrodes (on the scalp) relative to the source of the activity being measured (in the brain), and the spread of electric fields, EEG data have low anatomical specificity[95,96]. When analyzing electrode-level data, we are typically constrained to discussing signal origin at the level of lobes of the brain. For many research questions, this level of granularity is sufficient and the data will be further analyzed on

an electrode by electrode basis. This will be referred to as ‘sensor-space’. When additional spatial detail is desirable, the sensor-space data may be transformed in order to estimate the origins of the electrical activity within the brain[97]. When the data have been transformed in this way, they will be described as being in ‘source-space’. Sensor-space give us electrical potentials at a particular electrode on the scalp while source-space data give us estimates of electrical potentials at a particular coordinate within the brain.

There are many algorithms that have been designed to accomplish this conversion of sensor-space data into source-space data[97,98]. Collectively, these methods are called ‘source reconstruction’ or ‘source localization’. Source reconstruction is a very difficult problem to address because there are many more electrical sources in the brain than there are electrodes recording them but the activity observed at each electrode is an unknown combination of brain sources[99]. This results in an infinite number of possible combinations of brain sources that could produce the observed electrode signal[97,100]. The various methods of source reconstruction make different assumptions that place constraints upon how this problem can be solved in order to make unique solutions possible[101]. There are two source reconstruction methods that will be applied within this dissertation: exact low resolution brain electromagnetic tomography (eLORETA[102], Chapter 1) and dynamic causal modeling (DCM[103], Chapter 3). These methodologies allow us to make good estimates of brain activity with much greater precision than electrode-level data but they cannot entirely side-step the limited spatial resolution of EEG as a technology. The specific limitations of eLORETA and DCM will be discussed within their respective chapters and within the general conclusion of the dissertation.

Regardless of whether the EEG data are in sensor-space or source-space, the data can be analyzed in a myriad of different ways[104–106]. One of the most commonly used methods, and one that will be used extensively in chapters 1 & 2, is to treat the EEG as a summation of oscillations of varying frequencies. The time-varying EEG signal can be transformed into a frequency-based representation using analytical methods such as the Fourier transform or wavelet convolution[107]. The frequency domain signal allows researchers to quantify "how much" of the EEG signal belongs to a particular frequency range. This method has become particularly popular for EEG analysis because different frequency ranges have now been associated with a variety of biological and cognitive processes[108–112]. For example, the alpha band (8-14 Hz, peak at 10 Hz) activity becomes prominent over occipital cortex while awake and resting with eyes closed, but is largely absent when one's eyes are open[113–115]. Recent evidence suggests that that the alpha rhythm has supragranular cortical origins and reflects top-down information transfer[116,117]. Slow delta activity (1-4 Hz) is high during NREM sleep and general anesthesia but is rarely observable during wake or REM sleep in healthy individuals[118–120] . Delta activity can, however, be observed in awake individuals experiencing post-operative delirium, a transient state of cognitive dysfunction with temporal onset shortly after surgery[121,122]. By linking these frequency bands to different neural processes, researchers have been able to make inferences about, and identify biomarkers related to, specific brain states[108–112,123].

Aside from frequency-based analyses, many other methods of exploring the EEG signal exist[104–106]. Functional connectivity analyses assess how similar the activity is in two spatially distinct regions across time[124]. The simplest example would be a Pearson correlation calculated between the time series of two electrodes, but many more sophisticated measures exist as

well[105]. A related method is to build a network out of many functional connections then calculate some summary metric about that network[106,125]. These network or graph theory analyses have been used to make inferences about how information sharing is organized within the brain at a macro-scale[126]. Information theory or complexity measures have also gained popularity among EEG researchers. These measures, such as the Lempel-Ziv complexity or permutation entropy, quantify the degree of information coded within the EEG signal[127], and have been linked to consciousness in several studies[128–132]. Lastly, different frequency bands may also be related to one another through so-called cross-frequency coupling. These methods look for consistent relationships between the phases or amplitudes of different frequency bands[133]. For example, the amplitude of alpha oscillations has been shown to be maximal when coinciding with the trough of a delta wave during light anesthesia, but switch to being maximal at the peak of a delta wave during deep anesthesia[67,134]. Fundamentally, each of these methods captures different types of information embedded within the EEG signal and may serve as potential biomarkers for a particular brain state. Each of the above methodologies have been applied in the study of consciousness which has resulted in many putative EEG markers of consciousness within the scientific literature. Chapter 2 will explore how well these putative consciousness markers work when unconsciousness and disconnection are decoupled.

Pharmacological Impacts of Dexmedetomidine and Propofol on Endogenous Sleep Systems

As the data used throughout this dissertation were all derived through sleep or sedation studies (along with corresponding baseline data), I will provide a brief synopsis of the physiology of the sleep/arousal system and how the study drugs used within this dissertation interact with this system to produce states of sedation. States of sleep and arousal are

regulated by a complex interplay of wake and sleep promoting systems distributed throughout the brainstem, hypothalamus, and BF[135–138]. These systems tightly regulate one another through the use of a wide range of neurotransmitters, including (but not limited to) histaminergic, serotonergic, noradrenergic, orexinergic, dopaminergic, cholinergic, glutamatergic, and GABAergic signaling[139–147]. Lesions within these systems result in disproportionately high or low arousal, depending on if a sleep- or wake-promoting region is damaged, or in instability of arousal states (as seen in narcolepsy[148])[3,149]. Due to the powerful influence these regions have over general arousal (as well as connectedness and consciousness), the components of the sleep/arousal system serve as excellent pharmacological targets for achieving sedation or general anesthesia[65,150,151].

Dexmedetomidine is an alpha2-adrenergic receptor agonist that lowers LC activity by binding to pre-synaptic alpha2 receptors, resulting in hyperpolarization and reduced NA release[65,152]. During normal wake, the LC promotes waking states through excitatory and inhibitory mechanisms. The LC directly promotes wake through excitatory NA innervation to the BF, thalamus, and cortex[147]. The LC also indirectly promotes wake through an antagonistic relationship with the preoptic area of the hypothalamus (POA)[150]. When active, POA neurons release the inhibitory neurotransmitters GABA and galanin which suppress activity within wake promoting centers in the hypothalamus and brain stem[153,154]. During wake, the LC inhibits the POA through NA mediated signals[153,155,156]. By inhibiting the inhibitory signals of the POA, the LC promotes arousal. When the LC is inhibited by dexmedetomidine, the POA becomes disinhibited and is free to suppress arousal centers, thereby promoting sleep. This inhibition of the LC with subsequent loss of excitation to cortex, BF, and thalamus as well as disinhibition of

the POA mirrors what is seen physiologically in NREM sleep[65,150]. Indeed, electroencephalographic activity under moderate dexmedetomidine sedation is strikingly similar to the activity observed during stage-2 NREM sleep, exhibiting both delta oscillations and spindle activity[157,158].

Propofol is the most widely used anesthetic agent in clinical practice[65]. Propofol targets post-synaptic $GABA_A$ receptors where its binding potentiates inhibitory Cl^- through $GABA_A$ receptors and slows their desensitization[151,159]. $GABA_A$ receptors are distributed throughout cortex, thalamus, and brainstem[65,160]. Because of this broad spatial distribution of $GABA_A$ receptors, along with propofol's lipophilic nature, propofol is effectively able to enhance inhibitory activity across the entire brain. In addition to directly enhancing inhibition at the level of cortical pyramidal neurons, propofol also enhances GABAergic activity from the POA to arousal centers such as the tuberomammillary nucleus, the dorsal raphe nuclei, the ventral periaqueductal gray, and the LC[153]. In this way, propofol not only directly inhibits cortical activity, it also dampens the excitatory signals that would otherwise promote cortical activation. The resulting alterations in brain activity manifest in electrophysiological changes observable through EEG. At moderate doses, typical of sedation as opposed to general anesthesia, propofol will induce increased low-frequency delta activity as well as high frequency beta activity[65,161]. While the increase in delta activity is typical of NREM sleep[137] and many other drugs with sedative properties[65,150,158], the emergence of beta activity is atypical and seems to be a characteristic of drugs that target the $GABA_A$ receptor[65,161–163]. As the dose increases, the paradoxical beta activity appears to transition into alpha activity with high frontal coherence[65]. At high enough doses, propofol can induce an extreme state of neural quiescence

observable by EEG as “burst suppression”, an EEG pattern of short bursts of activity interspersed with electrical silence[164,165].

Conclusions

Objective assessment of consciousness and connectedness remains an outstanding challenge in clinical and research settings. Lack of such assessments limits accuracy in diagnosing DoC, ability to detect intraoperative awareness, and researchers’ ability to make strong inferences related to consciousness when subjective reports are unavailable. While substantial effort has been put forth to address these gaps, the majority of this work has relied upon observed loss of responsiveness as an index of unconsciousness, despite ample evidence that these are highly dissociable qualities. In the coming chapters of this dissertation, I will be making use of HD-EEG data, that I collected under the UN-ConsCIOUS project, to identify and validate signatures of consciousness and connectedness during sleep and anesthesia. The findings presented here are some of the first published works to explicitly distinguish between consciousness and connectedness while investigating conscious state specific neural signatures.

References

1. Tononi G. An information integration theory of consciousness. *BMC Neurosci*. 2004;5. doi:10.1186/1471-2202-5-42

2. Sanders RD, Tononi G, Laureys S, Sleigh JW. Unresponsiveness ≠ unconsciousness. *Anesthesiology*. 2012;116(4):946-959. doi:10.1097/ALN.0b013e318249d0a7

3. Lim MM, Szymusiak R. Neurobiology of Arousal and Sleep: Updates and Insights Into Neurological Disorders. *Curr Sleep Med Rep*. 2015;1(2):91-100. doi:10.1007/S40675-015-0013-0/TABLES/2

4. Siclari F, LaRocque JJ, Postle BR, Tononi G. Assessing sleep consciousness within subjects using a serial awakening paradigm. *Front Psychol*. 2013;4(AUG):542. doi:10.3389/FPSYG.2013.00542/BIBTEX

5. Malhotra RK, Avidan AY. Sleep Stages and Scoring Technique Introduction to Sleep Stage Scoring. *Atlas of Sleep Medicine*. Published online 2014:77-99. doi:10.1016/B978-1-4557-1267-0.00003-5

6. Aston-Jones G, Bloom FE. Activity of norepinephrine-containing locus coeruleus neurons in behaving rats anticipates fluctuations in the sleep-waking cycle. *J Neurosci*. 1981;1(8):876-886. doi:10.1523/JNEUROSCI.01-08-00876.1981

7. Hobson JA, Mccarley RW, Wyzinski PW. Sleep cycle oscillation: reciprocal discharge by two brainstem neuronal groups. *Science*. 1975;189(4196):55-58. doi:10.1126/SCIENCE.1094539

8. Xu M, Chung S, Zhang S, et al. Basal forebrain circuit for sleep-wake control. *Nat Neurosci*. 2015;18(11):1641-1647. doi:10.1038/NN.4143

9. Lee MG, Hassani OK, Alonso A, Jones BE. Cholinergic basal forebrain neurons burst with theta during waking and paradoxical sleep. *J Neurosci*. 2005;25(17):4365-4369. doi:10.1523/JNEUROSCI.0178-05.2005

10. Boucetta S, Cissé Y, Mainville L, Morales M, Jones BE. Discharge profiles across the sleep-waking cycle of identified cholinergic, GABAergic, and glutamatergic neurons in the pontomesencephalic tegmentum of the rat. *J Neurosci*. 2014;34(13):4708-4727. doi:10.1523/JNEUROSCI.2617-13.2014

11. Ozen Irmak S, de Lecea L. Basal Forebrain Cholinergic Modulation of Sleep Transitions. *Sleep*. 2014;37(12):1941. doi:10.5665/SLEEP.4246

12. Toscano A, Pancaro C, Peduto VA. Scopolamine Prevents Dreams during General Anesthesia. *Anesthesiology*. 2007;106(5):952-955. doi:10.1097/01.ANES.0000265154.24685.47

13. Meuret P, Backman SB, Bonhomme V, Plourde G, Fiset P. Physostigmine Reverses Propofol-induced Unconsciousness and Attenuation of the Auditory Steady State Response and Bispectral Index in Human Volunteers. *Anesthesiology*. 2000;93(3):708-717. doi:10.1097/00000542-200009000-00020

14. Mantz J. Alpha2-adrenoceptor agonists: Analgesia, sedation, anxiolysis, haemodynamics, respiratory function and weaning. *Bailliere's Best Practice and Research in Clinical Anaesthesiology*. 2000;14(2):433-448. doi:10.1053/BEAN.2000.0094

15. Carter ME, Yizhar O, Chikahisa S, et al. Tuning arousal with optogenetic modulation of locus coeruleus neurons. *Nat Neurosci*. 2010;13(12):1526-1535. doi:10.1038/NN.2682

16. Gompf HS, Budygin EA, Fuller PM, Bass CE. Targeted genetic manipulations of neuronal subtypes using promoter-specific combinatorial AAVs in wild-type animals. *Front Behav Neurosci*. 2015;9(JULY). doi:10.3389/FNBEH.2015.00152

17. Hayat H, Regev N, Matosevich N, et al. Locus coeruleus norepinephrine activity mediates sensory-evoked awakenings from sleep. *Sci Adv*. 2020;6(15). doi:10.1126/sciadv.aaz4232

18. Coull JT, Büchel C, Friston KJ, Frith CD. Noradrenergically Mediated Plasticity in a Human Attentional Neuronal Network. *Neuroimage*. 1999;10(6):705-715. doi:10.1006/NIMG.1999.0513

19. Gelbard-Sagiv H, Magidov E, Sharon H, Hendler T, Nir Y. Noradrenaline Modulates Visual Perception and Late Visually Evoked Activity. *Current Biology*. 2018;28(14):2239-2249.e6. doi:10.1016/J.CUB.2018.05.051

20. Sara SJ. The locus coeruleus and noradrenergic modulation of cognition. *Nature Reviews Neuroscience 2009 10:3*. 2009;10(3):211-223. doi:10.1038/nrn2573

21. Tononi G. Integrated information theory of consciousness: an updated account. *Arch Ital Biol*. 2012;150(4):293-329. doi:10.4449/aib.v149i5.1388

22. Tononi G. Consciousness as integrated information: A provisional manifesto. *Biological Bulletin*. 2008;215(3):216-242. doi:10.2307/25470707/ASSET/IMAGES/LARGE/Z1N0060832860010.JPEG

23. Mashour GA, Roelfsema P, Changeux JP, Dehaene S. Conscious Processing and the Global Neuronal Workspace Hypothesis. *Neuron*. 2020;105(5):776-798. doi:10.1016/J.NEURON.2020.01.026

24. Pal D, Li D, Dean JG, et al. Level of Consciousness Is Dissociable from Electroencephalographic Measures of Cortical Connectivity, Slow Oscillations, and Complexity. *Journal of Neuroscience*. 2020;40(3):605-618. doi:10.1523/JNEUROSCI.1910-19.2019

25. Bayne T, Hohwy J, Owen AM. Are There Levels of Consciousness? *Trends Cogn Sci*. 2016;20(6):405-413. doi:10.1016/J.TICS.2016.03.009

26. Nielsen TA. Changes in the kinesthetic content of dreams following somatosensory stimulation of leg muscles during REM sleep. *Dreaming*. 1993;3(2):99-113. doi:10.1037/H0094374

27. Schredl M, Atanasova D, Hörmann K, Maurer JT, Hummel T, Stuck BA. Information processing during sleep: the effect of olfactory stimuli on dream content and dream emotions. *J Sleep Res*. 2009;18(3):285-290. doi:10.1111/J.1365-2869.2009.00737.X

28. Leslie K, Ogilvie R. Vestibular dreams: The effect of rocking on dream mentation. *Dreaming*. 1996;6(1):1-16. doi:10.1037/H0094442

29. Nir Y, Tononi G. Dreaming and the brain: from phenomenology to neurophysiology. *Trends Cogn Sci*. 2010;14(2):88-100. doi:10.1016/J.TICS.2009.12.001

30. Meara JG, Leather AJM, Hagander L, et al. Global Surgery 2030: Evidence and solutions for achieving health, welfare, and economic development. *The Lancet*. 2015;386(9993):569-624. doi:10.1016/S0140-6736(15)60160-X

31. Sandin RH, Enlund G, Samuelsson P, Lennmarken C. Awareness during anaesthesia: a prospective case study. *The Lancet*. 2000;355(9205):707-711. doi:10.1016/S0140-6736(99)11010-9

32. Sebel PS, Bowdle TA, Ghoneim MM, et al. The incidence of awareness during anesthesia: A multicenter United States study. *Anesth Analg*. 2004;99(3):833-839. doi:10.1213/01.ANE.0000130261.90896.6C

33. Mashour GA, Shanks A, Tremper KK, et al. Prevention of Intraoperative Awareness with Explicit Recall in an Unselected Surgical Population: A Randomized Comparative Effectiveness Trial. *Anesthesiology*. 2012;117(4):717. doi:10.1097/ALN.0B013E31826904A6

34. Sanders RD, Gaskell A, Raz A, et al. Incidence of Connected Consciousness after Tracheal Intubation: A Prospective, International, Multicenter Cohort Study of the Isolated Forearm Technique. *Anesthesiology*. 2017;126(2):214-222. doi:10.1097/ALN.0000000000001479

35. Lennertz R, Pryor KO, Raz A, et al. Connected consciousness after tracheal intubation in young adults: an international multicentre cohort study. *Br J Anaesth*. Published online May 23, 2022. doi:10.1016/J.BJA.2022.04.010

36. Cascella M. Mechanisms underlying brain monitoring during anesthesia: Limitations, possible improvements, and perspectives. *Korean J Anesthesiol*. 2016;69(2):113-120. doi:10.4097/kjae.2016.69.2.113

37. Tunstall ME. Detecting wakefulness during general anaesthesia for caesarean section. *Br Med J*. 1977;1(6072):1321. doi:10.1136/BMJ.1.6072.1321-A

38. Tunstall ME. The reduction of amnesic wakefulness during caesarean section. *Anaesthesia*. 1979;34(4):316-319. doi:10.1111/J.1365-2044.1979.TB04928.X

39. Tunstall ME. ON BEING AWARE BY REQUEST. *Br J Anaesth*. 1980;52(10):1049-1053. doi:10.1093/bja/52.10.1049

40. Giacino JT, Katz DI, Schiff ND, et al. Comprehensive systematic review update summary: Disorders of consciousness: Report of the Guideline Development, Dissemination, and Implementation Subcommittee of the American Academy of Neurology; The American Congress of Rehabilitation Medicine; And the National Institute on Disability,

Independent Living, and Rehabilitati. *Neurology*. 2018;91(10):461-470. doi:10.1212/WNL.0000000000005928

41. Covelli V, Sattin D, Giovannetti AM, Scaratti C, Willems M, Leonardi M. Caregiver's burden in disorders of consciousness: a longitudinal study. *Acta Neurol Scand*. 2016;134(5):352-359. doi:10.1111/ANE.12550

42. Giacino JT, Katz DI, Schiff ND, et al. Comprehensive systematic review update summary: Disorders of consciousness: Report of the Guideline Development, Dissemination, and Implementation Subcommittee of the American Academy of Neurology; the American Congress of Rehabilitation Medicine; and the National Institute on Disability, Independent Living, and Rehabilitation Research. *Neurology*. 2018;91(10):461. doi:10.1212/WNL.0000000000005928

43. Schnakers C, Vanhaudenhuyse A, Giacino J, et al. Diagnostic accuracy of the vegetative and minimally conscious state: Clinical consensus versus standardized neurobehavioral assessment. *BMC Neurol*. 2009;9(1):35. doi:10.1186/1471-2377-9-35

44. Gosseries O, Zasler ND, Laureys S. Recent advances in disorders of consciousness: Focus on the diagnosis. *Brain Inj*. 2014;28(9):1141-1150. doi:10.3109/02699052.2014.920522

45. Regional Cerebral Dysfunction: Higher Mental Functions - ClinicalKey. Accessed October 13, 2022. https://www.clinicalkey.com/#!/content/book/3-s2.0-B9780323532662003738

46. Kreuer S, Biedler A, Larsen R, Schoth S, Altmann S, Wilhelm W. The narcotrend^{TM} - A new EEG monitor designed to measure the depth of anaesthesia: A comparison with bispectral index monitoring during propofol-remifentanil-anaesthesia. *Anaesthesist*. 2001;50(12):921-925. doi:10.1007/s00101-001-0242-0

47. Sigl JC, Chamoun NG. An introduction to bispectral analysis for the electroencephalogram. *J Clin Monit*. 1994;10(6):392-404. doi:10.1007/BF01618421

48. Prichep LS, Gugino LD, John ER, et al. The Patient State Index as an indicator of the level of hypnosis under general anaesthesia. *Br J Anaesth*. 2004;92(3):393-399. doi:10.1093/bja/aeh082

49. Koch C, Massimini M, Boly M, Tononi G. Neural correlates of consciousness: Progress and problems. *Nat Rev Neurosci*. 2016;17(5):307-321. doi:10.1038/nrn.2016.22

50. Boly M. Preserved Feedforward But Impaired Top-Down Processes in the Vegetative State. *Science (1979)*. 2011;46(5896):1-25. doi:10.1126/science.1245938

51. Kreuer S, Biedler A, Larsen R, Altmann S, Wilhelm W. *Narcotrend Monitoring Allows Faster Emergence and a Reduction of Drug Consumption in Propofol-Remifentanil Anesthesia*. Vol 99.; 2003.

52. Yli-Hankala A, Vakkuri A, Annila P, Korttila K. EEG bispectral index monitoring in sevoflurane or propofol anaesthesia: Analysis of direct costs and immediate recovery. *Acta Anaesthesiol Scand*. 1999;43(5):545-549. doi:10.1034/j.1399-6576.1999.430510.x

53. Song D, Joshi GP, White PF. Titration of volatile anesthetics using bispectral index facilitates recovery after ambulatory anesthesia. *Anesthesiology*. 1997;87(4):842-848. doi:10.1097/00000542-199710000-00018

54. Johansen JW, Sebel PS, Sigl JC. Clinical impact of hypnotic-titration guidelines based on EEG Bispectral Index (BIS) monitoring during routine anesthetic care. *J Clin Anesth*. 2000;12(6):433-443. doi:10.1016/S0952-8180(00)00187-2

55. Gan TJ, Glass PS, Windsor A, et al. Bispectral index monitoring allows faster emergence and improved recovery from propofol, alfentanil and nitrous oxide anesthesia. *Anesthesiology*. 1997;87(4):808-815. doi:10.1097/00000542-199710000-00014

56. Bannister CF, Brosius KK, Sigl JC, Meyer BJ, Sebel PS. The effect of bispectral index monitoring on anesthetic use and recovery in children anesthetized with sevoflurane in nitrous oxide. *Anesth Analg*. 2001;92(4):877-881. doi:10.1097/00000539-200104000-00015

57. Hirota K, Kubota T, Ishihara H, Matsuki A. The effects of nitrous oxide and ketamine on the bispectral index and 95% spectral edge frequency during propofol-fentanyl anaesthesia. *Eur J Anaesthesiol*. 1999;16(11):779-783. doi:10.1046/j.1365-2346.1999.00585.x

58. Schneider G, Wagner K, Reeker W, Hänel F, Werner C, Kochs E. Bispectral Index (BIS) May Not Predict Awareness Reaction to Intubation in Surgical Patients. *J Neurosurg Anesthesiol*. 2002;14(1):7-11. Accessed March 10, 2020. https://journals.lww.com/jnsa/Fulltext/2002/01000/Bispectral_Index__BIS__May_Not_Predict_Awareness.2.aspx

59. Schneider G, Gelb AW, Schmeller B, Tschakert R, Kochs E. Detection of awareness in surgical patients with EEG-based indices—bispectral index and patient state index. *Br J Anaesth*. 2003;91(3):329-335. doi:10.1093/BJA/AEG188

60. Russell IF. The Narcotrend 'depth of anaesthesia' monitor cannot reliably detect consciousness during general anaesthesia: an investigation using the isolated forearm technique. *Br J Anaesth*. 2006;96(3):346-352. doi:10.1093/BJA/AEL017

61. Chernik DA, Gillings D, Laine H, et al. Validity and reliability of the observer's assessment of alertness/sedation scale: Study with intravenous midazolam. *J Clin Psychopharmacol*. 1990;10(4):244-251. doi:10.1097/00004714-199008000-00003

62. Barttfelda P, Uhriga L, Sitta JD, Sigmane M, Jarrayaa B, Dehaene S. Signature of consciousness in the dynamics of resting-state brain activity. *Proc Natl Acad Sci U S A*. 2015;112(3):887-892. doi:10.1073/PNAS.1418031112/-/DCSUPPLEMENTAL

63. Sergent C, Naccache L. Imaging neural signatures of consciousness: "what", "when", "where" and "how" does it work? *Arch Ital Biol*. 2012;150(2-3):91-106. doi:10.4449/AIB.V150I2.1270

64. Bonhomme V, Staquet C, Montupil J, et al. General Anesthesia: A Probe to Explore Consciousness. *Front Syst Neurosci*. 2019;13:36. doi:10.3389/FNSYS.2019.00036/BIBTEX

65. Purdon PL, Sampson A, Pavone KJ, Brown EN. Clinical electroencephalography for anesthesiologists. *Anesthesiology*. 2015;123(4):937-960. doi:10.1097/ALN.0000000000000841

66. Warner DS, Purdon PL, Sampson A, Pavone KJ, Brown EN. The Electroencephalogram and Brain Monitoring under General Anesthesia Clinical Electroencephalography for Anesthesiologists Part I: Background and Basic Signatures. Published online 2015. Accessed June 6, 2019. www.anesthesiaEEG.com

67. Blain-Moraes S, Tarnal V, Vanini G, et al. Neurophysiological Correlates of Sevoflurane-induced Unconsciousness. *Anesthesiology*. 2015;122(2):307-316. doi:10.1097/ALN.0000000000000482

68. Li D, Hambrecht-Wiedbusch VS, Mashour GA. Accelerated recovery of consciousness after general anesthesia is associated with increased functional brain connectivity in the high-gamma bandwidth. *Front Syst Neurosci*. 2017;11:16. doi:10.3389/FNSYS.2017.00016/BIBTEX

69. Stephen EP, Hotan GC, Pierce ET, et al. Broadband slow-wave modulation in posterior and anterior cortex tracks distinct states of propofol-induced unconsciousness. *Scientific Reports 2020 10:1*. 2020;10(1):1-11. doi:10.1038/s41598-020-68756-y

70. Lee U, Ku S, Noh G, Baek S, Choi B, Mashour GA. Disruption of Frontal–Parietal Communication by Ketamine, Propofol, and Sevoflurane. *Anesthesiology*. 2013;118(6):1264-1275. doi:10.1097/ALN.0B013E31829103F5

71. Lee M, Sanders RD, Yeom SK, et al. Network Properties in Transitions of Consciousness during Propofol-induced Sedation. *Scientific Reports 2017 7:1*. 2017;7(1):1-13. doi:10.1038/s41598-017-15082-5

72. Fiset P, Paus T, Daloze T, et al. Brain mechanisms of propofol-induced loss of consciousness in humans: A positron emission tomographic study. *Journal of Neuroscience*. 1999;19(13):5506-5513. doi:10.1523/JNEUROSCI.19-13-05506.1999

73. Lee UC, Mashour GA, Kim S, Noh GJ, Choi BM. Propofol induction reduces the capacity for neural information integration: Implications for the mechanism of consciousness and general anesthesia. *Conscious Cogn*. 2009;18(1):56-64. doi:10.1016/J.CONCOG.2008.10.005

74. Plourde G, Belin P, Chartrand D, et al. Cortical Processing of Complex Auditory Stimuli during Alterations of Consciousness with the General Anesthetic Propofol. *Anesthesiology*. 2006;104(3):448-457. doi:10.1097/00000542-200603000-00011

75. Långsjö JW, Alkire MT, Kaskinoro K, et al. Returning from oblivion: Imaging the neural core of consciousness. *Journal of Neuroscience*. 2012;32(14):4935-4943. doi:10.1523/JNEUROSCI.4962-11.2012

76. Casali AG, Gosseries O, Rosanova M, et al. A theoretically based index of consciousness independent of sensory processing and behavior. *Sci Transl Med*. 2013;5(198):198ra105-198ra105. doi:10.1126/scitranslmed.3006294

77. Casarotto S, Comanducci A, Rosanova M, et al. Stratification of unresponsive patients by an independently validated index of brain complexity. *Ann Neurol*. 2016;80(5):718-729. doi:10.1002/ana.24779

78. Wang Y, Niu Z, Xia X, et al. Application of Fast Perturbational Complexity Index to the Diagnosis and Prognosis for Disorders of Consciousness. *IEEE Transactions on Neural Systems and Rehabilitation Engineering*. 2022;30:509-518. doi:10.1109/TNSRE.2022.3154772

79. Sinitsyn DO, Poydasheva AG, Bakulin IS, et al. Detecting the Potential for Consciousness in Unresponsive Patients Using the Perturbational Complexity Index. *Brain Sci*. 2020;10(12):1-12. doi:10.3390/BRAINSCI10120917

80. Kondziella D, Bender A, Diserens K, et al. European Academy of Neurology guideline on the diagnosis of coma and other disorders of consciousness. *Eur J Neurol*. 2020;27(5):741-756. doi:10.1111/ENE.14151

81. Jennett B. The vegetative state. *J Neurol Neurosurg Psychiatry*. 2002;73(4):355-357. doi:10.1136/JNNP.73.4.355

82. Ivan LP. The persistent vegetative state. *Transplant Proc*. 1990;22(3):993-994.

83. Tresch DD, Sims FH, Duthie EH, Goldstein MD, Lane PS. Clinical Characteristics of Patients in the Persistent Vegetative State. *Arch Intern Med*. 1991;151(5):930-932. doi:10.1001/ARCHINTE.1991.00400050078015

84. National Academies of Sciences E and M, Division H and M, Practice B on PH and PH, et al. The State of Health Disparities in the United States. *Communities in Action: Pathways to Health Equity*. Published online January 11, 2017:1-558. doi:10.17226/24624

85. Barshes NR, Minc SD. Healthcare disparities in vascular surgery: A critical review. *J Vasc Surg*. 2021;74(2):6S-14S.e1. doi:10.1016/J.JVS.2021.03.055

86. Siclari F, Baird B, Perogamvros L, et al. The neural correlates of dreaming. *Nat Neurosci*. 2017;20(6):872-878. doi:10.1038/nn.4545

87. Siclari F, Bernardi G, Cataldi J, Tononi G. Dreaming in NREM sleep: A high-density EEG study of slow waves and spindles. *Journal of Neuroscience*. 2018;38(43):9175-9185. doi:10.1523/JNEUROSCI.0855-18.2018

88. Bailey JM, Shafer SL. A Simple Analytical Solution to the Three-Compartment Pharmacokinetic Model Suitable for Computer-Controlled Infusion Pumps. *IEEE Trans Biomed Eng*. 1991;38(6):522-525. doi:10.1109/10.81576

89. Hannivoort LN, Eleveld DJ, Proost JH, et al. Development of an Optimized Pharmacokinetic Model of Dexmedetomidine Using Target-controlled Infusion in Healthy Volunteers. *Anesthesiology*. 2015;123(2):357-367. doi:10.1097/ALN.0000000000000740

90. Schnider TW, Minto CF, Gambus PL, et al. The influence of method of administration and covariates on the pharmacokinetics of propofol in adult volunteers. *Anesthesiology*. 1998;88(5):1170-1182. doi:10.1097/00000542-199805000-00006

91. Nunez PL, Srinivasan R. Electric Fields of the Brain: The neurophysics of EEG. *Electric Fields of the Brain: The neurophysics of EEG*. Published online May 1, 2006:1-611. doi:10.1093/ACPROF:OSO/9780195050387.001.0001

92. Kirschstein T, Köhling R. What is the source of the EEG? *Clin EEG Neurosci*. 2009;40(3):146-149. doi:10.1177/155005940904000305/ASSET/IMAGES/LARGE/10.1177_155005940904000305-FIG2.JPEG

93. Seeber M, Cantonas LM, Hoevels M, Sesia T, Visser-Vandewalle V, Michel CM. Subcortical electrophysiological activity is detectable with high-density EEG source imaging. *Nature Communications 2019 10:1*. 2019;10(1):1-7. doi:10.1038/s41467-019-08725-w

94. Rampil IJ. A Primer for EEG Signal Processing in Anesthesia. *Anesthesiology*. 1998;89(4):980-1002. doi:10.1097/00000542-199810000-00023

95. Nunez PL, Silberstein RB, Cadusch PJ, Wijesinghe RS, Westdorp AF, Srinivasan R. A theoretical and experimental study of high resolution EEG based on surface Laplacians and cortical imaging. *Electroencephalogr Clin Neurophysiol*. 1994;90(1):40-57. doi:10.1016/0013-4694(94)90112-0

96. Burle B, Spieser L, Roger C, Casini L, Hasbroucq T, Vidal F. Spatial and temporal resolutions of EEG: Is it really black and white? A scalp current density view. *International Journal of Psychophysiology*. 2015;97(3):210. doi:10.1016/J.IJPSYCHO.2015.05.004

97. Michel CM, Murray MM, Lantz G, Gonzalez S, Spinelli L, Grave De Peralta R. EEG source imaging. *Clinical Neurophysiology*. 2004;115(10):2195-2222. doi:10.1016/J.CLINPH.2004.06.001

98. Bradley A, Yao J, Dewald J, Richter CP. Evaluation of Electroencephalography Source Localization Algorithms with Multiple Cortical Sources. Published online 2016. doi:10.1371/journal.pone.0147266

99. Makeig S, Jung TP, Bell AJ, Sejnowski TJ. Independent Component Analysis of Electroencephalographic Data. *Adv Neural Inf Process Syst*. 1995;8.

100. Helmholtz H. Ueber einige Gesetze der Vertheilung elektrischer Ströme in körperlichen Leitern, mit Anwendung auf die thierisch-elektrischen Versuche (Schluss.). *Ann Phys*. 1853;165(7):353-377. doi:10.1002/ANDP.18531650702

101. DH Fender. Source localization of brain electrical activity. *Handbook of electroencephalography and clinical neurophysiology*. Published online 1987. Accessed October 26, 2022. https://ci.nii.ac.jp/naid/10009403747/

102. Pascual-Marqui RD, Lehmann D, Koukkou M, et al. Assessing interactions in the brain with exact low-resolution electromagnetic tomography. *Philosophical Transactions of the Royal Society A: Mathematical, Physical and Engineering Sciences*. 2011;369(1952):3768-3784. doi:10.1098/rsta.2011.0081

103. Kiebel SJ, Garrido MI, Moran RJ, Friston KJ. Dynamic causal modelling for EEG and MEG. *Cogn Neurodyn*. 2008;2(2):121-136. doi:10.1007/s11571-008-9038-0

104. Kaur J, Kaur A. A review on analysis of EEG signals. *Conference Proceeding - 2015 International Conference on Advances in Computer Engineering and Applications, ICACEA 2015*. Published online July 22, 2015:957-960. doi:10.1109/ICACEA.2015.7164844

105. Bastos AM, Schoffelen JM. A tutorial review of functional connectivity analysis methods and their interpretational pitfalls. *Front Syst Neurosci*. 2016;9(JAN2016):175. doi:10.3389/FNSYS.2015.00175/BIBTEX

106. Ismail LE, Karwowski W. A Graph Theory-Based Modeling of Functional Brain Connectivity Based on EEG: A Systematic Review in the Context of Neuroergonomics. *IEEE Access*. 2020;8:155103-155135. doi:10.1109/ACCESS.2020.3018995

107. Morales S, Bowers ME. Time-frequency analysis methods and their application in developmental EEG data. *Dev Cogn Neurosci*. 2022;54:101067. doi:10.1016/J.DCN.2022.101067

108. Noorlag L, van Klink NEC, Kobayashi K, Gotman J, Braun KPJ, Zijlmans M. High-frequency oscillations in scalp EEG: A systematic review of methodological choices and clinical findings. *Clinical Neurophysiology*. 2022;137:46-58. doi:10.1016/J.CLINPH.2021.12.017

109. Lee DJ, Kulubya E, Goldin P, Goodarzi A, Girgis F. Review of the neural oscillations underlying meditation. *Front Neurosci*. 2018;12(MAR):178. doi:10.3389/FNINS.2018.00178/BIBTEX

110. Klimesch W. EEG alpha and theta oscillations reflect cognitive and memory performance: A review and analysis. *Brain Res Rev*. 1999;29(2-3):169-195. doi:10.1016/S0165-0173(98)00056-3

111. Fernandez LMJ, Lüthi A. Sleep spindles: Mechanisms and functions. *Physiol Rev*. 2020;100(2):805-868. doi:10.1152/PHYSREV.00042.2018/ASSET/IMAGES/LARGE/Z9J0022029380013.JPEG

112. Niethard N, Ngo HV v., Ehrlich I, Born J. Cortical circuit activity underlying sleep slow oscillations and spindles. *Proc Natl Acad Sci U S A*. 2018;115(39):E9220-E9229. doi:10.1073/PNAS.1805517115/SUPPL_FILE/PNAS.1805517115.SM01.MP4

113. Adrian ED, Matthews BHC. THE BERGER RHYTHM: POTENTIAL CHANGES FROM THE OCCIPITAL LOBES IN MAN. *Brain*. 1934;57(4):355-385. doi:10.1093/BRAIN/57.4.355

114. Legewie H, Simonova O, Creutzfeldt OD. EEG changes during performance of various tasks under open- and closed-eyed conditions. *Electroencephalogr Clin Neurophysiol*. 1969;27(5):470-479. doi:10.1016/0013-4694(69)90187-4

115. Glass A, Kwiatkowski AW. Power spectral density changes in the EEG during mental arithmetic and eye-opening. *Psychol Forsch*. 1970;33(2):85-99. doi:10.1007/BF00424979

116. van Kerkoerle T, Self MW, Dagnino B, et al. Alpha and gamma oscillations characterize feedback and feedforward processing in monkey visual cortex. *Proc Natl Acad Sci U S A*. 2014;111(40):14332-14341. doi:10.1073/PNAS.1402773111

117. Halgren M, Ulbert I, Bastuji H, et al. The generation and propagation of the human alpha rhythm. *Proc Natl Acad Sci U S A*. 2019;116(47):23772-23782. doi:10.1073/PNAS.1913092116/SUPPL_FILE/PNAS.1913092116.SAPP.PDF

118. Jasper HH, Carmichael L. ELECTRICAL POTENTIALS FROM THE INTACT HUMAN BRAIN. *Science*. 1935;81(2089):51-53. doi:10.1126/SCIENCE.81.2089.51

119. Steriade M, Timofeev I, Grenier F. Natural waking and sleep states: a view from inside neocortical neurons. *J Neurophysiol*. 2001;85(5):1969-1985. doi:10.1152/JN.2001.85.5.1969

120. Adrian ED, Matthews BHC. The interpretation of potential waves in the cortex. *J Physiol*. 1934;81(4):440. doi:10.1113/JPHYSIOL.1934.SP003147

121. Rudolph JL, Marcantonio ER. Postoperative Delirium: Acute change with long-term implications. *Anesth Analg*. 2011;112(5):1202-1211. doi:10.1213/ANE.0B013E3182147F6D

122. Tanabe S, Mohanty R, Lindroth H, et al. Cohort study into the neural correlates of postoperative delirium: the role of connectivity and slow-wave activity. *Br J Anaesth*. 2020;125(1):55-66. doi:10.1016/J.BJA.2020.02.027

123. Başar E, Güntekin B. Review of delta, theta, alpha, beta, and gamma response oscillations in neuropsychiatric disorders. *Suppl Clin Neurophysiol*. 2013;62:303-341. doi:10.1016/B978-0-7020-5307-8.00019-3

124. Babaeeghazvini P, Rueda-Delgado LM, Gooijers J, Swinnen SP, Daffertshofer A. Brain Structural and Functional Connectivity: A Review of Combined Works of Diffusion Magnetic Resonance Imaging and Electro-Encephalography. *Front Hum Neurosci*. 2021;15:585. doi:10.3389/FNHUM.2021.721206/BIBTEX

125. van Wijk BCM, Stam CJ, Daffertshofer A. Comparing Brain Networks of Different Size and Connectivity Density Using Graph Theory. *PLoS One*. 2010;5(10):e13701. doi:10.1371/JOURNAL.PONE.0013701

126. Klados MA, Kanatsouli K, Antoniou I, et al. A Graph Theoretical Approach to Study the Organization of the Cortical Networks during Different Mathematical Tasks. *PLoS One*. 2013;8(8):e71800. doi:10.1371/JOURNAL.PONE.0071800

127. Timme NM, Lapish C. A Tutorial for Information Theory in Neuroscience. *eNeuro*. 2018;5(3). doi:10.1523/ENEURO.0052-18.2018

128. Sarasso S, Casali AG, Casarotto S, Rosanova M, Sinigaglia C, Massimini M. Consciousness and complexity: a consilience of evidence. *Neurosci Conscious*. 2021;2021(2):1-24. doi:10.1093/NC/NIAB023

129. Schartner MM, Pigorini A, Gibbs SA, et al. Global and local complexity of intracranial EEG decreases during NREM sleep. *Neurosci Conscious*. 2017;2017(1):1-12. doi:10.1093/NC/NIW022

130. Hudetz AG, Liu X, Pillay S, Boly M, Tononi G. Propofol anesthesia reduces Lempel-Ziv complexity of spontaneous brain activity in rats. *Neurosci Lett*. 2016;628:132. doi:10.1016/J.NEULET.2016.06.017

131. Schartner M, Seth A, Noirhomme Q, et al. Complexity of Multi-Dimensional Spontaneous EEG Decreases during Propofol Induced General Anaesthesia. Chialvo DR, ed. *PLoS One*. 2015;10(8):e0133532. doi:10.1371/journal.pone.0133532

132. Eagleman SL, Vaughn DA, Drover DR, et al. Do Complexity Measures of Frontal EEG Distinguish Loss of Consciousness in Geriatric Patients Under Anesthesia? *Front Neurosci*. 2018;12(SEP):645. doi:10.3389/FNINS.2018.00645/BIBTEX

133. Canolty RT, Knight RT. The functional role of cross-frequency coupling. *Trends Cogn Sci*. 2010;14(11):506. doi:10.1016/J.TICS.2010.09.001

134. Purdon PL, Pierce ET, Mukamel EA, et al. Electroencephalogram signatures of loss and recovery of consciousness from propofol. *Proc Natl Acad Sci U S A*. 2013;110(12). doi:10.1073/pnas.1221180110

135. Moruzzi G, Magoun HW. Brain stem reticular formation and activation of the EEG. *Electroencephalogr Clin Neurophysiol*. 1949;1(1-4):455-473. doi:10.1016/0013-4694(49)90219-9

136. Saper CB, Fuller PM, Pedersen NP, Lu J, Scammell TE. Sleep state switching. *Neuron*. 2010;68(6):1023-1042. doi:10.1016/J.NEURON.2010.11.032

137. Jones BE. Neurobiology of waking and sleeping. *Handb Clin Neurol*. 2011;98(C):131-149. doi:10.1016/B978-0-444-52006-7.00009-5

138. Brown RE, Basheer R, McKenna JT, Strecker RE, McCarley RW. Control of sleep and wakefulness. *Physiol Rev*. 2012;92(3):1087-1187. doi:10.1152/PHYSREV.00032.2011/ASSET/IMAGES/LARGE/Z9J0031226200013.JPEG

139. Haas HL, Sergeeva OA, Selbach O. Histamine in the nervous system. *Physiol Rev*. 2008;88(3):1183-1241. doi:10.1152/PHYSREV.00043.2007

140. Monti JM. Serotonin control of sleep-wake behavior. *Sleep Med Rev*. 2011;15(4):269-281. doi:10.1016/J.SMRV.2010.11.003

141. Jones BE. Modulation of Cortical Activation and Behavioral Arousal by Cholinergic and Orexinergic Systems. *Ann N Y Acad Sci*. 2008;1129(1):26-34. doi:10.1196/ANNALS.1417.026

142. Lu J, Jhou TC, Saper CB. Identification of wake-active dopaminergic neurons in the ventral periaqueductal gray matter. *J Neurosci*. 2006;26(1):193-202. doi:10.1523/JNEUROSCI.2244-05.2006

143. Dash MB, Douglas CL, Vyazovskiy V v., Cirelli C, Tononi G. Long-term homeostasis of extracellular glutamate in the rat cerebral cortex across sleep and waking states. *J Neurosci*. 2009;29(3):620-629. doi:10.1523/JNEUROSCI.5486-08.2009

144. John J, Ramanathan L, Siegel JM. Rapid changes in glutamate levels in the posterior hypothalamus across sleep-wake states in freely behaving rats. *Am J Physiol Regul Integr Comp Physiol*. 2008;295(6):R2041. doi:10.1152/AJPREGU.90541.2008

145. Gaus SE, Strecker RE, Tate BA, Parker RA, Saper CB. Ventrolateral preoptic nucleus contains sleep-active, galaninergic neurons in multiple mammalian species. *Neuroscience*. 2002;115(1):285-294. doi:10.1016/S0306-4522(02)00308-1

146. Szymusiak R, McGinty D. Hypothalamic regulation of sleep and arousal. *Ann N Y Acad Sci*. 2008;1129:275-286. doi:10.1196/ANNALS.1417.027

147. España RA, Berridge CW. Organization of noradrenergic efferents to arousal-related basal forebrain structures. *Journal of Comparative Neurology*. 2006;496(5):668-683. doi:10.1002/CNE.20946

148. Thannickal TC, Moore RY, Nienhuis R, et al. Reduced number of hypocretin neurons in human narcolepsy. *Neuron*. 2000;27(3):469-474. doi:10.1016/S0896-6273(00)00058-1

149. Young GB. Coma. *The Neurology of Consciousness*. Published online January 1, 2009:137-150. doi:10.1016/B978-0-12-374168-4.00011-3

150. Brown EN, Purdon PL, van Dort CJ. General Anesthesia and Altered States of Arousal: A Systems Neuroscience Analysis. *Annu Rev Neurosci*. 2011;34:601. doi:10.1146/ANNUREV-NEURO-060909-153200

151. Hemmings HC, Akabas MH, Goldstein PA, Trudell JR, Orser BA, Harrison NL. Emerging molecular mechanisms of general anesthetic action. *Trends Pharmacol Sci*. 2005;26(10):503-510. doi:10.1016/J.TIPS.2005.08.006

152. Coursin DB, Coursin DB, Maccioli GA. Dexmedetomidine. *Curr Opin Crit Care*. 2001;7(4):221-226. doi:10.1097/00075198-200108000-00002

153. Saper CB, Scammell TE, Lu J. Hypothalamic regulation of sleep and circadian rhythms. *Nature 2005 437:7063*. 2005;437(7063):1257-1263. doi:10.1038/nature04284

154. Sherin JE, Elmquist JK, Torrealba F, Saper CB. Innervation of Histaminergic Tuberomammillary Neurons by GABAergic and Galaninergic Neurons in the Ventrolateral Preoptic Nucleus of the Rat. *Journal of Neuroscience*. 1998;18(12):4705-4721. doi:10.1523/JNEUROSCI.18-12-04705.1998

155. Lu J, Sherman D, Devor M, Saper CB. A putative flip–flop switch for control of REM sleep. *Nature 2006 441:7093*. 2006;441(7093):589-594. doi:10.1038/nature04767

156. Osaka T, Matsumura H. Noradrenergic inputs to sleep-related neurons in the preoptic area from the locus coeruleus and the ventrolateral medulla in the rat. *Neurosci Res*. 1994;19(1):39-50. doi:10.1016/0168-0102(94)90006-X

157. Huupponen E, Maksimow A, Lapinlampi P, et al. Electroencephalogram spindle activity during dexmedetomidine sedation and physiological sleep. *Acta Anaesthesiol Scand*. 2008;52(2):289-294. doi:10.1111/J.1399-6576.2007.01537.X

158. Akeju O, Pavone KJ, Westover MB, et al. A comparison of propofol- and dexmedetomidineinduced electroencephalogram dynamics using spectral and coherence analysis. *Anesthesiology*. 2014;121(5):978-989. doi:10.1097/ALN.0000000000000419

159. Bai D, Pennefather PS, MacDonald JF, Orser BA. The General Anesthetic Propofol Slows Deactivation and Desensitization of GABAA Receptors. *The Journal of Neuroscience*. 1999;19(24):10635. doi:10.1523/JNEUROSCI.19-24-10635.1999

160. Bowery NG, Hudson AL, Price GW. GABAA and GABAB receptor site distribution in the rat central nervous system. *Neuroscience*. 1987;20(2):365-383. doi:10.1016/0306-4522(87)90098-4

161. Akeju O, Westover MB, Pavone KJ, et al. Effects of Sevoflurane and Propofol on Frontal Electroencephalogram Power and Coherence. *Anesthesiology*. 2014;121(5):990-998. doi:10.1097/ALN.0000000000000436

162. Porjesz B, Almasy L, Edenberg HJ, et al. Linkage disequilibrium between the beta frequency of the human EEG and a GABAA receptor gene locus. *Proc Natl Acad Sci U S A*. 2002;99(6):3729-3733. doi:10.1073/PNAS.052716399/ASSET/95150EF6-43E5-4824-A8F2-AAB3EB3F54A6/ASSETS/GRAPHIC/PQ0527163002.JPEG

163. McCarthy MM, Brown EN, Kopell N. Potential Network Mechanisms Mediating Electroencephalographic Beta Rhythm Changes during Propofol-Induced Paradoxical Excitation. *Journal of Neuroscience*. 2008;28(50):13488-13504. doi:10.1523/JNEUROSCI.3536-08.2008

164. Lukatch HS, Kiddoo CE, MacIver MB. Anesthetic-induced Burst Suppression EEG Activity Requires Glutamate-mediated Excitatory Synaptic Transmission. *Cerebral Cortex*. 2005;15(9):1322-1331. doi:10.1093/CERCOR/BHI015

165. Akrawi WP, Drummond JC, Kalkman CJ, Patel PM. A comparison of the electrophysiologic characteristics of EEG burst-suppression as produced by isoflurane, thiopental, etomidate, and propofol. *J Neurosurg Anesthesiol*. 1996;8(1):40-46. doi:10.1097/00008506-199601000-00010

CHAPTER I

This chapter was previously published as:

Casey CP, Tanabe S, Farahbakhsh Z, et al. Distinct EEG signatures differentiate unconsciousness and disconnection during anaesthesia and sleep. *Br J Anaesth* Elsevier; 2022;

Distinct EEG Signatures Differentiate Unconsciousness and Disconnection During Anaesthesia and Sleep

Cameron P. Casey[1], Sean Tanabe[1], Zahra Farahbakhsh[1], Margaret Parker[1], Amber Bo[1], Marissa White[1], Tyler Ballweg[1], Andrew Mcintosh[1], William Filbey[1], Yuri Saalmann[2], Robert A. Pearce[1], Robert D. Sanders[3-5]

1. Department of Anesthesiology, University of Wisconsin, Madison, USA.

2. Department of Psychology, University of Wisconsin, Madison, USA.

3. Specialty of Anaesthetics, University of Sydney, Camperdown, Australia

4. Department of Anaesthetics, Royal Prince Alfred Hospital, Camperdown, Australia

5. Institute of Academic Surgery, Royal Prince Alfred Hospital, Camperdown, Australia

Abstract

Background: How conscious experience becomes disconnected from the environment, or disappears, across arousal states remains a mystery. We sought to identify the neural correlates of sensory disconnection and unconsciousness using a novel serial awakening paradigm.

Methods: Volunteers were recruited to sedation with dexmedetomidine, propofol or natural sleep with high-density electroencephalogram (EEG)-monitoring, and serial awakenings to establish whether subjects were in states of disconnected consciousness or unconsciousness in the preceding 20s. Our primary outcome was the classification of conscious states by occipital delta power (0.5-4Hz). Secondary analyses included derivation (dexmedetomidine), and validation (sleep/propofol), studies of EEG signatures of conscious states.

Results: Occipital delta power differentiated disconnected and unconscious states for dexmedetomidine (area under the curve (AUC) for receiver operator characteristic 0.605 [95% CI 0.516, 0.694]) but not sleep/propofol (AUC 0.512 [95% CI 0.380, 0.645]). Distinct source localized signatures of sensory disconnection (AUC 0.999, [95% CI 0.9954, 1.0000]) and unconsciousness (AUC 0.972 [95% CI 0.9507, 0.9879]) were identified using Support Vector Machine classification of dexmedetomidine data. These findings generalized to sleep/propofol (validation dataset: sensory disconnection (AUC 0.743 [95% CI 0.6784, 0.8050]) and unconsciousness (AUC 0.622 [95% CI 0.5176, 0.7238])). We identified that sensory disconnection is associated with broad spatial and spectral changes. In contrast,

unconsciousness is associated with focal decreases in activity in anterior and posterior cingulate.

Conclusions: These findings pave the way for novel monitors of the anaesthetic state that can specifically characterize sensory disconnection and unconsciousness. These findings provide a novel lens through which to understand the biology of arousal.

Introduction

Understanding the neural correlates of sensory awareness and conscious experience remains an open problem of great clinical and scientific importance. Without this knowledge we are unable to adequately monitor the anaesthetic state, or diagnose disorders of consciousness, particularly when responsiveness to the environment is impaired[1–3]. Perhaps most intriguing are the mechanisms through which consciousness becomes disconnected from the physical world in dreaming; practically, an understanding of the mechanisms of sensory disconnection would inform the titration of anaesthetics, the development of therapies for insomnia and improve neurological diagnosis[4].

Prior research has made use of functional imaging technologies to study subjects who are sleeping or anaesthetized, contrasting baseline recordings with periods of putative "unconsciousness" to identify neural correlates of consciousness[5–9]. Such studies have yielded a variety of markers that have been ascribed to consciousness, however, their methodologies have confounded consciousness with responsiveness, making these results ambiguous. Unresponsive subjects may still be consciously aware of their environment or unaware of the environment but still having a conscious experience, e.g. dreaming[2,4,10]. Furthermore, anaesthetic studies that assign the label of "unconsciousness" to their data based solely on the dose of anaesthesia given suffer from the additional confound of drug concentration.

The limitations stated above have made it difficult to know which reported signatures are relevant to consciousness *per se*, i.e. the presence of phenomenological content, or specifically, perception of the external world. Serial awakening paradigms offer a way to tackle this problem. A prior study made use of this paradigm to distinguish between dreaming

consciousness and unconsciousness during sleep[11], implicating a "posterior hot zone"[12] of activity in the maintenance of consciousness. While this study made large improvements over previous experimental designs, the results were still limited in terms of external validity as the data were only derived under natural sleep conditions and they did not comment on the mechanisms of sensory disconnection. Attempts to define similar changes with sedatives have had insufficient data to contrast dreaming consciousness and unconsciousness[13].

Here, we combined the serial awakening paradigm with titration of sedatives and compare with natural sleep to probe for conserved, cross-state mechanisms of sensory disconnection and unconsciousness[4]. Additionally, we tested whether the neural correlates of consciousness solely included a posterior hot zone, as was previously reported. By collecting reports of sensory disconnection and unconsciousness across multiple conditions and drug concentrations, we present generalizable signatures of connectedness and consciousness.

Our primary outcome was chosen as a simple measure of brain activity over the "posterior hot zone", occipital delta power. *A priori* we also determined to conduct exploratory analyses to identify if superior markers of conscious state could be derived. Following the prior reports of a "posterior hot zone"[11,14], we conducted these secondary analyses in source space to obtain information on the regions involved in the different conscious states. We have previously hypothesized that perturbed noradrenergic signaling is a critical mechanism of sensory disconnection, hence we focused on dexmedetomidine (Dex). We also collected data on sleep and propofol (Prop), which we combined into a validation data set, on which we could test the generalizability of our findings.

Methods

Subjects and Drug Administration

Subjects were enrolled in the UNderstanding Consciousness Connectedness and Intra-Operative Unresponsiveness Study (UN-ConsCIOUS, NCT03284307). These participants are healthy volunteers with ages between 18 and 40 years old without prior contraindications to anaesthetics. The study was stopped prematurely due to the suspension of activity of the study due to the COVID-19 pandemic and the change of institution of the primary investigator (RDS). At that juncture, the primary dexmedetomidine dataset was complete. Data on ketamine was not included as conscious reports could not be obtained by serial awakening from unresponsive subjects. The sevoflurane arm was removed prior to suspending recruitment due to concerns over whether verbal reports would be intelligible through a facemask (no subjects were recruited to this arm).

Anaesthesia was administered, under the supervision of an anaesthetist, to achieve a series of stable drug plateaus throughout the visit. For dexmedetomidine, a rapid infusion of 3.0 μg $kg^{-1}hr^{-1}$ was initially administered over a 10-minute period followed by a 0.5 μg $kg^{-1}hr^{-1}$ maintenance infusion to achieve the first drug step. The second drug step was similarly achieved by a 10-minute infusion of 3.0 μg $kg^{-1}hr^{-1}$ followed by a 1.5 μg $kg^{-1}hr^{-1}$ maintenance infusion. Plasma dexmedetomidine concentration was estimated afterwards using pharmacokinetic-pharmacodynamic modeling[15,16]. Propofol administration was achieved using target-controlled infusion through the RUGLOOP (Ghent University, Gent, Belgium) according to the Schnider model[17]. The total duration of drug exposure was limited to 4 hours for each experiment.

Serial Wake Reports

Subjects were allowed to rest with their eyes closed for 2-10 minutes at a time during drug visits and 20-40 minutes at a time during sleep visits without researcher intervention. Each rest period was concluded by a researcher calling the participant's name and initiating a brief structured interview consisting of questions designed to assess if the participant had been having a conscious experience, directly prior to the name call, and if the experiences was connected to the environment through the senses (Fig. 1). Participant answers were evaluated by two members of the research team to code each wake reports as connected consciousness (CC; conscious awareness of the environment), disconnected consciousness (DC; a conscious experience but no awareness of the environment, like a dream), or unconscious (Unc; complete lack of experience). Both team members had to agree that a report could be unambiguously coded using the criteria in Fig. 1 for it to be included in analysis. Selected examples of subject reports available in Supplementary Figure 4. Importantly, if a subject was not rousable, they were not presumed unconscious and the attempted wakeup was excluded from analysis. Likewise, internally conflicting reports for which an unambiguous state could not be assigned were also excluded from analysis.

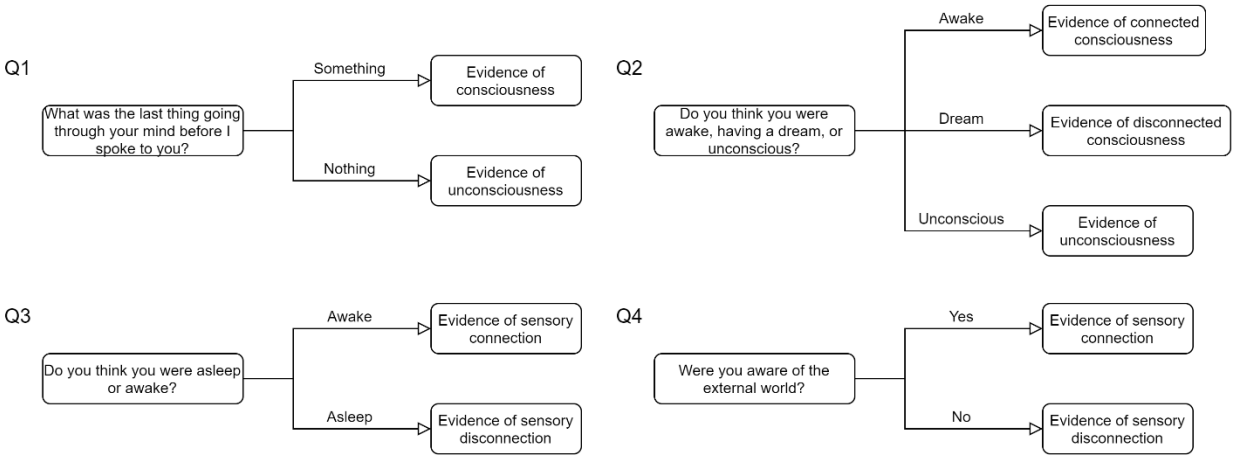

Figure 1. **Wake report questions.** Questions asked during wake reports to assess states of sensory connection and consciousness. Responses were evaluated by two members of the research team who had to agree on a state assignment of W, CC, DC, or Unc for a report to be included in the analyses.

EEG Data Acquisition

High-density EEG data were collected using a NA300 EGI system with 256-channel gel-caps. Electrodes were manually prepared with application of electrolyte electrode gel to achieve electrode impedances below 50 kΩ. Data are recorded using EGI's Net Station Acquisition 5.4 software.

All data processing was performed by a member of the research team, experienced in EEG analysis, while blinded to the assigned conscious state, using EEGLab[18]. Data were filtered between 0.1 and 55 Hz. Filtered data were then visually inspected for noisy channels and noisy epochs which were removed. Independent Components Analysis (ICA) were then computed using the InfoMax[19] algorithm and components dominated by eye movements or muscle artifacts were rejected. After these cleaning steps, data were average referenced and the last 20 seconds of data prior to the wake report was then segmented out for analysis. Sensor-space

power spectra were generated by computing the Welch power spectral density of the spline-based Laplacian transformed data[20].

Primary Outcome

Power spectral density in the Delta band (1-4 Hz) was averaged at electrode Oz and tested for differences between conscious states (DC vs CC and Unc vs DC) using linear mixed effects models (LMEMs) as implemented in the R lme4 library[21] (See *Statistical Methods* section below for more details on model specification). The predictive utility of our primary outcome was tested using empirical receiver operating characteristic (ROC) curves which were summarized by the area under the curve (AUC) with bootstrapped 95% confidence intervals.

Source Reconstruction

EEG data were imported into FieldTrip[22] and source reconstructed by frequency band using the eLORETA[23] algorithm. Frequency bands were specified as Slow Wave Activity (SWA; 0.5-1 Hz), Delta (1-4 Hz), Theta (4-8 Hz), Alpha (8-14 Hz), Beta (18-25 Hz), Gamma (28-55 Hz). An average brain model, taken from the SPM8 release (FieldTrip file cortex_20484.surf.gii) was used for the source model. The volume conductance model was a 3 shell Boundary Element Method (BEM) model with conductances of 0.33, 0.0041, and 0.33 for skin, skull, and brain respectively (FieldTrip file standard_bem.mat).

Statistical Methods

Source reconstructed data were analyzed voxel-wise using LMEMs, in which the log-transformed power at each voxel was regressed on wake state and predicted plasma drug concentration with a by-subject random intercepts and by-subject random slopes for predicted

plasma drug concentration to account for non-independence of repeated measures from the same subject. It is important to note that for all analyses involving the Sleep dataset, the baseline W coded data were used as the equivalent of CC as the sleep condition does not have a W/CC distinction equivalent to that of the Dex or Prop conditions. Wake state was treated as a dummy-coded variable to perform pairwise state contrasts. Drug concentration was treated as a continuous covariate to adjust for the non-specific effects of anaesthesia that are not relevant to connectedness or consciousness. P-values were generated using Type III ANOVA with Kenward-Roger degrees of freedom for the F-test. To correct for multiple comparisons, p-values corresponding to voxels within the same frequency band were adjusted using the Benjamini-Hochberg False Discovery Rate procedure. To ascribe anatomical labels to the significant results we masked the significant voxels against the automated anatomical labeling (AAL) atlas[21] from SPM8.

Machine Learning

Machine learning was performed separately for classification of DC vs CC and Unc vs DC wake reports, using Dex as a training set and Prop/Sleep as a test set. For the DC vs CC contrast, the source activation at each voxel across all frequency bands was included from training. These data were log transformed to improve normality and subjected to principal components analysis (PCA) to reduced dimensionality of the highly collinear data. The relative predictive value of each PC for classification was calculated using the random forest Recursive Feature Elimination algorithm implemented in the R caret library[21]. PCs with mean decrease in accuracy values greater than 0 were retained as training features. The number of features retained in each machine learning model are outlined in Supplementary Table 2.

Ensemble machine learning was performed by bootstrap aggregating 500 linear SVMs. To address the unbalanced nature of the training classes, balanced bootstrap samples were used to train each model. The *n* for each class was chosen as 50, the *n* of the smaller class (CC), i.e. each model was trained with a bootstrapped sample of 50 CC and 50 DC data points. The model cost tuning parameter was allowed to vary across models and was chosen from the range [0.1,0.25,0.5,1,2,4,8,16,32] based on the model that produced the largest kappa statistic. When applying the ensemble learner to the test set, each SVM produced a probability score for the DC/CC classification which were averaged across all 500 models and the class with the larger probability was chosen as the predicted class for the ensemble. See Fig. 4C for a graphical representation of the machine learning process. The machine learning process for the Unc vs DC classification problem was identical to that used for DC vs CC, except that only seed voxels for the Beta and Delta bands from the significant ROIs of the Beta/Delta ratio (Fig. 5B) were included. For quantification of SVM ensemble performance we calculated 95% confidence intervals for the AUC of each ROC and compared against chance levels of 0.5.

Results

States of consciousness show similar scalp level signatures across conditions.

To disentangle the constructs of connectedness and consciousness, we recruited healthy volunteers to record high-density EEG (256 channel) under anaesthesia with dexmedetomidine (Dex, n = 20), propofol (Prop, n = 6), or during natural sleep (n = 15). Anaesthesia was titrated to multiple drug steps to promote increasing somnolence (Fig. 2A). A total of 398, 104, and 202 wake-ups were attempted for Dex, Prop, and Sleep conditions

respectively. However, due to instances in which subjects did not give a verbal report or the report given was ambiguous, not all attempted wake-ups resulted in usable data. The final

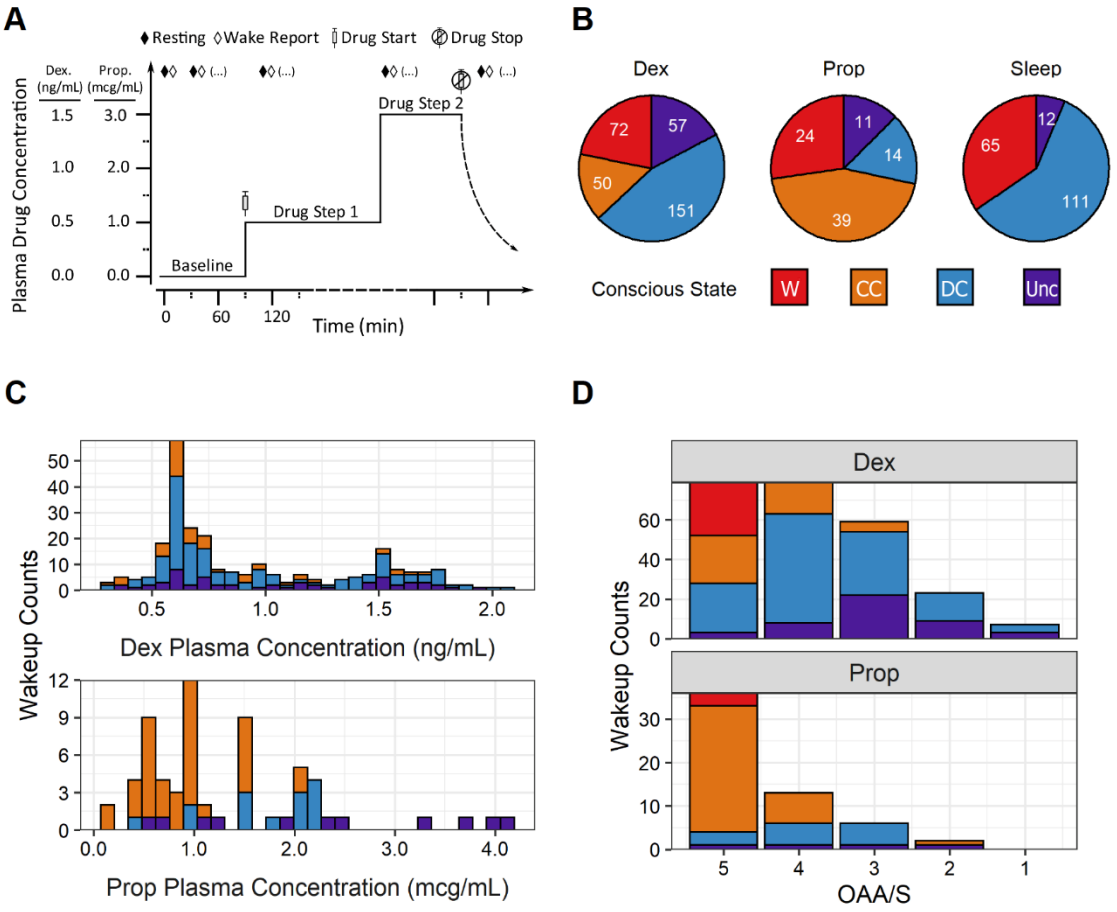

Figure 2. Drug administration and wake report collection. (A), Hypothetical drug dosing diagram illustrating experimental paradigm for serial wake reports, which results in multiple wake reports per subject. (B), Distribution of analyzed wake reports by state in each experimental condition. States coded as W (wake; connected consciousness pre-drug), CC (connected consciousness with drug), DC (disconnected consciousness), or Unc (unconsciousness). Additional wake-ups were attempted (Att) but the data were unusable due to either no verbal response (NVR) or ambiguous answers that could not be confidently classified (Amb). The final analyzed counts by condition consisted were: (Dex) $330 = 398_{Att} - 12_{NVR} - 56_{Amb}$, (Prop) $88 = 104_{Att} - 7_{NVR} - 9_{Amb}$, (Sleep) $188 = 202_{Att} - 2_{NVR} - 12_{Amb}$. (C), Distribution of wake states across modeled plasma drug concentrations of Dex. and Prop. (D), Distribution of wake states by level of responsiveness as assessed by the O/AAS.

counts of wake-ups analyzed were 330 for Dex, 88 for Prop, and 188 for Sleep (see Fig. 2B legend for additional details). Frequency of

each reported state (W, CC, DC, or Unc) varied across experimental conditions (Fig. 2B), predicted plasma drug concentration (Fig. 2C), and responsiveness (Fig. 2D), however, each state was observed, to some degree, across each of these variables.

Spectral analysis of the EEG data from the 20 seconds before each wake report showed similar (though not identical) patterns of activity in W/CC states and DC/Unc states (Fig. 3A). The most notable qualitative differences between connected (W/CC) and disconnected (DC) or unconscious (Unc) states being reduced high frequency power (16-55 Hz) and posterior alpha power (9-12 Hz) and increased low frequency power (0.5-9 Hz).

Primary Outcome

Occipital delta power showed a linear relationship with conscious state (Fig. 3B). Using a linear mixed effect model with by-subject random effects (intercept and predicted plasma drug concentration) and fixed effects for conscious state and predicted plasma drug concentration, we compared the effect of conscious state on Delta power using DC as the reference condition. Delta power during CC was, on average, 65.2% of that recorded during DC ($p < 0.001$) while Unc Delta power was, on average, 124.2% of that recorded during DC ($p = 0.030$) (Fig. 3C, Supplementary Table 1). Occipital Delta power showed a weak classification for disconnected and unconscious states (Fig. 3D), the primary outcome, for Dex (AUC for the ROC 0.605 [95% CI 0.516, 0.694]). However, this effect was not evident for Sleep/Prop (AUC 0.512 [95% CI 0.380, 0.645]), hence this marker is unlikely to represent a reliable marker of conscious state for

clinical application. To further interrogate the signatures of connectedness and consciousness, we source reconstructed the EEG data, allowing us to investigate the anatomical sources of spectral changes.

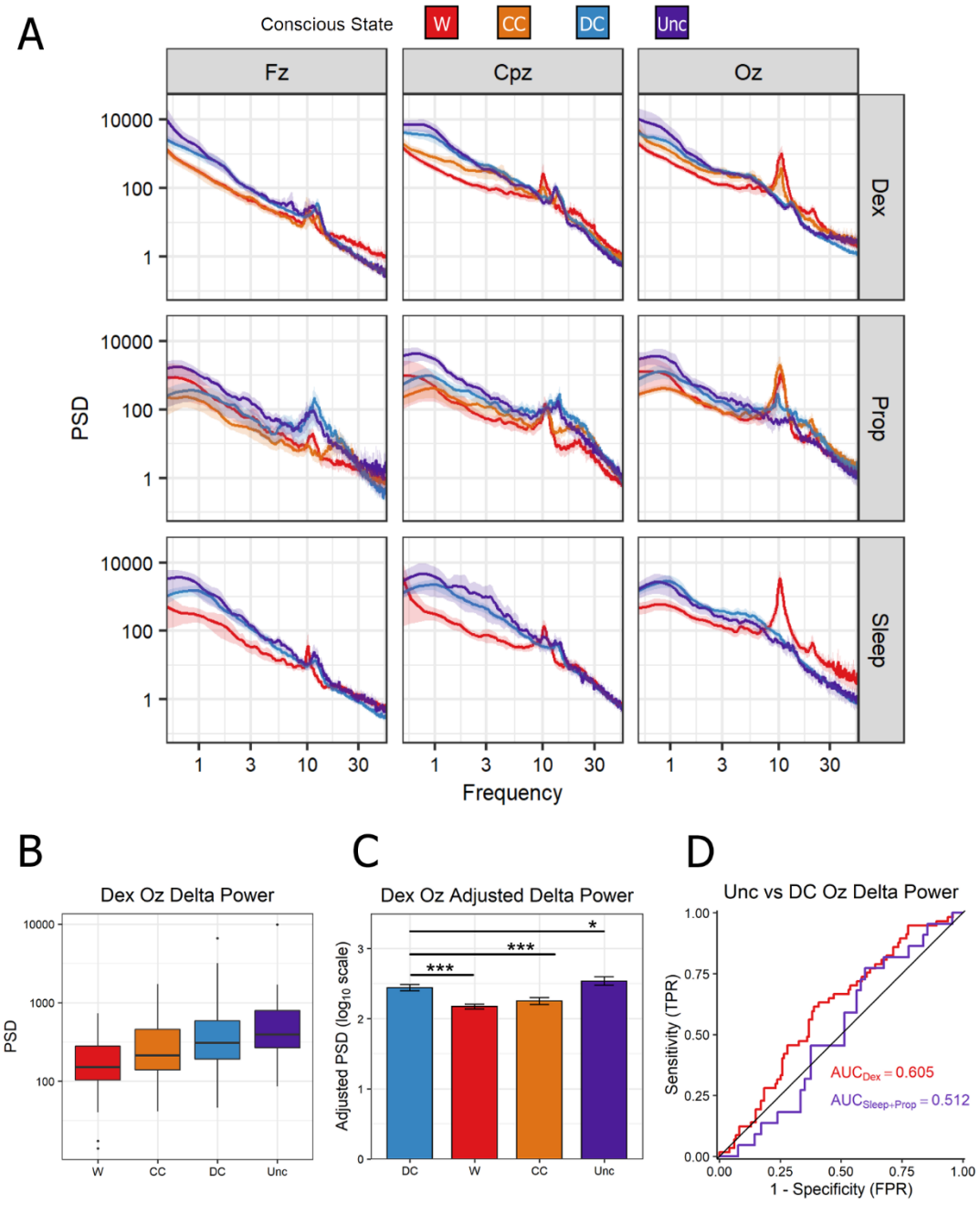

(See next page for figure legend.)

Figure 3. Scalp level power analysis. (A) Scalp level power spectral density (PSD) by frequency (average reference, Laplacian transformed) at canonical electrodes Fz (frontal, midline), Cpz (central, midline), and Oz (occipital, midline) across conditions. Experimental conditions show similar patterns of activity with a notable loss of occipital Alpha (~10 Hz) in DC and Unc relative to W and CC, as well as an increase in low frequency (0.5-9 Hz), activity and decrease in high frequency activity (16-55 Hz) across electrodes. (B) Box plots comparing mean Delta PSD at Oz across wake-ups in the Dex condition. (C) Bar plot of the adjusted Delta PSD values (on a $\log_{10}$ scale) from a LMEM contrasting DC against all other states while controlling for predicted plasma drug concentration and subject specific effects. Error bars represent bootstrapped standard errors. * $p < 0.05$, *** $p < 0.001$ (D) Empirical ROC curves for classifying Unc vs DC in Dex (red) and Sleep/Prop (purple). Black line represents chance performance (AUC = 0.5).

Disconnected consciousness differs from connected consciousness across multiple frequency bands across cortex.

Our primary motivation in this work was to investigate generalizable signatures of connectedness and consciousness. In-line with this goal, we adopted a machine learning analytical approach in which we divided the data into a discovery set with Dex and a generalizability test set (Prop and Sleep). We chose the α_2 adrenoceptor agonist, Dex, for the discovery dataset to identify whether perturbed noradrenergic signaling may offer a conserved mechanism of sensory disconnection, based on reduced locus coeruleus activity in the paradigmatic disconnected state of sleep[24] and the characteristics of this neuromodulator to provide gain across the sensory cortical hierarchy[25]. Within the Dex discovery set, we performed a source space voxel-wise analysis making use of linear mixed effects models (LMEMs) to predict spectral power as a function of wake report state while adjusting for predicted plasma drug concentration, overcoming a major limitation of prior studies of anaesthesia that did not dissect non-specific drug effects from conscious state.

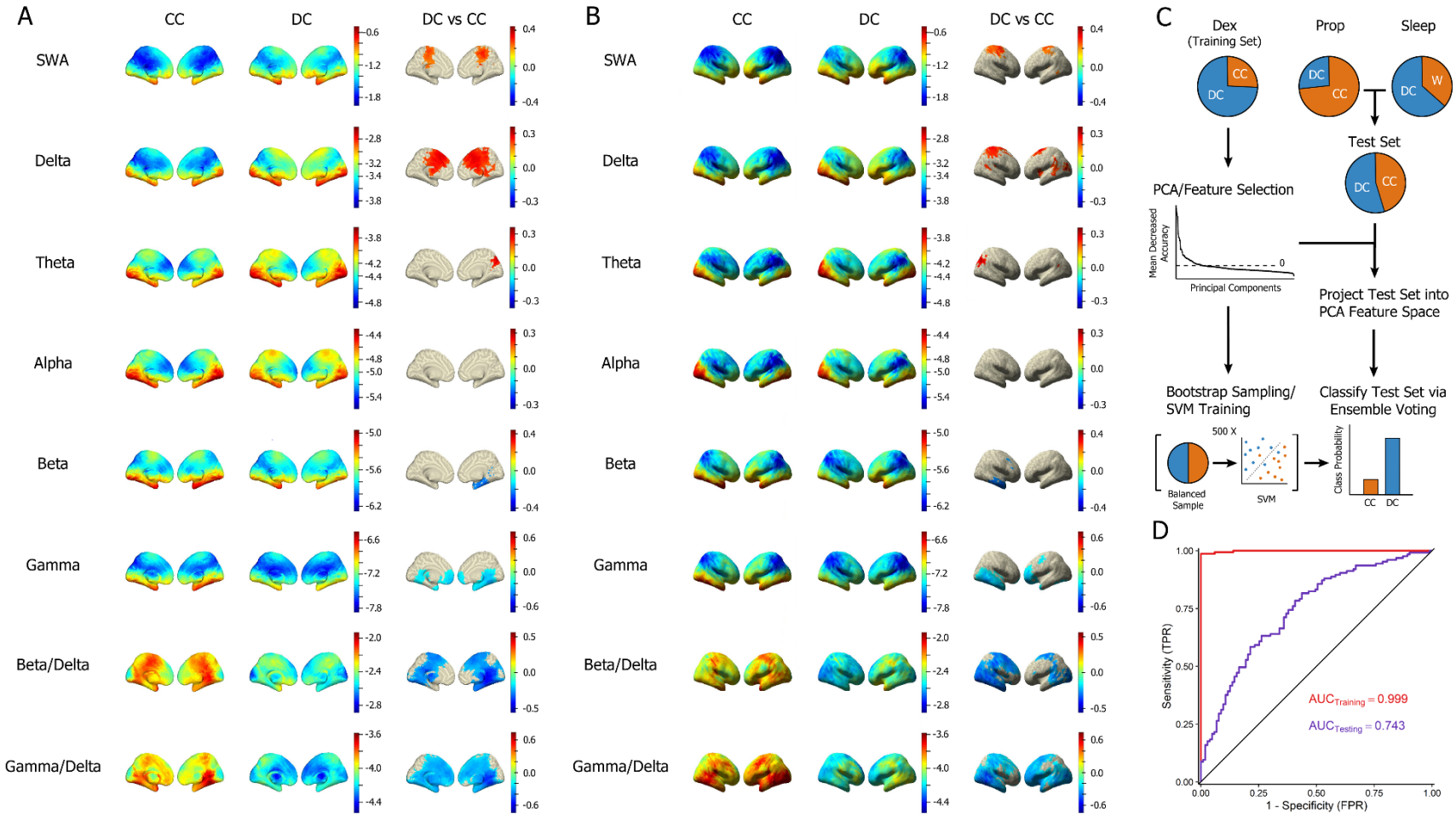

(See next page for figure legend.)

Figure 4. Disconnected consciousness compared to connected consciousness across frequency bands. (A) Medial view of voxel-wise predicted power (log_{10} scale color coded) from LMEMs for CC (left column) and DC (middle column) across frequency bands. Right column shows differences between DC and CC states for all significant voxels after FDR correction for multiple comparisons. (B) Same as in A but showing lateral view. (C) Depiction of machine learning approach used to classify DC and CC data. Briefly, Dex. data were used as a training set and subjected to PCA for dimensionality reduction prior to feature selection. The Prop. and Sleep test data were projected into the same feature space. Training features were used to generate an ensemble of 500 SVMs, each trained using a different subset of the training data, bootstrap sampled with balanced class representation. The ensemble was applied to the test data by averaging the probability scores of all 500 models and selecting the class with the higher average probability. (D) ROC curves for the ensemble learner, training using all bands except Alpha, applied to the training set and test set with AUC quantification. Black line represents chance performance (AUC = 0.5).

Our modeling approach highlighted significant differences in cortical rhythms in the slow wave activity (SWA), Delta, Theta, Beta, and Gamma bands (Fig. 4A-B). SWA and Delta activity was significantly greater ($p < 0.05$, FDR corrected) in fronto-medial cortex and surrounding the superior portion of the central sulcus in the DC condition. We also observed a small posterior cluster in the right hemisphere of increased Theta activity, in DC compared to CC, consistent with cuneus/precuneus. In contrast to the increased lower frequencies, the higher Beta and Gamma frequencies showed significant decreases in DC relative to CC. Beta showed decreases in the right temporal lobe while Gamma decreased bilaterally in both frontal and temporal lobes. Prior research defined a posterior hot zone of “conscious” activity based on reductions in high frequency power and increased low frequency power in unconsciousness relative to dreaming in sleep[11]. Hence, we tested the specificity of this marker by operationalizing it as a Beta/Delta ratio or a Gamma/Delta ratio. Conceptually, the ratio of high frequency to low frequency activity may represent how active an area of cortex is, given that cerebral metabolism is positively correlated with high frequency rhythms and negatively

correlated with low frequencies [26,27]. Notably, both ratios demonstrated more wide spread changes in DC vs CC than any of their constituent frequency bands.

We further investigated the predictive utility and generalizability of these power bands by using them as predictors in a machine learning classifier of sensory disconnection. We trained an ensemble of 500 support vector machines (SVMs) to classify the Dex DC and CC data, using all frequency bands except Alpha (which was omitted due to having no significant effects in the DC vs CC contrast), and tested its performance on the Prop and Sleep data (Fig. 4C). The ensemble had near perfect performance within the training set (AUC 0.999 [95% CI 0.9954, 1.0000]) and performed well above chance levels in the test set (AUC 0.743 [95% CI 0.6784, 0.8050]) demonstrating generalizability of the electrophysiological signatures of disconnection observed under Dex (Fig. 4D). Additional inclusion of the Alpha band did not substantially influence the model (Supplementary Figure 3A).

Unconsciousness differs from disconnected consciousness in Beta/Delta activity across cingulate cortex

In contrast to the broad spectral changes observed when contrasting DC and CC states, the differences between Unc and DC were much more specific. Unc demonstrated significant reductions in Beta/Delta ratio in a bilateral set of medial anterior and posterior voxels, as well as a lateral left hemispheric parietal cluster (Fig. 5A). These significant regions correspond with anterior cingulate cortex (ACC), middle and posterior cingulate cortex (MCC & PCC), and left supramarginal gyrus respectively. To test the generalizability of these clusters as markers of unconsciousness, we defined regions of interest (ROIs) as the average activity of all voxels

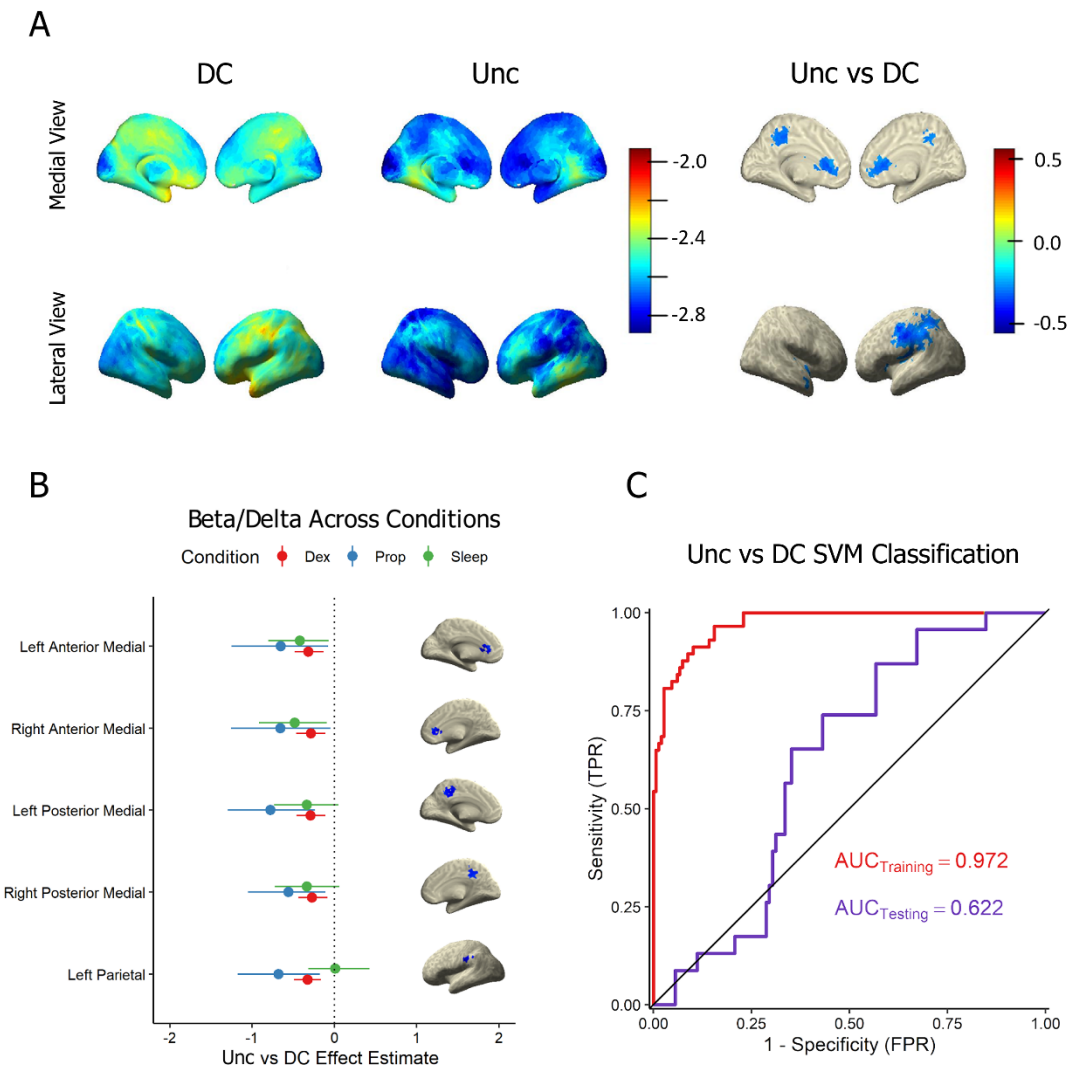

Figure 5. Unconsciousness compared to disconnected consciousness by Beta/Delta ratio. (A) Voxel-wise predicted power (log_{10} scale color coded) from LMEMs for DC (left column) and Unc (middle column) using Beta/Delta ratio. Right column shows differences between Unc and DC states for all significant voxels after FDR correction for multiple comparisons. (B) Unc vs DC effect estimates of Beta/Delta activity with bootstrapped 95% confidence intervals comparing experimental conditions within select ROIs. Anterior medial and posterior medial ROIs shows very similar effects across all three conditions. The Left parietal ROI was consistent between Dex and Prop but failed to generalize in Sleep data. (C) ROC curves for the ensemble learner, training using Beta/Delta activity in the five ROIs shown in c, applied to the training set and test set with AUC quantification. Black line represents chance performance (AUC = 0.5).

within 10 mm around the centroid of each cluster observed in the Dex dataset (Supplementary Table 3). Modeling the Beta/Delta power at these ROIs from the independent Prop and Sleep

data showed strikingly similar results to the Dex data (Fig. 5B, Supplementary Table 4). The one exception being the left parietal ROI, which was consistent for Dex and Prop but not for Sleep. Beta/Delta power within the anterior and posterior medial clusters, during Unc, ranged from 16.7 -53.2% of that recorded during DC (see Supplementary Table 4 for specific percentages in each cluster and condition). The non-significant results from the contrast of Unc and DC can be found in Supplementary Figure 2.

We again applied our ensemble SVM machine learning approach to these significant ROIs using the same methodology as described for the DC vs CC classification (Fig. 4C). The exception being that for this model we only trained our model using the Beta/Delta activity from voxels that were included as part of the ROIs, i.e. the same voxels shown in Fig. 5B. Again, the ensemble performed nearly perfectly within the training set (AUC 0.972 [95% CI 0.9507, 0.9879]), but also performed significantly above chance levels in the independent Prop and Sleep test set (AUC 0.622 [95% CI 0.5176, 0.7238]) (Fig. 5C). These significant results again support the generalizability and predictive utility of our findings in identifying unconsciousness under variable conditions. Because the left parietal ROI was not significant in the sleep condition, we performed a sensitivity analysis in which the ensemble was trained using only the four medial ROIs that were consistent across all conditions. This model performed comparably to the model with all five ROIs (AUC 0.635 [95% CI 0.5158, 0.7478]) (Supplementary Figure 3B).

Discussion

Diffuse increases in Delta and SWA, as well as wide spread suppression of Gamma and Beta bands, have been previously associated with anaesthetics and non-REM sleep[5,28–31]. Unfortunately, due to lack of subjective reports, these markers have often been assumed to be

markers of unconsciousness. Our data suggest that these broad spectral changes are more accurately described as markers of sensory disconnection, while more focal changes within cingulate cortex indicate loss of consciousness. However, the simple marker of occipital delta power did not show adequate classification of conscious state across anaesthetics and sleep.

The PCC is a core node of the default mode network (DMN), is highly active during autobiographical memory recall and introspection and has been implicated in a posterior hot zone proposed to represent the neural correlates of consciousness[12,32,33]. The ACC is also part of the anterior DMN[34,35] and has been proposed to be a key node supporting consciousness in the Global Neuronal Workspace model[36,37]. Both regions have previously been associated with deficits in consciousness individually[32,38]. Our data suggest that a both anterior and posterior cingulate regions of the DMN are critical for consciousness, challenging the recent notion of a "posterior hot zone"[6]. Moreover, recent fMRI work has shown reductions in DMN activation during behavioral unresponsiveness for multiple anaesthetics as well as unresponsive wakefulness syndrome, and a recent PET study identified reduced activity in ACC and PCC in unresponsive anaesthetized and sleeping subjects[13,39]. However, due to the limitations of responsiveness measurements, the authors were unable to conclusively say that these reductions were indicative of unconsciousness *per se*, as opposed to disconnected or covert consciousness. Our data build on this work by showing that reduced activity in these DMN nodes is associated with unconsciousness *per se*.

Notably our work is a significant advance on prior work as we disentangle disconnected conscious-dream states from unconsciousness[13]. Furthermore, many prior studies that claimed to study consciousness, used unresponsiveness as a marker of unconsciousness. We overcome

this substantial limitation as we used patient report to verify conscious state. These prior studies also ignored the confounding induced by changing drug concentrations to induce unresponsiveness. We have specifically adjusted for changes in pharmacological concentrations in our models, to remove non-specific drug effects from our analyses and focus our results on the change in conscious state.

Potential limitations in this study stem from our dependence on subjective reports as the "ground truth" of a subject's internal state. It is impossible to rule out subject error in reporting their state of consciousness. This is a substantial limitation to all present attempts to study consciousness and a primary motivation for the current study. Experiments with pharmacological interventions, such as our own, also run the risk of increasing self-report error due to memory interference. We reason that miscoded datapoints due to report error are only likely to increase the variance in our LMEMs which could lead to more false negative results but not false positives. Similarly, such miscoded datapoints would be expected to lower the estimated accuracy of our machine learning classifiers. Hence we believe that, if such errors are present, results that achieve statistical significance in spite of them are certainly robust.

We also acknowledge the limited spatial specificity of EEG technology. In principle this adds uncertainty to the anatomical sources of our statistical findings. However, the overlap with prior findings using other modalities, e.g. PET and fMRI, gives us confidence in these results, though these prior studies could not distinguish disconnected conscious and unconscious states.

Our findings provide evidence that sensory disconnection and unconsciousness have distinct electrophysiological signatures that are conserved across pharmacological and endogenous states. Furthermore, we find that sensory disconnection is accompanied by wide spread alterations in electrophysiological activity across many frequency bands while loss of consciousness is associated with a much more specific reduction in activity within anterior and posterior cingulate. This research is an important step in disentangling and quantifying the constructs of connectedness and consciousness which is necessary for progressing our understanding of these fundamental phenomena and our ability to objectively measure them for clinical and research purposes.

Author Contributions

RDS initiated the study and designed the experiments. The study was managed by RDS and RAP. CPC, ZF, ST, MP, AB, MW, TB, AM, and RDS collected EEG and wake report data. WF and RDS administered the anaesthesia for the Dex and Prop experiments. CPC, YS, RAP, and RDS designed the data analytic approaches which were conducted by CPC. CPC and RDS prepared the manuscript

Acknowledgments

We are grateful to advice from Prof Giulio Tononi, Dr. Brady Riedner, Dr David Plante and Dr. Melanie Boly (University of Wisconsin, USA) when setting up this project and for loan of the EEG equipment. We acknowledge Prof Michel MRF Struys, MD, PhD, FRCA, and Dr Tom De Smet, PhD from The University Medical Center Groningen, The Netherlands and Ghent University, Belgium for their assistance with RUGLOOP and infusion pump technology. In

addition, Prof Anthony Absalom (The University Medical Center Groningen, The Netherlands) provided advice on pharmacokinetic modelling of dexmedetomidine concentrations.

Funding

This work was supported by the Department of Anesthesiology at the University of Wisconsin and by NIH NIND 1R01NS117901-01.

References

1. Boly M, Sanders RD, Mashour GA, Laureys S. Consciousness and responsiveness: Lessons from anaesthesia and the vegetative state. *Curr Opin Anaesthesiol*. 2013;26(4):444-449. doi:10.1097/ACO.0b013e3283628b5d
2. Kotsovolis G, Komninos G. Awareness during anesthesia: How sure can we be that the patient is sleeping indeed? *Hippokratia*. 2009;13(2):83-89.
3. Cascella M. Mechanisms underlying brain monitoring during anesthesia: Limitations, possible improvements, and perspectives. *Korean J Anesthesiol*. 2016;69(2):113-120. doi:10.4097/kjae.2016.69.2.113
4. Sanders RD, Tononi G, Laureys S, Sleigh JW. Unresponsiveness ≠ unconsciousness. *Anesthesiology*. 2012;116(4):946-959. doi:10.1097/ALN.0b013e318249d0a7
5. Purdon PL, Pierce ET, Mukamel EA, et al. Electroencephalogram signatures of loss and recovery of consciousness from propofol. *Proc Natl Acad Sci U S A*. 2013;110(12). doi:10.1073/pnas.1221180110
6. Noreika V, Jylhänkangas L, Móró L, et al. Consciousness lost and found: Subjective experiences in an unresponsive state. *Brain Cogn*. 2011;77(3):327-334. doi:10.1016/j.bandc.2011.09.002
7. Ku SW, Lee U, Noh GJ, Jun IG, Mashour GA. Preferential Inhibition of Frontal-to-Parietal Feedback Connectivity Is a Neurophysiologic Correlate of General Anesthesia in Surgical Patients. Ward LM, ed. *PLoS One*. 2011;6(10):e25155. doi:10.1371/journal.pone.0025155
8. Lee U, Ku S, Noh G, Baek S, Choi B, Mashour GA. Disruption of frontal-parietal communication by ketamine, propofol, and sevoflurane. *Anesthesiology*. 2013;118(6):1264-1275. doi:10.1097/ALN.0b013e31829103f5

9. Långsjö JW, Alkire MT, Kaskinoro K, et al. Returning from oblivion: Imaging the neural core of consciousness. *Journal of Neuroscience*. 2012;32(14):4935-4943. doi:10.1523/JNEUROSCI.4962-11.2012

10. Sanders RD, Gaskell A, Raz A, et al. Incidence of Connected Consciousness after Tracheal Intubation: A Prospective, International, Multicenter Cohort Study of the Isolated Forearm Technique. *Anesthesiology*. 2017;126(2):214-222. doi:10.1097/ALN.0000000000001479

11. Siclari F, Baird B, Perogamvros L, et al. The neural correlates of dreaming. *Nat Neurosci*. 2017;20(6):872-878. doi:10.1038/nn.4545

12. Boly M, Massimini M, Tsuchiya N, Postle BR, Koch C, Tononi G. Are the neural correlates of consciousness in the front or in the back of the cerebral cortex? Clinical and neuroimaging evidence. *Journal of Neuroscience*. 2017;37(40):9603-9613. doi:10.1523/JNEUROSCI.3218-16.2017

13. Scheinin A, Kantonen O, Alkire M, et al. Foundations of human consciousness: Imaging the twilight zone. *Journal of Neuroscience*. 2021;41(8):1769-1778. doi:10.1523/JNEUROSCI.0775-20.2020

14. Boly M, Massimini M, Tsuchiya N, Postle BR, Koch C, Tononi G. Are the neural correlates of consciousness in the front or in the back of the cerebral cortex? Clinical and neuroimaging evidence. *Journal of Neuroscience*. 2017;37(40):9603-9613. doi:10.1523/JNEUROSCI.3218-16.2017

15. Bailey JM, Shafer SL. A Simple Analytical Solution to the Three-Compartment Pharmacokinetic Model Suitable for Computer-Controlled Infusion Pumps. *IEEE Trans Biomed Eng*. 1991;38(6):522-525. doi:10.1109/10.81576

16. Hannivoort LN, Eleveld DJ, Proost JH, et al. Development of an Optimized Pharmacokinetic Model of Dexmedetomidine Using Target-controlled Infusion in Healthy Volunteers. *Anesthesiology*. 2015;123(2):357-367. doi:10.1097/ALN.0000000000000740

17. Schnider TW, Minto CF, Gambus PL, et al. The influence of method of administration and covariates on the pharmacokinetics of propofol in adult volunteers. *Anesthesiology*. 1998;88(5):1170-1182. doi:10.1097/00000542-199805000-00006

18. Delorme A, Makeig S. EEGLAB: An open source toolbox for analysis of single-trial EEG dynamics including independent component analysis. *J Neurosci Methods*. 2004;134(1):9-21. doi:10.1016/j.jneumeth.2003.10.009

19. Bell AJ, Sejnowski TJ. An information-maximization approach to blind separation and blind deconvolution. *Neural Comput*. 1995;7(6):1129-1159. doi:10.1162/neco.1995.7.6.1129

20. Welch PD. The Use of Fast Fourier Transform for the Estimation of Power Spectra: A Method Based on Time Averaging Over Short, Modified Periodograms. *IEEE Transactions on Audio and Electroacoustics*. 1967;15(2):70-73. doi:10.1109/TAU.1967.1161901

21. Rolls ET, Huang CC, Lin CP, Feng J, Joliot M. Automated anatomical labelling atlas 3. *Neuroimage*. 2020;206:116189. doi:10.1016/j.neuroimage.2019.116189

22. Oostenveld R, Fries P, Maris E, Schoffelen JM. FieldTrip: Open Source Software for Advanced Analysis of MEG, EEG, and Invasive Electrophysiological Data. *Comput Intell Neurosci*. 2011;2011. doi:10.1155/2011/156869

23. Pascual-Marqui RD, Lehmann D, Koukkou M, et al. Assessing interactions in the brain with exact low-resolution electromagnetic tomography. *Philosophical Transactions of the Royal Society A: Mathematical, Physical and Engineering Sciences*. 2011;369(1952):3768-3784. doi:10.1098/rsta.2011.0081

24. Aston-Jones G, Bloom FE. Activity of norepinephrine-containing locus coeruleus neurons in behaving rats anticipates fluctuations in the sleep-waking cycle. *Journal of Neuroscience*. 1981;1(8):876-886. doi:10.1523/jneurosci.01-08-00876.1981

25. Sanders RD, Casey C, Saalmann YB. Predictive coding as a model of sensory disconnection: relevance to anaesthetic mechanisms. *Br J Anaesth*. 2021;126(1):37-40. doi:10.1016/j.bja.2020.08.017

26. Nishida M, Juhász C, Sood S, Chugani HT, Asano E. Cortical glucose metabolism positively correlates with gamma-oscillations in nonlesional focal epilepsy. *Neuroimage*. 2008;42(4):1275-1284. doi:10.1016/j.neuroimage.2008.06.027

27. Wisor JP, Rempe MJ, Schmidt MA, Moore ME, Clegern WC. Sleep slow-wave activity regulates cerebral glycolytic metabolism. *Cerebral Cortex*. 2013;23(8):1978-1987. doi:10.1093/cercor/bhs189

28. Brancaccio A, Tabarelli D, Bigica M, Baldauf D. Cortical source localization of sleep-stage specific oscillatory activity. *Scientific Reports 2020 10:1*. 2020;10(1):1-15. doi:10.1038/s41598-020-63933-5

29. Akeju O, Pavone KJ, Westover MB, et al. A comparison of propofol- and dexmedetomidineinduced electroencephalogram dynamics using spectral and coherence analysis. *Anesthesiology*. 2014;121(5):978-989. doi:10.1097/ALN.0000000000000419

30. Marzano C, Moroni F, Gorgoni M, Nobili L, Ferrara M, De Gennaro L. How we fall asleep: regional and temporal differences in electroencephalographic synchronization at sleep onset. *Sleep Med*. 2013;14(11):1112-1122. doi:10.1016/J.SLEEP.2013.05.021

31. Purdon PL, Sampson A, Pavone KJ, Brown EN. Clinical electroencephalography for anesthesiologists. *Anesthesiology*. 2015;123(4):937-960. doi:10.1097/ALN.0000000000000841

32. Vogt BA, Laureys S. Posterior cingulate, precuneal and retrosplenial cortices: Cytology and components of the neural network correlates of consciousness. *Prog Brain Res*. 2005;150:205-217. doi:10.1016/S0079-6123(05)50015-3

33. Koch C, Massimini M, Boly M, Tononi G. Neural correlates of consciousness: Progress and problems. *Nat Rev Neurosci*. 2016;17(5):307-321. doi:10.1038/nrn.2016.22

34. Buckner RL, Andrews-Hanna JR, Schacter DL. The brain's default network: Anatomy, function, and relevance to disease. *Ann N Y Acad Sci*. 2008;1124(1):1-38. doi:10.1196/annals.1440.011

35. Carter CS, Botvinick MM, Cohen JD. The contribution of the anterior cingulate cortex to executive processes in cognition. *Rev Neurosci*. 1999;10(1):49-57. doi:10.1515/REVNEURO.1999.10.1.49

36. Dehaene S, Kerszberg M, Changeux JP. A neuronal model of a global workspace in effortful cognitive tasks. *Proc Natl Acad Sci U S A*. 1998;95(24):14529-14534. doi:10.1073/pnas.95.24.14529

37. Mashour GA, Roelfsema P, Changeux JP, Dehaene S. Conscious Processing and the Global Neuronal Workspace Hypothesis. *Neuron*. 2020;105(5):776-798. doi:10.1016/j.neuron.2020.01.026

38. Qin P, Di H, Liu Y, et al. Anterior cingulate activity and the self in disorders of consciousness. *Hum Brain Mapp*. 2010;31(12):1993-2002. doi:10.1002/hbm.20989

39. Huang Z, Zhang J, Wu J, Mashour GA, Hudetz AG. Temporal circuit of macroscale dynamic brain activity supports human consciousness. *Sci Adv*. 2020;6(11):87-98. doi:10.1126/sciadv.aaz0087

CHAPTER II

This chapter is a draft of a manuscript currently being prepared for publication

Evaluating Putative Signatures of Consciousness in Anesthesia and Sleep Using Specific Definitions of Responsiveness, Connectedness and Consciousness

Cameron P. Casey*[1], Sean Tanabe[1], Zahra Z. Farahbakhsh[1], Margaret Parker[1], Amber Bo[1], Marissa White[1], Tyler Ballweg[1], Andrew Mcintosh[1], William Filbey[1], Matthew I. Banks[1], Yuri B. Saalmann[2], Robert A. Pearce[1], Robert D. Sanders*[3-5]

1. Department of Anesthesiology, University of Wisconsin, Madison, USA.

2. Department of Psychology, University of Wisconsin, Madison, USA.

3. Specialty of Anaesthetics & NHMRC Clinical Trials Centre, University of Sydney, Camperdown, Australia

4. Department of Anaesthetics, Royal Prince Alfred Hospital, Camperdown, Australia

5. Institute of Academic Surgery, Royal Prince Alfred Hospital, Camperdown, Australia

Abstract

Background: Understanding the neural correlates of consciousness remains an open problem with important ramifications for both theoretical understanding of consciousness as well as clinical applications. A substantial amount of work has previously been conducted to identify the neural correlates of consciousness, primarily based on electroencephalography, but also using other functional imaging methods. However, a major limitation in much of this work is the use of responsiveness as an index of consciousness. This methodological confound (responsiveness = consciousness) means that many reported "correlates of consciousness" might instead be correlates of responsiveness.

Methods: Here, we identified a collection of measures that were previously reported to be associated with unconsciousness, based on the assumption that unresponsive subjects are unconscious. Using electroencephalography data generated through the UN-ConsCIOUS (NCT03284307), we evaluated these putative correlates of consciousness across two different sedative conditions (dexmedetomidine and propofol) and natural sleep. Responsiveness data and subjective reports of conscious state were collected together with the electroencephalographic data, allowing us to 1) attempt to replicate prior findings related to responsiveness in an independent data set, and 2) evaluate the replicated findings for associations with consciousness *per se* and connectedness (sensory awareness).

Results: While many of the proposed markers were associated with consciousness *per se*, none was specific to consciousness alone – rather, each was also associated with connectedness. Of these markers, the spectral exponent and permutation entropy in the theta-beta range showed promise as measures that were significantly associated with consciousness across all three

experimental conditions. In addition, multiple markers showed no association with consciousness and were only associated with connectedness. Of the markers associated with connectedness, front-to-back normalized symbolic transfer entropy showed promise as the only measure to be significantly associated with connectedness in all three experimental conditions.

Conclusions: Our findings indicate that none of the proposed EEG-based neural correlates of consciousness correspond solely to either of the two underlying constructs (consciousness and connectedness). These results highlight the need for more conservative use of the term (un)consciousness, particularly when assessing unresponsive participants.

Introduction

Over the last several decades, advances in functional neuroimaging methodologies have enabled numerous investigations into the neural correlates of consciousness (NCCs)[1–19]. Identifying the neurobiological underpinnings of conscious experience would allow us to better understand the nature of consciousness and to develop better clinical tools for diagnosis/prognosis of disorders of consciousness (DoCs) as well as anesthetic monitoring[20–23]. In spite of the substantial amount of work that has been done in this domain, there is little consensus on the NCCs, and objective monitoring of consciousness remains an outstanding challenge in clinical research and consciousness neuroscience.

In the pursuit of identifying the NCCs, anesthesia has emerged as a useful experimental tool for manipulating consciousness[24]. A common paradigm is to record brain activity in awake participants, sedate them until they become unresponsive, then wait for them to become

responsive again. The neural activity during the period of unresponsiveness is then compared against the awake data from before and after the period of sedated unresponsiveness. The trouble with such paradigms is that they conflate loss of consciousness with loss of responsiveness, despite these being dissociable qualities[21]. From a theoretical perspective, consciousness *per se* is the existence of any phenomenological experience, i.e. there is something 'that it is like' to be in that state[25]. Importantly, this means that consciousness is not limited to waking states, but can also exist when an individual is unaware of their environment, such as during dreaming sleep[21,26]. To address this, we employ the terminology of "connectedness" and "consciousness" where connectedness (dichotomous, connected or disconnected) refers to an individual's sensory awareness of the world around them, while consciousness (dichotomous, conscious or unconscious) refers to an individual's state of phenomenological experience, i.e. consciousness *per se*[21]. An unresponsive participant could be unconscious, experiencing disconnected consciousness, or even in a covert state of connected consciousness in which they remain aware but unwilling or unable to communicate. With this in mind, it becomes clear that using responsiveness as a proxy for consciousness results in major limitations for the interpretability of any supposed NCCs derived under this assumption. Such findings may truly represent consciousness, but they could also easily represent connectedness, responsiveness, or any combination of these factors.

An additional challenge is that some putative markers of consciousness have only been assessed within a single experimental condition, e.g. only in the context of a single anesthetic agent[7,13,27]. This lack of replication across multiple pharmacological and non-pharmacological conditions raises the possibility that some proposed markers of 'consciousness' are actually

drug-specific effects representing particular pharmacology as opposed to a conserved phenomenological state. In such cases, the marker would likely have little utility in settings beyond those in which that particular drug is being used.

In the current study, we have selected a set of 10 previously published resting state electroencephalography- (EEG) based NCCs derived using unresponsiveness as a proxy for

Marker	Category	References
Lempel-Ziv complexity	Complexity	Schartner et al. 2015. PLOS ONE. Schartner et al. 2017. Neuroscience of Consciousness.
Permutation Entropy	Complexity	Kreuzer et al. 2020. Anesthesiology., Liang et al. 2015. Frontiers in Computational Neuroscience.
Normalized Symbolic Transfer Entropy	Connectivity	Lee et al. 2013. Anesthesiology. Li et al. 2017. Frontiers in Systems Neuroscience.
Frontal alpha (power & connectivity)	Connectivity + Power Spectrum	Purdon et al. 2013. PNAS. Banks et al. 2020. NeuroImage. Blain-Moraes et al. 2015. Anesthesiology.
Delta-alpha 'peak-max' coupling	Cross-Frequency Coupling	Purdon et al. 2013. PNAS. Stephen et al. 2020. Scientific Reports.
Delta-theta phase amplitude coupling (MI)	Cross-Frequency Coupling	Tsai et al. 2019. Scientific Reports.
Alpha global efficiency	Graph Theory	Blain-Moraes et al. 2017. Frontiers in Human Neuroscience.
Delta local efficiency	Graph Theory	Lee et al. 2017. Scientific Reports. Lee et al. 2020. Scientific Reports.
Spectral edge frequency 95%	Power Spectrum	Nieuwenhuijs et al. 2002. Anesthesia and Analgesia. Sleigh et al. 1999. Anesthesia & Analgesia. Bruhn et al. 2003. Anesthesiology.
Spectral Exponent	Power Spectrum	Colombo et al. 2019. NeuroImage. Gao et al. 2017. NeuroImage.

Table 1. List of previously reported proposed markers of unconsciousness investigated in this paper along with categorization of how the marker is derived and references to prior work investigating each one. The categories of complexity, connectivity, cross-frequency coupling, graph theory, and power spectrum serve to orient readers, who may not be familiar with each of the individual metrics, to the type of information they are derived from.

unconsciousness (Table 1). These markers have been split into broad categories of complexity, connectivity, cross-frequency coupling, graph theory, and power spectrum measures in order to orient readers to the type of information each metric captures. Further details on the specifics of each metric may be found in Supplementary Methods and by consulting the original publications investigating these measures as NCCs. We computed these measures using previously published resting state data[28] in which participants were directly assessed for connectedness and consciousness using subjective reports and for responsiveness using the OAA/S scale. These data were also recorded under multiple pharmacological and non-pharmacological conditions: dexmedetomidine sedation, propofol sedation, and natural sleep. Using this information rich dataset, we first attempted to replicate the prior findings which associated each of these markers with loss of responsiveness. The measures that were successful in replicating their previously published effects within our study data were then tested for associations with consciousness and connectedness to determine if they are correlates of consciousness *per se* or if they represent sensory awareness (connectedness).

The current study improves upon prior research by 1) explicitly measuring subjective consciousness and awareness of the environment (connectedness), allowing us to determine if the proposed metrics are related to consciousness *per se* or awareness of the environment, and 2) evaluating proposed metrics in multiple conditions (dexmedetomidine, propofol, and sleep) to test the generalizability of each measure. In doing so, we rigorously test each metric based on its association with consciousness. These analyses disentangle consciousness from connectedness and drug-specific effects and, in doing so, expand our understanding of the NCCs.

Methods

Subjects and Study Visits

Subjects were enrolled in the UNderstanding Consciousness Connectedness and Intra-Operative Unresponsiveness Study (UN-ConsCIOUS, NCT03284307). All subjects provided written consent for each study visit and data were collected in accordance with a protocol approved by the institutional review board at the University of Wisconsin-Madison. The collection of these resting state data has previously been reported in detail[28] and will be summarized briefly here. Study participants were healthy volunteers between 18 and 40 years old without prior contraindications to anesthetics. Study visits consisted of high-density recordings prior to and during natural sleep or sedation with dexmedetomidine or propofol (Fig 1A). During sedation visits, anesthesia was administered, under the supervision of an anesthetist, to achieve a series of stable drug plateaus throughout the visit (see[28] for drug dosing. The total duration of drug exposure was limited to 4 hours for each visit.

Subjects were allowed to rest with their eyes closed for 2-10 minutes at a time during drug visits and 20-40 minutes at a time during sleep visits without researcher intervention. Each rest period was concluded by a researcher calling the participant's name and initiating a brief structured interview consisting of questions designed to assess if the participant had been having a conscious experience, directly prior to the name call, and if the experiences was connected to the environment through the senses. During sedation visits, responsiveness was also assessed at this time using the OAA/S scale. OAA/S data were not collected during sleep visits because the study space required the researchers to be in a separate room and initiate wakeups via a microphone system, hence tactile stimulation could not be used if the subject

failed to respond to vocal stimuli. Each wake report was evaluated by two members of the research team as wake (W; conscious awareness of the environment without drug), connected consciousness (CC; conscious awareness of the environment with drug), disconnected consciousness (DC; a conscious experience but no awareness of the environment, like a dream), or unconscious (Unc; complete lack of experience). Wake report questions and sample responses can be found in Casey et al[28]. Rationale for the distinction between W and CC is given in the *Data Analysis* section below.

EEG Data Acquisition and Processing

EEG data were collected using a NA300 EGI system with 256-channel gel-caps. Electrodes were manually prepared with application of electrolyte electrode gel to achieve electrode impedances below 50 kΩ. Data are recorded using EGI's Net Station Acquisition 5.4 software. All EEG processing was performed by a member of the research team, experienced in EEG analysis, while blinded to the assigned conscious state. Data were filtered between 0.1 and 55 Hz then visually inspected for noisy channels and noisy epochs which were removed. Independent Components Analysis (ICA) was computed and components dominated by eye movements or muscle artifacts were rejected. After these cleaning steps, data were average referenced and the last 20 seconds of data prior to the wake report was then segmented out for analysis.

Metric Calculations

Due to the large number of metrics being assessed in this paper, the specifics of how each one was calculated have been included as Supplemental Methods.

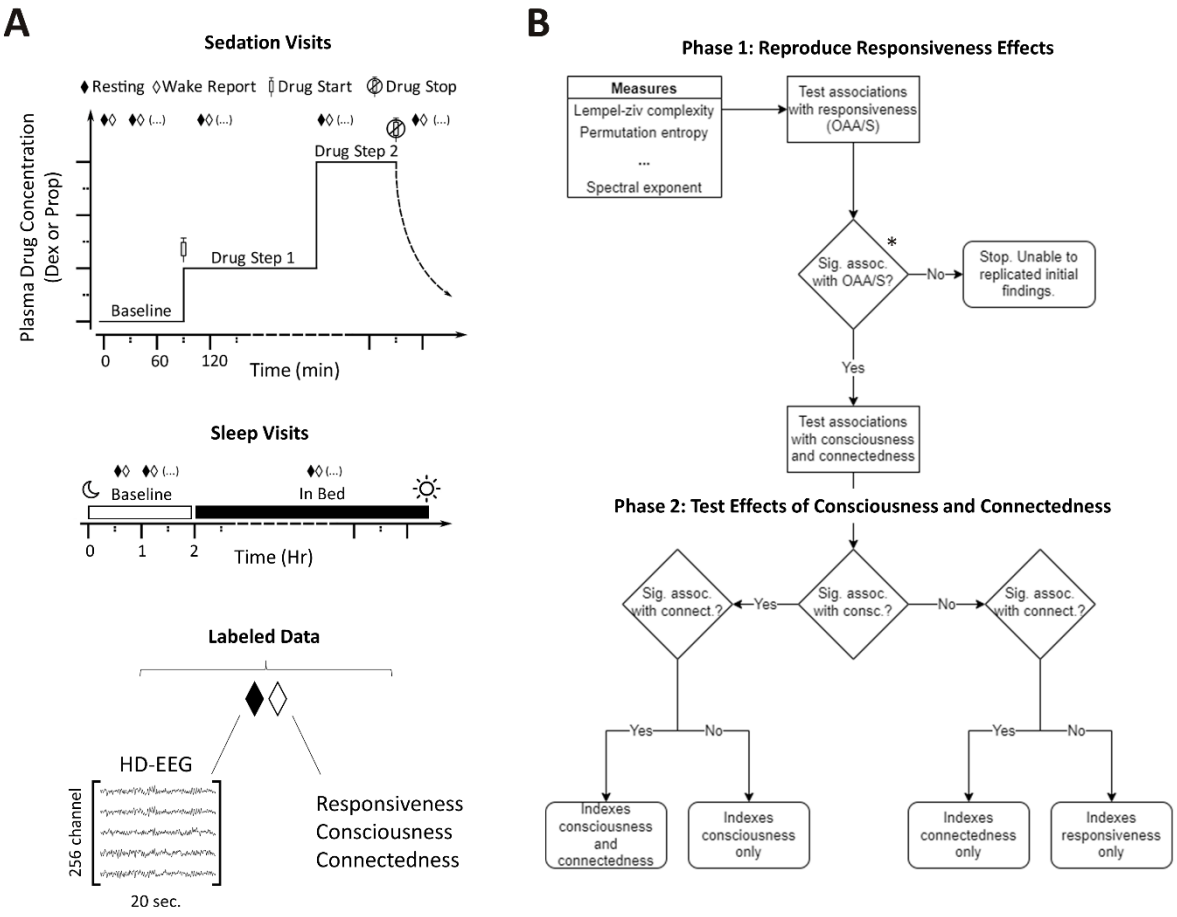

Figure 1. Data collection and analysis overview. A) Experimental design for data collection. Sedation visits consisted of EEG recordings before and during sedation with dexmedetomidine (Dex) or propofol (Prop). Increasing doses of drug were used over time to bias subjects towards deeper sedation levels. Sleep visits followed the same general framework but occurred overnight without any drugs administered. Throughout these study visits, eyes close resting EEG and matched subjective reports were collected. B) Flow diagram for the analysis of each EEG measure. Each metric was first tested for an association with low (OAA/S 0-2) vs high (OAA/S 4-5) responsiveness (Phase 1). Metrics that showed a significant association consistent with prior literature were then tested for associations with consciousness and connectedness (Phase 2). * Significant association with OAA/S consistent in direction with prior literature necessary to move to Phase 2.

Data Analysis

The first stage of analysis was to establish an association between each study metric and responsiveness. We reasoned that due to the scope of methodological variability among the studies that proposed these metrics, there could be many reasons a given metric would not

replicate in our own study, e.g. sedation visit vs natural sleep data, dosage of drugs, clinical or animal study, method of assessing responsiveness, etc. Therefore, we concluded that a fair assessment of each metric would involve first replicating the previous findings on responsiveness prior to testing for associations with consciousness and connectedness. If we failed to replicate an association with responsiveness, it would be unreasonable to further parse this effect into connectedness and consciousness since no such effect was present in our data.

For each metric, we tested for an association with loss of responsiveness (Fig. 1B Phase 1) in the dexmedetomidine and propofol data (sleep data were not used at this stage due to the lack of OAA/S measurements) using linear mixed effects models (LMEMs). The model specification was: Metric ~ OAAS.Bin + (1|Subject), where OAAS.Bin is a binarized version of the OAA/S scale contrasting high responsiveness (OAA/S 4-5) against low responsiveness (OAA/S 0-2), and (1|Subject) indicates the inclusion of by-subject random intercepts to account for subject-specific effects on the metric. Significance was assessed using Type III ANOVA with Kenward-Roger degrees of freedom for the F-test. P-values were adjusted for multiple comparisons using the Benjamini-Hochberg false discovery rate (FDR)[29] procedure across all metrics tested. If the OAAS.Bin term was significant ($p < 0.05$ after FDR correction) and consistent with the direction of the previously reported effects for that metric, that metric was considered to have successfully replicated in our study. If the OAAS.Bin term was non-significant or it was significant but opposite in direction from previous reports, the metric was deemed to have failed replication in our study.

Metrics that successfully replicated in our data were then assessed for associations with consciousness and connectedness (Fig. 1B Phase 2). We applied LMEMs to our sedation data (dexmedetomidine and propofol), with a model specification of: Metric ~ State + Cp + (1 + Cp|Subject). State is a set of dummy coded variables (0s and 1s) coding the states of W, CC, DC, or Unc, and Cp is the modeled plasma concentration of the drug. The (1 + Cp|Subject) term indicates the inclusion of by-subject random intercepts and by-subject random drug slopes to account for subject-specific effects. The sleep data were modeled as: Metric ~ State + (1|Subject), because there were no drug effects to include. W and CC data are phenomenologically identical (states of connected consciousness) but pharmacologically distinct; the latter was collected when subjects had anesthetic drugs in their system while the former was not. We model these data as separate states in order to best control for non-specific drug effects. The Cp term accounts for linear changes in the outcome variable dependent on plasma concentration of drug; however, nonlinear residual variance not captured by this term could instead be interpreted as an effect of connected consciousness if the W and CC data are pooled together. By splitting these data, we are able to directly contrast connected consciousness (with drug) against disconnected consciousness (with drug), which, we argue, is the best way to isolate effects of connectedness. As a final note, the above W/CC distinction is only relevant for the dexmedetomidine and propofol data, as the sleep data have no drugs involved. Because of this, the connectedness contrast for the sleep data is equivalent to DC vs W as opposed to DC vs CC.

Results

Collected and analyzed data

Data were collected from healthy volunteers during study visits in which they received dexmedetomidine (n = 20), propofol (n = 6), or completed a sleep visit (n = 15). Using a serial awakening paradigm, wake reports were initiated 390, 101, and 200 times for dexmedetomidine, propofol, and sleep respectively. Due to periods of unresponsiveness (no verbal reports) and reports that could not be coded because of internal inconsistencies, not all data could be analyzed. The data analyzed consisted of 322 conscious state reports and 339 OAA/S observations from dexmedetomidine, 86 conscious state reports and 89 OAA/S reports from propofol, and 187 conscious state reports from sleep. Here, "conscious state report" simply refers to an assessment of subjective consciousness and connectedness and does not mean that the reported state was a conscious one, i.e. the conscious state reports include reports of unconsciousness. Summaries of observed conscious state and OAA/s scores are included in Supplementary Table 1.

Associations with Responsiveness

The first step of our analysis was to attempt replicating the previously published effects of each measure by testing for an association with loss of responsiveness (Fig. 1B top). 'Successful replication' was assessed based on a significant association with OAA/S (0-2) vs OAA/S (4-5) with the effect going in the same direction (increasing or decreasing) as the published effect. Effect estimates from resulting LMEMs used for this assessment are shown in Fig. 2. The full list of effect estimates with confidence intervals and p-values can be found in Supplementary Table 2, but important observations are summarized here.

Dexmedetomidine			
Metric	LOC Effect	F-Statistic	P-Value (FDR)
Frontal alpha (power)	4.8E-2 [-3.3E-2, 1.2E-1]	F(1,303.82) = 1.55	0.308
Frontal alpha (connectivity)	3.1E-2 [1.3E-2, 4.8E-2]	F(1,306.61) = 10.8	0.004 *
Lempel-ziv complexity	-1.5E-2 [-3.7E-2, 4.8E-3]	F(1,296.85) = 2.18	0.229
Permutation Entropy (gamma)	-1.5E-2 [-2.4E-2, -5.6E-3]	F(1,302.84) = 10.69	0.004 *
Permutation Entropy (beta)	-1.4E-2 [-2.1E-2, -6.5E-3]	F(1,303.1) = 14.06	0.003 *
Permutation Entropy (alpha)	-1.3E-2 [-2.0E-2, -6.1E-3]	F(1,298.26) = 12.66	0.003 *
Permutation Entropy (theta)	-1.0E-2 [-1.8E-2, -2.0E-3]	F(1,299.55) = 6.18	0.025 *
Permutation Entropy (delta)	-4.1E-3 [-1.5E-2, 5.6E-3]	F(1,300.23) = 0.55	0.498
Spectral Exponent	-1.1E-1 [-1.9E-1, -3.1E-2]	F(1,297.47) = 9.02	0.007 *
Spectral edge frequency 95%	-6.0E-2 [-1.0E-1, -1.6E-2]	F(1,303.27) = 8.72	0.007 *
NSTE (back to front)	-5.6E-4 [-1.8E-3, 6.9E-4]	F(1,293.88) = 0.76	0.498
NSTE (front to back)	1.6E-6 [-1.2E-3, 1.3E-3]	F(1,296.59) = 0	0.998
NSTE (asymmetry)	1.8E-2 [-2.7E-2, 5.9E-2]	F(1,301.76) = 0.63	0.498
Propofol			
Metric	LOC Effect	F-Statistic	P-Value (FDR)
Frontal alpha (power)	1.1E-1 [-7.7E-2, 2.7E-1]	F(1,24.26) = 0.79	0.414
Frontal alpha (connectivity)	4.2E-2 [-2.3E-2, 1.1E-1]	F(1,54.99) = 1.4	0.314
Lempel-ziv complexity	-1.4E-1 [-2.3E-1, -6.3E-2]	F(1,21.64) = 6.2	0.045 *
Permutation Entropy (gamma)	-2.6E-2 [-4.5E-2, -4.8E-3]	F(1,38.66) = 4.88	0.056
Permutation Entropy (beta)	-3.1E-2 [-4.9E-2, -9.9E-3]	F(1,45.16) = 7.17	0.027 *
Permutation Entropy (alpha)	-3.9E-2 [-5.8E-2, -2.1E-2]	F(1,69.1) = 16.46	0.002 *
Permutation Entropy (theta)	-3.2E-2 [-4.6E-2, -1.7E-2]	F(1,66.11) = 13.67	0.003 *
Permutation Entropy (delta)	-2.1E-2 [-3.1E-2, -1.1E-2]	F(1,43.58) = 11.71	0.006 *
Spectral Exponent	-4.2E-1 [-6.0E-1, -2.0E-1]	F(1,19.4) = 8.94	0.024 *
Spectral edge frequency 95%	-1.3E-1 [-2.3E-1, -3.2E-2]	F(1,35.85) = 4.84	0.056
NSTE (back to front)	-1.8E-4 [-3.5E-3, 3.3E-3]	F(1,15.82) = 0.01	0.935
NSTE (front to back)	-3.7E-3 [-8.2E-3, 1.3E-3]	F(1,55.85) = 1.76	0.274
NSTE (asymmetry)	-8.1E-2 [-2.1E-1, 4.9E-2]	F(1,22.89) = 0.99	0.389
Sleep			
Metric	LOC Effect	F-Statistic	P-Value (FDR)
Frontal alpha (power)	5.6E-2 [-1.0E-1, 2.1E-1]	F(1,175.88) = 0.6	0.440
Frontal alpha (connectivity)	1.9E-2 [-1.3E-2, 5.2E-2]	F(1,156.44) = 1.26	0.311
Lempel-ziv complexity	-8.3E-2 [-1.5E-1, -2.2E-2]	F(1,183.03) = 6.2	0.036 *
Permutation Entropy (gamma)	-3.5E-2 [-6.2E-2, -1.3E-2]	F(1,183.03) = 7.41	0.031 *
Permutation Entropy (beta)	-2.8E-2 [-4.8E-2, -8.1E-3]	F(1,183.95) = 7.37	0.031 *
Permutation Entropy (alpha)	-2.3E-2 [-4.1E-2, -5.1E-3]	F(1,175.35) = 6.85	0.031 *
Permutation Entropy (theta)	-2.3E-2 [-3.9E-2, -7.6E-3]	F(1,175.63) = 8.6	0.031 *
Permutation Entropy (delta)	-1.6E-2 [-3.1E-2, -2.6E-3]	F(1,175.36) = 4.85	0.047 *
Spectral Exponent	-2.3E-1 [-4.3E-1, -4.5E-2]	F(1,171.07) = 5.46	0.038 *
Spectral edge frequency 95%	-1.3E-1 [-2.3E-1, -2.6E-2]	F(1,176.91) = 5.59	0.038 *
NSTE (back to front)	1.1E-3 [-7.5E-4, 3.2E-3]	F(1,178.84) = 1.07	0.327
NSTE (front to back)	-1.9E-3 [-5.0E-3, 1.1E-3]	F(1,182.87) = 1.49	0.290
NSTE (asymmetry)	-8.7E-2 [-1.9E-1, 2.1E-2]	F(1,170.44) = 3.03	0.120

Table 2. Effect estimates, F-statistics, and p-values from LMEMs testing the association between each metric and loss of consciousness (LOC, Unc vs DC) in dexmedetomidine, propofol, and sleep data. Effect estimates are listed as Mean [95% confidence interval]. P-values are corrected for multiple comparisons using the Benjamini-Hochberg false discovery rate (FDR) procedure. Asterisks (*) indicate significant p-values ($p < 0.05$).

Normalized Lempel-Ziv complexity (LZC) showed a significant reduction with loss of responsiveness in the propofol data ($p < 0.001$) and a trend towards decreases in the dexmedetomidine data ($p = 0.057$), consistent with prior findings[2,14,30]. Permutation Entropy (PE) showed significant reductions in at least 1 condition at each time-scale tested (delta-gamma), but the effects were not always consistent between the conditions. For example, gamma and beta (higher frequencies) only showed significant effects in the dexmedetomidine data, while delta only showed an effect with propofol. All observed effects on PE were decreasing with loss of responsiveness, consistent with prior findings[10]. Based on these results, each of the complexity-based metrics were selected for further testing against conscious state.

Anteriorization of alpha power, operationalized as the ratio of Fz/Oz alpha power, was significantly increased in both dexmedetomidine ($p < 0.001$) and propofol ($p = 0.004$), which was consistent with prior findings[1,7]. Frontal alpha wPLI connectivity similarly increased in both conditions (dexmedetomidine, $p < 0.001$, propofol, $p = 0.020$). Normalized symbolic transfer entropy (NSTE), which is a directed measure, was evaluated between clusters of frontal and posterior electrodes in both directions (front-to-back and back-to-front) and as a measure of asymmetry of front-to-back relative to back-to-front connectivity (see Supplementary Methods for details). Back-to-front connectivity decreased in dexmedetomidine ($p = 0.038$) but not propofol ($p = 0.855$), while front-to-back connectivity decreased in propofol ($p = 0.008$) but not dexmedetomidine ($p = 0.066$). The asymmetry index significantly decreased in propofol ($p = 0.003$), but not dexmedetomidine ($p = 0.912$). Lee et al., observed decreases in front-to-back but not back-to-front connectivity during sedation[12], consistent with our propofol findings, however, Pal et al. reported decreases in both directions[31]. As each NSTE measure showed

some evidence of decreasing in our data, they were all included in the subsequent consciousness/connectedness tests. Anteriorization of alpha power and frontal alpha wPLI were

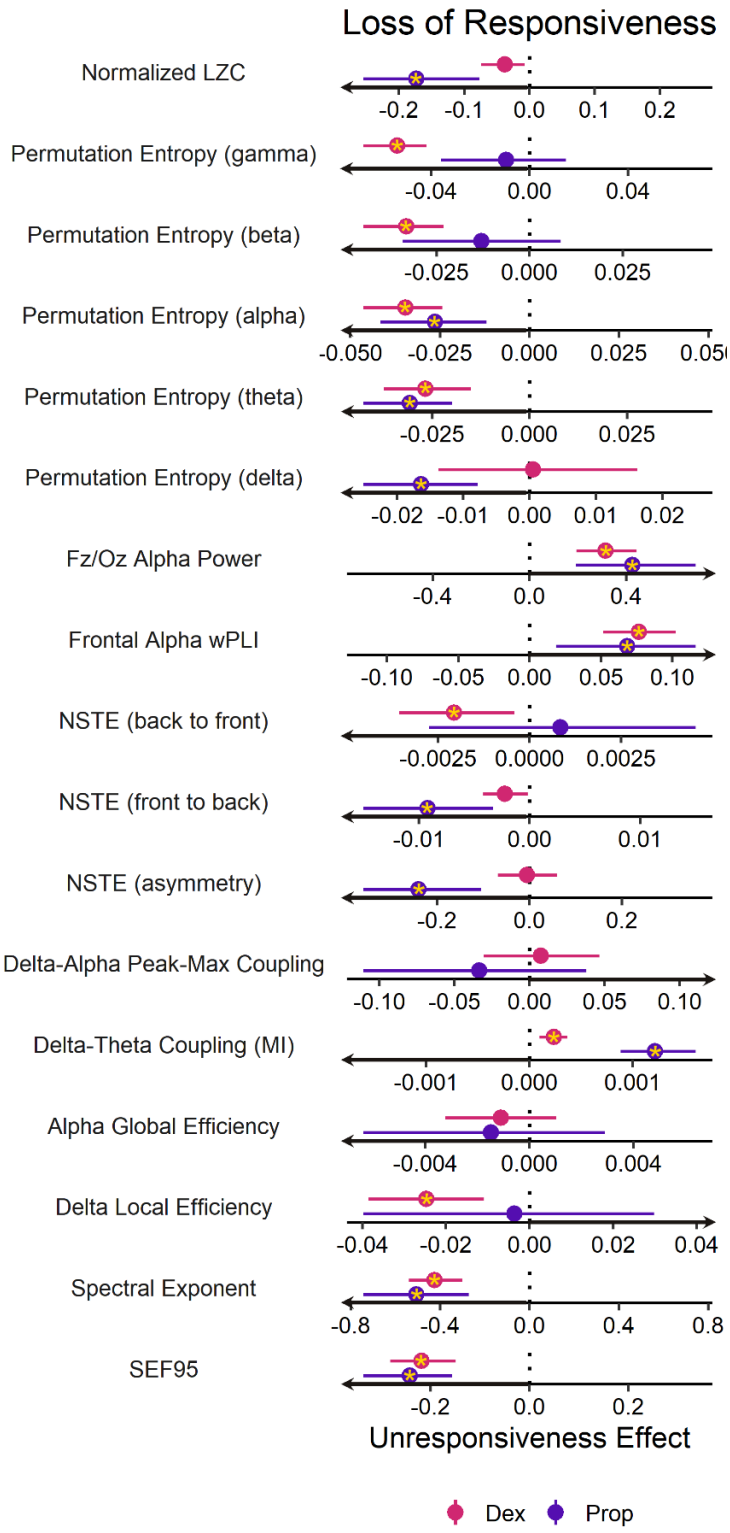

Figure 2. Association between metrics and loss of responsiveness. Effect estimates from LMEMs testing the association between each metric and loss of responsiveness (OAA/S 0-2 vs OAA/S 4-5) in dexmedetomidine (Dex) and propofol (Prop) data. Plots shoes the mean effect with 95% confidence intervals for each condition. The arrow on the X-axis of each subplot shows the *expected* direction of the effect based on prior literature. Metrics/conditions for which a statistically significant ($p < 0.05$ after FDR correction) association with loss of responsiveness are marked with a yellow asterisk (*). For simplicity of plotting, only the alpha global efficiency and delta local efficiency for networks thresholded to include only the top 30% of strongest edges are shown here. Results from networks using other threshold criteria can be found in Supplementary Figure 1.

also included.

Our data did not show an association between delta-alpha 'peak-max' coupling and loss of responsiveness within frontal channels in either dexmedetomidine ($p = 0.786$) or propofol ($p = 0.768$). In contrast, we did observe significant increases in delta-theta modulation index (MI) with loss of responsiveness in both dexmedetomidine ($p = 0.002$) and propofol ($p < 0.001$). However, prior work has proposed *decreased* delta-theta coupling as a marker of unconsciousness[5]. Because our delta-theta coupling results directly oppose the previously published findings, this was not considered a replication of results. As such, neither delta-alpha 'peak-max' coupling nor delta-theta MI were included in subsequent analyses.

Alpha global efficiency did not show significant changes in either dexmedetomidine ($0.089 \leq p \leq 0.935$) or propofol ($0.768 \leq p \leq 0.966$) across all networks tested. Delta local efficiency showed significant decreases with loss of responsiveness in dexmedetomidine networks containing 15-40% of the strongest edges ($0.001 \leq p \leq 0.022$) but not for any networks derived from propofol ($0.768 \leq p \leq 0.968$). While our dexmedetomidine data showed decreases in delta local efficiency, prior work proposes that *increased* efficiency indexes unconsciousness[6]. We therefore do not consider this a replication of results, and did not select either alpha global efficiency or delta local efficiency for further analysis. For simplicity, only the effects for the 30% edge density networks are shown in Fig. 2, however, complete results for all networks can be found in Supplementary Fig. 1.

The spectral edge frequency 95% (SEF95) showed significant decreases with loss of responsiveness in both dexmedetomidine ($p < 0.001$) and propofol ($p < 0.001$), consistent with

prior findings[8,9,18]. Similarly, the spectral exponent significantly decreased (became more negative) in both dexmedetomidine ($p < 0.001$) and propofol ($p < 0.001$) data, which agrees with prior findings[4,17]. Both of these spectral measures were considered to replicate prior findings and were selected for further analysis.

Associations with consciousness

Having successfully replicated prior findings in at least one drug condition, we proceeded to test LZC, PE, Fz/Oz alpha power, frontal alpha wPLI, NSTE, spectral exponent, and SEF95 for associations with consciousness within the dexmedetomidine, propofol, and sleep data. The effect estimates from the contrast of Unc vs DC, i.e. the effect of loss of consciousness from

these models are shown in Fig. 3. Raw data and adjusted model means for each state are presented in Supplemental Figs 3-15.

LZC showed significant reductions with loss of consciousness in the propofol ($p = 0.045$) and sleep ($p = 0.031$) data, but not dexmedetomidine ($p = 0.228$). All PE measures showed significant reductions with loss of consciousness. However, not all time scales showed significant changes in the same conditions, e.g. PE in the delta range showed significant decreases in propofol and sleep but not dexmedetomidine, while gamma range showed significant decreases in dexmedetomidine and sleep but not propofol (though the propofol p-values was borderline significant at $p = 0.056$). Beta, alpha, and theta range PE, however, showed significant reductions with loss of consciousness in all three conditions. See Table 2 for all p-values.

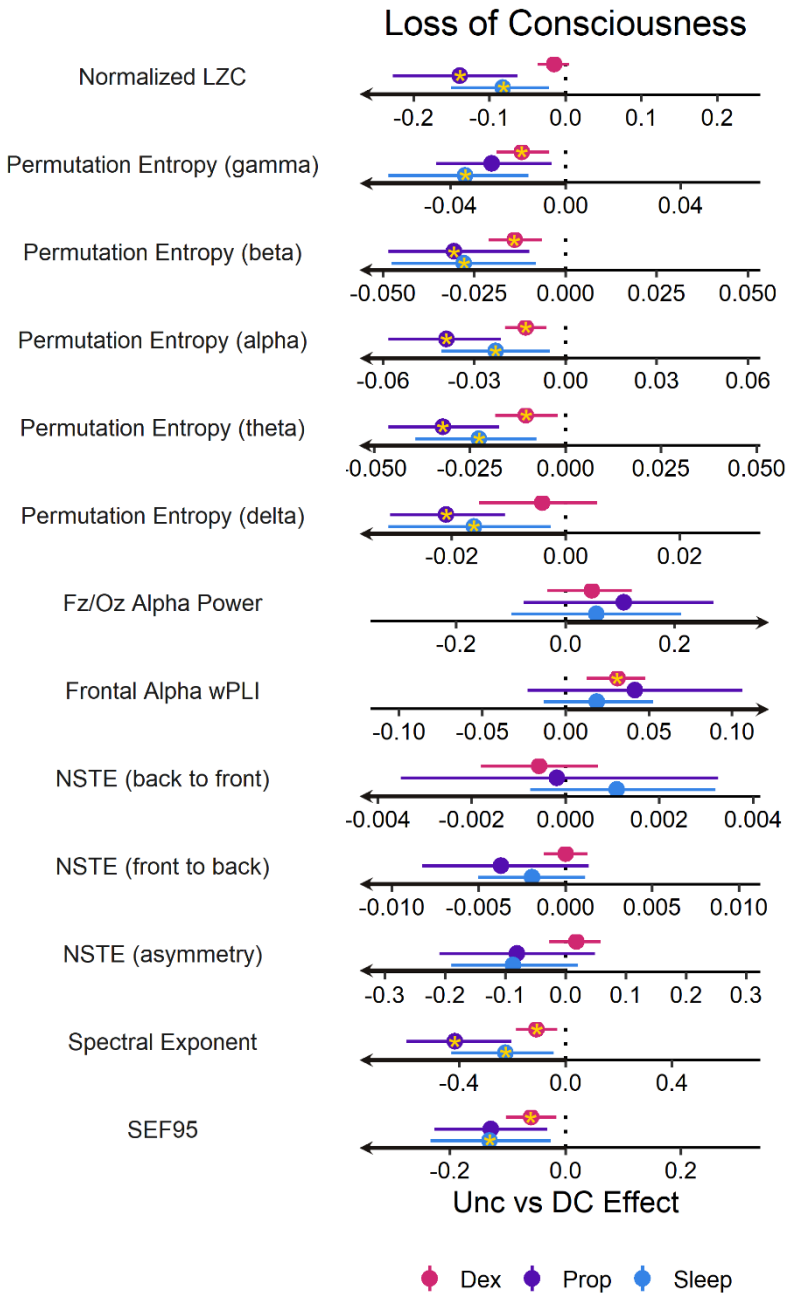

Figure 3. Association between metrics and loss of consciousness. Effect estimates from LMEMs testing the association between each metric and loss of consciousness (Unc vs DC) in dexmedetomidine (Dex), propofol (Prop), and sleep data. Plots shoes the mean effect with 95% confidence intervals for each condition. The arrow on the X-axis of each subplot shows the *expected* direction of the effect based on prior literature. Metrics/conditions for which a statistically significant ($p < 0.05$ after FDR correction) association with loss of responsiveness are marked with a yellow asterisk (*).

Surprisingly, none of the NSTE metrics showed significant changes with loss of consciousness in any experimental condition. We observed a modest visual trend of reduced front-to-back NSTE in propofol and sleep but no effect at all for dexmedetomidine, and a similar pattern with the asymmetry metric, however, none of these observations approached significance in the FDR corrected p-values (See Table 2).

Anteriorization of alpha power (Fz/Oz) showed a visual trend towards increasing with loss of consciousness in all conditions, but was not significant in any of them (Table 2). Frontal alpha wPLI, however, showed a significant increase in dexmedetomidine ($p = 0.003$), though not in either of the other conditions (propofol, $p = 0.314$, sleep, $p = 0.311$).

The metrics summarizing the entire power spectrum, SEF95 and the spectral exponent, also showed promise in tracking unconsciousness. The spectral exponent decreased (spectrum slope became steeper) with loss of consciousness in dexmedetomidine ($p = 0.007$), propofol ($p = 0.024$), and sleep ($p = 0.038$) data. Similarly, the SEF95 decreased significantly in dexmedetomidine ($p = 0.007$), and sleep ($p = 0.038$), but did not quite reach significance in propofol ($p = 0.056$).

Associations with connectedness

As mentioned before, consciousness and connectedness are often conflated in research and clinical assessment. To address this issue, we also tested each metric for associations with connectedness to see if proposed markers of consciousness might actually be better explained by connectedness. The effect estimates from the contrast of DC vs CC, i.e. the effect of loss of connectedness from these models are shown in Fig. 4.

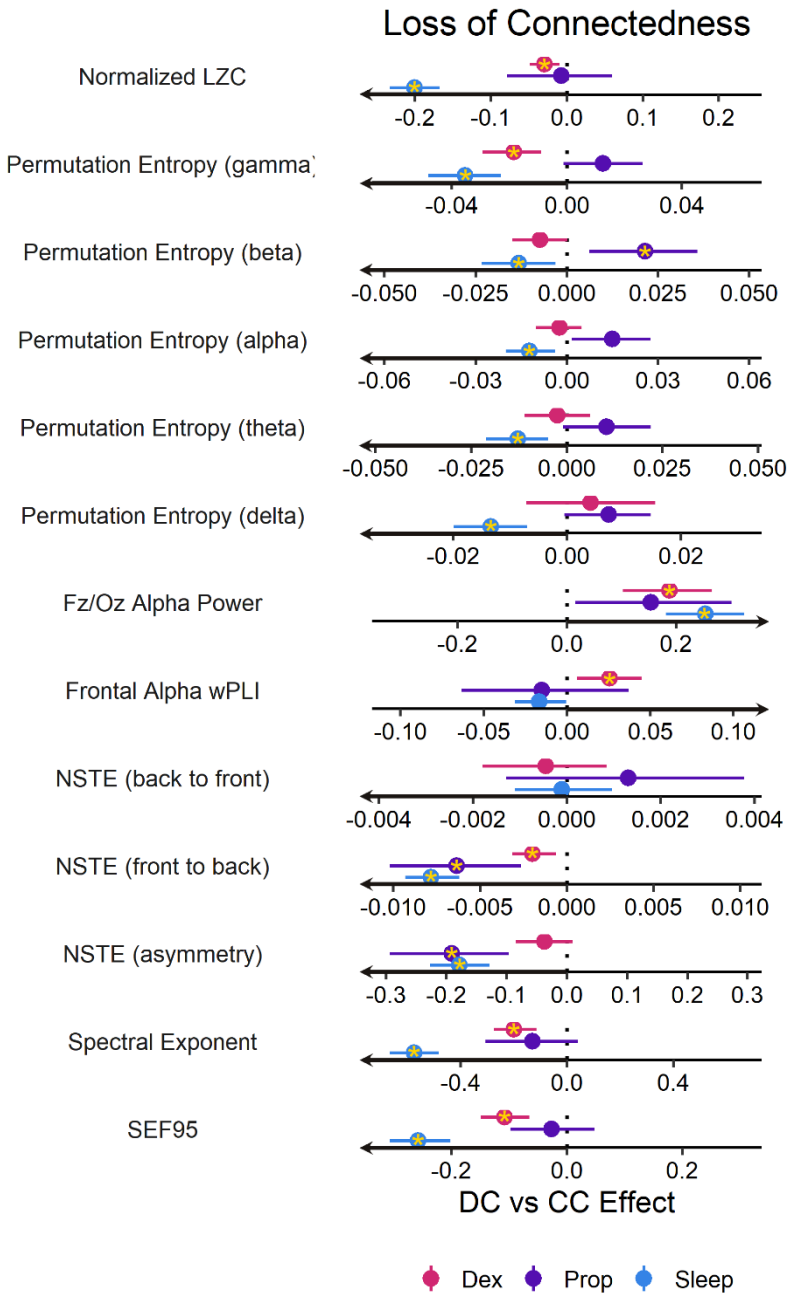

Figure 4. Association between metrics and loss of connectedness. Effect estimates from LMEMs testing the association between each metric and loss of connectedness (DC vs CC) in dexmedetomidine (Dex), propofol (Prop), and sleep data. Plots shoes the mean effect with 95% confidence intervals for each condition. The arrow on the X-axis of each subplot shows the *expected* direction of the effect based on prior literature. Metrics/conditions for which a statistically significant ($p < 0.05$ after FDR correction) association with loss of responsiveness are marked with a yellow asterisk (*).

For the complexity measures, LZC showed significant reductions with loss of connectedness in dexmedetomidine ($p = 0.012$) and sleep ($p < 0.001$) but not propofol ($p = 0.838$). PE, on the other hand, showed multiple condition and time scale-specific effects. The sleep data showed significant reductions in PE across all time scales (see Table 3 for p-values). However, dexmedetomidine only showed significant reductions in PE in the gamma range ($p < 0.001$). In contrast, propofol showed a trend towards *increased* PE across all time scales, but only reached significance for the beta range ($p = 0.044$).

As with the consciousness analysis, back-to-front NSTE showed no significant changes in any condition. However, front-to-back NSTE showed significant reductions in all conditions (dexmedetomidine, $p = 0.012$, propofol, $p = 0.018$, sleep, $p < 0.001$). The asymmetry metric showed significant reductions in propofol ($p = 0.010$) and sleep ($p < 0.001$) but not dexmedetomidine ($p = 0.181$). The effects of asymmetry can be explained easily as a mirror of the front-to-back results, as this metric is defined based on the degree of front-to-back relative to back-to-front NSTE (see Supplementary Methods).

Anteriorization of alpha significantly increased with loss of connectedness for dexmedetomidine ($p < 0.001$) and sleep ($p < 0.001$) but not propofol ($p = 0.155$). The frontal alpha wPLI was also significantly increased with loss of connectedness in dexmedetomidine ($p = 0.018$), but was not significant for either propofol ($p = 0.603$) or sleep ($p = 0.056$). Interestingly, though not significant, the trend in the sleep data was for a *decrease* rather than increase in frontal wPLI.

For the power spectrum measures, the spectral exponent significantly decreased in dexmedetomidine ($p < 0.001$) and sleep ($p < 0.001$) but not propofol ($p = 0.232$). Finally, the SEF95 also decreased in dexmedetomidine ($p < 0.001$) and sleep ($p < 0.001$) but not propofol ($p = 0.603$).

Dexmedetomidine			
Metric	LOCN Effect	F-Statistic	P-Value (FDR)
Frontal alpha (power)	1.9E-1 [2.7E-1, 1.0E-1]	F(1,299.34) = 21.24	<0.001 *
Frontal alpha (connectivity)	2.6E-2 [4.5E-2, 5.9E-3]	F(1,303.74) = 6.77	0.018 *
Lempel-ziv complexity	-2.9E-2 [-9.7E-3, -4.9E-2]	F(1,291.93) = 7.95	0.012 *
Permutation Entropy (gamma)	-1.8E-2 [-8.8E-3, -2.9E-2]	F(1,300.79) = 14.59	0.001 *
Permutation Entropy (beta)	-7.3E-3 [1.6E-4, -1.5E-2]	F(1,301.33) = 3.6	0.096
Permutation Entropy (alpha)	-2.4E-3 [4.9E-3, -1.0E-2]	F(1,299.61) = 0.4	0.559
Permutation Entropy (theta)	-2.5E-3 [6.1E-3, -1.1E-2]	F(1,298.96) = 0.34	0.559
Permutation Entropy (delta)	4.1E-3 [1.5E-2, -7.1E-3]	F(1,294.94) = 0.51	0.559
Spectral Exponent	-2.0E-1 [-1.1E-1, -2.7E-1]	F(1,297.31) = 27.58	<0.001 *
Spectral edge frequency 95%	-1.1E-1 [-6.5E-2, -1.5E-1]	F(1,300.26) = 26.08	<0.001 *
NSTE (back to front)	-4.5E-4 [8.4E-4, -1.8E-3]	F(1,304.56) = 0.43	0.559
NSTE (front to back)	-2.0E-3 [-6.3E-4, -3.2E-3]	F(1,295.34) = 7.79	0.012 *
NSTE (asymmetry)	-3.7E-2 [1.0E-2, -8.5E-2]	F(1,302.32) = 2.36	0.181
Propofol			
Metric	LOCN Effect	F-Statistic	P-Value (FDR)
Frontal alpha (power)	1.5E-1 [3.0E-1, 1.6E-2]	F(1,59.74) = 3.69	0.155
Frontal alpha (connectivity)	-1.5E-2 [3.7E-2, -6.3E-2]	F(1,70.44) = 0.35	0.603
Lempel-ziv complexity	-7.6E-3 [6.0E-2, -7.8E-2]	F(1,58.32) = 0.04	0.838
Permutation Entropy (gamma)	1.3E-2 [2.6E-2, -1.2E-3]	F(1,57.82) = 2.33	0.215
Permutation Entropy (beta)	2.1E-2 [3.6E-2, 6.1E-3]	F(1,66.59) = 7.02	0.044 *
Permutation Entropy (alpha)	1.5E-2 [2.7E-2, 1.7E-3]	F(1,69.37) = 4.23	0.141
Permutation Entropy (theta)	1.0E-2 [2.2E-2, -1.0E-3]	F(1,70.67) = 2.58	0.209
Permutation Entropy (delta)	7.3E-3 [1.5E-2, -4.4E-4]	F(1,59.41) = 2.77	0.209
Spectral Exponent	-1.3E-1 [4.0E-2, -3.1E-1]	F(1,58.49) = 2.02	0.232
Spectral edge frequency 95%	-2.7E-2 [4.8E-2, -9.8E-2]	F(1,58.14) = 0.41	0.603
NSTE (back to front)	1.3E-3 [3.8E-3, -1.3E-3]	F(1,58.85) = 0.86	0.466
NSTE (front to back)	-6.3E-3 [-2.7E-3, -1.0E-2]	F(1,68.85) = 9.62	0.018 *
NSTE (asymmetry)	-1.9E-1 [-9.6E-2, -2.9E-1]	F(1,61.04) = 12.64	0.010 *
Sleep			
Metric	LOCN Effect	F-Statistic	P-Value (FDR)
Frontal alpha (power)	2.5E-1 [3.2E-1, 1.8E-1]	F(1,172.42) = 51.59	<0.001 *
Frontal alpha (connectivity)	-1.7E-2 [-4.3E-4, -3.1E-2]	F(1,182.94) = 3.83	0.056
Lempel-ziv complexity	-2.0E-1 [-1.7E-1, -2.3E-1]	F(1,179.14) = 148.61	<0.001 *
Permutation Entropy (gamma)	-3.5E-2 [-2.3E-2, -4.8E-2]	F(1,176.25) = 31.43	<0.001 *
Permutation Entropy (beta)	-1.3E-2 [-3.1E-3, -2.3E-2]	F(1,177.5) = 6.8	0.012 *
Permutation Entropy (alpha)	-1.2E-2 [-3.8E-3, -2.0E-2]	F(1,181.22) = 7.86	0.007 *
Permutation Entropy (theta)	-1.3E-2 [-5.0E-3, -2.1E-2]	F(1,181.18) = 11.15	<0.001 *
Permutation Entropy (delta)	-1.3E-2 [-7.0E-3, -2.0E-2]	F(1,181.22) = 13.43	<0.001 *
Spectral Exponent	-5.7E-1 [-4.8E-1, -6.7E-1]	F(1,181.79) = 139.35	<0.001 *
Spectral edge frequency 95%	-2.6E-1 [-2.0E-1, -3.1E-1]	F(1,180.97) = 85.64	<0.001 *
NSTE (back to front)	-1.1E-4 [9.5E-4, -1.1E-3]	F(1,180.58) = 0.04	0.841
NSTE (front to back)	-7.8E-3 [-6.2E-3, -9.3E-3]	F(1,179.24) = 99.55	<0.001 *
NSTE (asymmetry)	-1.8E-1 [-1.3E-1, -2.3E-1]	F(1,181.86) = 50.61	<0.001 *

Table 3. Effect estimates, F-statistics, and p-values from LMEMs testing the association between each metric and loss of connectedness (LOCN, DC vs CC) in dexmedetomidine, propofol, and sleep data. Effect estimates are listed as Mean [95% confidence interval]. P-values are corrected for multiple comparisons using the Benjamini-Hochberg false discovery rate (FDR) procedure. Asterisks (*) indicate significant p-values ($p < 0.05$).

Metric	Loss of Responsiveness	Loss of Consciousness	Loss of Connectedness
Frontal alpha (power)	2/2	0/3	2/3
Frontal alpha (connectivity)	2/2	1/3	1/3
Lempel-ziv complexity	1/2	2/3	2/3
Delta-alpha peak-max coupling	0/2	-	-
Delta-theta phase amplitude coupling (MI)	2/2*	-	-
Permutation Entropy (gamma)	1/2	2/3	2/3
Permutation Entropy (beta)	1/2	3/3	2/3
Permutation Entropy (alpha)	2/2	3/3	1/3
Permutation Entropy (theta)	2/2	3/3	1/3
Permutation Entropy (delta)	1/2	2/3	1/3
Spectral Exponent	2/2	3/3	2/3
Spectral edge frequency 95%	2/2	2/3	2/3
NSTE (back to front)	1/2	0/3	0/3
NSTE (front to back)	1/2	0/3	3/3
NSTE (asymmetry)	1/2	0/3	2/3
Delta local efficiency	1/2*	-	-
Alpha global efficiency	0/2	-	-

Table 4. Counts of significant results from each experimental condition when testing for associations between each metric and loss of responsiveness, consciousness, and connectedness. Numerator indicates the number of conditions in which a significant result was observed, denominator indicates the number of conditions that were tested. For loss of responsiveness, the denominator represents Dex and Prop. For loss of consciousness and connectedness, denominator represents Dex, Prop, and sleep. Asterisks (*) indicate that while significant results were observed, the associations were opposite of what has been previously published within the paper(s) proposing that metric as a marker of unconsciousness.

Discussion

To our knowledge, the current study represents the most comprehensive assessment to date of proposed markers of consciousness, while controlling for confounds of sensory awareness (connectedness) and drug-specific effects. Of the markers evaluated (Table 1), frontal alpha (power and connectivity), Lempel-ziv complexity, permutation entropy, the spectral exponent, SEF95, and NSTE replicated previously published results within our study. However, when these markers were assessed using subjective reports of conscious state, rather than responsiveness, we observed that they were not all associated with consciousness *per se*. Rather, some markers specifically indexed connectedness while others were associated with both connectedness and consciousness (Table 4).

Notably, every marker that demonstrated a significant association with consciousness also showed a degree of association with connectedness, i.e. none of the markers of consciousness were *specific* to consciousness alone. The relative ubiquity of associations between these metrics and connectedness underscores the importance of this construct in explaining variance in responsiveness data that is often attributed to unconsciousness. This point is extremely important when considering the use of these markers for applications related to monitoring of consciousness. Monitors implementing heuristics developed from data in which connectedness and consciousness are conflated, e.g. responsiveness data, are likely to result in biased classifications due to the training data representing the joint effects of loss of connectedness and loss of consciousness. Accurate objective assessment of consciousness *per se* will require diligence in parsing out the effects of connectedness.

Our analyses identified Lempel-ziv complexity, permutation entropy, frontal alpha wPLI, spectral exponent, and SEF95 as metrics that significantly track consciousness *per se* even after adjusting for connectedness and predicted plasma drug concentration, at least in some conditions. Of these markers, permutation entropy in mid-frequency time scales (beta-theta) appears to be particularly useful in indexing loss of consciousness as significant effects were observed in all three conditions (dexmedetomidine, propofol, and sleep). If viewed in terms of metric categories (Table 1), our data support the utility of EEG complexity measures and metrics that summarize the relative predominance of low vs high frequency power as markers of (un)consciousness. These findings are consistent with another large-scale screening of markers of consciousness in the context of disorders of consciousness[32], which showed decreases in complexity measures and high frequency activity but increases in low frequency activity with progressive severity of the disorder. The complexity findings are also broadly consistent with integrated information theory (IIT) (and other information theory oriented theories), which count complexity of information among the central prerequisites of consciousness[33–35]. The power spectrum results match with one of the few published studies that also distinguished between consciousness and connectedness in sleeping subjects, which found an increase in low frequency power and decrease in high frequency power being associated with unconsciousness compared to disconnected consciousness[36].

Interestingly, every marker tested, with the exception of back-to-front NSTE, showed significant associations with connectedness after adjusting for consciousness and predicted plasma drug concentration. While back-to-front NSTE significantly decreased with loss of responsiveness in dexmedetomidine, this effect couldn't be explained by loss of consciousness

or loss of connectedness, however, it did exhibit a significant negative association with predicted plasma concentration of dexmedetomidine (data not shown), indicating the LOR effect is explainable as a drug specific effect of dexmedetomidine. Among the markers associated with connectedness, anteriorization of alpha power and front-to-back NSTE showed up as specifically related to connectedness, with no observed effects related to consciousness. Front-to-back NSTE appears especially promising as a generalizable marker specific to connectedness as it showed significant loss of connectedness effects in all three conditions. The front-to-back NSTE is thought to represent the directed information transfer from frontal to parietal cortex[12] while anteriorization of alpha is thought to represent an increase in thalamocortical synchronization frontally along with HCN channel-mediated disruption of occipital alpha rhythms[37–39]. Further investigation will be necessary to determine if these markers are independent or represent a joint mechanism of thalamocortical disruption of frontal to posterior information flow. In either case, they represent intriguing potential mechanisms of sensory disconnection. However, we recently investigated the impact of dexmedetomidine on frontotemporal connectivity using dynamic causal modelling of auditory evoked data, identifying increased feedback connectivity associated with sensory disconnection[40]. Whether this represents differences in the resting state vs. evoked paradigm or modelling approach needs further enquiry.

The fact that several markers (delta-alpha peak-max coupling, delta theta phase amplitude coupling, delta local efficiency, and alpha global efficiency) failed to replicate in the context of responsiveness within our study merits some discussion. There are many methodological reasons which might explain the lack of replication; for example, the prior work

on delta-theta phase amplitude coupling made use of ketamine and alfentanil for their anesthetic regimen[5]. Ketamine is well known to induce functional activity distinct from what is typically observed during GABAergic anesthesia, such as increased (rather than decreased) high-frequency power[27,41] and EEG complexity[42]. As such, the use of dexmedetomidine and propofol in our study may explain why we observed increased delta-theta coupling rather than the decreases reported under ketamine. Choice of anesthetic cannot explain all failed replications however. Frontal alpha connectivity, delta-alpha peak max coupling, and alpha global efficiency have all been investigated under propofol anesthesia, which was included in our study, yet we did not observe significant associations with loss of responsiveness[1,7,13]. This may be related to the depth of anesthesia achieved in our study compared to the prior works. In order to ensure that subjects were rousable so verbal reports could be acquired, anesthetic concentrations were kept relatively low in our study (predicted plasma concentrations under 2.0 μg/mL for the majority of data collected). These concentrations may have been insufficient to produce the signatures observed in prior studies utilizing higher doses of propofol (e.g. effect site concentration of 5.0 μg/mL[1]). In general, it is challenging for any one study to perfectly replicate the methodologies of so many prior studies simultaneously. It is for this very reason that our analytical procedures focused on first demonstrating that our data could replicate prior findings based on responsiveness before testing for effects of consciousness and connectedness.

Our findings highlight the need for improved specificity in reporting results within the neuroscience of consciousness community. As researchers, it is unavoidable that the tools we use to measure our constructs of interest will be imperfect. We do not advocate that

assessments of responsiveness be thrown out as tools used in the study of consciousness. Indeed, doing so would be a major detriment to the field as there are many scenarios in which responsiveness is the only proxy of consciousness that is available to us, such as during clinical anesthesia or in animal studies. These are critical sources of data that the field must continue to leverage in order to make progress in understanding the mechanisms of consciousness. In fact, the current findings underscore the utility of such data, as many of the evaluated markers, derived based on assessments of responsiveness, showed significant associations with *consciousness per se*. However, in cases where responsiveness is used as a proxy of consciousness, we argue that it is of great importance that researchers be explicit about this when publishing their findings and include the conflation of disconnection and unconsciousness as a limitation of the work. Furthermore, when designing future studies, we urge investigators to evaluate whether direct assessment of consciousness distinct from connectedness, through subjective reporting, is a viable strategy within their research context. If so, implementing these assessments is encouraged as it provides greater specificity to the claims that can be made about consciousness based on the data collected.

The current work provides methodological advances by explicitly distinguishing between connectedness and consciousness, but it is not free of limitations. The most fundamental limitation is the dependency on subjective reports as “ground truth” of conscious state. Due to the subjective nature of these reports, we cannot rule out human error from participants in assessing their own mental state. Until the field arrives at a sufficiently accurate objective marker of consciousness, human reporting error will remain an unavoidable source of noise in the data. However, this is still a major advance over assuming unconsciousness based on

unresponsiveness[21]. As mentioned above, we are also limited in our ability to simultaneously replicate the various prior studies to a degree that allows us to rule out methodological differences, such as sample sizes or peak drug concentrations, as a source of difference in the data. To mitigate this issue, we first focused on replicating prior findings based on responsiveness to identify markers for which methodological differences did not produce differences in effects. This allows us to be more confident that the effects we observed for consciousness and connectedness are not specific to methodological idiosyncrasies of our study. Finally, we readily acknowledge that the current work is not comprehensive of all proposed markers of consciousness. The markers evaluated in this study were chosen based on prior evidence of indexing consciousness (as measured by responsiveness) within an anesthetic context to best match with our experimental procedures. Furthermore, they were selected to cover the general categories of complexity, connectivity, cross-frequency coupling, graph theory, and power spectra summaries, to ensure different dimensions of the EEG signal were being evaluated. Additional future work will be necessary to evaluate markers not covered in this this paper for associations with consciousness *per se* and connectedness.

In summary, the current study demonstrates that measures of unconsciousness based on responsiveness are not necessarily specific to unconsciousness *per se*, rather, the majority track changes in both consciousness and connectedness, though some were specific to connectedness alone. Though none of the measures tested in this study were specific to unconsciousness alone, a majority did show significant associations with unconsciousness independent of their associations with connectedness. These findings highlight the importance of distinguishing between connectedness and consciousness when attempting to study one or

the other. While not all experimental paradigms are amenable to acquiring subjective reports for distinguishing connectedness and consciousness, adopting these measurements where possible is indicated.

Data Availability

Data may be made available upon request at the discretion of the University of Wisconsin-Madison Institutional Review Board.

Acknowledgments

We are grateful to advice from Prof Giulio Tononi, Dr. Brady Riedner, Dr David Plante and Dr. Melanie Boly (University of Wisconsin, USA) when setting up this project and for loan of the EEG equipment. We acknowledge Prof Michel MRF Struys, MD, PhD, FRCA, and Dr Tom De Smet, PhD from The University Medical Center Groningen, The Netherlands and Ghent University, Belgium for their assistance with RUGLOOP and infusion pump technology. In addition, Prof Anthony Absalom (The University Medical Center Groningen, The Netherlands) provided advice on pharmacokinetic modelling of drug concentrations.

Competing Interests

The authors have no competing interests to declare.

Funding

This work was supported by the Department of Anesthesiology at the University of Wisconsin-Madison and by NIH NIND 1R01NS117901-01.

References

1. Purdon PL, Pierce ET, Mukamel EA, et al. Electroencephalogram signatures of loss and recovery of consciousness from propofol. *Proc Natl Acad Sci U S A*. 2013;110(12). doi:10.1073/pnas.1221180110

2. Schartner M, Seth A, Noirhomme Q, et al. Complexity of Multi-Dimensional Spontaneous EEG Decreases during Propofol Induced General Anaesthesia. Chialvo DR, ed. *PLoS One*. 2015;10(8):e0133532. doi:10.1371/journal.pone.0133532

3. Banks MI, Krause BM, Endemann CM, et al. Cortical functional connectivity indexes arousal state during sleep and anesthesia. *Neuroimage*. 2020;211:116627. doi:10.1016/j.neuroimage.2020.116627

4. Colombo MA, Napolitani M, Boly M, et al. The spectral exponent of the resting EEG indexes the presence of consciousness during unresponsiveness induced by propofol, xenon, and ketamine. *Neuroimage*. 2019;189:631-644. doi:10.1016/J.NEUROIMAGE.2019.01.024

5. Tsai FF, Fan SZ, Cheng HL, Yeh JR. Multi-timescale phase-amplitude couplings in transitions of anesthetic-induced unconsciousness. *Scientific Reports 2019 9:1*. 2019;9(1):1-11. doi:10.1038/s41598-019-44238-8

6. Lee M, Sanders RD, Yeom SK, et al. Network Properties in Transitions of Consciousness during Propofol-induced Sedation. *Scientific Reports 2017 7:1*. 2017;7(1):1-13. doi:10.1038/s41598-017-15082-5

7. Blain-Moraes S, Tarnal V, Vanini G, et al. Network Efficiency and Posterior Alpha Patterns Are Markers of Recovery from General Anesthesia: A High-Density Electroencephalography Study in Healthy Volunteers. *Front Hum Neurosci*. 2017;11:328. doi:10.3389/FNHUM.2017.00328

8. Nieuwenhuijs D, Coleman EL, Douglas NJ, Drummond GB, Dahan A. Bispectral index values and spectral edge frequency at different stages of physiologic sleep. *Anesth Analg*. 2002;94(1):125-129. doi:10.1213/00000539-200201000-00024

9. Sleigh JW, Andrzejowski J, Steyn-Ross A, Steyn-Ross M. The Bispectral Index. *Anesth Analg*. 1999;88(3):659-661. doi:10.1213/00000539-199903000-00035

10. Liang Z, Wang Y, Sun X, et al. EEG entropy measures in anesthesia. *Front Comput Neurosci*. 2015;9(JAN). doi:10.3389/FNCOM.2015.00016/ABSTRACT

11. Kreuzer M, Stern MA, Hight D, et al. Spectral and Entropic Features Are Altered by Age in the Electroencephalogram in Patients under Sevoflurane Anesthesia. *Anesthesiology*. 2020;132(5):1003-1016. doi:10.1097/ALN.0000000000003182

12. Lee U, Ku S, Noh G, Baek S, Choi B, Mashour GA. Disruption of Frontal–Parietal Communication by Ketamine, Propofol, and Sevoflurane. *Anesthesiology*. 2013;118(6):1264-1275. doi:10.1097/ALN.0B013E31829103F5

13. Stephen EP, Hotan GC, Pierce ET, et al. Broadband slow-wave modulation in posterior and anterior cortex tracks distinct states of propofol-induced unconsciousness. *Scientific Reports 2020 10:1*. 2020;10(1):1-11. doi:10.1038/s41598-020-68756-y

14. Schartner MM, Pigorini A, Gibbs SA, et al. Global and local complexity of intracranial EEG decreases during NREM sleep. *Neurosci Conscious*. 2017;2017(1):1-12. doi:10.1093/NC/NIW022

15. Li D, Hambrecht-Wiedbusch VS, Mashour GA. Accelerated recovery of consciousness after general anesthesia is associated with increased functional brain connectivity in the high-gamma bandwidth. *Front Syst Neurosci*. 2017;11:16. doi:10.3389/FNSYS.2017.00016/BIBTEX

16. Lee JM, Kim PJ, Kim HG, et al. Analysis of brain connectivity during nitrous oxide sedation using graph theory. *Scientific Reports 2020 10:1*. 2020;10(1):1-11. doi:10.1038/s41598-020-59264-0

17. Gao R, Peterson EJ, Voytek B. Inferring synaptic excitation/inhibition balance from field potentials. *Neuroimage*. 2017;158:70-78. doi:10.1016/J.NEUROIMAGE.2017.06.078

18. Bruhn J, Bouillon TW, Radulescu L, Hoeft A, Bertaccini E, Shafer SL. Correlation of Approximate Entropy, Bispectral Index, and Spectral Edge Frequency 95 (SEF95) with Clinical Signs of “Anesthetic Depth” during Coadministration of Propofol and Remifentanil. *Anesthesiology*. 2003;98(3):621-627. doi:10.1097/00000542-200303000-00008

19. Blain-Moraes S, Tarnal V, Vanini G, et al. Neurophysiological Correlates of Sevoflurane-induced Unconsciousness. *Anesthesiology*. 2015;122(2):307-316. doi:10.1097/ALN.0000000000000482

20. Boly M, Sanders RD, Mashour GA, Laureys S. Consciousness and responsiveness: Lessons from anaesthesia and the vegetative state. *Curr Opin Anaesthesiol*. 2013;26(4):444-449. doi:10.1097/ACO.0b013e3283628b5d

21. Sanders RD, Tononi G, Laureys S, Sleigh JW. Unresponsiveness ≠ unconsciousness. *Anesthesiology*. 2012;116(4):946-959. doi:10.1097/ALN.0b013e318249d0a7

22. Cascella M. Mechanisms underlying brain monitoring during anesthesia: Limitations, possible improvements, and perspectives. *Korean J Anesthesiol*. 2016;69(2):113-120. doi:10.4097/kjae.2016.69.2.113

23. Kotsovolis G, Komninos G. Awareness during anesthesia: How sure can we be that the patient is sleeping indeed? *Hippokratia*. 2009;13(2):83-89.

24. Bonhomme V, Staquet C, Montupil J, et al. General Anesthesia: A Probe to Explore Consciousness. *Front Syst Neurosci*. 2019;13:36. doi:10.3389/FNSYS.2019.00036/BIBTEX

25. Koch C, Massimini M, Boly M, Tononi G. Neural correlates of consciousness: Progress and problems. *Nat Rev Neurosci*. 2016;17(5):307-321. doi:10.1038/nrn.2016.22

26. Sanders RD, Casey C, Saalmann YB. Predictive coding as a model of sensory disconnection: relevance to anaesthetic mechanisms. *Br J Anaesth*. 2021;126(1):37-40. doi:10.1016/j.bja.2020.08.017

27. Purdon PL, Sampson A, Pavone KJ, Brown EN. Clinical electroencephalography for anesthesiologists. *Anesthesiology*. 2015;123(4):937-960. doi:10.1097/ALN.0000000000000841

28. Casey CP, Tanabe S, Farahbakhsh Z, et al. Distinct EEG signatures differentiate unconsciousness and disconnection during anaesthesia and sleep. *Br J Anaesth*. Published online February 9, 2022. doi:10.1016/J.BJA.2022.01.010

29. Benjamini Y, Hochberg Y. Controlling the False Discovery Rate: A Practical and Powerful Approach to Multiple Testing. *Journal of the Royal Statistical Society: Series B (Methodological)*. 1995;57(1):289-300. doi:10.1111/J.2517-6161.1995.TB02031.X

30. Hudetz AG, Liu X, Pillay S, Boly M, Tononi G. Propofol anesthesia reduces Lempel-Ziv complexity of spontaneous brain activity in rats. *Neurosci Lett*. 2016;628:132. doi:10.1016/J.NEULET.2016.06.017

31. Pal D, Silverstein BH, Lee H, Mashour GA. Neural Correlates of Wakefulness, Sleep, and General AnesthesiaAn Experimental Study in Rat. *Anesthesiology*. 2016;125(5):929-942. doi:10.1097/ALN.0000000000001342

32. Sitt JD, King JR, el Karoui I, et al. Large scale screening of neural signatures of consciousness in patients in a vegetative or minimally conscious state. *Brain*. 2014;137(8):2258-2270. doi:10.1093/brain/awu141

33. Tononi G. An information integration theory of consciousness. *BMC Neurosci*. 2004;5. doi:10.1186/1471-2202-5-42

34. Tononi G. Integrated information theory of consciousness: an updated account. *Arch Ital Biol*. 2012;150(4):293-329. doi:10.4449/aib.v149i5.1388

35. Seth AK, Barrett AB, Barnett L. Causal density and integrated information as measures of conscious level. *Philosophical Transactions of the Royal Society A: Mathematical,*

Physical and Engineering Sciences. 2011;369(1952):3748-3767. doi:10.1098/RSTA.2011.0079

36. Siclari F, Baird B, Perogamvros L, et al. The neural correlates of dreaming. *Nat Neurosci*. 2017;20(6):872-878. doi:10.1038/nn.4545

37. Ching S, Cimenser A, Purdon PL, Brown EN, Kopell NJ. Thalamocortical model for a propofol-induced α-rhythm associated with loss of consciousness. *Proc Natl Acad Sci U S A*. 2010;107(52):22665-22670. doi:10.1073/PNAS.1017069108/SUPPL_FILE/PNAS.201017069SI.PDF

38. Vijayan S, Kopell NJ. Thalamic model of awake alpha oscillations and implications for stimulus processing. *Proc Natl Acad Sci U S A*. 2012;109(45):18553-18558. doi:10.1073/PNAS.1215385109/SUPPL_FILE/PNAS.201215385SI.PDF

39. Vijayan S, Ching SN, Purdon PL, Brown EN, Kopell NJ. Thalamocortical Mechanisms for the Anteriorization of Alpha Rhythms during Propofol-Induced Unconsciousness. *The Journal of Neuroscience*. 2013;33(27):11070. doi:10.1523/JNEUROSCI.5670-12.2013

40. Casey CP, Tanabe S, Farahbakhsh Z, et al. Dynamic causal modelling of auditory surprise during disconnected consciousness: The role of feedback connectivity. *Neuroimage*. 2022;263:119657. doi:10.1016/J.NEUROIMAGE.2022.119657

41. Akeju O, Song AH, Hamilos AE, et al. Electroencephalogram signatures of ketamine anesthesia-induced unconsciousness. *Clinical Neurophysiology*. 2016;127(6):2414-2422. doi:10.1016/J.CLINPH.2016.03.005

42. Li D, Mashour GA. Cortical dynamics during psychedelic and anesthetized states induced by ketamine. *Neuroimage*. 2019;196:32-40. doi:10.1016/j.neuroimage.2019.03.076

CHAPTER III

This chapter was previously published as:

Casey CP, Tanabe S, Farahbakhsh Z, et al. Dynamic causal modelling of auditory surprise during disconnected consciousness: the role of feedback connectivity. *NeuroImage* Academic Press Inc.; 2022;

Dynamic Causal Modelling of Auditory Surprise During Disconnected Consciousness: The Role of Feedback Connectivity

Cameron P. Casey*[1], Sean Tanabe[1], Zahra Farahbakhsh[1], Margaret Parker[1], Amber Bo[1], Marissa White[1], Tyler Ballweg[1], Andrew Mcintosh[1], William Filbey[1], Matthew I. Banks[1], Yuri B. Saalmann[2], Robert A. Pearce[1], Robert D. Sanders*[3-5]

1. Department of Anesthesiology, University of Wisconsin, Madison, USA.

2. Department of Psychology, University of Wisconsin, Madison, USA.

3. Specialty of Anaesthetics, University of Sydney, Camperdown, Australia

4. Department of Anaesthetics, Royal Prince Alfred Hospital, Camperdown, Australia

5. Institute of Academic Surgery, Royal Prince Alfred Hospital, Camperdown, Australia

*Cameron P. Casey and Robert D. Sanders are the corresponding authors

Email: robert.sanders@sydney.edu.au, cpcasey3@wisc.edu

Abstract

The neural mechanisms through which individuals lose sensory awareness of their environment during anesthesia remains poorly understood despite being of vital importance to the field. Prior research has not distinguished between sensory awareness of the environment (connectedness) and consciousness itself. In the current study, we investigated the neural correlates of sensory awareness by contrasting neural responses to an auditory roving oddball paradigm during consciousness with sensory awareness (connected consciousness) and consciousness without sensory awareness (disconnected consciousness). These states were captured using a serial awakening paradigm with the sedative alpha2 adrenergic agonist dexmedetomidine, chosen based on our published hypothesis that suppression of noradrenaline signaling is key to induce a state of sensory disconnection. High-density electroencephalography was recorded from 18 human subjects before and after administration of dexmedetomidine. By investigating event-related potentials and taking advantage of advances in Dynamic Causal Modeling (DCM), we assessed alterations in effective connectivity between nodes of a previously established auditory processing network. We found that during disconnected consciousness, the scalp-level response to standard tones produced a P3 response that was absent during connected consciousness. This P3 response resembled the response to oddball tones seen in connected consciousness. DCM showed that disconnection produced increases in standard tone feedback signaling throughout the auditory network. Simulation analyses showed that these changes in connectivity, most notably the increase in feedback from right superior temporal gyrus to right A1, can explain the new P3 response. Together these findings show that during disconnected consciousness there is a disruption of

normal predictive coding processes, so that all incoming auditory stimuli become similarly surprising.

Introduction

An estimated 313 million surgical procedures are performed globally each year, with this figure projected to increase dramatically with growing populations and spread of medical coverage[1,2]. General anesthesia has become an essential component of surgery, allowing physicians to perform operations by preventing patient movement and protecting patients from awareness of surgery. However, this is under ideal circumstances. While intraoperative awareness is not generally evident in clinical practice, focused investigations have shown it remains a pernicious problem, with estimated occurrence rates of roughly 5%[3] in the general population and 11% among young adults[4]. This implies that at least 15.6 million cases of intraoperative awareness occur each year. In order to better address this problem, it is essential that we develop a better understanding of how the brain becomes disconnected from the environment under general anesthesia.

A great deal of prior research has been conducted on the effects of anesthesia on the brain, especially in relation to loss of consciousness[5–9]. However, a common theme in this field of work is to assume that loss of consciousness has occurred when there is a loss of motor responsiveness to sensory input. This approach is problematic for our understanding of these processes because it conflates awareness of the environment, conscious experience itself, and motor responsiveness. Without experimentally distinguishing these processes, we face a fundamental limitation in our ability to understand the effects of anesthesia on the brain. Specifically, to understand sensory disconnection from the environment, it is necessary to

directly compare states of ‘consciousness with sensory awareness’ versus ‘consciousness without sensory awareness’. We refer to the former as connected consciousness and the later as disconnected consciousness[10,11].

Electroencephalography (EEG) offers a convenient method for real time assessment of neurophysiology in a clinical setting. However, routine EEG signal metrics, such as spectral power or functional connectivity measures, are limited in what they can reveal about causal mechanisms within the brain. Recent advances in generative modeling methods now allow for more sophisticated inferences to be drawn from EEG data, permitting researchers to test mechanistic hypotheses about directed information flow within the brain. One such approach is dynamic causal modeling (DCM), which provides a framework for modeling functional relationships within an anatomically defined network, and importantly, the ability to test the effects of external stimuli on that network[12–14].

In the current study, we employ an auditory roving oddball paradigm with high-density EEG recording and DCM modeling to probe sensory processing during connected and disconnected consciousness. To experimentally bias our participants towards a disconnected state, we administered dexmedetomidine, a commonly used sedative and anesthetic. We then confirmed sensory disconnection using serial awakenings with structured interviews. We hypothesized that disconnected consciousness would be associated with a loss of feedforward connectivity in response to auditory stimulation, indicating a reduction in environmental information in-flow to higher-order cerebral cortex[15]. To our knowledge, the current work represents the first attempt to study the changes in sensory processing of auditory cues associated with loss of sensory awareness but maintenance of consciousness.

Methods

Subjects and Drug Administration

The subjects presented here were enrolled in the UNderstanding Consciousness Connectedness and Intra-Operative Unresponsiveness Study (UN-ConsCIOUS, NCT03284307). The resting-state data from this study has been previously published [11], however, the data presented here have not. In brief, 20 healthy volunteers, ages 18 to 32 years old, without prior contraindications to anesthetics, were recruited for dexmedetomidine administration. Due to an early revision in the study protocol, the first two subjects were presented with a different auditory paradigm than the latter 18 and were thus excluded from analyses. Drug administration occurred under the supervision of an anesthetist, to achieve a series of stable drug plateaus throughout the visit (Fig. 1A). A rapid infusion of 3.0 μg $kg^{-1}hr^{-1}$ was initially given over a 10-minute period followed by a 0.5 μg $kg^{-1}hr^{-1}$ maintenance infusion to achieve the first drug step. The second drug step was similarly achieved by a 10 minute infusion of 3.0 μg $kg^{-1}hr^{-1}$ followed by a 1.5 μg $kg^{-1}hr^{-1}$ maintenance infusion. The total duration of drug exposure was limited to 4 hours for each subject.

Roving Oddball Paradigm

We implemented an auditory roving oddball paradigm (Fig. 1B) based on the work of Garrido et al[16,17]. Participants were presented with a series of single frequency tones with a pseudo-random number of repetitions, between 2 and 11 repeats, constituting a stimulus block.

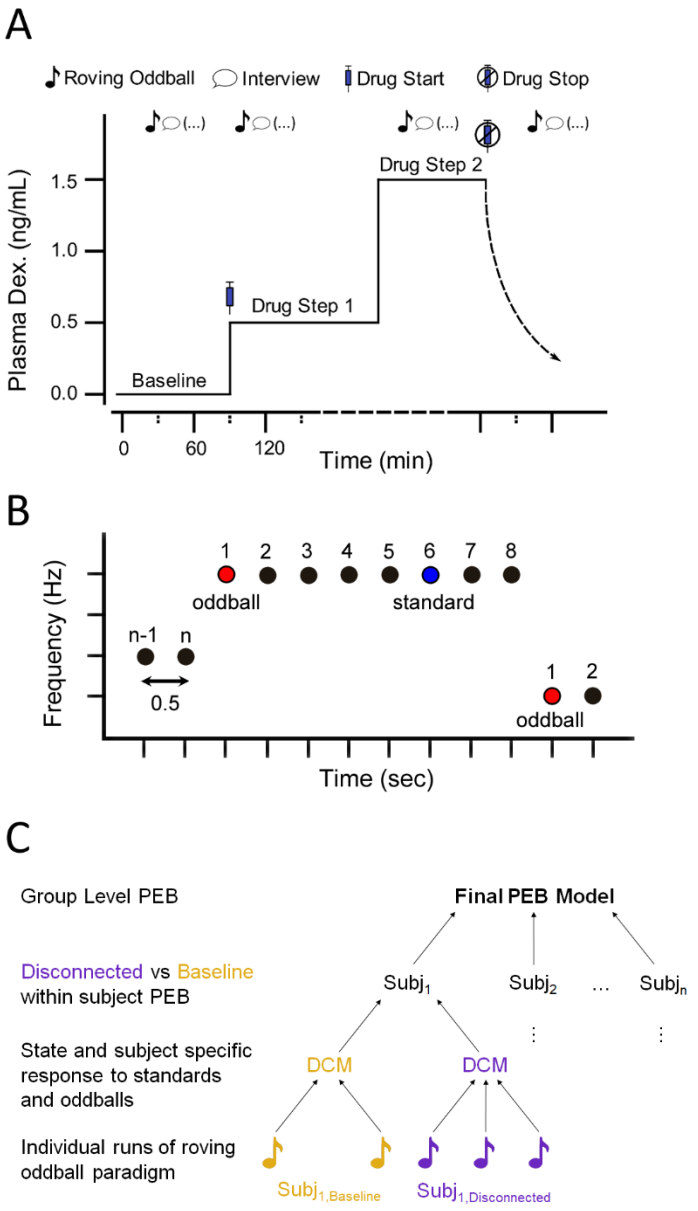

Figure 1. Experimental Overview. A) Hypothetical drug dosing diagram illustrating the format of each subject's study visit. Roving oddball auditory stimulation was administered throughout the visit and paired with subjective report information to assess the subject's state of sensory awareness and consciousness during the auditory paradigm. B) A graphical illustration of the roving oddball paradigm. Tones were played in blocks for which the 1st tone (red) is considered and oddball and the 6th tone (blue) is considered a standard. C) An illustration of the hierarchical PEB modeling approach (PEB of PEBs) that was applied to the DCM results. At the first level, a PEB model is generated for each subject to contrast their baseline and disconnected data. At the second level, a PEB of PEBs models the group level effect of sensory disconnection.

Each stimulus block was followed by a block of a different auditory tone, for a duration of 7 minutes. The first tone in a new block was classified as an auditory oddball while the 6th repetition of a tone was considered an auditory standard. The auditory stimuli were presented through a set of headphones using E-Prime (Psychology Software Tools, Inc., Pittsburgh, PA, USA). The volume of tones was calibrated to each participant's comfort level during the visit baseline. The paradigm was run a variable number of times for each subject through the sedation visit, interspersed between other study paradigms as time allowed. However, it was run at least once at baseline and per each drug infusion concentration.

EEG Data Acquisition, Processing, and ERP Extraction

High-density EEG data were collected using a NA300 EGI system with 256-channel gel-caps. Electrodes were manually prepared with application of electrolyte electrode gel to achieve electrode impedances below 50 kΩ. Data are recorded using EGI's Net Station Acquisition 5.4 software.

Subjects were allowed to rest with their eyes closed for up to 17 minutes (10 minutes of silence + 7 minutes of roving oddball paradigm) at a time without researcher intervention. Each rest period was concluded by a researcher calling the participant's name and initiating a brief structured interview which has been discussed in detail previously[11]. Briefly, participants were asked to recount the last thing going through their mind, whether they were awake or asleep, whether they were awake, dreaming, or unconscious, and whether they were aware of the external world around them. Participants who reported having an experience, being asleep, dreaming, and unaware of the world around them were considered to be in a state of disconnected consciousness. Participants who reported having an experience, being awake, and

aware of the world around them were considered to be in a state of connected consciousness. Reports of no experience and unconsciousness as well as conflicting reports that could not be confidently labeled were excluded from analysis.

All data processing was performed by a member of the research team experienced in EEG analysis but blinded to the conscious state, using EEGLab (v14.1.2b)[18]. Data were filtered between 1 and 30 Hz. Filtered data were visually inspected for noisy channels and noisy epochs, which were removed. Independent Components Analysis (ICA) were then computed using the InfoMax[19] algorithm and components dominated by eye movements or muscle artifacts were rejected. After these cleaning steps, data were average referenced, linearly detrended, and baseline corrected by subtracting the average amplitude over the 50 ms preceding each trial.

Scalp ERP Analysis

Grand-average ERPs were generated by averaging all trials for a particular tone-type (standard or oddball) and condition (baseline or disconnection). The baseline data, collected before dexmedetomidine administration, were used as the connected consciousness condition. This averaging procedure resulted in 4 ERPs: baseline-standard, baseline-oddball, disconnection-standard, and disconnection-oddball. Topographical views of each ERP over time were plotted using functions from FieldTrip toolbox (v20201229, https://www.fieldtriptoolbox.org/). An *a prioi* decision was made to make statistical comparisons between ERPs across time at electrode Cpz based on prior studies[16,20]. Statistical comparisons were made using within-subject permutations (n_{perm}=1000) of data labels (either tone-type or condition depending on the contrast) with significance defined based on a Welch t-statistic greater than 95% of t-statistics in the permutation-based null distribution. The null

distribution was constructed by storing the most extreme t-statistic, across all time points, from each permutation. Because the null distribution is based on the entire time window, the results of this test are inherently corrected for multiple-comparisons over timepoints[21]. Regions of significance, i.e. one or more significant sequential time point, are summarized in the results section using the maximum t-value within that range and its corresponding p-value. In cases where no significant differences are observed, a time range is reported and the maximum t-value/p-value are reported for that range. As an exploratory analysis, the same permutation testing was applied across all 256 electrodes. The resulting p-values were corrected for multiple comparisons across electrodes using the Benjamini-Hochberg false discovery rate procedure[22].

Dynamic Causal Modeling with Bayesian Model Selection

The DCM for ERPs framework, as implemented in SPM12 (*https://www.fil.ion.ucl.ac.uk/spm*), was used to estimate source level effective connectivity between brain regions in response to auditory stimulation. The DCM framework, as applied to EEG, may be conceptualized as a source reconstruction procedure with additional Bayesian priors, based on experimentally derived physiological constants, that constrain the estimation of the inverse model[13]. This model, based on biologically plausible neuronal architecture, allows for inferences to be made about the origins of the observed neural responses as well as the flow of information (effective connectivity) between those sources.

DCMs were fit using the ERP mode within SPM12, which models each source with three interacting subpopulations of neurons: pyramidal cells, spiny stellate cells, and inhibitory interneurons[13,23]. Within this framework, all extrinsic (between source) connections are modeled as excitatory, while the intrinsic (self-connections) are inhibitory. Models were fit to

the ERP data between 0 and 400 ms after stimulus onset using 8 empirical modes. Modulatory effects (B-matrix) were modeled using standards as the reference trials and oddballs as the change trials (i.e., standards = 0, oddballs = 1). The cortical surface (IMG) method was chosen for the electromagnetic model. The auditory stimulus was modeled as a Gaussian (M = 50, SD = 16) arriving at auditory cortex 50 ms after tone presentation based on SPM12 recommendations for auditory paradigms.

The model space investigated here (Fig. 3C) was based upon previously published work applying DCM to the auditory roving oddball paradigm[20,24–26]. This space consisted of 30 models (M1-M30) varying in their anatomical sources and connectivity. The full model (M30) consisted of left A1 (L-A1), right A1 (R-A1), left superior temporal gyrus (L-STG), right superior temporal gyrus (R-STG), left inferior frontal gyrus (L-IFG), and right inferior frontal gyrus (R-IFG) (Fig. 3A), with feedforward (FF), feedback (FB), lateral (Lat), and intrinsic (Self) connections. All connections included within a model were also allowed to be modulated differently by standard and oddball tones. M1-M29 are all subsets of M30.

The 30 model specifications were compared using random-effects Bayesian model selection (BMS). Each subject's baseline and disconnected consciousness data were modeled separately. Individual models and model families based on number of modeled regions (2, 4, 5, or 6) and connection types (None, FF, FF/FB, or FF/FB/Self) were compared. This procedure was applied to the baseline and disconnected data separately as well as pooled together.

Parametric Empirical Bayes (PEB)

Because M30 outperformed all other models regardless of how the data were subdivided, this model was selected for further analysis using PEB[27]. A within-subjects hierarchical approach[28] was applied (Fig. 1C); at the first level, each subject's disconnected consciousness and baseline DCMs were contrasted using PEB; at the second level, each subject's PEB model was used as input to a group level PEB (a PEB of PEBs) which tested for consistent group level effects. Both the 'A' and 'B' matrices were included in the PEB analysis, representing the effective connectivity observed in response to standards and the modulation of that connectivity by oddballs respectively. The contrast was specified such that positive values indicate parameters that were greater in the disconnected condition than in baseline, while negative values indicate the reverse. Parameters with a posterior probability of being non-zero of >95% were considered to have sufficient evidence for interpretation.

DCM Simulations

In order to test the relationship between the PEB and scalp ERP findings, we simulated scalp level ERPs of standard tone responses using DCMs with varying connectivity strengths. First, an average DCM (M30 architecture) was generated by averaging all data across subjects. PEB coefficients for the connection with >95% confidence of differing between disconnected and connected consciousness (Fig. 4A-B, yellow and purple connections) were then extracted for use in modifying the DCM connectivity strength. DCM connectivity strength was adjusted by adding multiples, from 1 to 4 by intervals of 0.1, of the PEB coefficients to the average parameter values and simulating scalp ERPs at electrode Cpz. More formally:

$$d_i = D + a_i(P \circ C) \quad \text{(Eq. 1)}$$

$$a_i = 1, 1.1, 1.2, \ldots, 4$$

Where, d_i is the new set of connectivity strengths, D is the set of connectivity strengths (A-matrix) from the average DCM, P is the set of PEB coefficients, C is a vector where $C_k = 1$ if P_k has >95% of differing between disconnected and connected consciousness and is 0 otherwise, and a_i is the current PEB scaling factor. The ∘ operator indicates the elementwise multiplication of P and C, such that only the coefficients with >95% confidence of difference will have non-zero values added to D. ERPs were simulated using SPM's 'spm_dcm_simulate' function. In essence, the DCM was iteratively pushed the direction of disconnected consciousness using PEB derived parameter scaling to observe the impact on simulated ERP waveforms. The choice of 1 to 4 was largely arbitrary and simply served as a way to find a range where all connections demonstrated linear scaling activity, making them easier to compare.

To test the impact of each connection on ERP morphology, one parameter was fixed at its average value while the other 8 were scaled by their PEB coefficients. The ERPs for each fixed parameter were compared to the ERPs generated when all 9 parameters were scaled to determine the impact of that parameter on P3 scaling. P3 amplitude was quantified by tracking the mean amplitude between 300-400 ms for each scaling factor. Due to the observation of consistent linear scaling between scaling factors of 1-3 (Fig. 5A, Supplementary Figure 3), P3 scaling was quantified as the slope of the P3 amplitude over scaling factor (from 1 to 3), calculated using linear regression. Lastly connections that showed an effect on simulated P3 scaling when they were fixed were evaluated in combination to determine which parameters were necessary or sufficient to produce the same degree of scaling observed when all 9 parameters were modulated.

Results

At baseline, 31 instances of connected consciousness (24.6% of all reports) were reported during the roving oddball paradigm, including reports by all 18 subjects. All baseline reports were of connected consciousness. 43 instances of disconnected consciousness (34.1% of all reports) were reported after sedation began, including reports from 17/18 subjects (i.e. one subject did not report any instances of disconnected consciousness during the sedation). Reports of unconsciousness (no experience) and reports that could not be confidently labeled, due to internally conflicting responses or loss of responsiveness, were not included in the analyses.

At baseline, oddball tones elicit pronounced N1 (~100 ms), N2 (~175 ms), and P3 (~250 ms) waveforms (Fig. 2A top, B top-left). In contrast, standard tones only reproducibly evoke an N1 component which is smaller in magnitude than that observed from oddball tones. The increased negative amplitude between 100-200 ms and positive amplitude between 200-300 ms observed in oddballs relative to standards produces a stereotyped mismatch negativity and P3 in the difference waveform respectively (Fig. 2B top-left black trace), consistent with prior literature[16,20]. Both the 100-200 ms (N2) and 200-300 ms (P3) periods show significant differences between oddballs and standards in the baseline condition (N2 oddballs vs standards: $t_{max} = 4.54$, $p = 0.001$, P3 oddballs vs standards $t_{max} = 6.32$, $p < 0.001$).

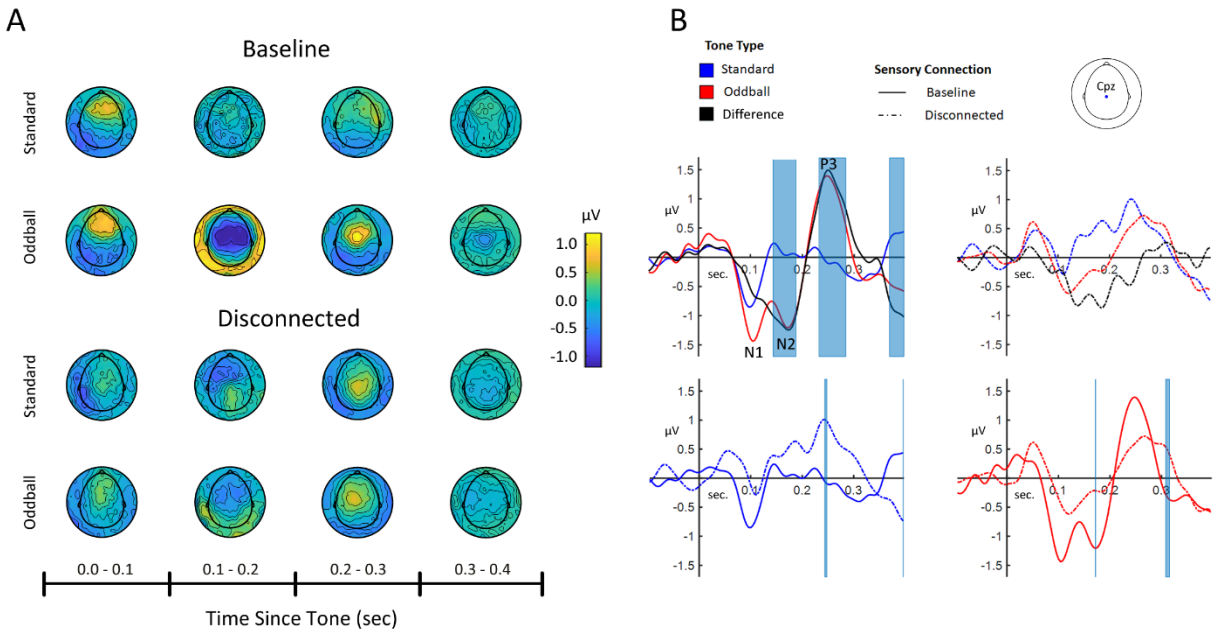

Figure 2. Scalp Event Related Potentials of Standards and Oddballs. A) Topographical view of scalp potentials over time (0 to 400ms) in response to standard and oddball tones in baseline and disconnected data. Plots represent grand averages across all subjects. B) ERPs over time at electrode Cpz (inset shows the location of this electrode on the scalp). Subplots show response to standards and oddballs at baseline (top-left) and during disconnection (top-right) as well as comparisons of baseline and disconnection response to standards (bottom-left) and oddballs (bottom-right). Blue highlighted regions indicate times where significant differences ($p < 0.05$) were observed between the contrasted conditions or tones based on permutation tests. The statistical contrasts were: top-left, baseline oddball vs baseline standard; top-right, disconnected oddball vs disconnected standard; bottom-left, disconnected standard vs baseline standard; bottom-right, disconnected oddball vs baseline oddball. N1, N2, and P3 components are labeled in the baseline condition. Note that "baseline" always refers to the pre-sedation data, *not* the pre-stimulus period of the ERP.

In contrast to the baseline ERPs, the disconnected consciousness data showed smaller amplitude responses to oddball tones (Fig. 2A bottom, B top-right). These oddball amplitudes were significantly smaller in disconnection compared to baseline during both the N2 (t_{max} = 3.39, p = 0.036) and P3 (t_{max} = 3.68, p = 0.020) periods (Fig. 2B bottom-right). Standard tones also showed a visual reduction in amplitude in disconnection compared to baseline at N1, though this was non-significant (t_{max} = 2.29, p = 0.624, 75-125 ms), and a significantly increased

amplitude for the P3 (t_{max} = 3.55, p = 0.038) component (Fig. 2B bottom-left). Notably, the addition of a P3 in response to standards during disconnection produced an ERP that resembled the oddball response during connected consciousness. In addition, oddballs and standards during periods of disconnected consciousness showed no significant differences (t_{max} = 1.38, p = 1.00, 0-400 ms) (Fig. 2B top-right). The loss of significance from baseline to disconnection cannot be explained away as a limitation of statistical power as we collected more disconnection data than baseline data and thus have greater power to detect a difference in this condition, making the absence of difference a conspicuous finding. Exploratory analyses evaluating the spatial distribution of these effects can be found in Supplementary Figure 1. These results demonstrate that the observed differences between oddballs and standards during baseline generalize across a wide range of centrally oriented electrodes (not just Cpz). Similarly, the observed lack of difference between standards and oddballs in disconnection also generalized, with no significant differences being found at any electrode.

To investigate the neural mechanisms underpinning the observed alterations in ERPs, we employed DCM to explore changes in effective connectivity (EC) between connected and disconnected consciousness. To establish the optimum model, we applied Bayesian model selection (BMS). BMS identified the fully connected model (M30) as having the greatest model evidence in both the baseline and disconnected data separately, as well as when they were pooled together (Fig. 3B, left column). Similarly, all subdivisions of data showed that models with all 6 regions of interest (ROIs) outperform model families with fewer regions, despite being more complex and thus more heavily penalized (Fig. 3B, middle column). Finally, models

containing FF, FB, and intrinsic self-modulation outperformed those with no connections, only FF connections,

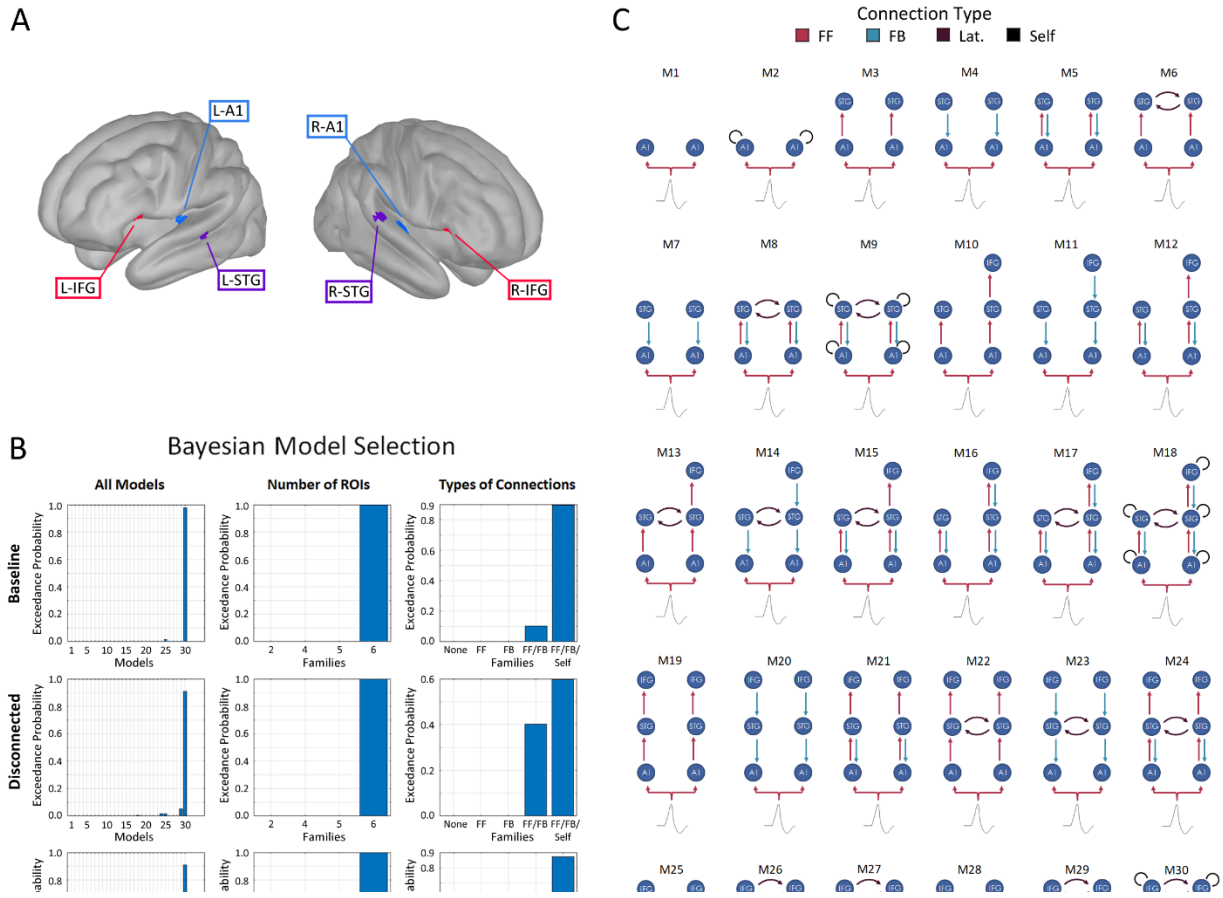

Figure 3. Bayesian Model Selection. A) 3D brain models showing the spatial location of each region of interest included in the DCM model space. The MNI coordinates used as source priors, presented as ROI [X, Y, Z], were L-A1 [-42, -22, 7], R-A1 [46, -14, 8], L-STG [-61, -32, 8], R-STG [59, -25, 8], L-IFG [-46, 20, 8], and R-IFG [46, 20, 8]. B) Exceedance probabilities for each model specification indicating how much relative evidence there is for each model. BMS results are shown for the baseline data alone (top row), the disconnected data alone (middle row), and all the data pooled together (bottom row). In addition to the individual models (left column), we present family-level evidence based on the number of ROIs (middle column), and the types of connections included in the models (right column). C) Model specifications for all 30 models included in the BMS model space.

only FB connections, and FF and FB connections (without self-modulation), in all subdivisions (Fig. 3B right column).

Due to M30 outperforming all other models by a large margin, we selected this model for further analysis of individual parameters using PEB. Interestingly, all FB connections showed increased connectivity in response to standard tones in disconnection relative to baseline (Fig. 4A-B). We also observed two connections with a higher response to standard tones in the baseline condition: a FF connection between L-STG and L-IFG and a lateral connection from R-STG to L-STG. The modulation of connection strength by oddball tones showed a predominance of connections with greater connectivity during sensory disconnection, including all but one of the FF connections but none of the feedback connections (Fig. 4C-D). Again, two connections showed higher oddball modulation in the baseline condition: a FB connection from R-IFG to R-STG and a lateral connection from L-STG to R-STG.

In order to understand how these PEB results relate to the prior scalp ERP findings, namely the emergence of a P3 in response to standard tones during disconnection, we simulated scalp ERPs for standard tones, at Cpz, using an average DCM (averaged across subjects). When DCM connectivity strengths were modulated by adding multiples of the PEB coefficients (Fig. 4A-B, only yellow and purple connections), we observed increased amplitudes in the P3 range (300-400 ms) (Fig. 5A left). This scaling of simulated ERPs as a function of PEB scaling factor was used as the reference for the subsequent simulation analyses.

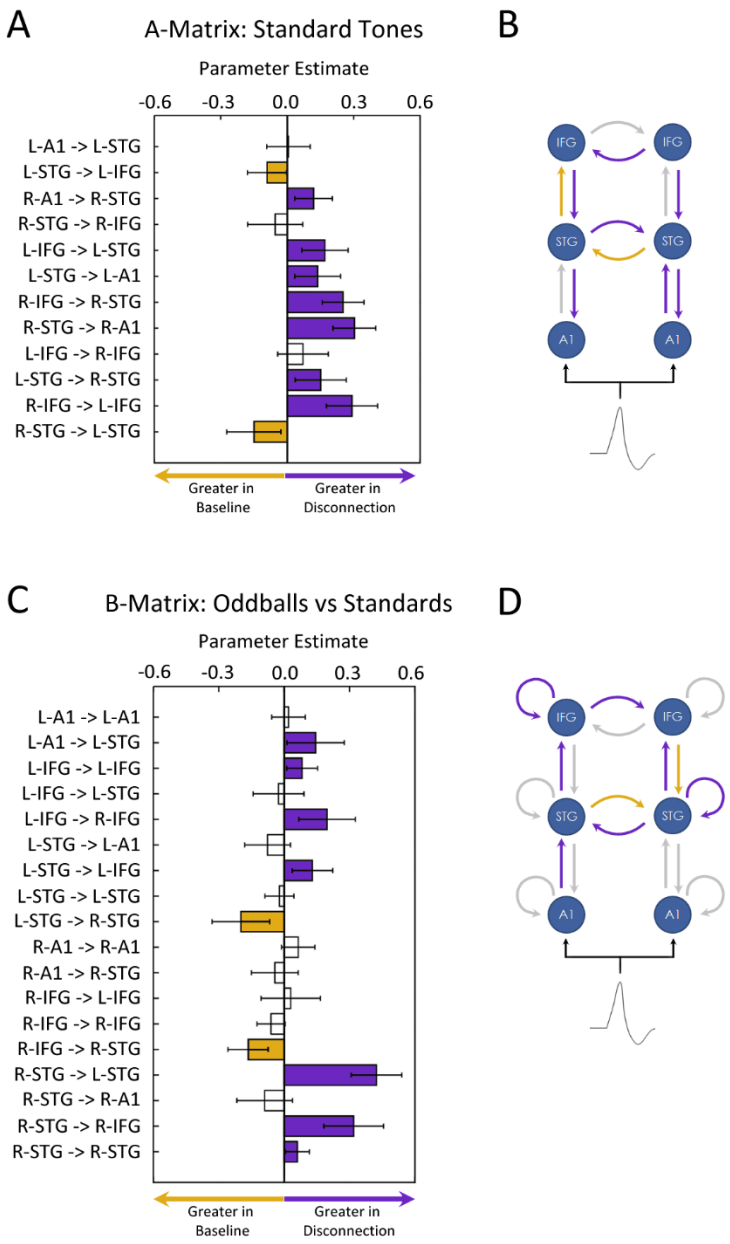

Figure 4. PEB Changes Associated with Sensory Disconnection. A) Final PEB model results (corresponding to Fig. 1C top level) for the A-matrix, modeling the difference in response to standard tones in disconnection compared to baseline. Negative values indicate a greater response in baseline while positive values indicate greater response with disconnection. Parameters estimated as different from 0 with >95% confidence are color filled yellow if negative or purple if positive. B) Model architecture of M30 with connections colored to match the A-matrix PEB results seen in **A**. As before, purple arrows indicated connections greater in disconnection compared to baseline (>95% confidence), while yellow arrows indicate connections greater in baseline compared to disconnection (>95% confidence). C) Same as **A** but illustrating results from the B-matrix, representing the difference in oddball vs standard effect in disconnection compared to baseline. D) Same as **B** but results correspond to the B-matrix.

To determine which model connections contributed to the observed P3 emergence, we repeated the same PEB scaling simulations with a different parameter being fixed at its average value each time. Changes in P3 morphology (shape and amplitude) were observed when R-A1 to R-STG, R-IFG to R-STG, and R-STG to R-A1 were fixed at their average values (Supplementary Figure 2). The most notable changes being observed when R-STG to A1 was fixed and P3 scaling was greatly reduced. These changes in P3 scaling were quantified by examining changes in the P3 scaling slope (Supplementary Figure 3) relative to the reference (Fig. 5A right). When fixed to their average values, we observed reductions in P3 scaling, relative to reference, of 22.6%, 32.9%, and 77.7% for R-A1 to R-STG, R-IFG to R-STG, and R-STG to R-A1, respectively (Fig. 5B). Lastly, we scaled the DCM connectivity strengths using all combinations of these three connections, but fixing all others to their average, to determine which connection(s) would be necessary or sufficient to produce the reference P3 scaling (Supplementary Figures 4-5). Only when all three connections were modulated did we observe the full scaling effect, 102% of reference (Fig. 5C). Notably scaling only R-STG to R-A1 was sufficient to produce 55.3% of the reference scaling, while scaling R-A1 to R-STG and R-IFG to R-STG together (without R-STG to R-A1) only produced 22.1% of reference scaling.

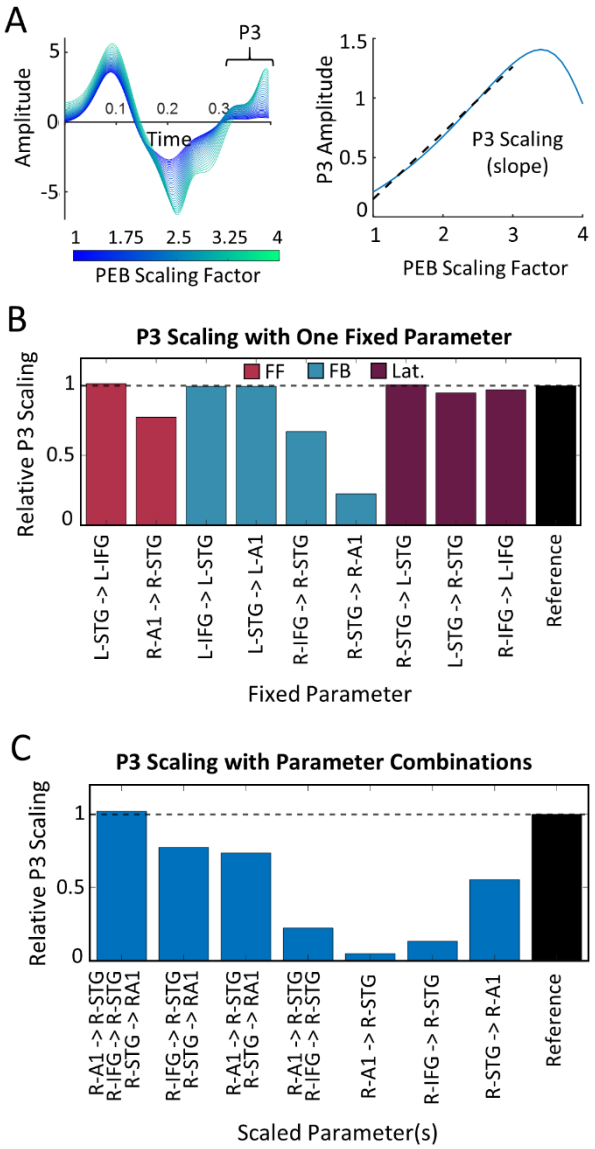

Figure 5. Impact of DCM Connectivity Strength on P3 Scaling. A) (Left) Simulated ERPs at electrode Cpz generated from an averaged DCM model with connectivity strengths modulated based on PEB coefficients for the 9 parameters with >95% confidence of differing between baseline and disconnection. (Right) P3 amplitude (averaged between 300-400 ms) vs the scaling factor the PEB coefficients were multiplied by. Black dashed line shows the regression line calculated from scaling factors between 1 and 3. The slope of this line is used as the Reference P3 Scaling. B) P3 scaling observed when 8 parameters are scaled and 1 is fixed at the average. Data are normalized to the reference (shown in **A**). Values less than 1 indicate a reduction in P3 scaling when that parameter is not scaled. Bars color coded by the type of connection: feedforward (red), feedback (green-blue), lateral (purple). C) P3 scaling, relative to reference, when *only* the x-axis parameters are scaled by their PEB coefficients. All other coefficients are fixed at their averages. Values less than 1 indicate a given parameter combination is insufficient for producing the full P3 scaling effect.

Discussion

The aim of this work was to assess perturbations in predictive processing within auditory pathways that may explain how the conscious brain handles sensory input when connected to the environment vs disconnected from the environment. Our results demonstrate that disconnected consciousness is associated with altered responses to both expected (standard tones) and unexpected (oddball tones) stimuli and that these differences may be explained by changes in connectivity within auditory networks. This study advances our understanding of the mechanisms the brain may use to achieve a state of disconnection from the environment.

Our scalp level ERP data show that disconnected consciousness is associated with a loss of discriminability between standard and oddball tones. Notably, the response to standards during disconnection looks remarkably similar to the oddball response. This similarity arises from the addition of a P3 component in response to standard tones (Fig. 2B bottom-left) and a loss of N2 amplitude in response to oddball tones (Fig. 2B bottom-right). This finding is quite striking as the P3 is typically associated with stimulus perception and involuntary attention recruitment[29–31]. This interpretation of the P3 does not align with the current sensory disconnection data where the subjects, by definition, did not consciously perceive or attend to the tones. It should also be noted that the P3 response has been shown to correlate with how unexpected the stimulus is[32,33]. Viewing the P3 as an index of expectation, the finding of a P3 in response to standard tones could be interpreted as a loss of neural habituation in response to repeated stimuli. In essence, the similar neural response to standards and oddballs suggests

that in a state of disconnected consciousness, every stimulus is surprising due to a mismatch in internally generated predictions and externally generated stimuli.

It has been proposed that the auditory N2 consists of overlapping, but distinct, ERP components, namely the N2a and N2b[29,31]. Both components are triggered by deviant stimuli but the N2a does not require conscious perception of deviance while the N2b does[29,34]. The observed loss of N2 amplitude during disconnection is thus consistent with loss of the N2b. We have previously hypothesized that higher order thalamus (e.g. the pulvinar) plays a key role in mediating sensory disconnection via control of precision weighting of error signals[15]. We suggest that reduced precision weighting, and thus reduced cortical gain, in response to sensory signals could explain the loss of N2b. Lower precision weighting of sensory signals is also consistent with the view that standards and oddballs become similarly surprising. Low precision information should not be given undue weight when updating one's model predictions about the world as it is not very trustworthy. Loss of model updating would result in a loss of habituation to repeated tones, thus even tones that have been heard many times before would remain surprising. However, the stage of information processing within the cortical hierarchy at which perturbations (potentially through precision weighting) are impacting the ERPs is not clear based on scalp level analysis alone.

Our use of DCM begins to address the question of where in the processing hierarchy information transfer is being perturbed. The BMS results show that both sensory connected and disconnected states are best represented by a 6-ROI model containing FF, FB, lateral, and self-connections. This implies that, though signaling within the network may be altered, there is not a complete breakdown of its fundamental functional architecture during disconnection. The

family-level analysis further highlights that no class of connection types (FF, FB, or Self) is systematically lost in disconnected consciousness. Though there is a reduced exceedance probability for the FF/FB/Self family relative to FF/FB in disconnection compared to baseline, caution should be taken in interpreting this result as model evidence is only comparable when the models have been fitted to the same data[14].

While BMS informs us about the general model architecture, PEB gives us deeper insight into the 'between-conditions' differences within an established model. Rather than observing a loss of EC, as one might expect for a state defined by loss of sensory connectedness, we observe a predominance of connections with increased parameter estimates in the disconnected consciousness data. In particular, we observed increased EC in all FB connections in disconnection relative to baseline (Fig. 4A-B). This finding is of particular note in the context of the previously mentioned P3 response to standard tones. Previous modeling work has demonstrated that the late components of the oddball ERP are dependent on FB connections[25]. Therefore, the increased FB connectivity appears a likely explanation for the emergence of a standard P3 during disconnected consciousness. The evaluation of this possibility through ERP simulations is discussed further below.

The modulation of connectivity by oddball tones shows perturbation across a bilateral frontotemporal network for which R-STG appears to be a key hub (Fig. 4D). We observed increased connectivity from R-STG to R-IFG both directly and indirectly (R-STG to L-STG, L-STG to L-IFG, and L-IFG to R-IFG) during disconnected consciousness. At the same time, we observed reductions in FB connectivity from R-IFG to R-STG and lateral input from L-STG to R-STG. Together these changes point to a shift in the balance of information flow at the level of the R-

STG towards more outflow and less inflow. The exact implications of this altered frontotemporal network during disconnected consciousness are not obvious but merit further investigation as it may represent a physiological substrate of sensory disconnection.

The above PEB findings seemed a likely explanation for the observed P3 response to standard tones during disconnection, however, based on these two separate analyses, it is unclear which changed connection(s) may contribute to the effect. Our simulation analyses link our scalp ERP and PEB findings by demonstrating that a subset of connections contribute to P3 amplitude while the majority do not. Namely, FF connectivity from R-A1 to R-STG, and FB connectivity from R-STG to R-A1 and from R-IFG to R-STG play important roles in the increased P3 amplitude observed when DCM EC strengths were scaled by their disconnection PEB parameters (Fig. 5B). Furthermore, these three connections together are sufficient to produce comparable P3 scaling as a model where all 9 connections are modulated (Fig. 5C). Conversely, leaving out any one of these three parameters results in reduced P3 scaling compared to the reference. These three connections do not contribute equally, however. FB from R-STG to R-A1 was sufficient to produce 55.3% of the reference scaling, but R-A1 to R-STG and R-IFG to R-STG together could only produce 22.1% of reference scaling. This suggests that while FB from R-STG to R-A1 is the primary driver of P3 emergence, R-A1 to R-STG and R-IFG to R-STG play synergistic roles, resulting in a P3 larger than the sum of their parts.

We previously proposed a model in which sensory disconnection is defined by a reduction in FF connectivity with maintenance of FB connectivity[15]. The relative excess of FB over FF signaling, we argued, would explain the phenomenological state of dreaming (disconnected consciousness), where conscious experience is internally driven and not related

to the external world. While we hypothesized that sensory disconnection would be associated with a reduction of FF connectivity, our data indicated that this was generally not the case. In fact, only one connection showed lower FF connectivity in disconnection compared to baseline: the standard response from R-STG to R-IFG. Rather, our findings suggest that sensory disconnection is associated with an *increase* in *FB* connectivity in response to standard stimuli. Interestingly, the end result of increased FB connectivity, with preserved FF connectivity, could be qualitatively similar to a loss of FF connectivity with preserved FB connectivity. In both cases, a state where FB signaling dominates is achieved. We suggest that new information is still being passed forward to the cortex (through FF connections), however, the brain's internally generated experience (communicated through FB connections) predominates through a relative enhancement of FB precision compared to FF precision; preserving the integrity of the endogenous state. Hence, each standard tone is a surprising event as it is mismatched to the internal model of the world (the dream), which we argue is supported by the finding of a P3 in response to standard tones. This interpretation also appears consistent with the recently proposed 'apical drive' hypothesis of dreaming[35]. This hypothesis states that dreaming (disconnected consciousness) occurs when input to the apical dendrites, carrying feedback signals, of layer-5 pyramidal neurons are able to directly drive spiking activity at the cell body. This in contrast to normal cellular behavior found during wake (connected consciousness), where apical inputs only selectively amplify the neuronal response to somatic inputs carrying information about the environment. The observed increased FB connectivity may represent a state of apical drive. Whether all brain regions respond in a homogenous manner however remains to be determined.

Physiologically, dexmedetomidine acts as an α2-adrenergic receptor agonist which inhibits noradrenaline release from the locus coeruleus (LC), producing a state similar to physiological sleep[36,37]. LC activity can be tonic or phasic, with tonic activity tracking general level of arousal (and causally impacting sensory evoked awakenings[38]) and phasic activity occurring in response to unexpected stimuli[38–40]. Indeed, phasic activity in the LC has been suggested to code for prediction errors[41] and such phasic activity can still be elicited during sleep, when tonic activity is low[38]. Multiple models have been proposed in which phasic LC activity plays a key role in facilitating internal prediction updates in response to new information[42–44]. Finally, phasic LC activity has been previously linked to P3 generation[45]. Together, these findings are consistent with a model of sensory disconnection as a state of low tonic but evocable phasic LC activity. This phasic activity, however, is no longer coupled to successful prediction updates. This hypothesis could be further tested in animal models, sedated with an α2-adrenergic receptor agonist, by recording LC activity in response to an oddball paradigm. If this model is correct, we would expect to find similar phasic LC activity in response to standards and oddballs in the sedated animals.

We note that while we interpret the disconnected standard P3 as evidence of the stimulus becoming surprising and that the increase in FB connectivity during disconnection could explain *why* the stimulus is surprising, not all FB connections appear to contribute to the P3. FB from R-IFG to R-STG and from R-STG to R-A1 were critical for P3 emergence in our simulation analyses, but the left hemisphere connections were not. FF from R-A1 to R-STG also played a role, though this connection seems to have the smallest contribution of the three. The observation that only right hemispheric connections contribute to P3 scaling is not necessarily a

surprising one, as many prior studies have demonstrated right lateralized dominance in auditory processing[46–51]. This appears to be especially common for tasks that don't require much language processing demand or that do require precise frequency monitoring[46,52], both of which are qualities of the roving oddball paradigm. As such, it seems reasonable that P3 generation under this paradigm would also be right lateralized.

As with all research, the current study has several limitations. One major limitation in this field is the lack of accurate objective markers of sensory awareness vs consciousness. Because of this, we relied on subjective reports from each subject as the ground truth of their experience. While subjective reports have limitations due to the possibility of human error in assessing one's own mental state, using such methods are currently the only way to separate out disconnected consciousness and unconsciousness, which is critical for this research. In a related vein, we are limited by our inability to experimentally *assign* subjects to a disconnected consciousness condition. Using pharmacological intervention, we can bias subjects to states of either disconnected consciousness or unconsciousness, but we cannot directly control which state they will enter. Because of this, different subjects will report being in a state of disconnected consciousness more or less frequently than others, resulting in unequal amounts of disconnection data for each subject. Fortunately, the Bayesian framework that DCM is built upon mitigates the consequences of this issue. Each subject's DCM contains not only the prior estimate of each parameter, but also the full posterior distribution. This allows group level analyses, like PEB, to weight each model based on the confidence of parameter estimates when estimating the whole group effect. We also acknowledge that while we propose thalamic controlled precision weighting as a plausible mechanism to explain our findings, imaging

modalities with better spatial accuracy, such as fMRI, would be better suited to testing this hypothesis as EEG is known to have poor accuracy and sensitivity when estimating source activity in deep subcortical structures[53–55].

In the current work, we experimentally isolated sensory connectedness by controlling for conscious experience in our contrasting conditions (participants were conscious in both groups). By capitalizing on recent advances in the generative modeling technique of DCM, we demonstrate that sensory disconnection is associated with an increase of FB connectivity within the auditory processing network in response to standard (predictable) tones, while oddball (unpredictable) tones elicit altered information flow within a frontotemporal subnetwork consisting of bilateral STG and IFG. We also demonstrate that a subset of connections showing altered response to standard tones during disconnection can explain the emergence of a P3 (surprise) response observed in the scalp ERP data. We interpret these DCM results together with our ERP findings as evidence that disconnected consciousness is associated with a breakdown in predictive coding processes, resulting in all incoming stimuli being 'surprising' from a neuronal perspective. These findings provide useful targets for future study on the mechanisms of sensory disconnection and may develop into clinically relevant biomarkers of awareness for use in anesthetic monitoring.

Author Contributions

RDS initiated the study and designed the experiments. The study was managed by RDS and RAP. CPC, ZF, ST, MP, AB, MW, TB, AM, and RDS collected EEG and wake report data. WF and RDS administered the anesthesia. CPC, YBS, RAP, MIB, and RDS designed the data analytic approaches which were conducted by CPC. CPC and RDS prepared the manuscript

Acknowledgments

We are grateful to advice from Prof Giulio Tononi, Dr. Brady Riedner, Dr David Plante and Dr. Melanie Boly (University of Wisconsin, USA) when setting up this project and for loan of the EEG equipment.

Competing Interests

The authors have no competing interests to declare.

Funding

This work was supported by the Department of Anesthesiology at the University of Wisconsin and by NIH NIND 1R01NS117901-01

References

1. Weiser TG, Haynes AB, Molina G, et al. Estimate of the global volume of surgery in 2012: an assessment supporting improved health outcomes. *The Lancet*. 2015;385:S11. doi:10.1016/S0140-6736(15)60806-6
2. Meara JG, Leather AJM, Hagander L, et al. Global Surgery 2030: Evidence and solutions for achieving health, welfare, and economic development. *The Lancet*. 2015;386(9993):569-624. doi:10.1016/S0140-6736(15)60160-X
3. Sanders RD, Gaskell A, Raz A, et al. Incidence of Connected Consciousness after Tracheal Intubation: A Prospective, International, Multicenter Cohort Study of the Isolated Forearm Technique. *Anesthesiology*. 2017;126(2):214-222. doi:10.1097/ALN.0000000000001479
4. Lennertz R, Pryor KO, Raz A, et al. Connected consciousness after tracheal intubation in young adults: an international multicentre cohort study. *Br J Anaesth*. Published online May 23, 2022. doi:10.1016/J.BJA.2022.04.010
5. Ku SW, Lee U, Noh GJ, Jun IG, Mashour GA. Preferential Inhibition of Frontal-to-Parietal Feedback Connectivity Is a Neurophysiologic Correlate of General Anesthesia in Surgical Patients. Ward LM, ed. *PLoS One*. 2011;6(10):e25155. doi:10.1371/journal.pone.0025155

6. Noreika V, Jylhänkangas L, Móró L, et al. Consciousness lost and found: Subjective experiences in an unresponsive state. *Brain Cogn*. 2011;77(3):327-334. doi:10.1016/j.bandc.2011.09.002

7. Lee U, Ku S, Noh G, Baek S, Choi B, Mashour GA. Disruption of frontal-parietal communication by ketamine, propofol, and sevoflurane. *Anesthesiology*. 2013;118(6):1264-1275. doi:10.1097/ALN.0b013e31829103f5

8. Blain-Moraes S, Tarnal V, Vanini G, et al. Neurophysiological Correlates of Sevoflurane-induced Unconsciousness. *Anesthesiology*. 2015;122(2):307. doi:10.1097/ALN.0000000000000482

9. Purdon PL, Pierce ET, Mukamel EA, et al. Electroencephalogram signatures of loss and recovery of consciousness from propofol. *Proceedings of the National Academy of Sciences*. 2013;110(12):E1142-E1151. doi:10.1073/PNAS.1221180110

10. Sanders RD, Tononi G, Laureys S, Sleigh JW. Unresponsiveness ≠ unconsciousness. *Anesthesiology*. 2012;116(4):946-959. doi:10.1097/ALN.0b013e318249d0a7

11. Casey CP, Tanabe S, Farahbakhsh Z, et al. Distinct EEG signatures differentiate unconsciousness and disconnection during anaesthesia and sleep. *Br J Anaesth*. Published online February 9, 2022. doi:10.1016/J.BJA.2022.01.010

12. Friston KJ, Harrison L, Penny W. Dynamic causal modelling. *Neuroimage*. 2003;19(4):1273-1302. doi:10.1016/S1053-8119(03)00202-7

13. Kiebel SJ, Garrido MI, Moran RJ, Friston KJ. Dynamic causal modelling for EEG and MEG. *Cogn Neurodyn*. 2008;2(2):121-136. doi:10.1007/s11571-008-9038-0

14. Stephan KE, Penny WD, Moran RJ, den Ouden HEM, Daunizeau J, Friston KJ. Ten simple rules for dynamic causal modeling. *Neuroimage*. 2010;49(4):3099-3109. doi:10.1016/j.neuroimage.2009.11.015

15. Sanders RD, Casey C, Saalmann YB. Predictive coding as a model of sensory disconnection: relevance to anaesthetic mechanisms. *Br J Anaesth*. 2021;126(1):37-40. doi:10.1016/j.bja.2020.08.017

16. Garrido MI, Kilner JM, Kiebel SJ, Stephan KE, Friston KJ. Dynamic causal modelling of evoked potentials: A reproducibility study. *Neuroimage*. 2007;36(3):571-580. doi:10.1016/j.neuroimage.2007.03.014

17. Garrido MI, Friston KJ, Kiebel SJ, Stephan KE, Baldeweg T, Kilner JM. The functional anatomy of the MMN: A DCM study of the roving paradigm. *Neuroimage*. 2008;42(2):936-944. doi:10.1016/j.neuroimage.2008.05.018

18. Delorme A, Makeig S. EEGLAB: An open source toolbox for analysis of single-trial EEG dynamics including independent component analysis. *J Neurosci Methods*. 2004;134(1):9-21. doi:10.1016/j.jneumeth.2003.10.009

19. Bell AJ, Sejnowski TJ. An information-maximization approach to blind separation and blind deconvolution. *Neural Comput*. 1995;7(6):1129-1159. doi:10.1162/neco.1995.7.6.1129

20. Boly M. Preserved Feedforward But Impaired Top-Down Processes in the Vegetative State. *Science (1979)*. 2011;46(5896):1-25. doi:10.1126/science.1245938

21. Groppe DM, Urbach TP, Kutas M. Mass univariate analysis of event-related brain potentials/fields I: A critical tutorial review. *Psychophysiology*. 2011;48(12):1711-1725. doi:10.1111/j.1469-8986.2011.01273.x

22. Benjamini Y, Hochberg Y. Controlling the False Discovery Rate: A Practical and Powerful Approach to Multiple Testing. *Journal of the Royal Statistical Society: Series B (Methodological)*. 1995;57(1):289-300. doi:10.1111/J.2517-6161.1995.TB02031.X

23. David O, Harrison L, Friston KJ. Modelling event-related responses in the brain. *Neuroimage*. 2005;25(3):756-770. doi:10.1016/J.NEUROIMAGE.2004.12.030

24. Garrido MI, Friston KJ, Kiebel SJ, Stephan KE, Baldeweg T, Kilner JM. The functional anatomy of the MMN: A DCM study of the roving paradigm. *Neuroimage*. 2008;42(2):936-944. doi:10.1016/j.neuroimage.2008.05.018

25. Garrido MI, Kilner JM, Kiebel SJ, Friston KJ. Evoked brain responses are generated by feedback loops. *Proc Natl Acad Sci U S A*. 2007;104(52):20961-20966. doi:10.1073/pnas.0706274105

26. Rosch RE, Auksztulewicz R, Leung PD, Friston KJ, Baldeweg T. Selective Prefrontal Disinhibition in a Roving Auditory Oddball Paradigm Under N-Methyl-D-Aspartate Receptor Blockade. *Biol Psychiatry Cogn Neurosci Neuroimaging*. 2019;4(2):140. doi:10.1016/J.BPSC.2018.07.003

27. Friston KJ, Litvak V, Oswal A, et al. Bayesian model reduction and empirical Bayes for group (DCM) studies. *Neuroimage*. 2016;128:413-431. doi:10.1016/J.NEUROIMAGE.2015.11.015

28. Zeidman P, Jafarian A, Seghier ML, et al. A guide to group effective connectivity analysis, part 2: Second level analysis with PEB. *Neuroimage*. 2019;200:12-25. doi:10.1016/J.NEUROIMAGE.2019.06.032

29. Fitzgerald K, Todd J. Making Sense of Mismatch Negativity. *Front Psychiatry*. 2020;11:468. doi:10.3389/FPSYT.2020.00468/BIBTEX

30. Friedman D, Cycowicz YM, Gaeta H. The novelty P3: an event-related brain potential (ERP) sign of the brain's evaluation of novelty. *Neurosci Biobehav Rev*. 2001;25(4):355-373. doi:10.1016/S0149-7634(01)00019-7

31. Patel SH, Azzam PN. Characterization of N200 and P300: Selected Studies of the Event-Related Potential. *Int J Med Sci*. 2005;2(4):147. doi:10.7150/IJMS.2.147

32. Ravden D, Polich J. Habituation of P300 from visual stimuli. *International Journal of Psychophysiology*. 1998;30(3):359-365. doi:10.1016/S0167-8760(98)00039-7

33. Romero R, Polich J. P3(00) habituation from auditory and visual stimuli. *Physiol Behav*. 1996;59(3):517-522. doi:10.1016/0031-9384(95)02099-3

34. Sams M, Paavilainen P, Alho K, Näätänen R. Auditory frequency discrimination and event-related potentials. *Electroencephalography and Clinical Neurophysiology/Evoked Potentials Section*. 1985;62(6):437-448. doi:10.1016/0168-5597(85)90054-1

35. Aru J, Siclari F, Phillips WA, Storm JF. Apical drive—A cellular mechanism of dreaming? *Neurosci Biobehav Rev*. 2020;119:440-455. doi:10.1016/j.neubiorev.2020.09.018

36. HUUPPONEN E, MAKSIMOW A, LAPINLAMPI P, et al. Electroencephalogram spindle activity during dexmedetomidine sedation and physiological sleep. *Acta Anaesthesiol Scand*. 2008;52(2):289-294. doi:10.1111/J.1399-6576.2007.01537.X

37. Purdon PL, Sampson A, Pavone KJ, Brown EN. Clinical electroencephalography for anesthesiologists. *Anesthesiology*. 2015;123(4):937-960. doi:10.1097/ALN.0000000000000841

38. Hayat H, Regev N, Matosevich N, et al. Locus coeruleus norepinephrine activity mediates sensory-evoked awakenings from sleep. *Sci Adv*. 2020;6(15). doi:10.1126/sciadv.aaz4232

39. Rajkowski J, Kubiak P, Aston-Jones G. Locus coeruleus activity in monkey: Phasic and tonic changes are associated with altered vigilance. *Brain Res Bull*. 1994;35(5-6):607-616. doi:10.1016/0361-9230(94)90175-9

40. Aston-Jones G, Bloom FE. Activity of norepinephrine-containing locus coeruleus neurons in behaving rats anticipates fluctuations in the sleep-waking cycle. *Journal of Neuroscience*. 1981;1(8):876-886. doi:10.1523/JNEUROSCI.01-08-00876.1981

41. Ferreira-Santos F. The role of arousal in predictive coding. *Behavioral and Brain Sciences*. 2016;39:e207. doi:10.1017/S0140525X15001788

42. Aston-Jones G, Cohen JD. An integrative theory of locus coeruleus-norepinephrine function: adaptive gain and optimal performance. *Annu Rev Neurosci*. 2005;28:403-450. doi:10.1146/ANNUREV.NEURO.28.061604.135709

43. Bouret S, Sara SJ. Network reset: a simplified overarching theory of locus coeruleus noradrenaline function. *Trends Neurosci*. 2005;28(11):574-582. doi:10.1016/J.TINS.2005.09.002

44. Sales AC, Friston KJ, Jones MW, Pickering AE, Moran RJ. Locus Coeruleus tracking of prediction errors optimises cognitive flexibility: An Active Inference model. *PLoS Comput Biol*. 2019;15(1):e1006267. doi:10.1371/JOURNAL.PCBI.1006267

45. Nieuwenhuis S, Aston-Jones G, Cohen JD. Decision making, the P3, and the locus coeruleus-norepinephrine system. *Psychol Bull*. 2005;131(4):510-532. doi:10.1037/0033-2909.131.4.510

46. Zatorre RJ, Belin P, Penhune VB. Structure and function of auditory cortex: music and speech. *Trends Cogn Sci*. 2002;6(1):37-46. doi:10.1016/S1364-6613(00)01816-7

47. Boemio A, Fromm S, Braun A, Poeppel D. Hierarchical and asymmetric temporal sensitivity in human auditory cortices. *Nature Neuroscience 2005 8:3*. 2005;8(3):389-395. doi:10.1038/nn1409

48. Abrams DA, Nicol T, Zecker S, Kraus N. Right-Hemisphere Auditory Cortex Is Dominant for Coding Syllable Patterns in Speech. *Journal of Neuroscience*. 2008;28(15):3958-3965. doi:10.1523/JNEUROSCI.0187-08.2008

49. Abrams DA, Nicol T, Zecker S, Kraus N. Abnormal Cortical Processing of the Syllable Rate of Speech in Poor Readers. *Journal of Neuroscience*. 2009;29(24):7686-7693. doi:10.1523/JNEUROSCI.5242-08.2009

50. Telkemeyer S, Rossi S, Koch SP, et al. Sensitivity of Newborn Auditory Cortex to the Temporal Structure of Sounds. *Journal of Neuroscience*. 2009;29(47):14726-14733. doi:10.1523/JNEUROSCI.1246-09.2009

51. Doelling KB, Arnal LH, Ghitza O, Poeppel D. Acoustic landmarks drive delta–theta oscillations to enable speech comprehension by facilitating perceptual parsing. *Neuroimage*. 2014;85:761-768. doi:10.1016/J.NEUROIMAGE.2013.06.035

52. Assaneo MF, Rimmele JM, Orpella J, Ripollés P, de Diego-Balaguer R, Poeppel D. The lateralization of speech-brain coupling is differentially modulated by intrinsic auditory and top-down mechanisms. *Front Integr Neurosci*. 2019;13:28. doi:10.3389/FNINT.2019.00028/XML/NLM

53. Piastra MC, Nüßing A, Vorwerk J, Clerc M, Engwer C, Wolters CH. A comprehensive study on electroencephalography and magnetoencephalography sensitivity to cortical and subcortical sources. *Hum Brain Mapp*. 2021;42(4):978. doi:10.1002/HBM.25272

54. Attal Y, Schwartz D. Assessment of Subcortical Source Localization Using Deep Brain Activity Imaging Model with Minimum Norm Operators: A MEG Study. *PLoS One*. 2013;8(3):e59856. doi:10.1371/JOURNAL.PONE.0059856

55. Hillebrand A, Barnes GR. A Quantitative Assessment of the Sensitivity of Whole-Head MEG to Activity in the Adult Human Cortex. *Neuroimage*. 2002;16(3):638-650. doi:10.1006/NIMG.2002.1102

SUMMARY, LIMITATIONS, AND FUTURE DIRECTIONS

Summary

Within the previous chapters of this dissertation, I describe data collected and analyzed under the UNderstanding Consciousness Connectedness and Intra-Operative Unresponsiveness Study (UN-ConsCIOUS) in order to disentangle the EEG signatures of unconsciousness from sensory disconnection.

In Chapter 1 (Fig. 1 top row), I explored the anatomical signatures of disconnection and unconsciousness using frequency-based analysis of resting state EEG activity in source space. These analyses demonstrated that connected and disconnected consciousness differ across a wide range of frequency bands throughout the brain while loss of consciousness is associated with focal changes in the ratio of beta/delta activity, particularly within the anterior and posterior cingulate cortex (ACC & PCC). These signatures also generalized across dexmedetomidine and propofol sedation, as well as natural sleep, indicating specificity to unconsciousness rather than experimental condition.

In Chapter 2 (Fig. 1 middle row), I evaluated a selection of ten putative markers of unconsciousness that have been previously published under the assumption that anesthetized and unresponsive participants are unconscious. This work showed that some proposed markers of unconsciousness are actually specific to sensory disconnection. Several markers did show significant associations with loss of consciousness even while statistically adjusting for the effect of disconnection, however, none of these markers were specific to loss of consciousness, i.e. each marker that showed an effect related to unconsciousness was also related to disconnection. These findings indicate that a substantial number of effects published as being

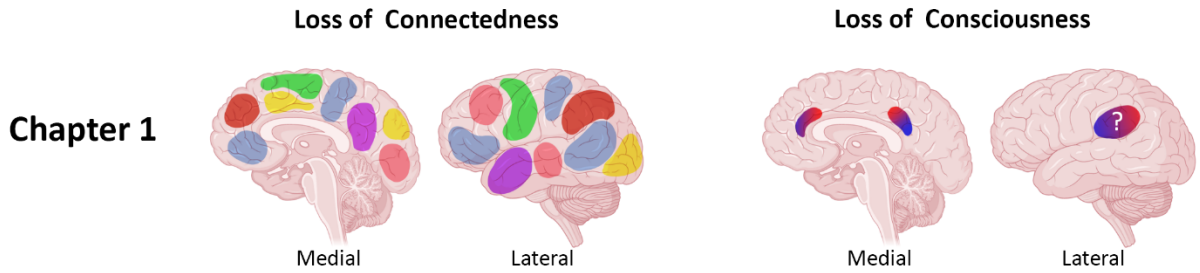

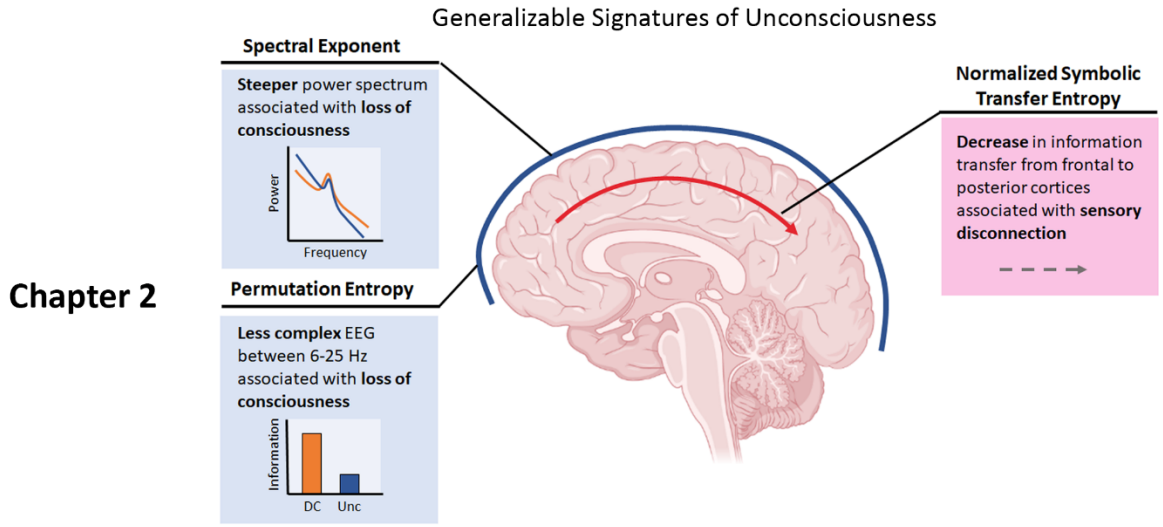

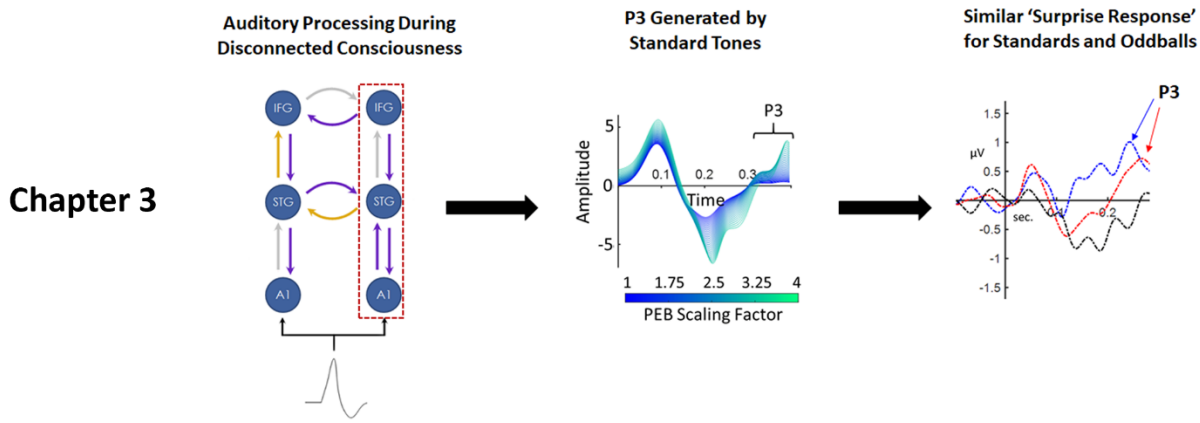

(See next page for figure legend.)

Figure 1. Summary of major findings (Top) Loss of connectedness was found to be associated with changes in multiple frequency bands, represented by the different colors, across cortex. Loss of consciousness, on the other hand, was associated with focal decreases in beta relative to delta activity in anterior and posterior cingulate cortex as well as temporoparietal cortex. The temporoparietal effect was only observed in the sedation experiments, not the sleep experiments, indicating this may be a sedation specific effect rather than a general effect of consciousness. (Middle) Loss of consciousness was associated with slowing of the EEG and a decrease in complexity within the theta-beta range. Loss of connectedness was associated with a decrease in directed connectivity from the front to the back of the brain. (Bottom) During disconnected consciousness, a subset of perturbed connections within the auditory network, specifically ones connected to the right superior temporal gyrus, were able to account for a new P3 response elicited by standard tones.

related to loss of consciousness are in part, and in some cases entirely, related to loss of connectedness. This work provides evidence in support of a more conservative use of the term "unconsciousness" when phenomenological state has not been assessed.

Lastly, in Chapter 3 (Fig. 1 bottom row), I tested the neural mechanisms of sensory disconnection using an auditory roving oddball paradigm and dynamic causal modeling (DCM). These analyses showed that during disconnected consciousness, participants produced a P3 novelty response to predictable stimuli, indistinguishable from their responses to unpredictable stimuli. Furthermore, disconnected consciousness showed a marked increase in feedback connectivity throughout the auditory network relative to connected consciousness. Together, these findings suggest that disconnected consciousness is a state in which internally generated (feedback) signals predominate over environmental (feedforward) signals, resulting in a mismatch between the environment and one's internal state. This mismatch results in all incoming information being 'surprising' even when it seems entirely predictable to an outside observer.

This body of work builds upon decades of interdisciplinary work studying consciousness empirically. While prior works have identified a myriad of statistically robust effects, very few have distinguished between disconnected consciousness and unconsciousness in their methodology. This dissertation expands on the existing literature by explicitly contrasting disconnected consciousness against connected consciousness and unconsciousness, isolating effects of disconnection and loss of consciousness respectively. In doing so, these studies add phenomenological specificity that has been largely absent from the field. This work is a step towards understanding the neural basis of consciousness and connectedness, but at the same time it faces its own limitations and presents new questions and avenues for future inquiry, which will be explored below.

Limitations

The Accuracy of Subjective Reports

A common limitation to all of the work in this dissertation is the reliance on subjective reports as ground truth of mental state. As was noted in the Introduction, subjective report is currently the nearest we can come to accessing the experiences of another person. In this regard, little has changed since Descartes published the phrase “cogito ergo sum” (“I think, therefore I am”) in 1637[1]. This famous quote is interpreted to mean that the only thing one can know is that they exist, by virtue of the fact that they are thinking. Until reliable objective markers of consciousness are developed, the existence of consciousness in anyone other than oneself can only be inferred[i]. During day to day life we constantly make inferences about the

[i] If this were not the case, the work of this dissertation would be largely irrelevant!

consciousness of others based on the presence of complex behaviors we identify as being consistent with our own directed conscious behaviors. However, disconnected consciousness and unconsciousness are behaviorally identical. Because of this, the only way to study the difference between these states, at present, is to obtain verbal reports of subjective experience.

While subjective reports allow us to distinguish between disconnected consciousness and unconsciousness, they introduce a degree of memory dependence to the outcome variable (i.e. conscious state). Subjective reports can only be acquired while the participant is in a state of connected consciousness, therefore we must collect reports on what their mental state *was* prior to the start of the interview. The risk of memory error increases along with the length of time between recall and the event being recalled[2]. It is for this reason that the questions making up the subjective reports used in UN-ConsCIOUS begin with "Just before I started speaking to you…" (see Chapter 1 Fig. 1 for endings to this prompt). By doing this, we minimize time dependent errors in our reports. For resting state analyses (Chapters 1 & 2), we also limited the EEG data analyzed in association with the reports to the 20 seconds before the interview was initiated (see Appendix A, Fig 2 for sensitivity analysis demonstrating consistent findings across time scales but loss of statistical power outside of the 20-60 second range). This improves our confidence that the EEG data analyzed correspond, as closely as possible, to the subjective report acquired. For the ERP analyses of Chapter 3, it was not possible to confine the analyzed data to such a short timeframe due to the need for dozens to hundreds of trials, depending on signal to noise ratio of the data, to produce robust ERPs[3]. Because of this, there is

a higher probability of a participant's state of consciousness being non-stationary during the period of the roving oddball compared to the resting state data.

Beyond the matter of subjective reports inherently depending on short-term memory, there is also the valid concern that short-term memory processes could be pharmacologically impaired by the drugs used during sedation visits. Both propofol and dexmedetomidine have been shown to impair episodic memory[4,5]. The presence of memory errors cannot be ruled out from these data. That said, I argue that the most likely outcome of memory impairment would be to forget having a conscious experience when there was one, resulting in a period of disconnected consciousness being labeled as unconsciousness. This effect could show up in the contrast of disconnected conscious and unconscious data by increasing the variance within the 'unconscious' data and bringing the mean of the unconscious group closer to that of the disconnected conscious group. The ramifications of this would be a reduction in statistical power and an increase in false negatives. While not ideal, this should not compromise the validity of the effects that were observed and effects that were significant under these conditions would certainly have to be robust.

Sample Size of Propofol and Sleep Data

One major limitation of the current work is that, due to the global COVID-19 pandemic and the loss of the study anesthesiologist, I was unable to obtain the amount of data I had originally planned on. The study was designed to obtain data from 20 participants in each condition, however, at the time that recruitment was frozen, we had only met this goal for the dexmedetomidine visits. The propofol and sleep visits ended with 6 and 15 participants respectively. Because of this, only the dexmedetomidine dataset was statistically powered for

the planned analyses. In order to address these limitations in data, I had to make adjustments to my methods in the analyses that became Chapters 1 and 3.

My original plan for the exploratory analyses of Chapter 1 was to perform voxel-wise analyses in each condition to identify signatures of disconnection and unconsciousness in each. I would then compare the significant differences from each condition to identify overlapping signatures that generalized. Due to having less data than expected, however, exploratory analysis of the propofol and sleep data were expected to have a very high false negative rate. Instead, I conducted the voxel-wise exploratory analyses only within the dexmedetomidine data and then tested the generalizability of those findings within the propofol and sleep data. In doing so, I only had to apply voxel-wise multiple comparison corrections to the dexmedetomidine data, which reduced the risk of false negatives within the sleep and propofol data. The drawback of this approach is that we don't have a complete picture of which dexmedetomidine derived features generalized well in the other conditions. This is not so much an issue for the signatures of unconsciousness, which were limited to the beta/delta ratio in cingulate and parietal cortex, making it easy to test each effect in propofol and sleep data. However, the signatures of sensory disconnection were widespread across regions and frequency bands. Voxel-wise analyses in the propofol and sleep data may have revealed that not all of the changes observed under dexmedetomidine generalize to the other conditions. The *general* signatures of disconnection may actually be a limited subset of what was observed under dexmedetomidine.

The DCM work in Chapter 3 were also originally planned as cross-condition analyses between dexmedetomidine and propofol. The sleep data were not planned for use in this

analysis because we prioritized resting state data during those recording periods due to the limited number of wakeups in each session. Unfortunately, in the propofol visits, only 2/6 participants reported disconnected consciousness during roving oddball presentation. I judged that analyzing 2 subjects worth of data in a second condition would not be productive as it would not be enough data to make strong inferences on its own but adding those subjects to the dexmedetomidine data would risk mixing condition specific effects in an uncontrolled way. Instead, I chose to only focus on the dexmedetomidine data in Chapter 3 with the caveat that these effects should undergo further validation in other drug conditions in the future. This will be discussed further in the *Future Directions* section below.

Source Reconstruction Accuracy

Two of the chapters of this dissertation make heavy use of source reconstruction methods for the analyses. As such, I think it is important to elaborate on what these methods can and cannot tell us about functional brain activity. It is well known that, compared to methods such as functional magnetic resonance imaging (fMRI) or positron emission tomography (PET), EEG has quite poor spatial resolution[6]. This is a matter of physics that is unlikely to ever be completely solved by computational means. Concerns around localization accuracy (i.e. the spatial accuracy of the reconstructed data) are particularly relevant for resting state analyses in which the entire cortical sheet is modeled, as was done in Chapter 1. Later I will explain how DCM ameliorates this issue, though it comes with its own set of limitations.

In Chapter 1, I made use of the exact low resolution brain electromagnetic tomography (eLORETA)[7] algorithm to estimate cortical level activity across the brain using resting state data. The major advantage of this algorithm over prior methods is that it removed issues of

localization bias when estimating deep structures, which is important to note given that the main findings of this chapter revolved around the anterior and posterior cingulate[7]. But an unbiased measure is not necessarily a precise measure; substantial error may still exist in the absence of bias. Localization errors for eLORETA have been estimated to be around 1-4 cm[7,8]. 4 cm is roughly the distance from the genu of the corpus callosum to the frontal pole (estimate based on MNI atlas space). In principle, this means that the anterior and posterior cingulate sources from Chapter 1 could feasibly represent neighboring regions such as the medial prefrontal cortex (mPFC) and precuneus respectively. The ACC and PCC are our best guesses given the data we have, but not definitive truth. With that said, convergent results from other studies support the involvement of these regions.

Scheinin et al. conducted a very similar experiment to our UN-ConsCIOUS using PET but didn't distinguish between unconsciousness and disconnected consciousness[9]. One of the major findings of this study was reduced activity in ACC and PCC in their unresponsive participants. However, their propofol data also showed reduced precuneus and mPFC activity. fMRI work from Huang et al. showed reduced default mode network (DMN) activity in unresponsive subjects across multiple anesthetics as well[10]. The core nodes of the DMN are the mPFC, the PCC, and temporal parietal junction, however, extended specifications of the network involve the ACC and precuneus as well[11,12]. Taken together with the findings of Chapter 1, these results suggest that unconsciousness *per se* is associated with decreases in DMN activity and that our source localization is reasonably accurate.

In contrast to the whole brain analyses using eLORETA, DCM models a limited number of regions (typically fewer than 10, though this is a choice made by the individual researcher). The

choice of model becomes critical for the validity of the results and requires a degree of prior knowledge as to what brain regions will be involved in the process being studied[13]. Provided that reasonable sources are included in the model, the issue of spatial accuracy becomes relatively less important than for eLORETA. This is because, while the user provides coordinates for each source to model, the provided coordinates are used as spatial priors rather than absolute locations. Provided that there is a true source in the proximity of the specified coordinates, the Bayesian optimization of the DCM will hone in on that source by combining the data with the spatial prior[14]. But again, this is all dependent on the researcher having sufficient prior knowledge in order to specify a reasonable model to optimize[13].

Researchers can depend on the data to identify an appropriate model to a limited extent by using Bayesian Model Selection (BMS) to compare a range of models based on their fit to the data[13]. I applied this method when choosing a final model within Chapter 3. However, the utility of this method is still limited by the model space that the researcher specifies in the comparison. BMS can only inform the user of the best model *in the model space*. There is no way of knowing if the 'real' model specification exists in the model space. Therefore, the best model based on BMS could still be very different from reality. However, it is important to note that evaluating a model that differs from the ground truth does not imply that the subsequent inferences from that model are wrong. Simulation analyses demonstrate that correct inferences can be consistently drawn even when the model architecture deviates from reality[15], though it becomes less likely to detect true effects as the model fit worsens[13]. In other words, the primary concern with absolute model fit is not false positive results, but rather false negatives.

The model space investigated within Chapter 3 is based on substantial prior literature investigating the neural responses of the auditory roving oddball[16–21]. Indeed, one of the major advantages of using this auditory paradigm to study sensory disconnection is that it has been so well characterized previously. Because this model architecture has been informed and validated by many prior studies, in multiple imaging modalities, there is little concern that the model space does not contain a model that is sufficient to fit the data well enough to find group differences. Indeed, if the model was a poor fit, we would likely not observe any of the effects seen in the parametric empirical Bayes (PEB) contrasts of Chapter 3[13]. Even so, we may still be missing important connections that also differ outside of this relatively simple auditory network[15]. The network investigating in the model space of Chapter 3 constitutes the ventral stream of the auditory processing network, however, there is also a dorsal stream that is currently completely neglected in the model[22]. This omission is likely justified given that the roving oddball did not elicit responses in dorsal stream regions in the previous neuroimaging studies[16,17]. This makes sense as the ventral stream is primarily associated with the 'what' of sound and the roving oddball only manipulates the 'what' quality of tone frequency[22]. The dorsal stream encodes the 'where' of sound, which is not manipulated by the roving oddball paradigm[22]. Even so, it is still possible that dorsal stream effects could be contributing the EEG data and that these effects are not captured by the models in Chapter 3.

Future Directions

Resolving the Role of Feedback Connectivity in Sensory Disconnection

Feedback connectivity has long been proposed as a critical feature of systems that can support consciousness[23–26]. This proposition was used as a theoretical basis for the use of

normalized symbolic transfer entropy (NSTE) from frontal to posterior electrodes by Lee et al[27]. This metric was designed to measure the information flow from frontal to parietal cortex as an index of feedback connectivity [27]. They hypothesized that due to the theoretical importance of feedback connectivity to consciousness, unconsciousness should be measurable based on a decrease in this connectivity. Indeed, participants administered ketamine, propofol, or sevoflurane all showed decreases in front-to-back NSTE, which was interpreted as an effect related to loss of consciousness[ii]. Based on these findings, the front-to-back NSTE was included in the set of measures I evaluated for associations with connectedness and consciousness in Chapter 2. The analyses of Chapter 2 demonstrated the front-to-back NSTE showed no significant effects related to loss of consciousness, however, all three experimental conditions showed significant reductions in NSTE with sensory disconnection. Provided that the NSTE from frontal to posterior electrodes is an accurate assessment of feedback connectivity (this assumption will be discussed further later), the results of Chapter 2 imply that disconnected consciousness is associated with a decrease in feedback connectivity.

Interestingly, the NSTE findings in Chapter 2 are in direct conflict with the DCM results presented in Chapter 3. When evaluating changes in connectivity strength in response to auditory stimulation between connected and disconnected consciousness, disconnection was associated with significantly *greater* feedback connectivity. It seems paradoxical that two assessments of feedback connectivity would result in opposite effects when contrasting

[ii] The authors of this paper did make note that "…study assessed only connected or external consciousness (i.e., consciousness of environmental stimuli), which is thought to be mediated by lateral frontoparietal networks, rather than disconnected or internal consciousness (e.g.,dream states)". However, their discussion proceeds to discuss how their findings relate to consciousness more generally, not just "external" or connected consciousness.

connected and disconnected consciousness within the same study. How then might these findings be reconciled? There are three probable explanations for the discrepancy: 1) modeling approach, 2) resting vs evoked data, and 3) construct validity. Each of these explanations with be described below and experimental methods for addressing each hypothesized source of difference will be presented.

The first explanation of modeling approach refers to differences in how the data are transformed and represented in order to derive a final measure of connectivity. The most notable difference in the NSTE and DCM approaches is that the NSTE was calculated using the sensor level data while DCM is performed in source space[28]. It is possible that the process of source reconstruction alters the representation of feedback signaling in some critical, though unknown, way. Though not clear what specifically about source vs sensor analyses would result in such dramatic changes in feedback connectivity, this explanation could be evaluated by comparing both methods using the same data. The data used in evaluating the NSTE could be source reconstructed to produce source space time series data, allowing the front-to-back NSTE to be calculated explicitly as a frontal to parietal NSTE. A reversal of the NSTE effect could rule this in as an explanation, though due to additional modeling differences between DCM and 'standard' source reconstruction[28], a negative result wouldn't rule out modeling approach as a source of difference. The source reconstructed data should also be assessed for frontal to temporal connectivity, i.e. inferior frontal gyrus to superior temporal gyrus, to determine if the differences can be explained by the regions used for the connectivity estimation.

The second explanation is simply that the data used for the NSTE and DCM analyses are fundamentally different in that the former reflects the brain at rest while the latter represents a

dynamic response to external stimuli. Evoked activity is, by definition, not the same as resting activity, therefore we cannot assume that observations made from one will automatically apply to the other. It is biologically plausible that, during disconnected consciousness, there is *less* feedback signaling at rest and *more* feedback activity in response to sensory stimulation compared to connected consciousness. For example, the observed evoked feedback could be specific to the P3 surprise response that was observed in Chapter 2. Indeed, the DCM simulation analysis showed that 2/4 of the feedback connections in the model were essential to the standard-tone P3. The evoked feedback could also be a sort of disconnection maintenance mechanism, preventing sensory evoked state transition to connected consciousness. Feedback activity could be dynamically upregulated in order to preserve a predominance of internally generated information. Such mechanisms of "sleep defense" have previously been attributed to K-complexes within the sleep literature[29–31]. Either mechanism of P3 generation or disconnection maintenance (or a combination of both) could explain an increase of feedback activity that would only be relevant in response to sensory stimuli.

In order to determine if the differences in observed feedback connectivity are related to resting vs evoked data, it would be useful to apply NSTE to evoked data or DCM to resting data. It has yet to be demonstrated that NSTE produces stable estimates of connectivity when applied to short (sub-second) time windows (previous studies have used at least 10 seconds of data per window[27,32]). Thus, it would be important to validate the stability of the measure before applying it to event related data. DCM, on the other hand, has recently been expanded to include methods for modeling resting state EEG data[33]. Comparing DCM results from resting and evoked data would be doubly informative as finding decreases in feedback in resting data

(consistent with the NSTE findings) would suggest that the differences can be explained based on resting vs evoked data, while a finding of increased feedback (consistent with prior DCM analysis) would suggest the difference are related to methodology.

The final explanation is one that researchers much always be mindful of: whether our measures are representative of the phenomena they are meant to assess. Measures that fail to recapitulate the underlying construct they are intended to evaluate are said to lack construct validity. The construct of interest in this case is feedback signaling in the brain. It is possible that the NSTE or DCM effective connectivity (or both) are measuring something other than true feedback signaling. Evaluating this is non-trivial as it requires knowledge of the ground truth feedback signaling to compare each measure against. Of course, if we had access to this ground truth, we wouldn't be using indirect estimates like NSTE and DCM in the first place. DCM, which is continually being updated by the lab that originated the method, has undergone iterative validation to demonstrate accuracy[34–36]. The major caveat here is that the accuracy of the model is dependent on the accuracy of its specification[37]. NSTE is not reliant upon model specification, however, it has also not yet been evaluated against any ground truth datasets. In order to establish ground truth and validate the feedback connectivity findings, a new dataset would be needed.

Animal model experiments would be a productive means of generating complementary data to the above human subject work for a finer grain interrogation of feedback signaling within the brain. Recent advances in optogenetic technology has allowed for unprecedented control of neural circuits[38]. These tools could be applied to directly stimulate or inhibit feedback projections within mouse auditory cortex with simultaneous multichannel extracellular

recording. For example, one could select two regions with known reciprocal hierarchical connectivity, such as A1 and A2 (mouse A2 is roughly homologous to STG in humans[39]). Excitatory (e.g. ChR2[40]) or inhibitory (e.g. eNpHR[41]) rhodopsins could be injected within A2 (the higher-order area) and A2 efferents to A1 selectively regulated with photo-stimulation within A1. Using this general setup, several questions could be addressed.

First, using an excitatory rhodopsin, feedback activity could be stimulated and the resulting effect on A1 measured extracellularly across cortical layers in different physiological states. As mice are not capable of providing subjective reports of dreaming experiences, assuming disconnection would be necessary. Presently, the best physiological proxy of disconnected consciousness is likely REM sleep which exhibits dream rates of roughly 80% in humans[42]. Contrasting REM and wake would thus be a reasonable approximation of disconnected vs connected consciousness. If disconnected consciousness is associated with increased feedback signaling, one could expect to see more frequent and/or stronger depolarizations among L1 afferents in A1 (where cortico-cortical feedback is largely targeted[43]) during REM compared to wake. When stimulating A2 efferents during REM compared to wake, we might also see larger depolarizations in A1 and a reduced threshold of light stimulation required to elicit depolarization.

Second, using an inhibitory rhodopsin, feedback could be inhibited during REM sleep and the effects on arousal assessed. One of the hypotheses I mentioned above regarding putative roles for feedback connectivity increasing during disconnected consciousness was that it might be a compensatory response to environmental stimuli that preserves disconnection. By presenting auditory stimuli during REM, with or without inhibition of feedback, one could

determine if inhibiting feedback signaling increases the probability of sensory evoked awakening. If so, that would support the idea that high feedback signaling has a disconnection protective role.

Lastly, this experimental model could be used to further validate the validity of NSTE and DCM in measuring directed connectivity. To do this, signaling between A1 and A2 could be bidirectionally regulated optogenetically while recording EEG across auditory cortex. Because feedforward and feedback activity are being experimentally manipulated by the researcher, there is a known ground truth of when each signaling type is high and low. The EEG recording from electrodes positioned over A1 and A2 could then be modeled using NSTE and DCM to see how well each method corresponds with the ground truth signaling. A better understanding of the accuracy of these indirect connectivity measures would be beneficial for future human subject research.

The experiments outlined above provide a general framework for evaluating the role of feedback connectivity within auditory processing during disconnected consciousness. While relatively simple on paper, there are significant technical challenges posed by trying to optogenetically manipulate A1 and A2 in mouse brains. In the examples above, I chose A1 and A2 as analogs of human A1 and STG in order to make the findings easily comparable to those of the DCM analyses. But in practice, targeting these regions may be infeasible. Mouse brains are extremely small compared to primate brains and A1/A2 are directly adjacent to one another[44]. The proximity of these regions would likely make specific targeting of the viral injection to A2 extremely difficult to achieve. In 2018, Nagode et al. showed that orbitofrontal cortex in mice directly regulates activity in A1 through feedback projections and proposed these to be

analogous to inferior frontal projections to auditory cortex in primates[45]. Rather than injecting viral vector into A2, one could inject orbitofrontal cortex, without the concern of viral diffusion into A1. The compromise of choosing orbitofrontal cortex over A2 is that a frontal to A1 connection does not exist within the DCM model, preventing a direct connection-to-connection comparison of the results. However, for the purposes of broadly understanding auditory feedback signaling during disconnected consciousness, this is likely a reasonable tradeoff for the gains in practicality.

Replication and Expansion of Conditions

As noted above under the Limitations section, I was unable to collect the originally planned sample sizes for the propofol and sleep conditions due to the extenuating circumstances of COVID-19. While I adjusted my analytical approaches as best as I was able to draw meaningful conclusions from the data I was able to collect, these experimental conditions are fundamentally statistically underpowered. Because of this, there is a high probability of false negatives within these conditions, particularly for propofol which had the smallest sample size by far. In order to address this, future work should be conducted to collect additional propofol and sleep data analogous to the data already collected. This would allow us to validate the current findings and perform comprehensive exploratory analyses, comparable to those of Chapter 1, within sleep and propofol data. By comparing these results with those derived from dexmedetomidine, we may identify a more specific set of signatures associated with sensory disconnection across all conditions.

The work of studying differences between disconnection and unconsciousness is still in its infancy, and the data collected thus far represent only a small sample of the possible

pharmacological manipulations of these states. Using dexmedetomidine and propofol, we have manipulated noradrenergic and GABAergic activity, respectively. However, there are many other drugs, with different modes of action, that could be applied under similar experimental conditions. Even drugs with shared primary pharmacological targets, e.g. propofol and etomidate both act on $GABA_A$ receptors, may have different physiological effects due to differences in secondary binding sites, e.g. propofol also acts through HCN1 channels but etomidate does not[46]. In expanding the repertoire of experimental manipulations, and comparing the results of these different experiments, we can test the limits of generalizability of the currently available signatures of consciousness and connectedness. These additional data may also reveal new signatures that could be tested against the current data. Continuing to expand the experimental conditions in which consciousness and connectedness are evaluated will be necessary to further improve the discriminatory power and external validity of the work.

Non-pharmacological Modulatory Interventions

A major question for all scientific work that makes use of observational correlations is whether or not the observed effects have a causal association. The experimental protocol used in UN-ConsCIOUS do not allow for causal inferences to be drawn regarding each of the studied biomarkers and consciousness/connectedness. However, there are emerging technologies, such as transcranial alternating current stimulation (tACS)[47] and closed-loop slow wave enhancement[48], that may allow for non-invasive experimental manipulation of neural activity separate from pharmacological intervention in future studies.

tACS makes use of electrodes placed on the scalp to deliver sinusoidal currents that can alter neuronal spiking probabilities within the brain[49]. A major advantage of using a sinusoidal

stimulation profile is that it allows researchers to entrain specific rhythms in the brain, rather than just establishing a fixed current dipole as is the case for transcranial direct current stimulation (tDCS)[50]. This means that particular frequencies of biological interest can be targeted and causally manipulated[iii]. For example, recent work by Cheng et al. demonstrated that beta stimulation (20 Hz), which has previously been associated with visual processing[51], improved short term visual memory for seen, but not unseen, stimuli[52]. Onoda et al. targeted tACS to the anterior cingulate cortex and showed that stimulating theta activity, which is endogenously produced within anterior cingulate during cognitive control tasks[53], significantly altered fMRI connectivity, while gamma stimulation had no effect[54]. The analyses of Chapter 1 pointed to low vs high frequency activity in the anterior and posterior cingulate as a distinguishing feature of unconsciousness compared to disconnected consciousness. These regions would make prime targets for a causal test using tACS. By stimulating in the beta or delta frequency ranges during sleep or sedation, one could observe if these frequencies play a causal role in rates of consciousness and unconsciousness. Based on the findings of Chapter 1, I would predict that beta stimulation would increase rates of disconnected consciousness, while delta stimulation would increase rates of unconsciousness, if there is a causal relationship.

[iii] This statement comes with some caveats. While multiple studies have shown that targeting tACS to specific frequencies produces cognitive effects consistent with the putative roles of those oscillations[60], entraining a particular rhythm does not guarantee that the oscillation of interest has been manipulated. Oscillations are emergent properties of neuronal networks generated through repeating patterns of activity that are defined by that network's functional architecture[65,66]. That does not imply that all neurons within a network are simultaneously oscillating at the same frequency. Enforcing entrainment using external currents (tACS) may result in the same frequency of activity as the intended oscillation, but the underlying neuronal activity may very well differ from that of the endogenous oscillation in biologically important ways.

The findings of Chapter 1-2 suggest that unconsciousness is associated with decreased beta activity along with increased delta activity (seen as the beta/delta ratio in Chapter 1 and the spectral exponent in Chapter 2). Ideally, a causal manipulation experiment would involve simultaneous manipulation of beta and delta rather than one or the other. Unfortunately, the current state of tACS does not allow for simultaneous enhancement and inhibition of distinct frequency bands. However, such manipulations may be possible by combining tACS beta stimulation with closed-loop auditory slow wave suppression. By timing auditory stimuli to different phases of endogenous slow waves, subsequent slow waves can either be enhanced or suppressed[55]. This method could be used to suppress low frequency activity while tACS is used to enhance high frequency activity, which may hypothetically result in higher rates of disconnected consciousness.

Though still limited, non-invasive neuromodulation methods offer unique opportunities to manipulate neural oscillations non-pharmacologically in human participants. Despite their potential, these technologies have not seen much use as means of manipulating putative markers of consciousness to test for causal associations. Transcranial magnetic stimulation (TMS) has been applied in tandem with EEG to measure changes in brain responsivity during sleep, anesthesia, and disorders of consciousness, but these studies have been aimed at diagnostics rather than intervention (see[56] for a review of this work). Closed-loop slow wave enhancement is currently being developed as a sleep aid technology[57,58], but has yet to be applied in anesthetic settings or as a means of biasing conscious state. tACS and tDCS studies have primarily focused on manipulating cognitive performance such as memory or stimulus perception, but not consciousness (see[59,60] for review). I argue that these technologies

represent an untapped (or at the very least “under-tapped”) resource as experimental tools in the study of consciousness. Future application of non-invasive neurostimulation has the potential to add important insight in our developing understanding of how the correlates of consciousness relate to the phenomenon itself.

Investigation of Temporal Dynamics and Microstates

The resting states analyses of Chapters 1 and 2 only made use of the last 20 seconds of EEG data prior to when the wake report was collected. As mentioned before, this choice was made to ensure that each analyzed epoch was likely to reflect only the internal state matching the phenomenological report. While this decision was important for these initial analyses demonstrating detectable differences between disconnected consciousness and unconsciousness, it also resulted in the vast majority of the collected EEG being excluded from analysis. However, these data may still hold extremely useful information, even if they cannot be confidently associated with a subjective report.

An alternative approach for analyzing the EEG would be to evaluate the temporal dynamics of the topographical signal in order to identify repeating patterns of activity that may represent a recurring brain state. These so-called ‘EEG microstates’ provide a data driven way to characterize brain activity with high temporal resolution[61]. This approach has been previously used to characterize differences in activity between NREM with and without dreams[62] as well as to track depth of sedation[63].

The UN-ConsCIOUS data could also be analyzed using a microstate procedure. By clustering the data into microstates, in a data driven manner, then comparing those clusters to

the activity patterns observed immediately preceding subjective reports, one may be able to establish a correspondence between certain microstates and the presence of consciousness/connectedness. By tracking transition probabilities between microstates, it may also be possible to identify EEG states that are predictive of a returning awareness, which would be highly desirable for depth of anesthesia monitors. Even microstates without a clear phenomenological correlate within the current data could be very useful for structuring future studies. For example, microstates of unknown phenomenology could be used as targets in future studies such that wake reports are initiated once the participant enters that state. Qualitative analysis of reports derived from these target microstates could then be used to characterize their phenomenological correlates.

Concluding Remarks

While discourse on the nature of consciousness has existed for millennia, empirical study of the phenomenon only emerged in the late 19th and early 20th century[64]. Since then, the technologies and experimental designs we employ have advanced in leaps and bounds, but our fundamental understanding of how consciousness arises from the brain remains limited. In this dissertation, I have argued that a major limitation in our ability to study consciousness arises from experimentally confounding unresponsiveness and sensory disconnection with unconsciousness. These confounds not only hinder scientific progress, they also manifest in limitations in our ability to clinically evaluate disorders of consciousness and anesthetic efficacy. The work I have presented here demonstrates that connectedness and consciousness can be experimentally decoupled and that doing so has important consequences for our scientific findings. I believe these results to be an important step forward in studying both consciousness

per se and sensory connection to the environment. Even so, this work only begins to scratch the surface of these complex phenomena. Moving forward, we must continue to strive for greater specificity in our experimental methods, statistical controls, and results reporting. Only then will we successfully disentangle disconnection and unconsciousness.

References

1. René Descartes. *Discourse on the Method*.; 1637.
2. Peterson L, Peterson MJ. Short-term retention of individual verbal items. *J Exp Psychol*. 1959;58(3):193-198. doi:10.1037/H0049234
3. Boudewyn MA, Luck SJ, Farrens JL, Kappenman ES. How Many Trials Does It Take to Get a Significant ERP Effect? It Depends. *Psychophysiology*. 2018;55(6):e13049. doi:10.1111/PSYP.13049
4. Veselis RA, Reinsel RA, Feshchenko VA, Johnson R. Information Loss over Time Defines the Memory Defect of Propofol: A Comparative Response with Thiopental and Dexmedetomidine. *Anesthesiology*. 2004;101(4):831. doi:10.1097/00000542-200410000-00006
5. Veselis RA, Pryor KO, Reinsel RA, Li Y, Mehta M, Johnson R. Propofol and midazolam inhibit conscious memory processes very soon after encoding: An event related potential study of familiarity and recollection in volunteers. *Anesthesiology*. 2009;110(2):295. doi:10.1097/ALN.0B013E3181942EF0
6. Walsh V, Cowey A. Transcranial magnetic stimulation and cognitive neuroscience. *Nature Reviews Neuroscience 2000 1:1*. 2000;1(1):73-80. doi:10.1038/35036239
7. Pascual-Marqui RD, Lehmann D, Koukkou M, et al. Assessing interactions in the brain with exact low-resolution electromagnetic tomography. *Philosophical Transactions of the Royal Society A: Mathematical, Physical and Engineering Sciences*. 2011;369(1952):3768-3784. doi:10.1098/rsta.2011.0081
8. Tait L, Özkan A, Szul MJ, Zhang J. A systematic evaluation of source reconstruction of resting MEG of the human brain with a new high-resolution atlas: Performance, precision, and parcellation. *Hum Brain Mapp*. 2021;42(14):4685-4707. doi:10.1002/HBM.25578
9. Scheinin A, Kantonen O, Alkire M, et al. Foundations of human consciousness: Imaging the twilight zone. *Journal of Neuroscience*. 2021;41(8):1769-1778. doi:10.1523/JNEUROSCI.0775-20.2020

10. Huang Z, Zhang J, Wu J, Mashour GA, Hudetz AG. Temporal circuit of macroscale dynamic brain activity supports human consciousness. *Sci Adv*. 2020;6(11):87-98. doi:10.1126/sciadv.aaz0087

11. Buckner RL, Andrews-Hanna JR, Schacter DL. The brain's default network: Anatomy, function, and relevance to disease. *Ann N Y Acad Sci*. 2008;1124(1):1-38. doi:10.1196/annals.1440.011

12. Carter CS, Botvinick MM, Cohen JD. The contribution of the anterior cingulate cortex to executive processes in cognition. *Rev Neurosci*. 1999;10(1):49-57. doi:10.1515/REVNEURO.1999.10.1.49

13. Stephan KE, Penny WD, Moran RJ, den Ouden HEM, Daunizeau J, Friston KJ. Ten simple rules for dynamic causal modeling. *Neuroimage*. 2010;49(4):3099-3109. doi:10.1016/j.neuroimage.2009.11.015

14. Henson RN, Flandin G, Friston KJ, Mattout J. A Parametric Empirical Bayesian framework for fMRI-constrained MEG/EEG source reconstruction. *Hum Brain Mapp*. 2010;31(10):1512-1531. doi:10.1002/HBM.20956

15. Protzner AB, McIntosh AR. Testing effective connectivity changes with structural equation modeling: What does a bad model tell us? *Hum Brain Mapp*. 2006;27(12):935-947. doi:10.1002/HBM.20233

16. Opitz B, Rinne T, Mecklinger A, von Cramon DY, Schröger E. Differential Contribution of Frontal and Temporal Cortices to Auditory Change Detection: fMRI and ERP Results. *Neuroimage*. 2002;15(1):167-174. doi:10.1006/NIMG.2001.0970

17. Doeller CF, Opitz B, Mecklinger A, Krick C, Reith W, Schröger E. Prefrontal cortex involvement in preattentive auditory deviance detection: Neuroimaging and electrophysiological evidence. *Neuroimage*. 2003;20(2):1270-1282. doi:10.1016/S1053-8119(03)00389-6

18. Rosch RE, Auksztulewicz R, Leung PD, Friston KJ, Baldeweg T. Selective Prefrontal Disinhibition in a Roving Auditory Oddball Paradigm Under N-Methyl-D-Aspartate Receptor Blockade. *Biol Psychiatry Cogn Neurosci Neuroimaging*. 2019;4(2):140. doi:10.1016/J.BPSC.2018.07.003

19. Garrido MI, Friston KJ, Kiebel SJ, Stephan KE, Baldeweg T, Kilner JM. The functional anatomy of the MMN: A DCM study of the roving paradigm. *Neuroimage*. 2008;42(2):936-944. doi:10.1016/j.neuroimage.2008.05.018

20. Gjini K, Casey C, Tanabe S, et al. Greater tau pathology is associated with altered predictive coding. *Brain Commun*. 2022;4(5). doi:10.1093/BRAINCOMMS/FCAC209

21. Boly M. Preserved Feedforward But Impaired Top-Down Processes in the Vegetative State. *Science (1979)*. 2011;46(5896):1-25. doi:10.1126/science.1245938

22. Rauschecker JP, Scott SK. Maps and streams in the auditory cortex: nonhuman primates illuminate human speech processing. *Nat Neurosci*. 2009;12(6):718-724. doi:10.1038/nn.2331

23. Dehaene S, Changeux JP. Experimental and Theoretical Approaches to Conscious Processing. *Neuron*. 2011;70(2):200-227. doi:10.1016/J.NEURON.2011.03.018

24. Crick F, Koch C. A framework for consciousness. *Nature Neuroscience 2003 6:2*. 2003;6(2):119-126. doi:10.1038/nn0203-119

25. Llinás R, Ribary U, Contreras D, Pedroarena G. The neuronal basis for consciousness. *Philosophical Transactions of the Royal Society B: Biological Sciences*. 1998;353(1377):1841-1849. doi:10.1098/RSTB.1998.0336

26. Tononi G, Boly M, Massimini M, Koch C. Integrated information theory: from consciousness to its physical substrate. *Nature Reviews Neuroscience 2016 17:7*. 2016;17(7):450-461. doi:10.1038/nrn.2016.44

27. Lee U, Ku S, Noh G, Baek S, Choi B, Mashour GA. Disruption of Frontal–Parietal Communication by Ketamine, Propofol, and Sevoflurane. *Anesthesiology*. 2013;118(6):1264-1275. doi:10.1097/ALN.0B013E31829103F5

28. Kiebel SJ, Garrido MI, Moran RJ, Friston KJ. Dynamic causal modelling for EEG and MEG. *Cogn Neurodyn*. 2008;2(2):121-136. doi:10.1007/s11571-008-9038-0

29. Jahnke K, von Wegner F, Morzelewski A, et al. To wake or not to wake? The two-sided nature of the human K-complex. *Neuroimage*. 2012;59(2):1631-1638. doi:10.1016/J.NEUROIMAGE.2011.09.013

30. Halász P. K-complex, a reactive EEG graphoelement of NREM sleep: an old chap in a new garment. *Sleep Med Rev*. 2005;9(5):391-412. doi:10.1016/J.SMRV.2005.04.003

31. Halasz P, Pal I, Rajna P. K-complex formation of the EEG in sleep. A survey and new examinations. *Acta Physiol Hung*. 1985;65(1):3-35. Accessed October 31, 2022. https://europepmc.org/article/med/3993393

32. Li D, Hambrecht-Wiedbusch VS, Mashour GA. Accelerated recovery of consciousness after general anesthesia is associated with increased functional brain connectivity in the high-gamma bandwidth. *Front Syst Neurosci*. 2017;11:16. doi:10.3389/FNSYS.2017.00016/BIBTEX

33. van de Steen F, Almgren H, Razi A, Friston K, Marinazzo D. Dynamic causal modelling of fluctuating connectivity in resting-state EEG. *Neuroimage*. 2019;189:476-484. doi:10.1016/J.NEUROIMAGE.2019.01.055

34. Moran RJ, Symmonds M, Stephan KE, Friston KJ, Dolan RJ. An In Vivo Assay of Synaptic Function Mediating Human Cognition. *Current Biology*. 2011;21(15):1320-1325. doi:10.1016/J.CUB.2011.06.053

35. Moran RJ, Jung F, Kumagai T, et al. Dynamic Causal Models and Physiological Inference: A Validation Study Using Isoflurane Anaesthesia in Rodents. Uversky VN, ed. *PLoS One*. 2011;6(8):e22790. doi:10.1371/journal.pone.0022790

36. Moran RJ, Stephan KE, Kiebel SJ, et al. Bayesian estimation of synaptic physiology from the spectral responses of neural masses. *Neuroimage*. 2008;42(1):272-284. doi:10.1016/j.neuroimage.2008.01.025

37. Friston KJ, Preller KH, Mathys C, et al. Dynamic causal modelling revisited. *Neuroimage*. 2019;199:730-744. doi:10.1016/J.NEUROIMAGE.2017.02.045

38. Lee C, Lavoie A, Liu J, Chen SX, Liu BH. Light Up the Brain: The Application of Optogenetics in Cell-Type Specific Dissection of Mouse Brain Circuits. *Front Neural Circuits*. 2020;14:18. doi:10.3389/FNCIR.2020.00018/BIBTEX

39. Loomba S, Straehle J, Gangadharan V, et al. Connectomic comparison of mouse and human cortex. *Science (1979)*. 2022;377(6602). doi:10.1126/SCIENCE.ABO0924/SUPPL_FILE/SCIENCE.ABO0924_MDAR_REPRODUCIBILITY_CHECKLIST.PDF

40. Nagel G, Szellas T, Huhn W, et al. Channelrhodopsin-2, a directly light-gated cation-selective membrane channel. *Proc Natl Acad Sci U S A*. 2003;100(SUPPL. 2):13940-13945. doi:10.1073/PNAS.1936192100/SUPPL_FILE/6192FIG5B.PDF

41. Zhang F, Wang LP, Brauner M, et al. Multimodal fast optical interrogation of neural circuitry. *Nature 2007 446:7136*. 2007;446(7136):633-639. doi:10.1038/nature05744

42. Siclari F, LaRocque JJ, Postle BR, Tononi G. Assessing sleep consciousness within subjects using a serial awakening paradigm. *Front Psychol*. 2013;4(AUG):542. doi:10.3389/FPSYG.2013.00542/BIBTEX

43. Bastos AM, Usrey WM, Adams RA, Mangun GR, Fries P, Friston KJ. Canonical Microcircuits for Predictive Coding. *Neuron*. 2012;76(4):695-711. doi:10.1016/j.neuron.2012.10.038

44. Tsukano H, Horie M, Hishida R, Takahashi K, Takebayashi H, Shibuki K. Quantitative map of multiple auditory cortical regions with a stereotaxic fine-scale atlas of the mouse brain. *Scientific Reports 2016 6:1*. 2016;6(1):1-12. doi:10.1038/srep22315

45. Winkowski DE, Nagode DA, Donaldson KJ, et al. Orbitofrontal Cortex Neurons Respond to Sound and Activate Primary Auditory Cortex Neurons. *Cerebral Cortex*. 2018;28(3):868-879. doi:10.1093/CERCOR/BHW409

46. Chen X, Shu S, Bayliss DA. HCN1 Channel Subunits Are a Molecular Substrate for Hypnotic Actions of Ketamine. *The Journal of Neuroscience*. 2009;29(3):600. doi:10.1523/JNEUROSCI.3481-08.2009

47. Antal A, Boros K, Poreisz C, Chaieb L, Terney D, Paulus W. Comparatively weak after-effects of transcranial alternating current stimulation (tACS) on cortical excitability in humans. *Brain Stimul*. 2008;1(2):97-105. doi:10.1016/J.BRS.2007.10.001

48. Ngo HVV, Martinetz T, Born J, Mölle M. Auditory Closed-Loop Stimulation of the Sleep Slow Oscillation Enhances Memory. *Neuron*. 2013;78(3):545-553. doi:10.1016/J.NEURON.2013.03.006

49. Ozen S, Sirota A, Belluscio MA, et al. Transcranial Electric Stimulation Entrains Cortical Neuronal Populations in Rats. *Journal of Neuroscience*. 2010;30(34):11476-11485. doi:10.1523/JNEUROSCI.5252-09.2010

50. Herrmann CS, Rach S, Neuling T, Strüber D. Transcranial alternating current stimulation: A review of the underlying mechanisms and modulation of cognitive processes. *Front Hum Neurosci*. 2013;0(MAY):279. doi:10.3389/FNHUM.2013.00279/BIBTEX

51. Hanslmayr S, Aslan A, Staudigl T, Klimesch W, Herrmann CS, Bäuml KH. Prestimulus oscillations predict visual perception performance between and within subjects. *Neuroimage*. 2007;37(4):1465-1473. doi:10.1016/J.NEUROIMAGE.2007.07.011

52. Cheng PX, Grover S, Wen W, et al. Dissociable rhythmic mechanisms enhance memory for conscious and nonconscious perceptual contents. *Proc Natl Acad Sci U S A*. 2022;119(44):e2211147119. doi:10.1073/PNAS.2211147119/SUPPL_FILE/PNAS.2211147119.SAPP.PDF

53. Cavanagh JF, Frank MJ. Frontal theta as a mechanism for cognitive control. *Trends Cogn Sci*. 2014;18(8):414-421. doi:10.1016/J.TICS.2014.04.012

54. Onoda K, Kawagoe T, Zheng H, Yamaguchi S. Theta band transcranial alternating current stimulations modulates network behavior of dorsal anterior cingulate cortex. *Scientific Reports 2017 7:1*. 2017;7(1):1-9. doi:10.1038/s41598-017-03859-7

55. Bellesi M, Riedner BA, Garcia-Molina GN, Cirelli C, Tononi G. Enhancement of sleep slow waves: underlying mechanisms and practical consequences. *Front Syst Neurosci*. 2014;8:208. doi:10.3389/fnsys.2014.00208

56. Napolitani M, Bodart O, Canali P, et al. Transcranial magnetic stimulation combined with high-density EEG in altered states of consciousness.

https://doi.org/103109/026990522014920524. 2014;28(9):1180-1189. doi:10.3109/02699052.2014.920524

57. Garcia-Molina G, Tsoneva T, Jasko J, et al. Closed-loop system to enhance slow-wave activity. *J Neural Eng*. 2018;15(6):066018. doi:10.1088/1741-2552/aae18f

58. Ferster ML, Lustenberger C, Karlen W. Configurable Mobile System for Autonomous High-Quality Sleep Monitoring and Closed-Loop Acoustic Stimulation. *IEEE Sens Lett*. 2019;3(5):1-4. doi:10.1109/LSENS.2019.2914425

59. Berryhill ME, Martin D. Cognitive Effects of Transcranial Direct Current Stimulation in Healthy and Clinical Populations: An Overview. *Journal of ECT*. 2018;34(3):e25-e35. doi:10.1097/YCT.0000000000000534

60. Klink K, Paßmann S, Kasten FH, Peter J. The Modulation of Cognitive Performance with Transcranial Alternating Current Stimulation: A Systematic Review of Frequency-Specific Effects. *Brain Sciences 2020, Vol 10, Page 932*. 2020;10(12):932. doi:10.3390/BRAINSCI10120932

61. Michel CM, Koenig T. EEG microstates as a tool for studying the temporal dynamics of whole-brain neuronal networks: A review. *Neuroimage*. 2018;180:577-593. doi:10.1016/J.NEUROIMAGE.2017.11.062

62. Bréchet L, Brunet D, Perogamvros L, Tononi G, Michel CM. EEG microstates of dreams. *Scientific Reports 2020 10:1*. 2020;10(1):1-9. doi:10.1038/s41598-020-74075-z

63. Artoni F, Maillard J, Britz J, et al. EEG microstate dynamics indicate a U-shaped path to propofol-induced loss of consciousness. *Neuroimage*. 2022;256:119156. doi:10.1016/J.NEUROIMAGE.2022.119156

64. LeDoux JE, Michel M, Lau H. A little history goes a long way toward understanding why we study consciousness the way we do today. *Proc Natl Acad Sci U S A*. 2020;117(13):6976-6984. doi:10.1073/PNAS.1921623117/SUPPL_FILE/PNAS.1921623117.SAPP.PDF

65. Buzsáki G, Draguhn A. Neuronal Oscillations in Cortical Networks. *Science (1979)*. 2004;304(5679):1926-1929. doi:10.1126/SCIENCE.1099745

66. Whittington MA, Traub RD, Adams NE. A future for neuronal oscillation research. *https://doi.org/101177/2398212818794827*. 2019;2:239821281879482. doi:10.1177/2398212818794827

APPENDIX A: SUPPLEMENTAL MATERIALS FOR CHAPTER I

Supplementary Table 1. Model predictions of Delta power at electrode Oz across conscious states using data from the Dex condition. These results correspond to those presented in Fig. 3C of the main text.

State	Adjusted Delta PSD ($log_{10}(\mu V^2)$)	Std. Err. ($log_{10}(\mu V^2)$)	Adjusted Delta PSD (μV^2)	% Change vs DC	P-Value vs DC
DC	2.457	0.044	286.418	-	-
W	2.182	0.034	152.055	53.1%	<0.001
CC	2.271	0.049	186.638	65.2%	<0.001
Unc	2.551	0.059	355.631	124.2%	0.030

Supplementary Table 2. Number of features selected by Random Feature Elimination in each machine learning model out of the total number of possible features. Because each feature accounts for a different portion of the overall variance in the training data, the sum of the variance across the selected features is also presented for reference.

Model	Corresponding Figure	Features Selected	%Variance Accounted for by Selected Features
DC vs CC. All voxels, no Alpha band.	Fig. 2d	50/198	56.4%
DC vs CC. All voxels, Alpha included.	Supp. Fig. 1a	44/198	60.2%
NE vs DC. 5 ROIs, Beta/Delta.	Fig. 3d	44/138	33.8%
NE vs DC. 4 ROIs, Beta/Delta.	Supp. Fig. 1b	52/110	33.4%
NE vs DC. All voxels, all bands.	Supp. Fig. 1c	55/205	29.5%

Supplementary Table 3. MNI Coordinates for the centroids of significant clusters. Linear Mixed Effects Model analysis of the Dex data revealed 5 clusters of voxels with significantly reduced Beta/Delta ratio in Unc vs DC wake ups.

Region of Interest	X	Y	Z
Left Parietal	-50.4	-26.8	33.6
Left Anterior Medial	-3.7	29.4	5.8
Right Anterior Medial	5.6	32.9	3.4
Left Posterior Medial	-10.8	-42.1	43
Right Posterior Medial	6.1	-42.4	41.6

Supplementary Table 4. Source localized Beta/Delta effect estimates for contrast of Unc vs DC states across conditions. These results correspond to the data presented in Fig. 5B. The effect estimates and confidence intervals (middle column) represent the difference in Beta/Delta activity, on a $\log_{10}$ scale, in Unc vs DC data. For ease of interpretation, these effects are also presented as an average percentage change in Unc vs DC (right column).

	ROI	Effect Estimate [95 % CI]	% Change vs DC
Dex	Left Parietal	-0.326 [-0.493, -0.165]	47.2%
	Left Anterior Medial	-0.315 [-0.482, -0.136]	48.4%
	Left Posterior Medial	-0.291 [-0.459, -0.111]	51.1%
	Right Anterior Medial	-0.288 [-0.466, -0.109]	51.5%
	Right Posterior Medial	-0.274 [-0.440, -0.086]	53.2%
Prop	Left Parietal	-0.678 [-1.178, -0.180]	21.0%
	Left Anterior Medial	-0.651 [-1.255, -0.077]	22.3%
	Left Posterior Medial	-0.777 [-1.299, -0.236]	16.7%
	Right Anterior Medial	-0.657 [-1.256, -0.050]	22.0%
	Right Posterior Medial	-0.558 [-1.053, -0.113]	27.7%
Sleep	Left Parietal	0.011 [-0.317, 0.426]	102.6%
	Left Anterior Medial	-0.419 [-0.804, -0.069]	38.1%
	Left Posterior Medial	-0.335 [-0.733, 0.052]	46.3%
	Right Anterior Medial	-0.481 [-0.915, -0.092]	33.0%
	Right Posterior Medial	-0.333 [-0.724, 0.060]	46.4%

Supplementary Figure 1. Validation of primary outcome (Delta power) results across varying time lengths (10-180 seconds) of EEG data as the unit of analysis. We made the decision to use the 20 seconds of EEG immediately before the wake report *a priori* based on previous literature (Siclari, 2017). Here we test if this choice has appreciable effects on the raw power spectral density (PSD) (top row) or our statistical findings (bottom row). (Top row) Raw Delta PSD estimates remained highly consistent across all time lengths analyzed. (Bottom row) Adjust PSD estimates were also highly consistent across all time lengths analyzed, though the significance of the state contrasts varied slightly. The 45 and 60 second time windows had comparable p-values to those of the 20 second window reported in the main text. Below 20 seconds and above 60 seconds we observed reduced significance of p-values. Our interpretation is that below 20 seconds, the reduced amount of data lowers the stability of the PSD estimates, increasing variability, while above 60 seconds the data become less reflective of the wake report, reducing the statistical association between the EEG data and the report. Overall, our findings do not appear to be specific to the 20 second window selected *a priori*.

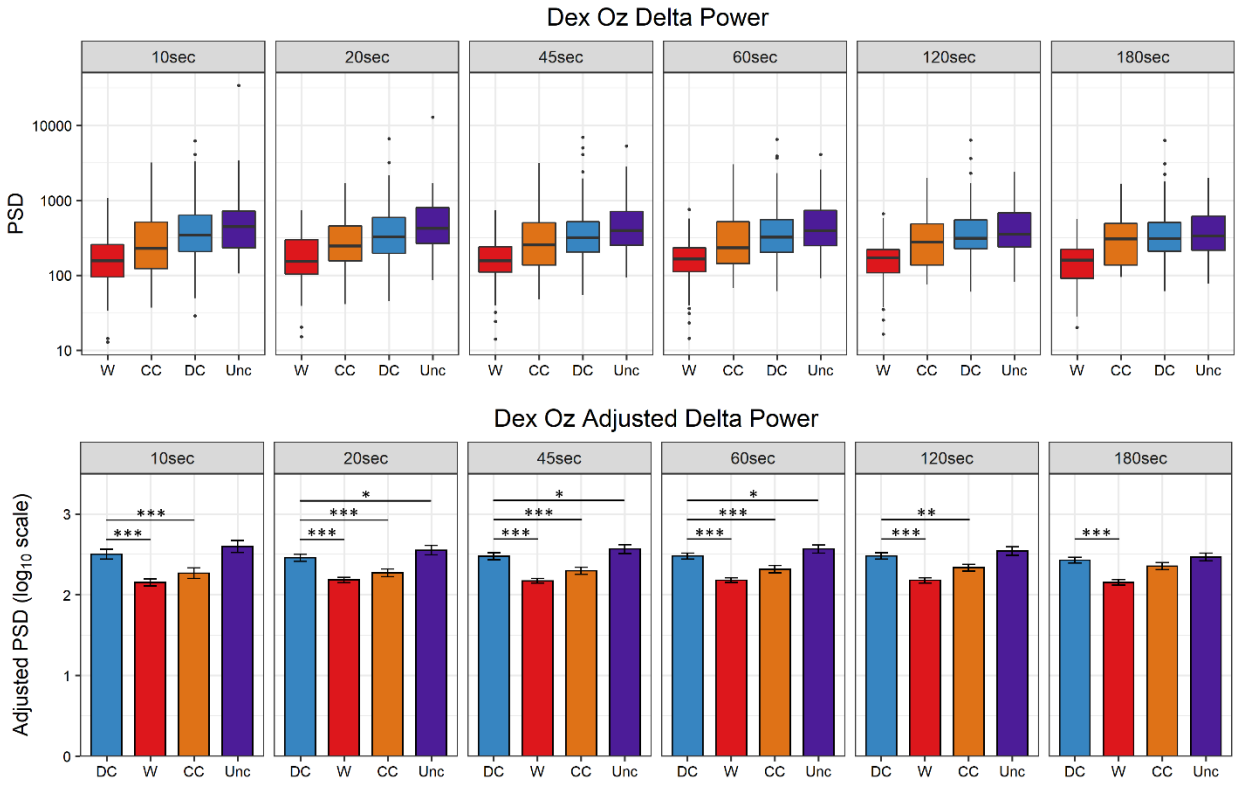

Supplementary Figure 2. (A) Medial view of voxel-wise predicted power (log_{10} scale color coded) from LMEMs for DC (left column) and Unc (middle column) across all frequency bands. Right column shows differences between Unc and DC states for all significant voxels after FDR correction for multiple comparisons. (B) Same as in A but showing lateral view.

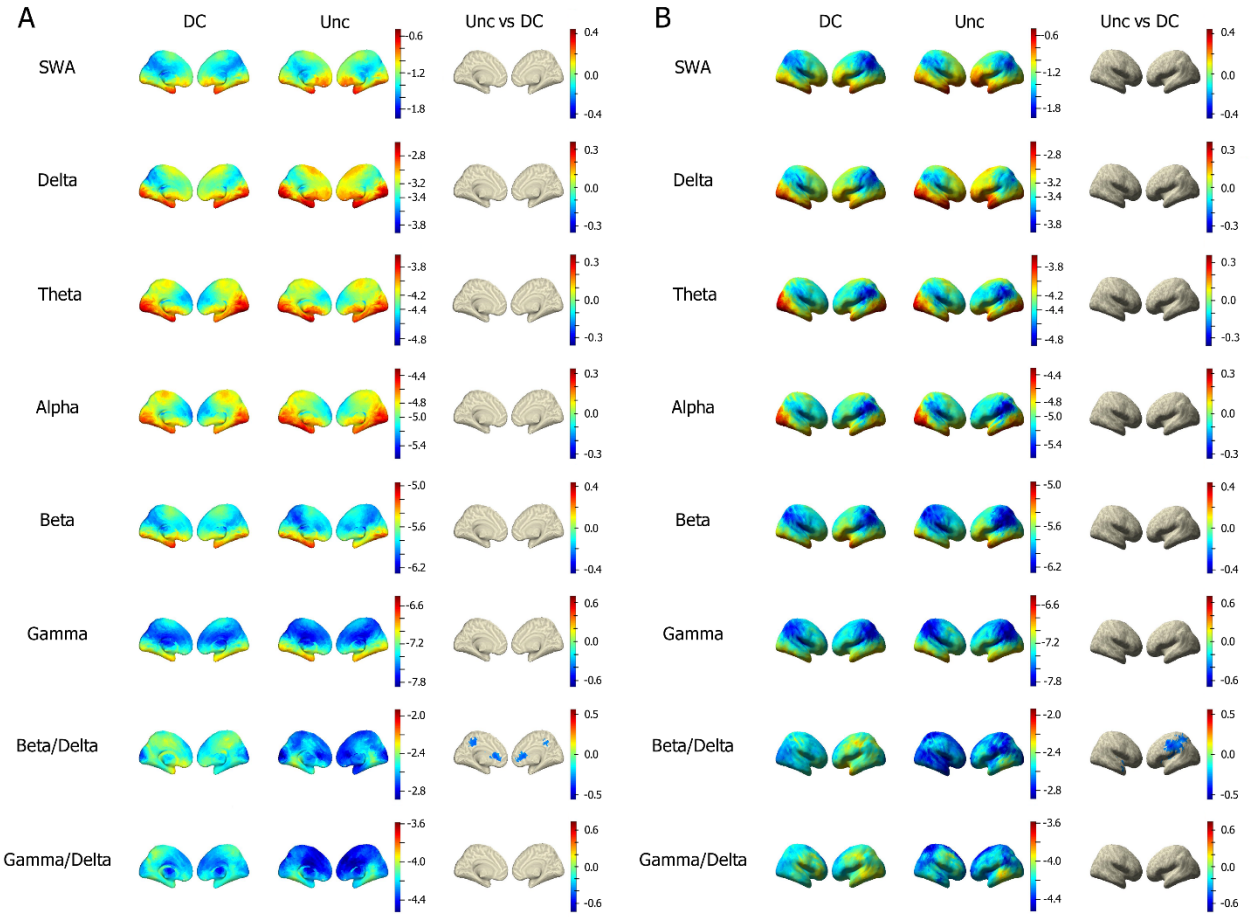

Supplementary Figure 3. Receiver operator characteristic curves for sensitivity analyses. **A**, Classification of DC vs CC using all frequency bands, i.e. same as model presented in main text but with addition of Alpha band. $AUC_{Training}$ = 0.996 [0.9899, 1.0000], $AUC_{Testing}$ = 0.793 [0.7315, 0.8467]. **B**, Classification of NE vs DC using Beta/Delta ratio of the left anterior medial, right anterior medial, left posterior medial, and right posterior medial ROIs, i.e. same as model presented in main text but excluding the left parietal ROI which failed to generalize to the Sleep data in the LMEM analysis. **C**, Classification of NE vs DC using all frequency bands and all voxels. $AUC_{Training}$ = 0.986 [0.9724, 0.9966], $AUC_{Testing}$ = 0.414 [0.2939, 0.5444].

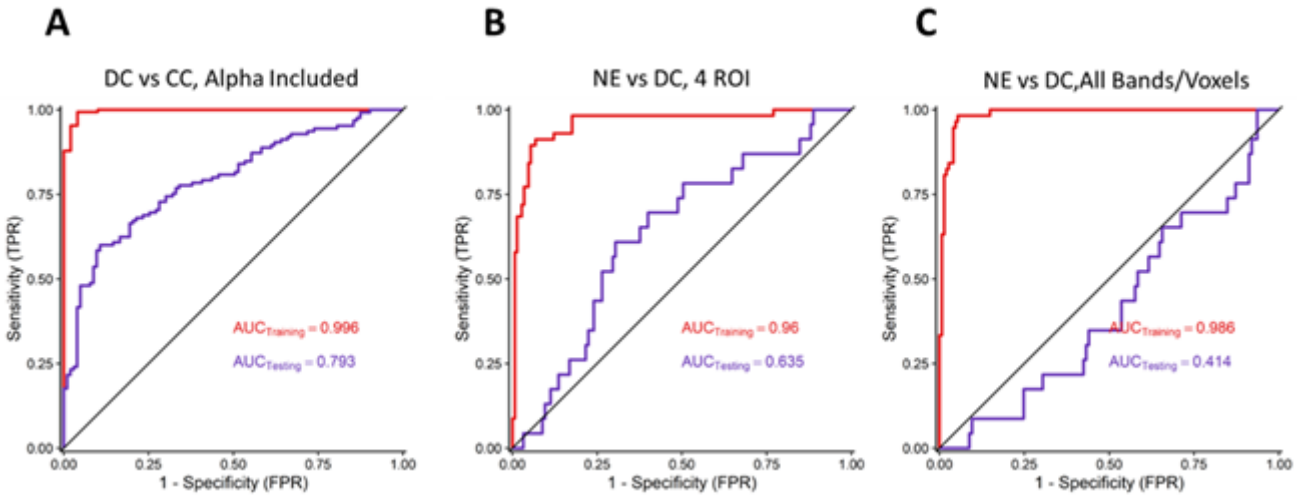

Supplementary Figure 4. Sample wake reports.

UNC10, Prop Visit. Coded: CC

What was the last thing going through your mind before I spoke to you?

My socks. They have squirrels on them.

Do you think you were awake, having a dream, or unconscious?

Awake.

Do you think you were asleep or awake?

Awake.

Were you aware for the external world?

Yes.

UNC30, Dex Visit. Coded: Unc

What was the last thing going through your mind before I spoke to you?

Mind was empty. I think I was unconscious.

Do you think you were awake, having a dream, or unconscious?

Unconscious.

Do you think you were asleep or awake?

Asleep.

Were you aware for the external world?

No.

UNC13, Dex Visit. Coded: DC

What was the last thing going through your mind before I spoke to you?

I was doing some activity. Talking to somebody.

Do you think you were awake, having a dream, or unconscious?

Dreaming.

Do you think you were asleep or awake?

Asleep.

Were you aware for the external world?

No.

UNC20, Sleep Visit. Coded: DC

What was the last thing going through your mind before I spoke to you?

Something to do with my shoes. One kind of fell apart so I was going around trying to get them fixed.

Do you think you were awake, having a dream, or unconscious?

Dreaming.

Do you think you were asleep or awake?

Asleep.

Were you aware for the external world?

No.

UNC27, Dex Visit. Coded: Ambiguous (excluded from analysis)

What was the last thing going through your mind before I spoke to you?

I don't know. I guess I was just glad to be done.

Do you think you were awake, having a dream, or unconscious?

Not sure.

Do you think you were asleep or awake?

Not sure.

Were you aware for the external world?

No.

UNC23, Prop Visit. Coded: CC

What was the last thing going through your mind before I spoke to you?

Thinking about my neighbors.

Do you think you were awake, having a dream, or unconscious?

Awake.

Do you think you were asleep or awake?

Awake.

Were you aware for the external world?

Yes.

UNC30, Dex Visit. Coded: Ambiguous (excluded from analysis)

What was the last thing going through your mind before I spoke to you?

Dreaming, it felt very realistic.

Do you think you were awake, having a dream, or unconscious?

Dreaming.

Do you think you were asleep or awake?

Asleep.

Were you aware for the external world?

Yes. (Report of external awareness conflicts with reports of sleeping and dreaming)

APPENDIX B: SUPPLEMENTAL MATERIALS FOR CHAPTER II

Supplemental Methods

Lempel-Ziv Complexity

The Lempel-Ziv complexity (LZC) of the data was calculated following the methods of Schartner et al[1]. Each EEG channel was Hilbert transformed and binarized around the mean absolute value of the subsequent analytical signal such that all values equal to or above the mean were coded as 1 and all values below the median were 0. The algorithm outline in Casali et al[2] was used to calculate the LZC of this binary string. To account for bias in the LZC measurement, the LZC values for each segment of data were normalized against LZCs generated by shuffling the binarized data of that same segment (LZC_{shuf}). We tested the variation in LZC_{shuf} values across 50 randomly selected channels and files by calculating the variance across 100 shuffles each and found that, in all cases, the variance was under 0.01% of the mean (M = 0.005%, SD = 7.83×10^{-4}%). Because the variation across shuffles was negligible, we opted to normalize against an LZC_{shuf} from a single shuffle to save computational time.

Permutation Entropy

Permutation entropy is calculated following the equation presented by Liang et al[3]. for normalized Shannon permutation entropy (PE).

$$PE = \frac{\sum_{j=1}^{m!} p_j log p_j}{\log(m!)} \quad \text{(Eq. 1)}$$

Where m is the embedding dimension used to symbolize the EEG data and p_j is the probability of the jth symbol occurring. This procedure also depends upon a time delay variable, τ, which controls the spacing between time points being used in the symbolization procedure. Because τ

is measured in time samples, the meaning of the time scale of τ depends on the sampling rate of the data. To ensure that PE would be comprehensively assessed, we computed the metric for a range of τ values. Specifically, we chose values of τ corresponding to various frequency bands of biological interest (τ = 6, 40 Hz, gamma; τ = 13, 19 Hz, beta; τ = 25, 10 Hz, alpha; τ = 41, 6 Hz, theta; and τ = 83, 3 Hz, delta). *m* was set to 6 following the selection made by Liang et al[3]. and proposed by Li et al[4].

Alpha Power and Connectivity

Alpha power was calculated by averaging over the Welch power spectral density[5] from 8-14 Hz at each channel. Due to high positive skew, power data were log-transformed to improve normality and homoskedasticity of variance. To measure the degree of alpha anteriorization, the ratio of alpha power at Fz/Oz was taken (computed as log(Fz)-log(Oz) = log(Fz/Oz)).

Alpha connectivity was estimated using the weighted phase lag index (wPLI) of the EEG data filtered between 8-14 Hz. Pairwise connectivity was computed across all 256 channels using the 'wpli_debiased' procedure in FieldTrip[6] (https://www.fieldtriptoolbox.org/). This whole scalp alpha wPLI was used as the connectivity metric for the alpha global efficiency metric below. To compute frontal alpha connectivity, the pairwise connectivity across 8 frontal channels (Supplementary Fig. 2A) were averaged.

Spectral Exponent

The spectral exponent was estimated at each channel by calculating the slope of the Welch power spectrum, between 0.5 and 55 Hz, in log-log space, following the procedure

outlined in Colombo et al[7]. Because the logarithm compresses the spacing of the frequency bins, the log-transformed power spectrum was resampled using evenly spaced frequency bins to prevent the higher frequencies from being given disproportionate weight during the regression-based slope estimation.

Spectral Edge Frequency 95%

The spectral edge frequency 95% (SEF95) is defined as the frequency boundary below which 95% of the spectral power resides[5]. SEF95 was calculated by first computing the Welch power spectrum of each channel and filtering between 0.5 and 55 Hz. The cumulative integral of each power spectrum was then computed using trapezoidal integration and normalized against the total integral. The first frequency at which the normalized cumulative integral exceeded 0.95 was selected as the SEF95. Due to high positive skew, SEF95 data were log-transformed to improve normality and homoskedasticity of variance during statistical modeling.

Normalized Symbolic Transfer Entropy

The normalized symbolic transfer entropy (NSTE) was calculated following the procedures outlined in Lee et al[8] using modified scripts from the Neuroscience Information Theory Toolbox (https://github.com/cascam07/Neuroscience-Information-Theory-Toolbox-CC)[9]. Consistent with prior work[8], we set the embedding dimension to 3 (d_E = 3), the prediction time was selected to be the value between 1 and 100 (δ = 1-100; 4-400 ms) producing the greatest cross-correlation between signals, and selected a time delay between 1 and 30 (τ = 1-30; 12-360 ms) based on the value the resulted in the greatest NSTE value. The NSTE was calculated pairwise between 8 frontal channels and 8 posterior channels (Supplementary Fig. 2B) in both directions. The averages of all frontal to posterior connections (front-to-back NSTE,

$NSTE_{f\rightarrow p}$) and all posterior to frontal connections (back-to-front NSTE, $NSTE_{p\rightarrow f}$) were then computed. Finally, the asymmetry in information flow was computed as

$$DF_{f\rightarrow p} = \frac{NSTE_{f\rightarrow p} - NSTE_{p\rightarrow f}}{NSTE_{f\rightarrow p} + NSTE_{p\rightarrow f}} \quad \text{(Eq. 2)}$$

such that positive values indicate a predominance of frontal to posterior connectivity while negative values favor the reverse.

Delta-Alpha Trough-Max Coupling

In order to operationalize the 'trough-max' pattern of delta-alpha phase-amplitude coupling[10], we applied the correlation metric previously implemented by Stephen et al[11]. Briefly, the EEG signal, at each channel, was bandpass filtered from 0.5-4 Hz to isolate the delta band and from 8-14 Hz to isolate the alpha band. A Hilbert transform was then applied to the alpha band to acquire the instantaneous amplitude, calculated as the magnitude of the analytical signal. The Pearson correlation coefficient was then computed between the delta band and the amplitude of the analytical alpha band. A Fisher Z-transform was then applied to the correlation coefficients to improve normality prior to statistical analysis[12].

Delta-Theta Phase-Amplitude Coupling

The delta-theta phase-amplitude coupling (PAC) was calculated following the procedures outlined in Tsai et al[13]. Briefly, the EEG signal, at each channel, was bandpass filtered from 2-4 Hz to isolate the high-delta band and from 4-8 Hz to isolate the theta band. Both bands were Hilbert transformed to extract the phase from the delta band and the amplitude envelope from the theta band. Next, the phases were partitioned into 16 equally spaced bins and the average amplitudes of the data points in each bin were computed. The

mean amplitudes were then normalized against the sum across bins, resulting in a normalized modulogram. The modulation index (MI) of each channel was calculated according to the following:

$$MI = \frac{\log(N) + \sum_{j=1}^{N} P(j)\log\left(P(j)\right)}{\log(N)} \quad \text{(Eq. 3)}$$

Where *P(j)* is the normalized mean amplitude of bin *j* and *N* is the total number of bins (16).

Alpha Global Efficiency and Delta Local Efficiency

The network global and local efficiency metrics were computed using the wPLI (see *Alpha Power and Connectivity*) applied from 8-14 Hz for alpha connectivity and from 0.5-4 Hz for delta activity. Following the procedures outline in Blain-Moraes et al[14] and Lee et al[15], each wPLI adjacency matrix was converted into a binary undirected network. Converting weighted parameters into a binary network requires thresholding the connectivity data based on some criteria to determine which connections will be included, however, the choice of threshold can impact the results of downstream analyses and should be made with care[16–19]. Rather than select a single threshold value arbitrarily, a range of edge density thresholds (5%, 10%, 15%, 20%, 25%, 30%, 35%, 40%) were applied and global/local efficiencies were computed from the resulting networks. Statistics were run for each threshold value (see *Statistical Modeling*).

The global efficiency of each alpha network and the local efficiency of each delta network was calculated using the Brain Connectivity Toolbox (https://sites.google.com/site/bctnet/)[20]. Each network's efficiency values were normalized against the average efficiency (global or local) of 10 randomized networks, generated by shuffling the real network edges while maintaining the same distribution of node degrees[14].

References

1. Schartner M, Seth A, Noirhomme Q, et al. Complexity of Multi-Dimensional Spontaneous EEG Decreases during Propofol Induced General Anaesthesia. Chialvo DR, ed. *PLoS One*. 2015;10(8):e0133532. doi:10.1371/journal.pone.0133532

2. Casali AG, Gosseries O, Rosanova M, et al. A theoretically based index of consciousness independent of sensory processing and behavior. *Sci Transl Med*. 2013;5(198):198ra105-198ra105. doi:10.1126/scitranslmed.3006294

3. Liang Z, Wang Y, Sun X, et al. EEG entropy measures in anesthesia. *Front Comput Neurosci*. 2015;9(JAN). doi:10.3389/FNCOM.2015.00016/ABSTRACT

4. Li X, Cui S, Voss LJ. Using Permutation Entropy to Measure the Electroencephalographic Effects of Sevoflurane. *Anesthesiology*. 2008;109(3):448-456. doi:10.1097/ALN.0B013E318182A91B

5. Welch PD. The Use of Fast Fourier Transform for the Estimation of Power Spectra: A Method Based on Time Averaging Over Short, Modified Periodograms. *IEEE Transactions on Audio and Electroacoustics*. 1967;15(2):70-73. doi:10.1109/TAU.1967.1161901

6. Oostenveld R, Fries P, Maris E, Schoffelen JM. FieldTrip: Open source software for advanced analysis of MEG, EEG, and invasive electrophysiological data. *Comput Intell Neurosci*. 2011;2011. doi:10.1155/2011/156869

7. Colombo MA, Napolitani M, Boly M, et al. The spectral exponent of the resting EEG indexes the presence of consciousness during unresponsiveness induced by propofol, xenon, and ketamine. *Neuroimage*. 2019;189:631-644. doi:10.1016/J.NEUROIMAGE.2019.01.024

8. Lee U, Ku S, Noh G, Baek S, Choi B, Mashour GA. Disruption of Frontal–Parietal Communication by Ketamine, Propofol, and Sevoflurane. *Anesthesiology*. 2013;118(6):1264-1275. doi:10.1097/ALN.0B013E31829103F5

9. Timme NM, Lapish C. A Tutorial for Information Theory in Neuroscience. *eNeuro*. 2018;5(3). doi:10.1523/ENEURO.0052-18.2018

10. Purdon PL, Pierce ET, Mukamel EA, et al. Electroencephalogram signatures of loss and recovery of consciousness from propofol. *Proc Natl Acad Sci U S A*. 2013;110(12). doi:10.1073/pnas.1221180110

11. Stephen EP, Hotan GC, Pierce ET, et al. Broadband slow-wave modulation in posterior and anterior cortex tracks distinct states of propofol-induced unconsciousness. *Scientific Reports 2020 10:1*. 2020;10(1):1-11. doi:10.1038/s41598-020-68756-y

12. Silver NC, Dunlap WP. Averaging Correlation Coefficients: Should Fisher's z Transformation Be Used? *Journal of Applied Psychology*. 1987;72(1):146-148. doi:10.1037/0021-9010.72.1.146

13. Tsai FF, Fan SZ, Cheng HL, Yeh JR. Multi-timescale phase-amplitude couplings in transitions of anesthetic-induced unconsciousness. *Scientific Reports 2019 9:1*. 2019;9(1):1-11. doi:10.1038/s41598-019-44238-8

14. Blain-Moraes S, Tarnal V, Vanini G, et al. Network Efficiency and Posterior Alpha Patterns Are Markers of Recovery from General Anesthesia: A High-Density Electroencephalography Study in Healthy Volunteers. *Front Hum Neurosci*. 2017;11:328. doi:10.3389/FNHUM.2017.00328

15. Lee M, Sanders RD, Yeom SK, et al. Network Properties in Transitions of Consciousness during Propofol-induced Sedation. *Scientific Reports 2017 7:1*. 2017;7(1):1-13. doi:10.1038/s41598-017-15082-5

16. van Wijk BCM, Stam CJ, Daffertshofer A. Comparing Brain Networks of Different Size and Connectivity Density Using Graph Theory. *PLoS One*. 2010;5(10):e13701. doi:10.1371/JOURNAL.PONE.0013701

17. Ismail LE, Karwowski W. A Graph Theory-Based Modeling of Functional Brain Connectivity Based on EEG: A Systematic Review in the Context of Neuroergonomics. *IEEE Access*. 2020;8:155103-155135. doi:10.1109/ACCESS.2020.3018995

18. Drakesmith M, Caeyenberghs K, Dutt A, Lewis G, David AS, Jones DK. Overcoming the effects of false positives and threshold bias in graph theoretical analyses of neuroimaging data. *Neuroimage*. 2015;118:313-333. doi:10.1016/j.neuroimage.2015.05.011

19. Buchanan CR, Bastin ME, Ritchie SJ, et al. The effect of network thresholding and weighting on structural brain networks in the UK Biobank. *Neuroimage*. 2020;211:116443. doi:10.1016/J.NEUROIMAGE.2019.116443

20. Rubinov M, Sporns O. Complex network measures of brain connectivity: Uses and interpretations. *Neuroimage*. 2010;52(3):1059-1069. doi:10.1016/J.NEUROIMAGE.2009.10.003

Supplemental Figures & Tables

	Dex	Prop	Sleep
Conscious State			
W	69	23	64
CC	49	39	-
DC	147	13	111
Unc	57	11	12
OAA/S			
5	132	57	-
4	102	19	-
3	72	8	-
2	25	2	-
1	8	2	-
0	0	1	-

Supplementary Table 1. Counts of wake reports from each experimental condition, split by conscious state (top), or OAA/S score (bottom). Experimental conditions are dexmedetomidine sedation (Dex), propofol sedation (Prop) or natural sleep. Conscious states are baseline connected consciousness (W), connected consciousness with drug (CC), disconnected consciousness (DC), and unconsciousness (Unc).

Dexmedetomidine			
Metric	LOR Effect	F-Statistic	P-Value
Frontal alpha (power)	3.1E-1 [1.9E-1, 4.4E-1]	F(1,249.11) = 24.75	<0.001 *
Frontal alpha (connectivity)	7.7E-2 [5.2E-2, 1.0E-1]	F(1,227.04) = 34.17	<0.001 *
Lempel-ziv complexity	-3.8E-2 [-7.4E-2, -7.2E-3]	F(1,264.72) = 4.68	0.057
Delta-alpha peak-max coupling	7.5E-3 [-3.1E-2, 4.7E-2]	F(1,235.94) = 0.14	0.786
Delta-theta phase amplitude coupling (MI)	2.4E-4 [9.9E-5, 3.7E-4]	F(1,241.38) = 11.18	0.002 *
Permutation Entropy (gamma)	-5.4E-2 [-6.8E-2, -4.2E-2]	F(1,257.98) = 63.42	<0.001 *
Permutation Entropy (beta)	-3.3E-2 [-4.5E-2, -2.3E-2]	F(1,252.34) = 41.51	<0.001 *
Permutation Entropy (alpha)	-3.5E-2 [-4.6E-2, -2.4E-2]	F(1,241.26) = 42.87	<0.001 *
Permutation Entropy (theta)	-2.7E-2 [-3.7E-2, -1.5E-2]	F(1,253.39) = 21.72	<0.001 *
Permutation Entropy (delta)	5.2E-4 [-1.4E-2, 1.6E-2]	F(1,264.71) = 0	0.946
Spectral Exponent	-4.2E-1 [-5.4E-1, -3.0E-1]	F(1,208.46) = 46.93	<0.001 *
Spectral edge frequency 95%	-2.2E-1 [-2.8E-1, -1.5E-1]	F(1,206.39) = 42.7	<0.001 *
NSTE (back to front)	-2.1E-3 [-3.5E-3, -4.1E-4]	F(1,195.47) = 5.52	0.038 *
NSTE (front to back)	-2.2E-3 [-4.2E-3, -1.7E-4]	F(1,205.07) = 4.34	0.066
NSTE (asymmetry)	-5.9E-3 [-6.8E-2, 5.9E-2]	F(1,223.7) = 0.03	0.912
Delta local efficiency (5% edges)	-6.5E-2 [-1.4E-1, 1.0E-2]	F(1,118.25) = 3.25	0.104
Delta local efficiency (10% edges)	-3.9E-2 [-8.4E-2, 7.2E-3]	F(1,118.25) = 2.92	0.121
Delta local efficiency (15% edges)	-4.0E-2 [-7.0E-2, -1.3E-2]	F(1,118.25) = 6.7	0.022 *
Delta local efficiency (20% edges)	-3.4E-2 [-5.7E-2, -1.3E-2]	F(1,118.25) = 9.18	0.007 *
Delta local efficiency (25% edges)	-2.8E-2 [-4.5E-2, -1.1E-2]	F(1,118.25) = 10.39	0.004 *
Delta local efficiency (30% edges)	-2.5E-2 [-3.6E-2, -1.1E-2]	F(1,118.25) = 12.99	0.001 *
Delta local efficiency (35% edges)	-2.1E-2 [-3.1E-2, -1.1E-2]	F(1,118.25) = 14.65	0.001 *
Delta local efficiency (40% edges)	-1.6E-2 [-2.4E-2, -7.1E-3]	F(1,118.25) = 12.86	0.001 *
Alpha global efficiency (5% edges)	1.5E-2 [-9.5E-4, 3.2E-2]	F(1,167.59) = 3.36	0.101
Alpha global efficiency (10% edges)	3.4E-3 [-5.6E-3, 1.3E-2]	F(1,174.68) = 0.47	0.612
Alpha global efficiency (15% edges)	-4.0E-4 [-6.6E-3, 6.0E-3]	F(1,134.67) = 0.01	0.935
Alpha global efficiency (20% edges)	-1.3E-3 [-6.1E-3, 3.0E-3]	F(1,118.25) = 0.29	0.681
Alpha global efficiency (25% edges)	-1.0E-3 [-4.3E-3, 2.1E-3]	F(1,134.34) = 0.42	0.619
Alpha global efficiency (30% edges)	-1.1E-3 [-3.4E-3, 1.0E-3]	F(1,138.69) = 0.95	0.429
Alpha global efficiency (35% edges)	-1.4E-3 [-2.9E-3, 8.0E-5]	F(1,123.32) = 3.67	0.090
Alpha global efficiency (40% edges)	-9.4E-4 [-1.9E-3, 7.0E-5]	F(1,144.22) = 3.66	0.090
Propofol			
Metric	LOR Effect	F-Statistic	P-Value
Frontal alpha (power)	5.4E-6 [4.2E-1, 1.9E-1]	F(1,74.89) = 11.36	0.004 *
Frontal alpha (connectivity)	9.0E-8 [6.8E-2, 1.9E-2]	F(1,77.44) = 7.65	0.020 *
Lempel-ziv complexity	5.7E-2 [-1.7E-1, -2.5E-1]	F(1,75.25) = 17.4	<0.001 *
Delta-alpha peak-max coupling	7.9E-1 [-3.4E-2, -1.1E-1]	F(1,77.64) = 0.8	0.768

Delta-theta phase amplitude coupling (MI)	2.5E-3 [1.2E-3, 8.8E-4]	F(1,78.94) = 38.06	<0.001 *
Permutation Entropy (gamma)	1.7E-12 [-9.5E-3, -3.6E-2]	F(1,75.64) = 0.59	0.768
Permutation Entropy (beta)	3.7E-9 [-1.3E-2, -3.4E-2]	F(1,75.43) = 1.57	0.554
Permutation Entropy (alpha)	3.6E-9 [-2.6E-2, -4.2E-2]	F(1,76.88) = 11.65	0.004 *
Permutation Entropy (theta)	2.0E-5 [-3.1E-2, -4.3E-2]	F(1,76.78) = 25.63	<0.001 *
Permutation Entropy (delta)	9.5E-1 [-1.6E-2, -2.5E-2]	F(1,76.02) = 13.85	0.002 *
Spectral Exponent	1.3E-9 [-5.1E-1, -7.4E-1]	F(1,75.31) = 19.18	<0.001 *
Spectral edge frequency 95%	3.7E-9 [-2.4E-1, -3.4E-1]	F(1,75.58) = 25.08	<0.001 *
NSTE (back to front)	3.8E-2 [8.3E-4, -2.7E-3]	F(1,78.97) = 0.22	0.855
NSTE (front to back)	6.6E-2 [-9.2E-3, -1.5E-2]	F(1,76.64) = 9.64	0.008 *
NSTE (asymmetry)	9.1E-1 [-2.4E-1, -3.6E-1]	F(1,77.96) = 12.37	0.003 *
Delta local efficiency (5% edges)	1.0E-1 [-1.0E-1, -3.2E-1]	F(1,77.87) = 0.9	0.768
Delta local efficiency (10% edges)	1.2E-1 [1.6E-2, -1.1E-1]	F(1,78.97) = 0.07	0.932
Delta local efficiency (15% edges)	2.2E-2 [1.8E-2, -5.9E-2]	F(1,78.25) = 0.19	0.855
Delta local efficiency (20% edges)	6.7E-3 [6.3E-3, -5.0E-2]	F(1,78.28) = 0.05	0.932
Delta local efficiency (25% edges)	3.9E-3 [-1.5E-3, -4.1E-2]	F(1,78.19) = 0	0.967
Delta local efficiency (30% edges)	1.4E-3 [-3.6E-3, -4.2E-2]	F(1,77.8) = 0.04	0.932
Delta local efficiency (35% edges)	7.2E-4 [-5.7E-4, -2.8E-2]	F(1,77.96) = 0	0.967
Delta local efficiency (40% edges)	1.4E-3 [-2.2E-3, -2.6E-2]	F(1,78.07) = 0.04	0.932
Alpha global efficiency (5% edges)	1.0E-1 [1.7E-2, -2.6E-2]	F(1,78.93) = 0.79	0.768
Alpha global efficiency (10% edges)	6.1E-1 [7.8E-3, -1.2E-2]	F(1,76.99) = 0.57	0.768
Alpha global efficiency (15% edges)	9.4E-1 [-5.4E-3, -2.0E-2]	F(1,78.18) = 0.52	0.768
Alpha global efficiency (20% edges)	6.8E-1 [-3.6E-3, -1.4E-2]	F(1,77.45) = 0.47	0.768
Alpha global efficiency (25% edges)	6.2E-1 [-2.6E-3, -1.0E-2]	F(1,76.96) = 0.47	0.768
Alpha global efficiency (30% edges)	4.3E-1 [-1.5E-3, -6.1E-3]	F(1,76.82) = 0.34	0.792
Alpha global efficiency (35% edges)	9.0E-2 [2.3E-4, -3.0E-3]	F(1,76.72) = 0.01	0.966
Alpha global efficiency (40% edges)	9.0E-2 [8.1E-4, -1.5E-3]	F(1,76.74) = 0.36	0.792

Supplementary Table 2. Effect estimates, F-statistics, and p-values from LMEMs testing the association between each metric and loss of responsiveness (LOR) in dexmedetomidine and propofol data. Effect estimates are listed as Mean [95% confidence interval]. P-values are corrected for multiple comparisons using the Benjamini-Hochberg false discovery rate (FDR) procedure. Asterisks (*) indicate significant p-values ($p < 0.05$).

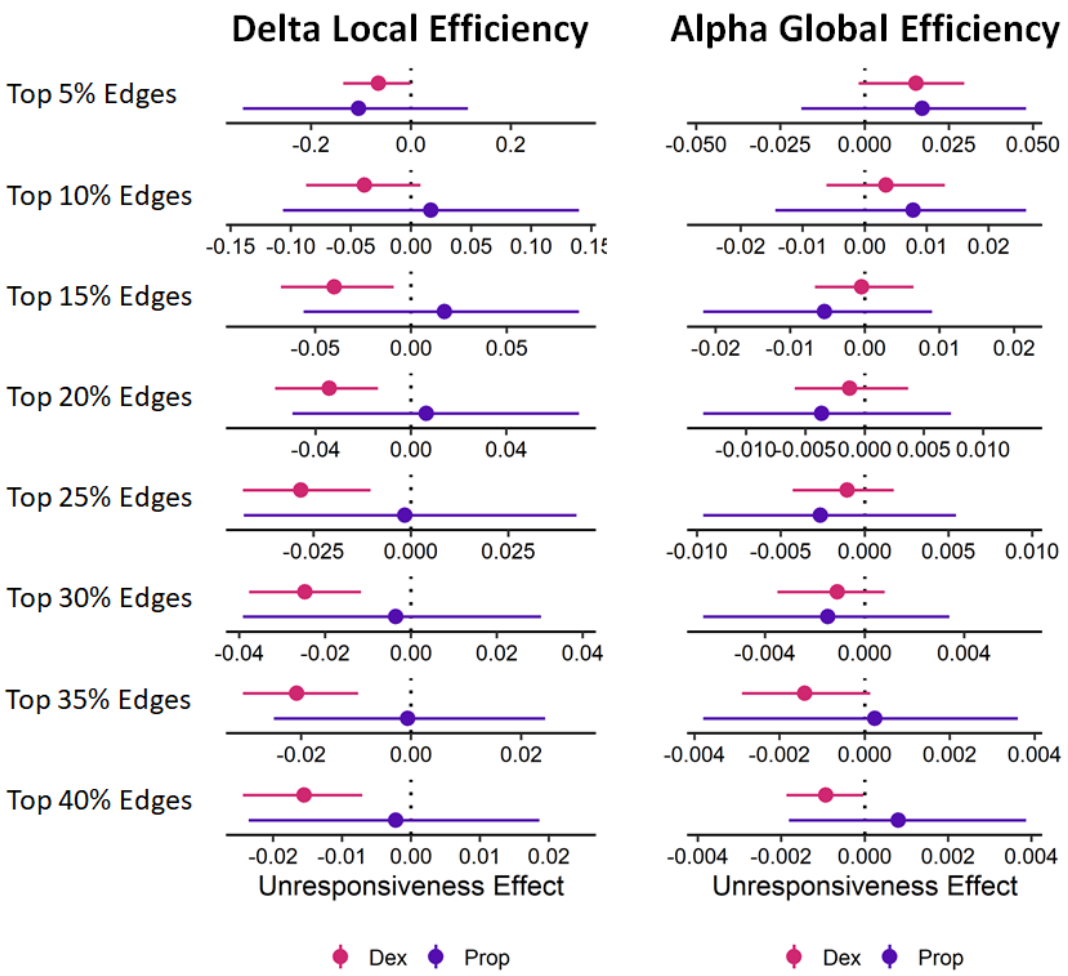

Supplementary Figure 1. Effect estimates from LMEMs testing the association between delta local efficiency or alpha global efficiency with low responsiveness in dexmedetomidine (Dex) and propofol (Prop) data. Plots show the mean effect with 95% confidence intervals. Each row indicates a different threshold applied to the wPLI network prior to calculating the efficiency metrics.

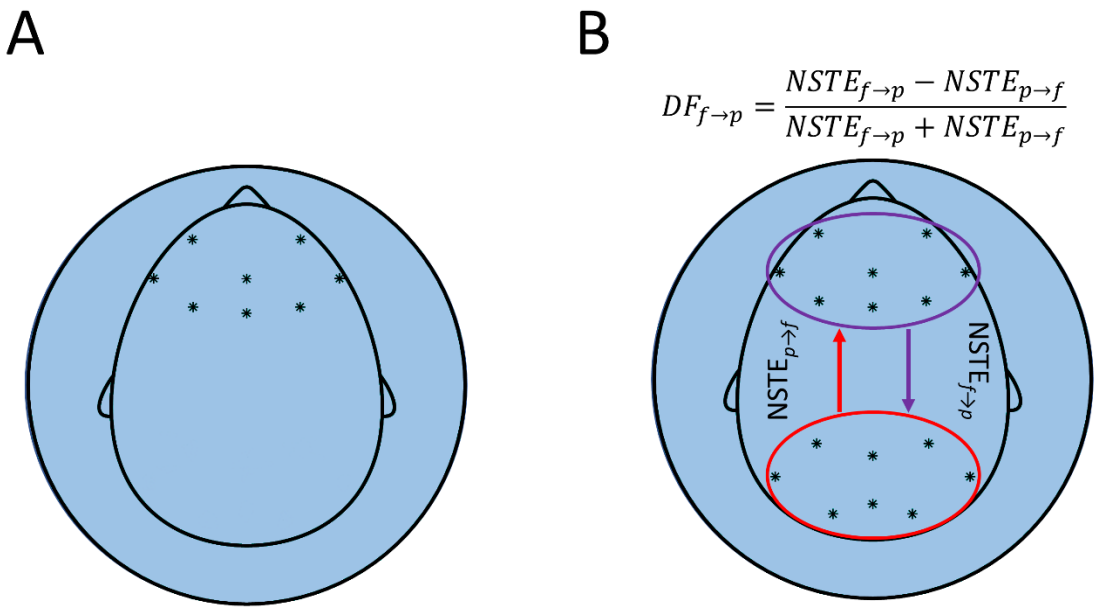

Supplementary Figure 2. A) Locations of the frontal electrodes used for computing the average pair-wise frontal alpha wPLI. B) Locations of the frontal (purple grouping) and posterior (red grouping) electrodes used to calculate the NSTE. The equation included is that of Eq. 2 in the Supplementary Methods, which defines the asymmetry in front-to-back relative to back-to-front directed connectivity.

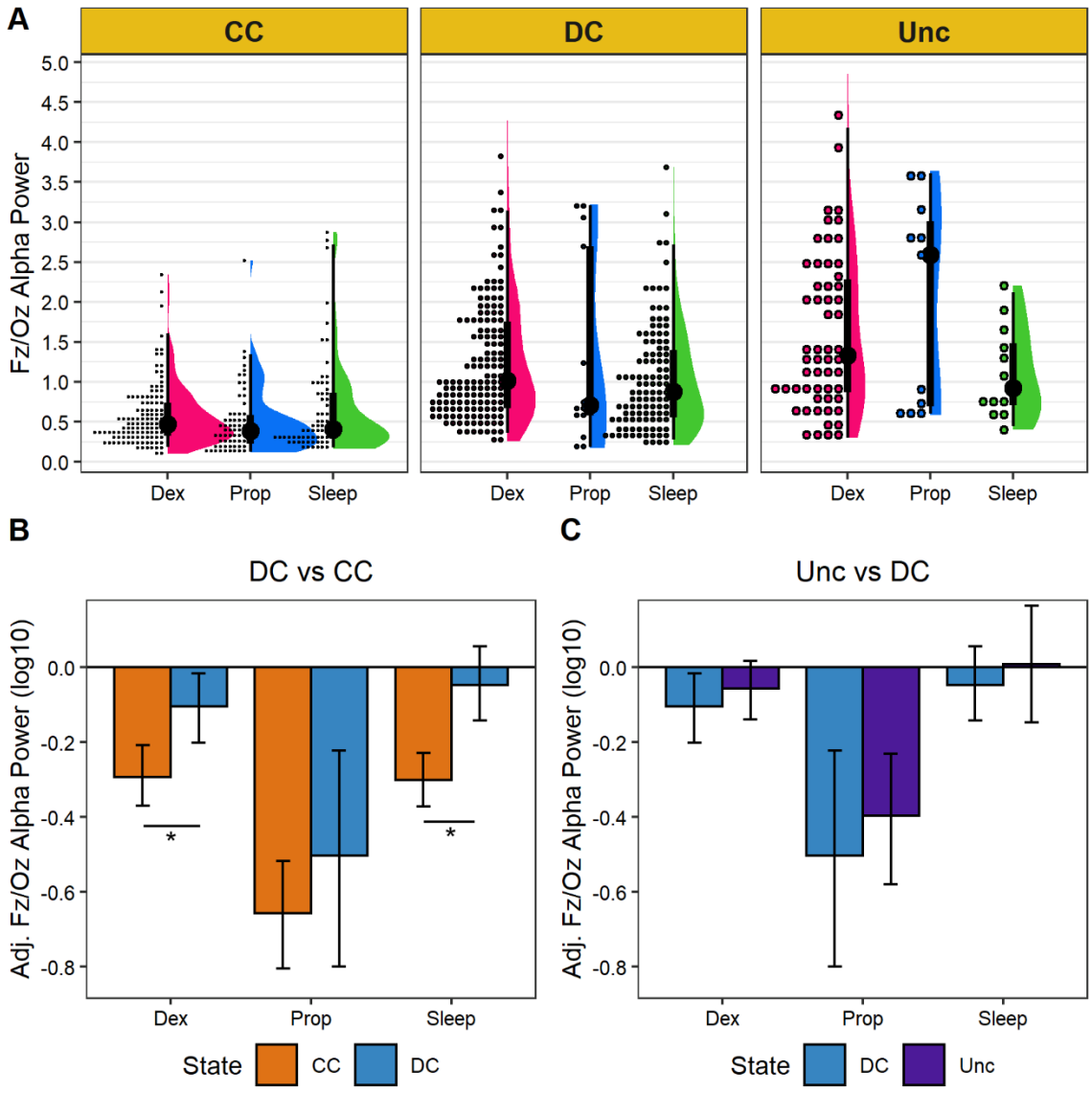

Supplementary Figure 3. A) Density plots of raw data for Fz/Oz alpha power in each conscious state (CC, DC, or Unc) and experimental condition (Dex, Prop, Sleep). B) Adjusted means (i.e. model predictions) of Fz/Oz alpha power in CC and DC. C) Adjusted means (i.e. model predictions) of Fz/Oz alpha power in DC and Unc. Asterisks (*) indicate contrasts in which differences between states were statistically significant after correcting for multiple comparison, $p_{FDR} < 0.05$.

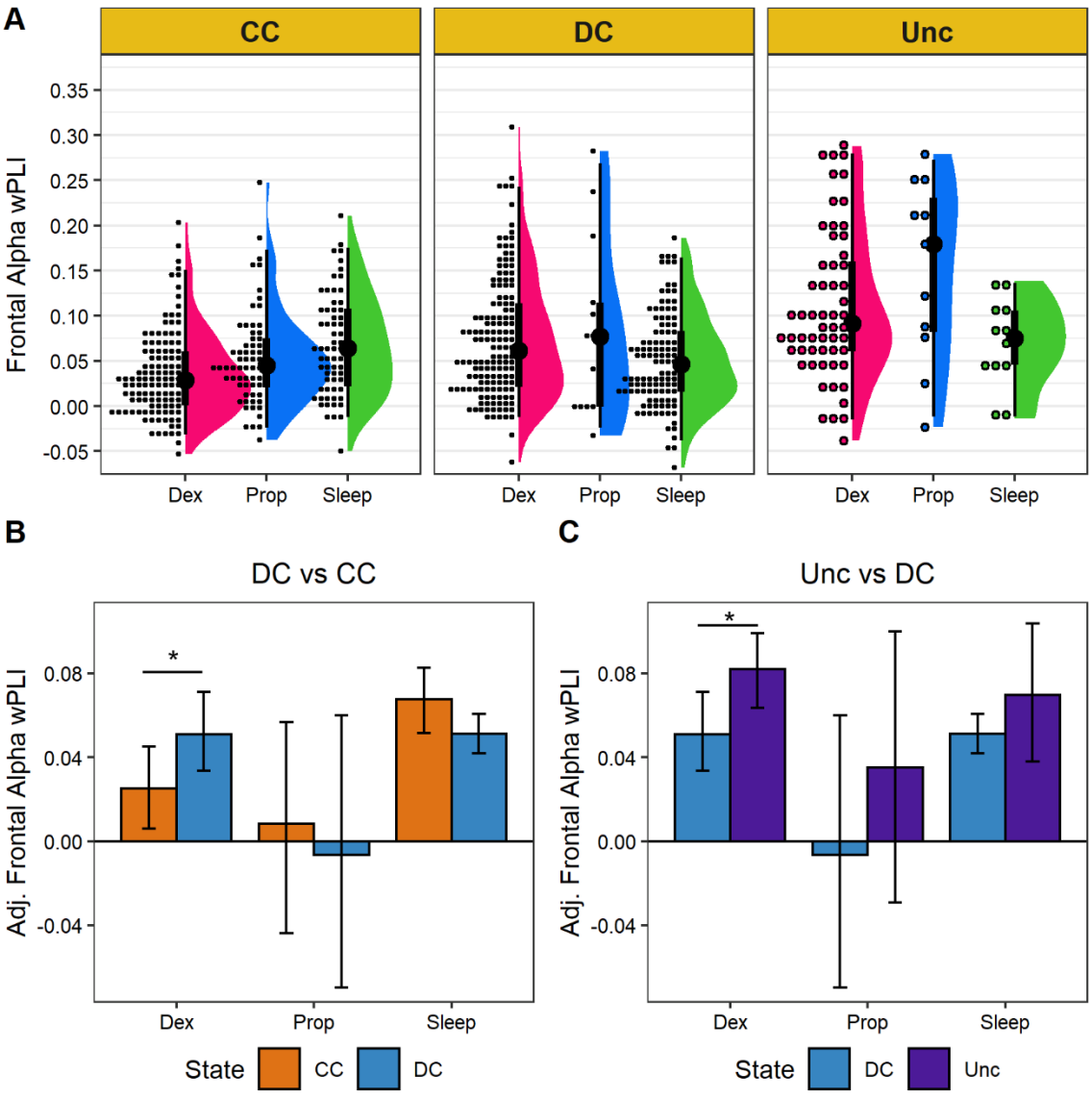

Supplementary Figure 4. A) Density plots of raw data for frontal alpha wPLI in each conscious state (CC, DC, or Unc) and experimental condition (Dex, Prop, Sleep). B) Adjusted means (i.e. model predictions) of frontal alpha wPLI in CC and DC. C) Adjusted means (i.e. model predictions) of frontal alpha wPLI in DC and Unc. Asterisks (*) indicate contrasts in which differences between states were statistically significant after correcting for multiple comparison, $p_{FDR} < 0.05$.

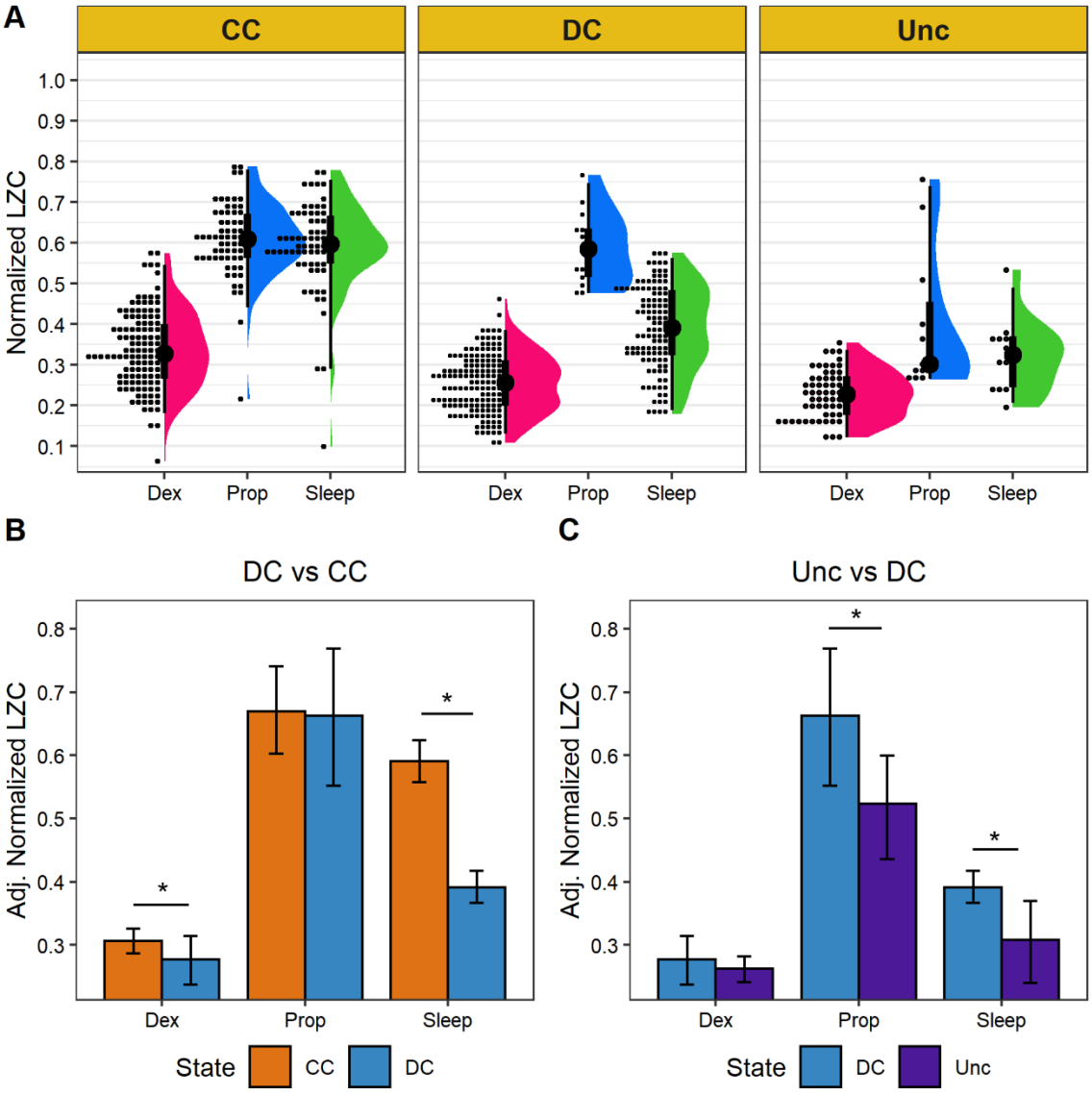

Supplementary Figure 5. A) Density plots of raw data for Lempel-Ziv complexity in each conscious state (CC, DC, or Unc) and experimental condition (Dex, Prop, Sleep). B) Adjusted means (i.e. model predictions) of Lempel-Ziv complexity in CC and DC. C) Adjusted means (i.e. model predictions) of Lempel-Ziv complexity in DC and Unc. Asterisks (*) indicate contrasts in which differences between states were statistically significant after correcting for multiple comparison, $p_{FDR} < 0.05$.

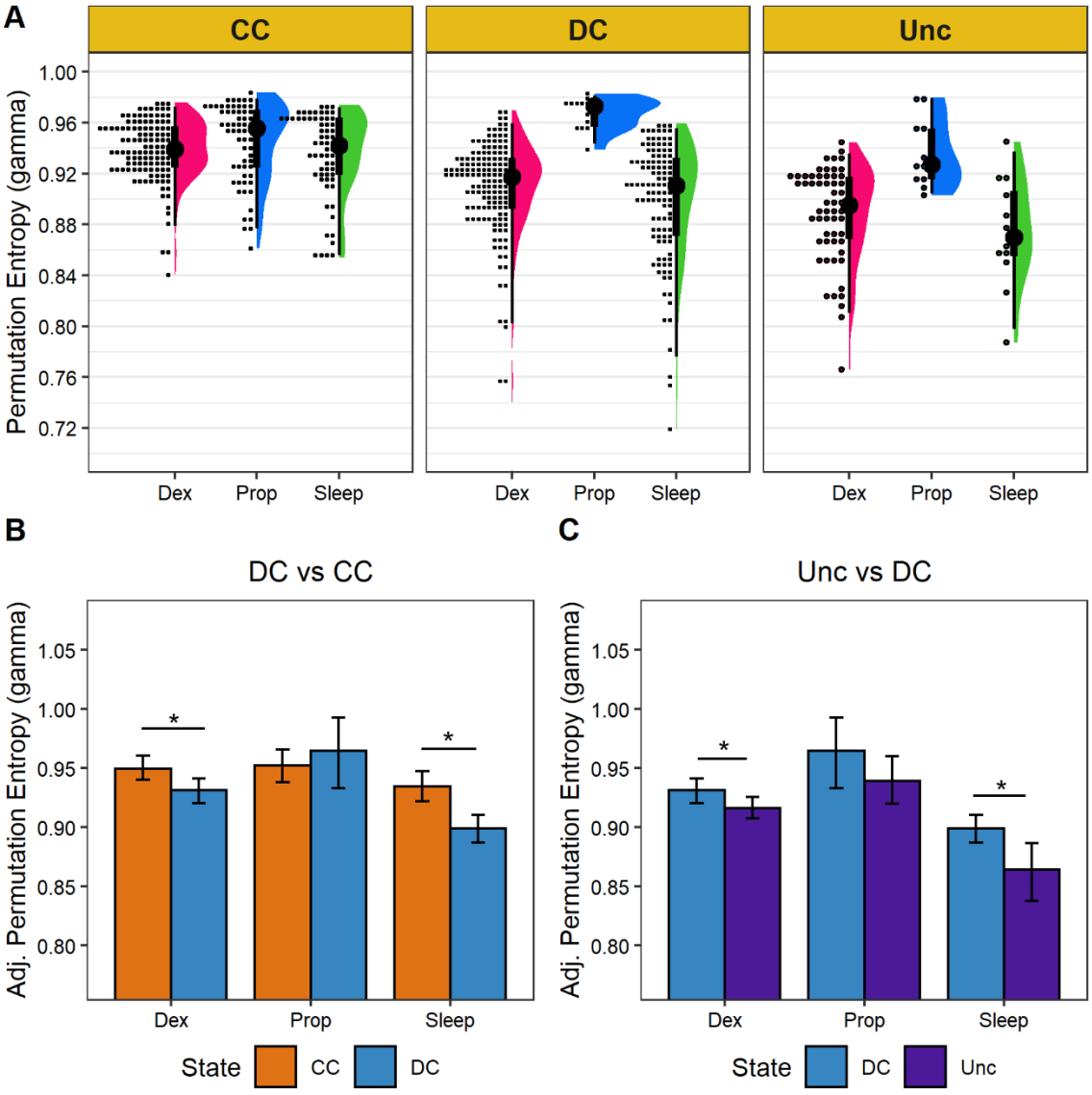

Supplementary Figure 6. A) Density plots of raw data for gamma permutation entropy in each conscious state (CC, DC, or Unc) and experimental condition (Dex, Prop, Sleep). B) Adjusted means (i.e. model predictions) of gamma permutation entropy in CC and DC. C) Adjusted means (i.e. model predictions) of gamma permutation entropy in DC and Unc. Asterisks (*) indicate contrasts in which differences between states were statistically significant after correcting for multiple comparison, $p_{FDR} < 0.05$.

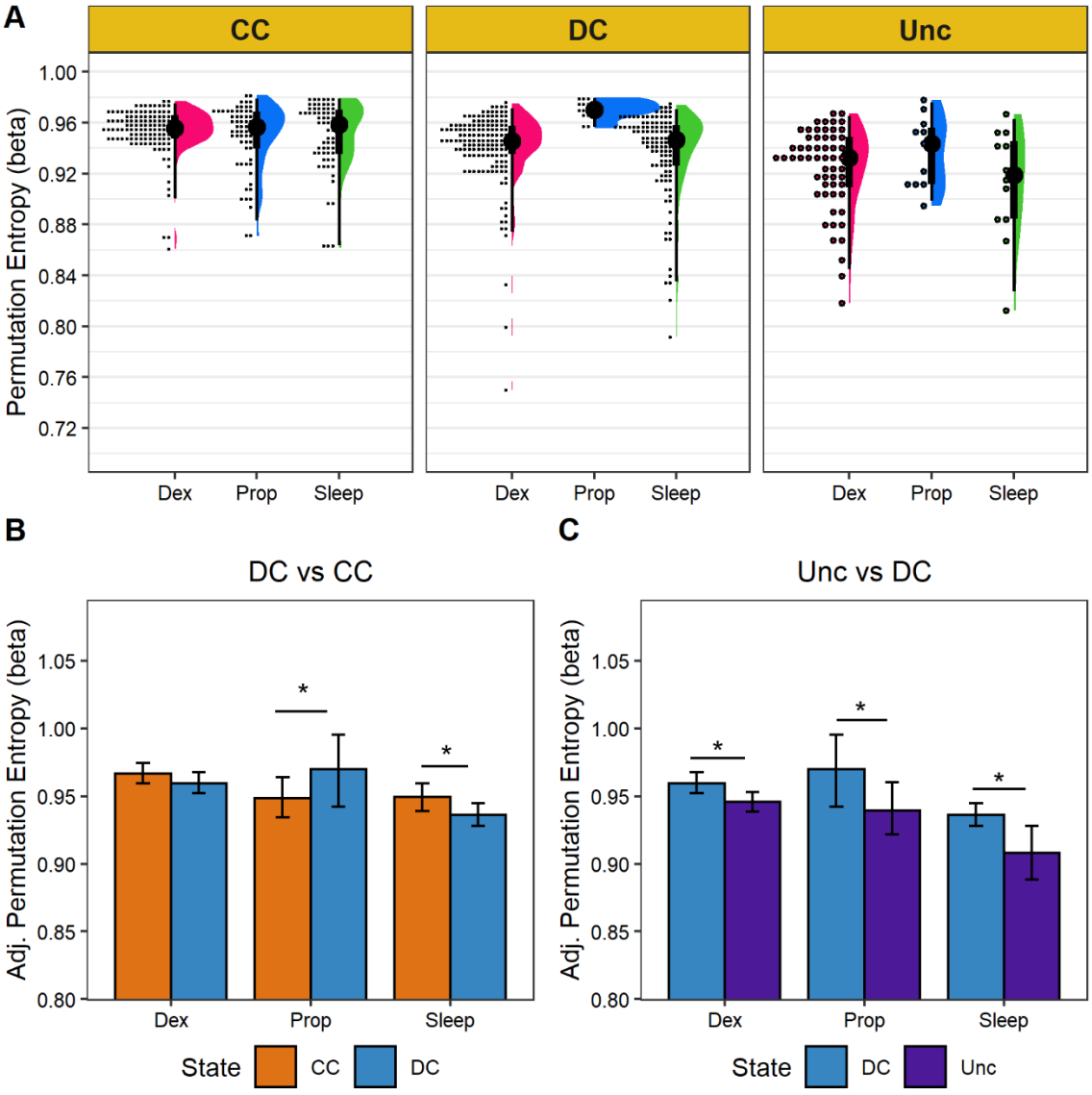

Supplementary Figure 7. A) Density plots of raw data for beta permutation entropy in each conscious state (CC, DC, or Unc) and experimental condition (Dex, Prop, Sleep). B) Adjusted means (i.e. model predictions) of beta permutation entropy in CC and DC. C) Adjusted means (i.e. model predictions) of beta permutation entropy in DC and Unc. Asterisks (*) indicate contrasts in which differences between states were statistically significant after correcting for multiple comparison, $p_{FDR} < 0.05$.

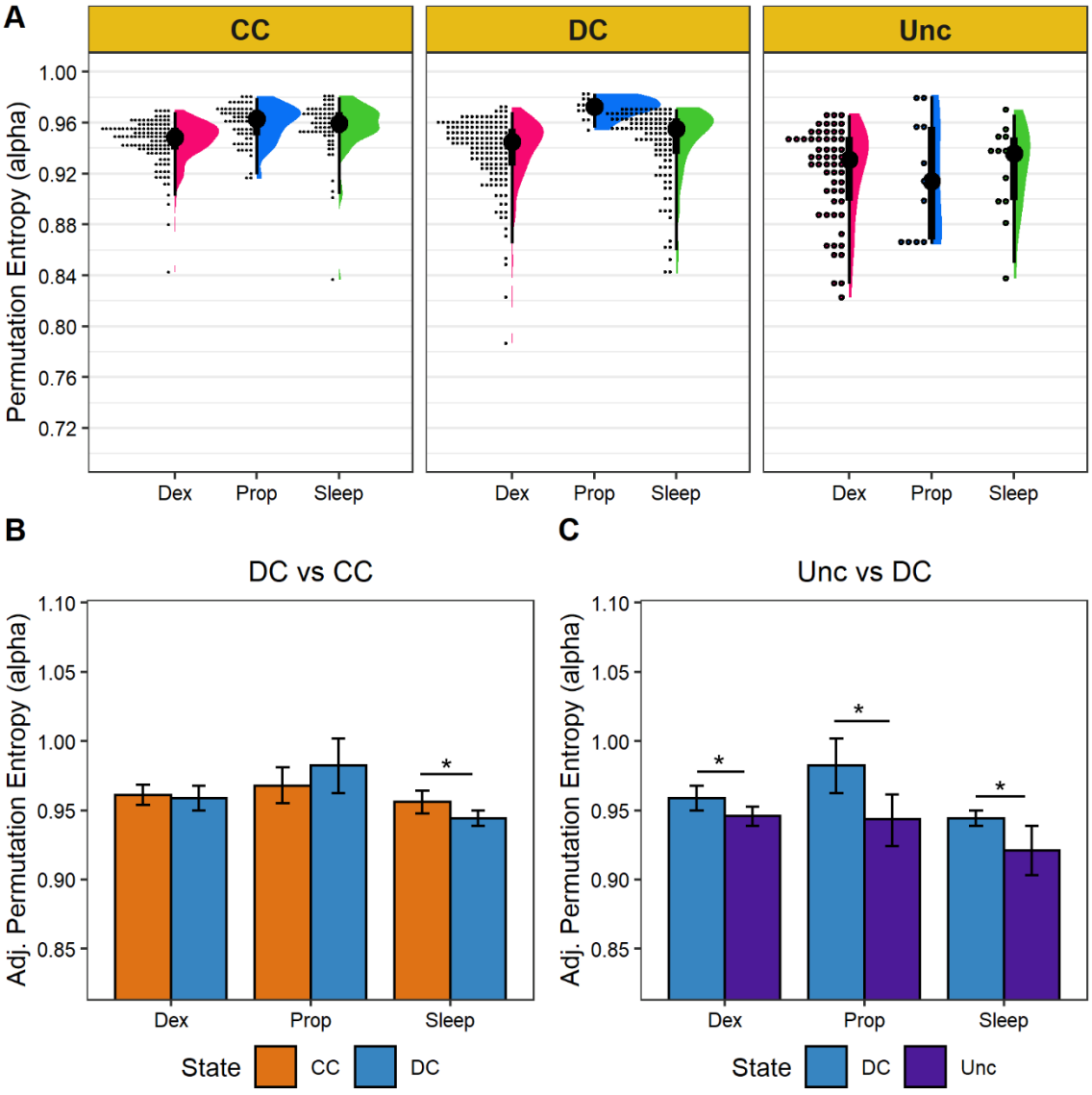

Supplementary Figure 8. A) Density plots of raw data for alpha permutation entropy in each conscious state (CC, DC, or Unc) and experimental condition (Dex, Prop, Sleep). B) Adjusted means (i.e. model predictions) of alpha permutation entropy in CC and DC. C) Adjusted means (i.e. model predictions) of alpha permutation entropy in DC and Unc. Asterisks (*) indicate contrasts in which differences between states were statistically significant after correcting for multiple comparison, $p_{FDR} < 0.05$.

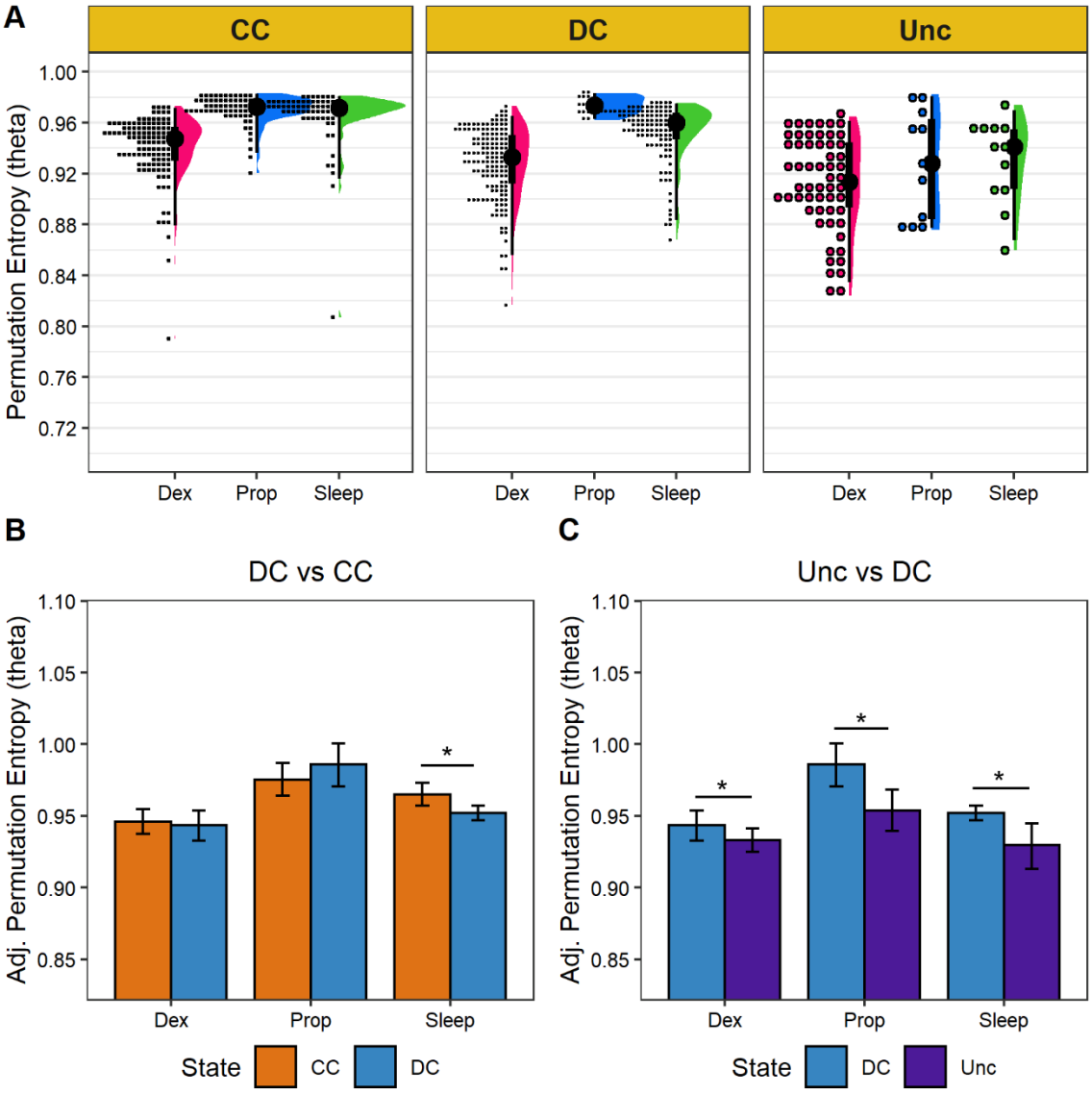

Supplementary Figure 9. A) Density plots of raw data for theta permutation entropy in each conscious state (CC, DC, or Unc) and experimental condition (Dex, Prop, Sleep). B) Adjusted means (i.e. model predictions) of theta permutation entropy in CC and DC. C) Adjusted means (i.e. model predictions) of theta permutation entropy in DC and Unc. Asterisks (*) indicate contrasts in which differences between states were statistically significant after correcting for multiple comparison, $p_{FDR} < 0.05$.

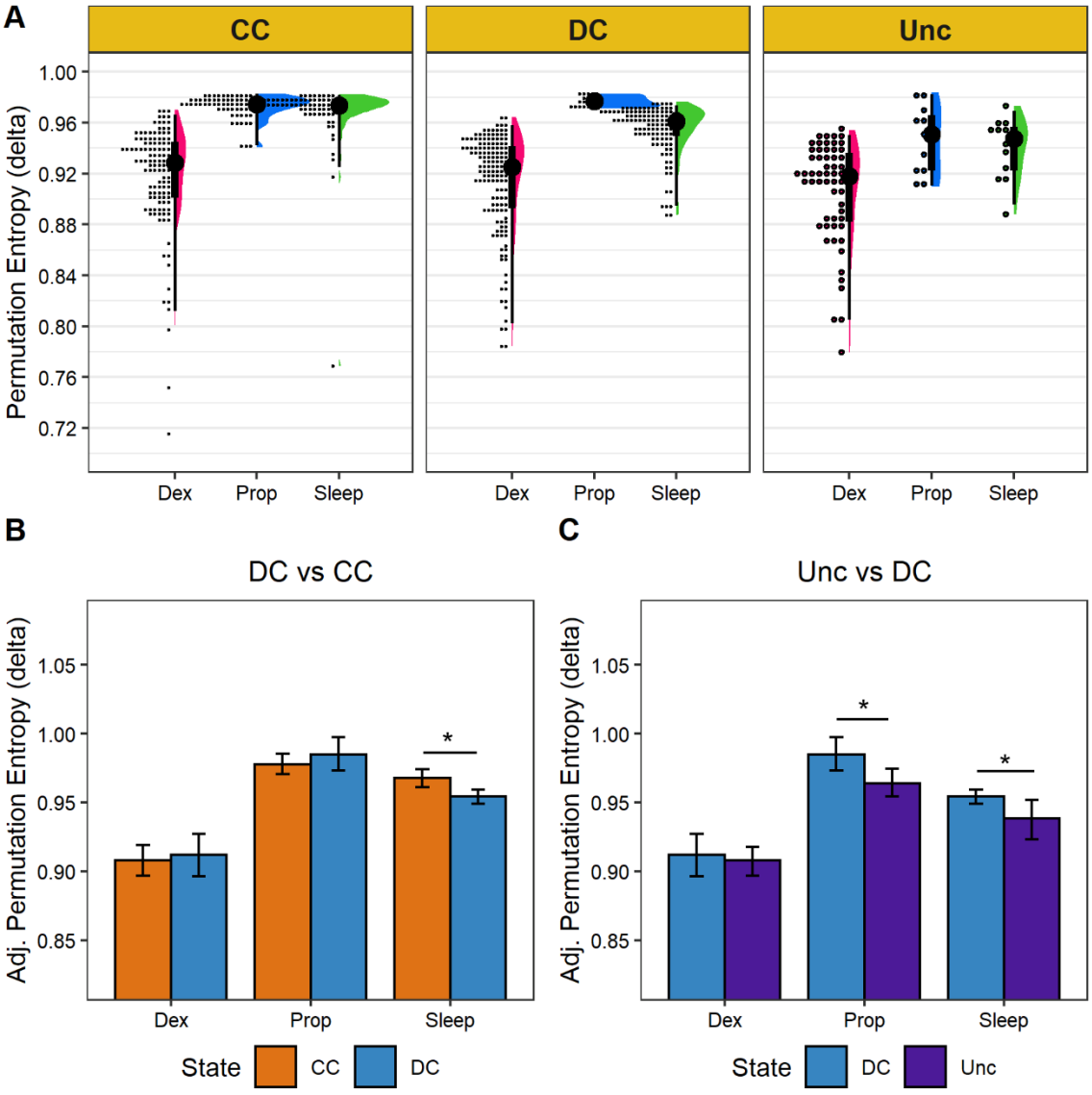

Supplementary Figure 10. A) Density plots of raw data for delta permutation entropy in each conscious state (CC, DC, or Unc) and experimental condition (Dex, Prop, Sleep). B) Adjusted means (i.e. model predictions) of delta permutation entropy in CC and DC. C) Adjusted means (i.e. model predictions) of delta permutation entropy in DC and Unc. Asterisks (*) indicate contrasts in which differences between states were statistically significant after correcting for multiple comparison, $p_{FDR} < 0.05$.

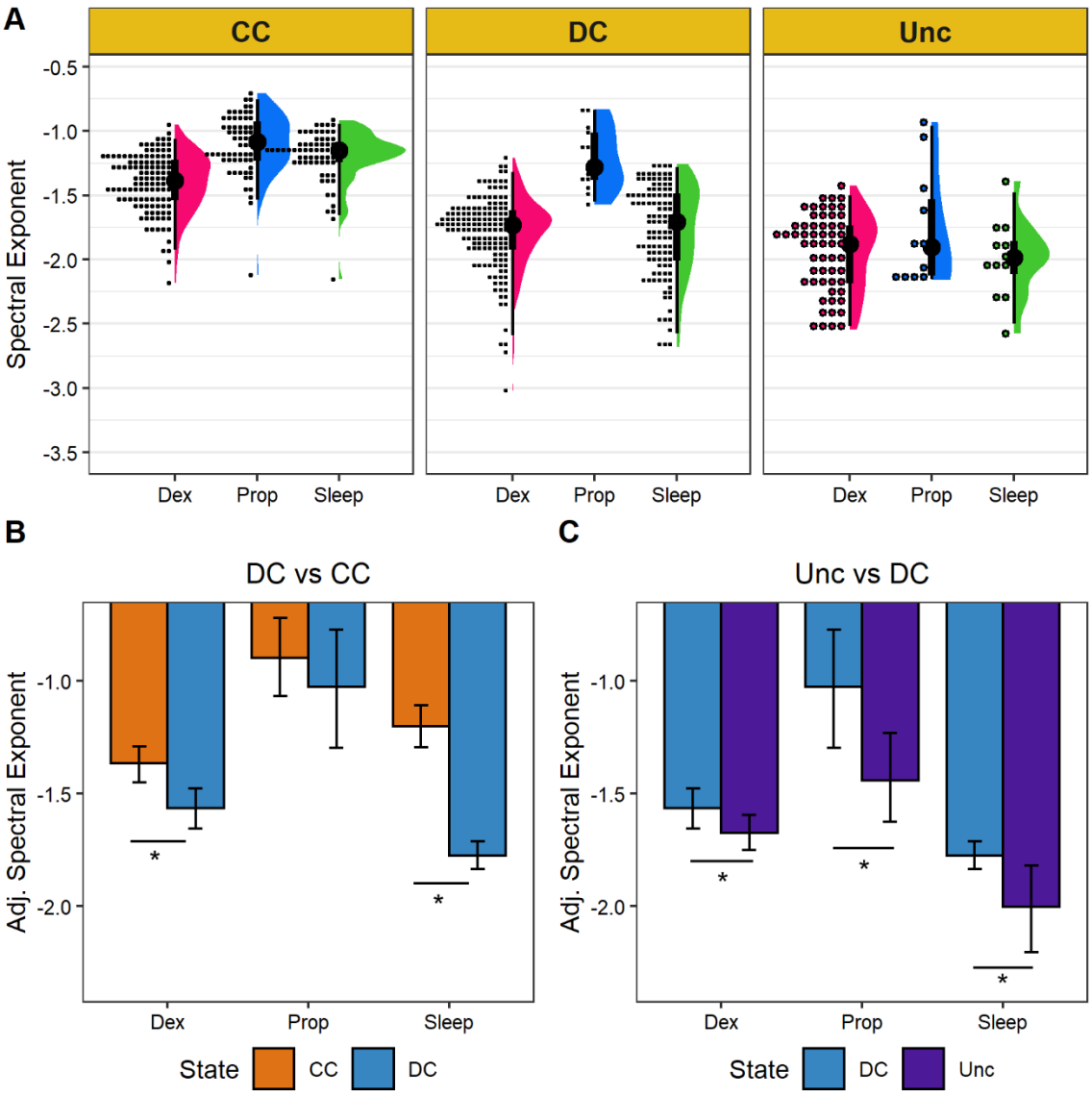

Supplementary Figure 11. A) Density plots of raw data for the spectral exponent in each conscious state (CC, DC, or Unc) and experimental condition (Dex, Prop, Sleep). B) Adjusted means (i.e. model predictions) of the spectral exponent in CC and DC. C) Adjusted means (i.e. model predictions) of the spectral exponent in DC and Unc. Asterisks (*) indicate contrasts in which differences between states were statistically significant after correcting for multiple comparison, $p_{FDR} < 0.05$.

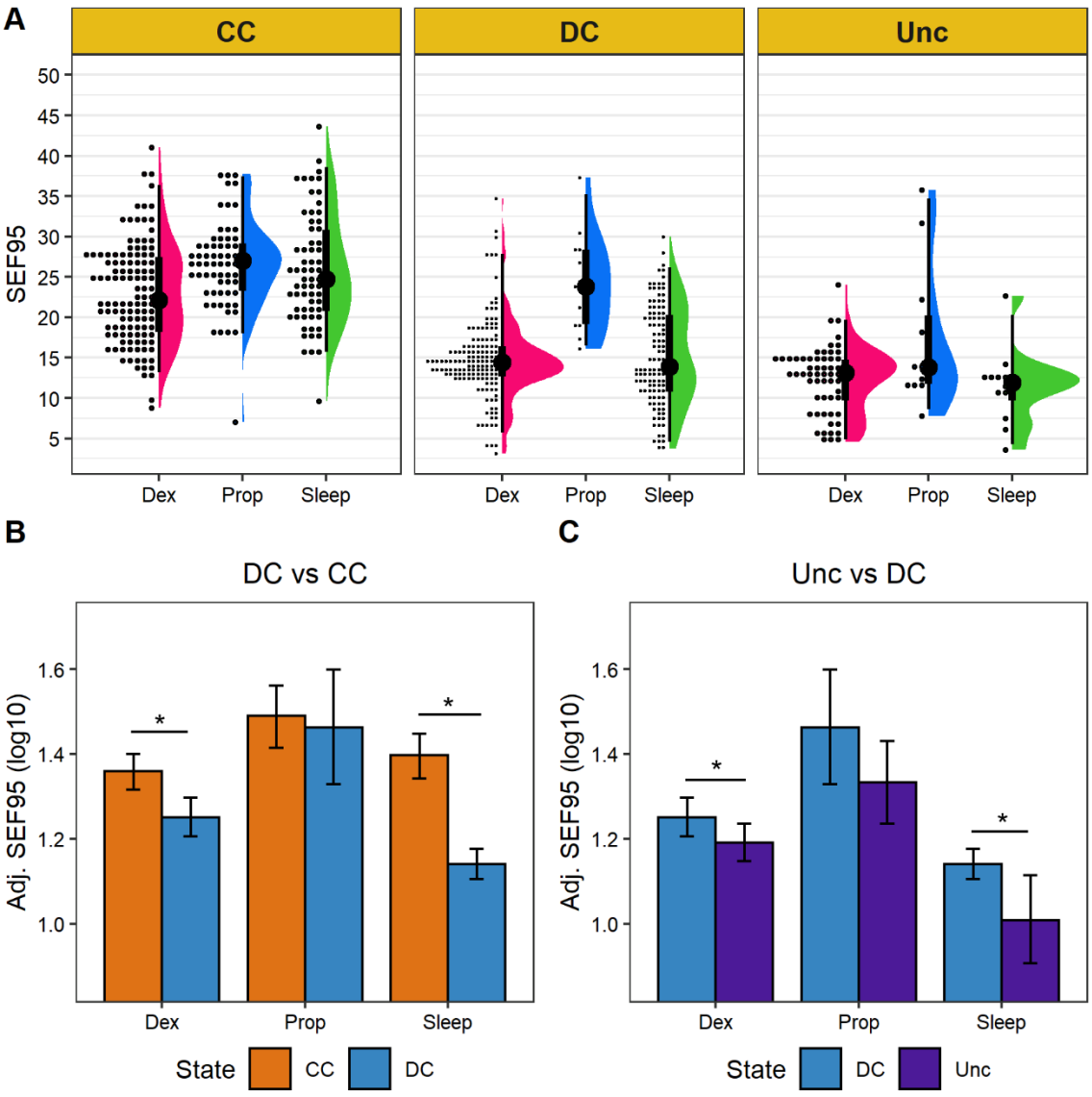

Supplementary Figure 12. A) Density plots of raw data for the spectral edge frequency 95% (SEF95) in each conscious state (CC, DC, or Unc) and experimental condition (Dex, Prop, Sleep). B) Adjusted means (i.e. model predictions) of SEF95 in CC and DC. C) Adjusted means (i.e. model predictions) of SEF95 in DC and Unc. Asterisks (*) indicate contrasts in which differences between states were statistically significant after correcting for multiple comparison, $p_{FDR} < 0.05$.

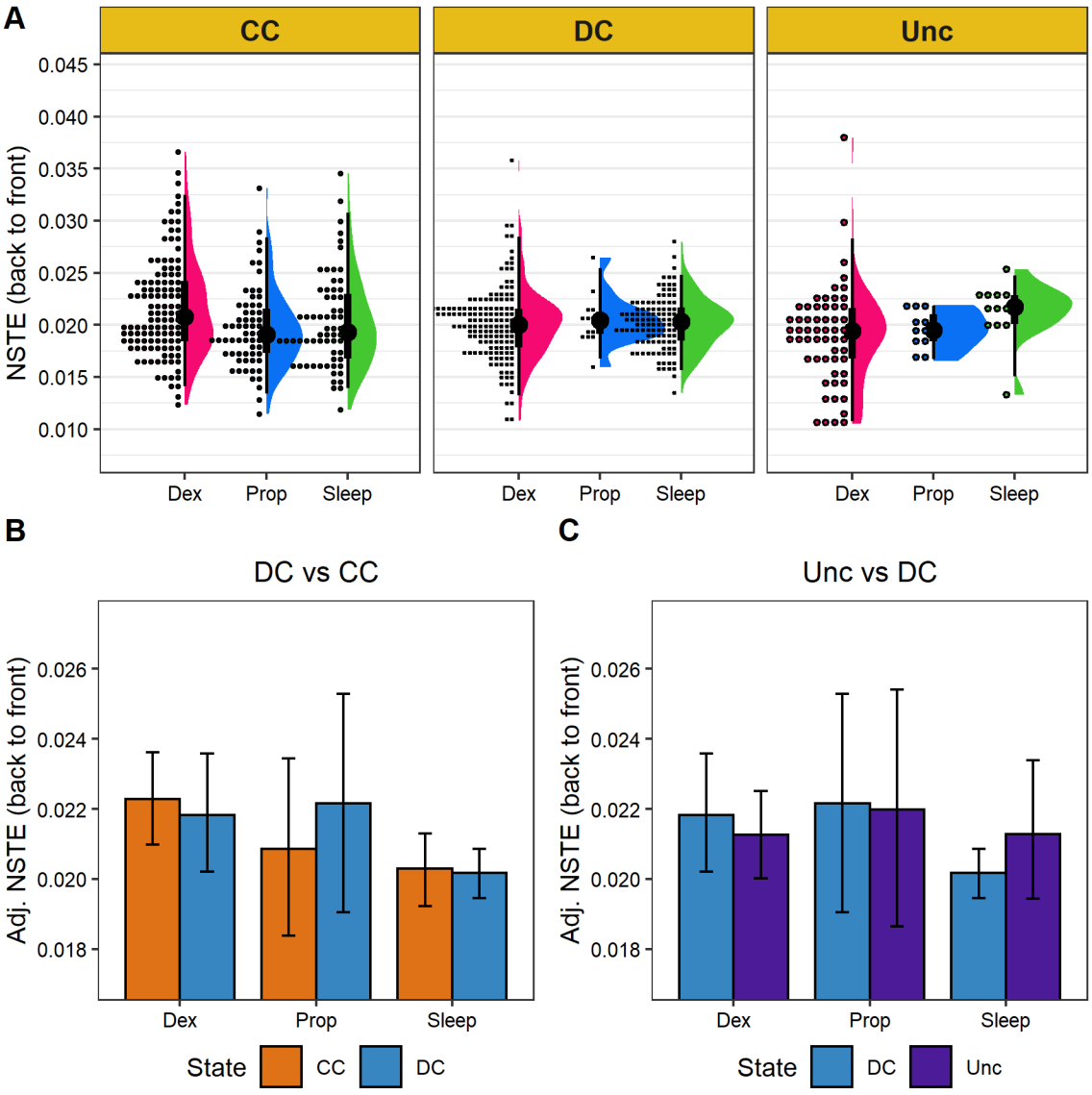

Supplementary Figure 13. A) Density plots of raw data for the normalized symbolic transfer entropy (NSTE) from back-to-front in each conscious state (CC, DC, or Unc) and experimental condition (Dex, Prop, Sleep). B) Adjusted means (i.e. model predictions) of back-to-front NSTE in CC and DC. C) Adjusted means (i.e. model predictions) of back-to-front NSTE in DC and Unc. Asterisks (*) indicate contrasts in which differences between states were statistically significant after correcting for multiple comparison, $p_{FDR} < 0.05$.

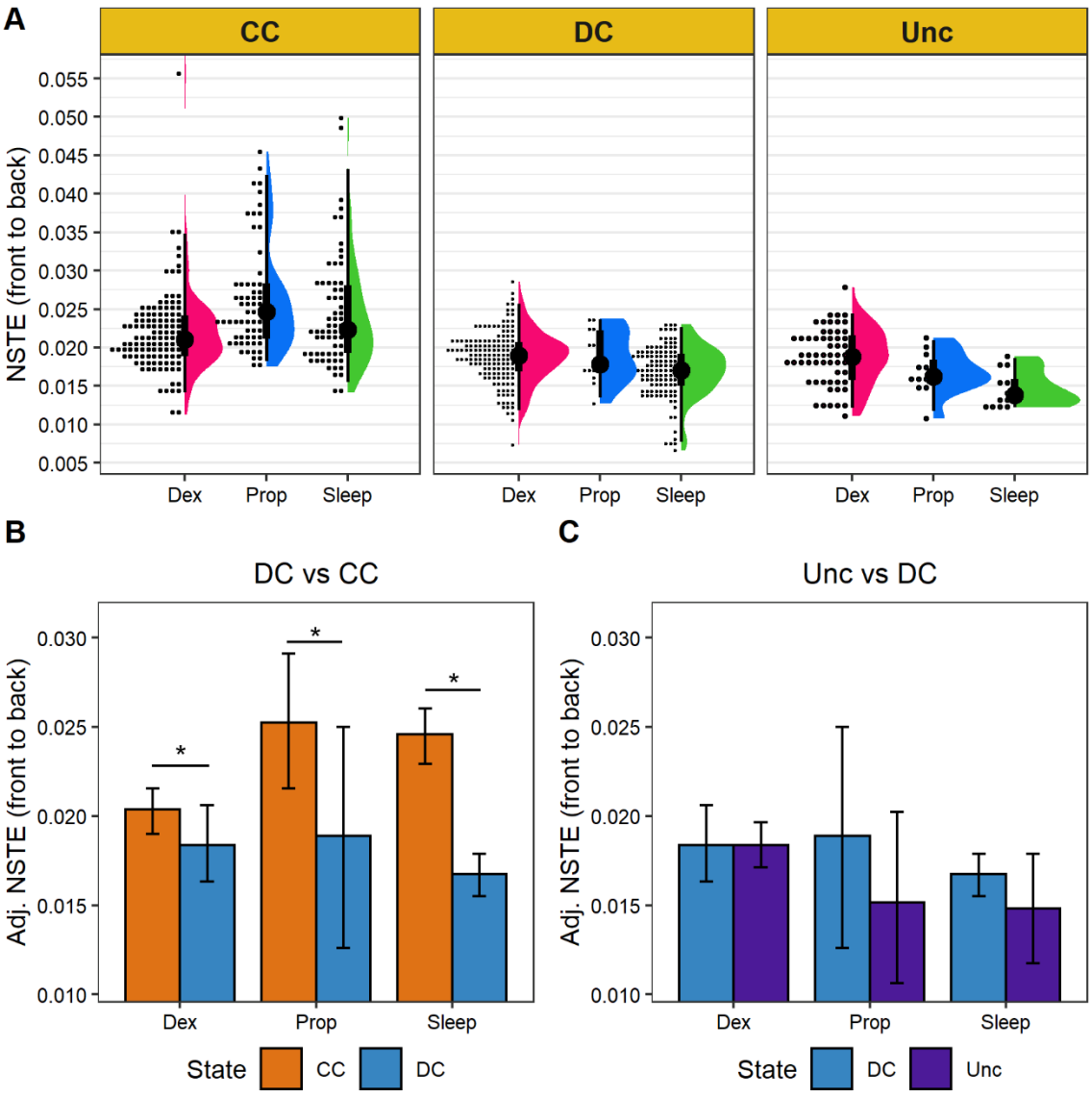

Supplementary Figure 14. A) Density plots of raw data for the normalized symbolic transfer entropy (NSTE) from front-to-back in each conscious state (CC, DC, or Unc) and experimental condition (Dex, Prop, Sleep). B) Adjusted means (i.e. model predictions) of front-to-back NSTE in CC and DC. C) Adjusted means (i.e. model predictions) of front-to-back NSTE in DC and Unc. Asterisks (*) indicate contrasts in which differences between states were statistically significant after correcting for multiple comparison, $p_{FDR} < 0.05$.

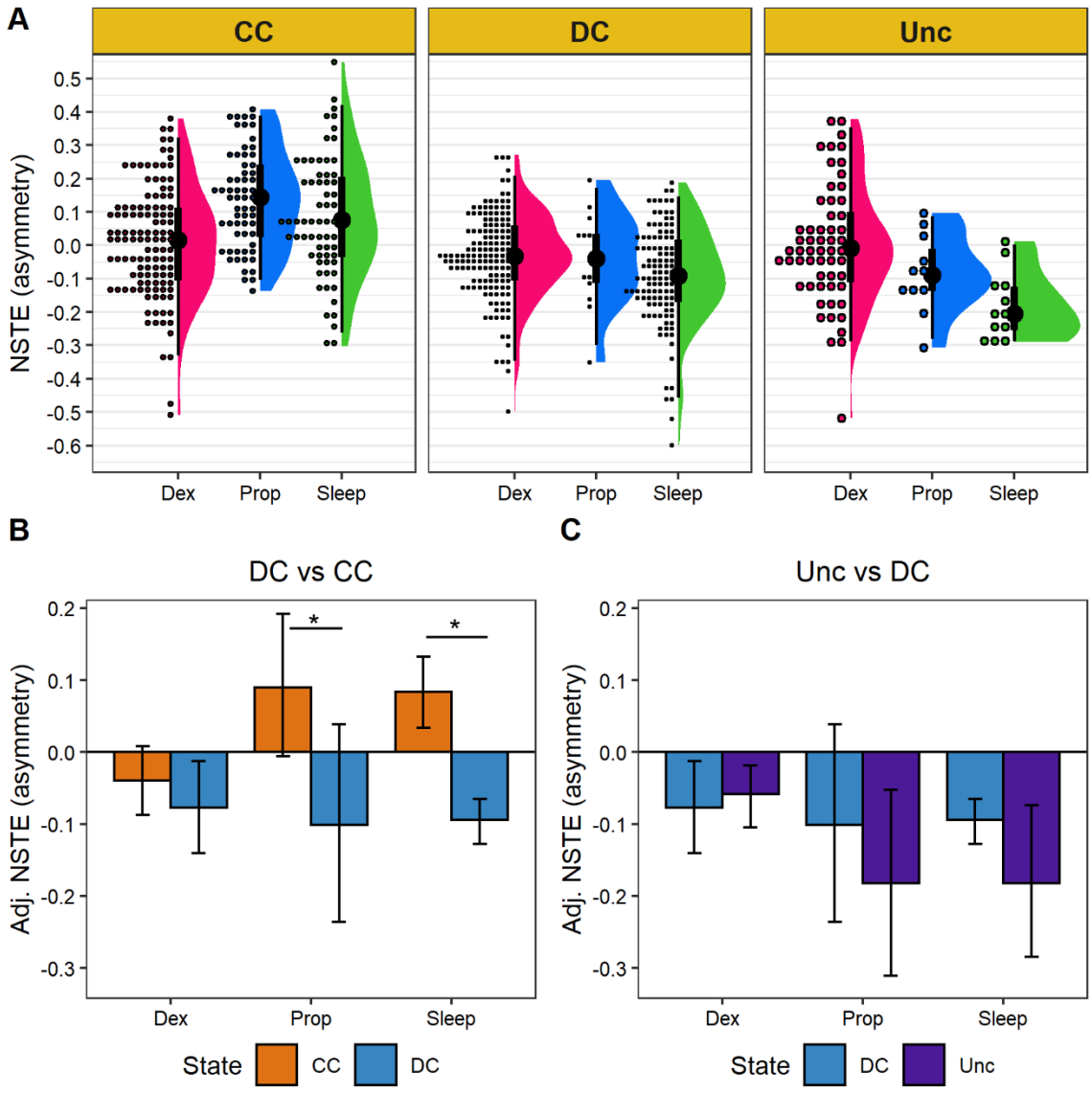

Supplementary Figure 15. A) Density plots of raw data for the normalized symbolic transfer entropy (NSTE) asymmetry in each conscious state (CC, DC, or Unc) and experimental condition (Dex, Prop, Sleep). B) Adjusted means (i.e. model predictions) of NSTE asymmetry in CC and DC. C) Adjusted means (i.e. model predictions) of NSTE asymmetry in DC and Unc. Asterisks (*) indicate contrasts in which differences between states were statistically significant after correcting for multiple comparison, $p_{FDR} < 0.05$.

APPENDIX C: SUPPLEMENTAL MATERIALS FOR CHAPTER III

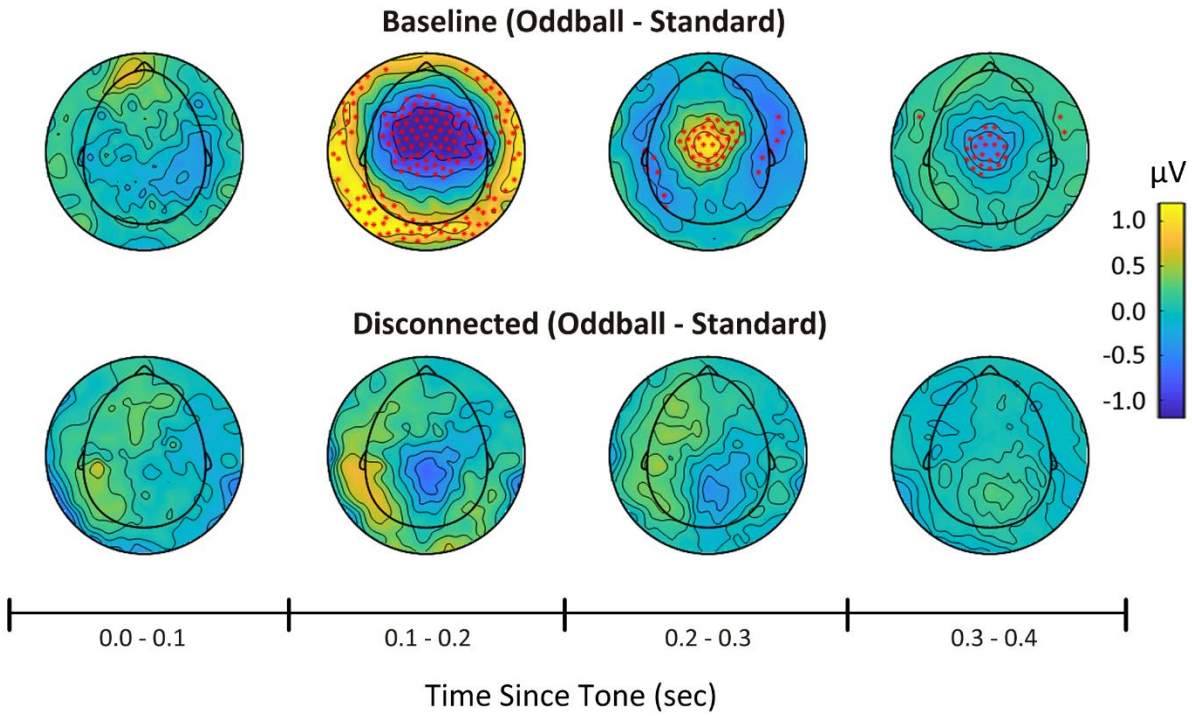

Supplementary Figure 1. Permutation tests comparing oddballs and standards in Baseline and Disconnected data. Plots show the topographical distribution of the oddball – standard difference waveform over time. Red asterisks (*) indicate electrodes where a significant ($p < 0.05$, FDR corrected) difference between oddballs and standards was detected within the time range given on the time scale.

Matrix	Parameter Type	Connection	Baseline Strength	Disconnected Strength
A	FB	left IFG -> left STG	0.308	0.412
A	FB	left STG -> left A1	2.579	0.503
A	FB	right IFG -> right STG	0.442	0.998
A	FB	right STG -> right A1	1.845	0.074
A	FF	left A1 -> left STG	0.352	0.078
A	FF	left STG -> left IFG	0.194	0.327
A	FF	right A1 -> right STG	0.064	0.262
A	FF	right STG -> right IFG	0.223	0.190
A	Lat	left IFG -> right IFG	1.347	1.567
A	Lat	left STG -> right STG	0.095	5.554
A	Lat	right IFG -> left IFG	0.106	1.104
A	Lat	right STG -> left STG	0.659	5.587
B	FB	left IFG -> left STG	-0.821	-0.818
B	FB	left STG -> left A1	-0.311	2.201
B	FB	right IFG -> right STG	0.935	-0.580
B	FB	right STG -> right A1	-1.008	0.245
B	FF	left A1 -> left STG	-1.850	-0.941
B	FF	left STG -> left IFG	0.920	1.097
B	FF	right A1 -> right STG	-0.041	-0.755
B	FF	right STG -> right IFG	2.359	0.909
B	Lat	left IFG -> right IFG	0.901	-1.711
B	Lat	left STG -> right STG	1.417	-0.856
B	Lat	right IFG -> left IFG	2.605	0.790
B	Lat	right STG -> left STG	-1.027	-1.517
B	Self	left A1 -> left A1	-0.372	0.277
B	Self	left IFG -> left IFG	0.218	0.115
B	Self	left STG -> left STG	0.308	0.044
B	Self	right A1 -> right A1	-0.102	-0.202
B	Self	right IFG -> right IFG	-0.093	-0.009
B	Self	right STG -> right STG	0.069	0.448

Supplementary Table 1. Connectivity parameters (extracted from the Ep.A and Ep.B matrices) from averaged DCM models of the Baseline and Disconnected data.

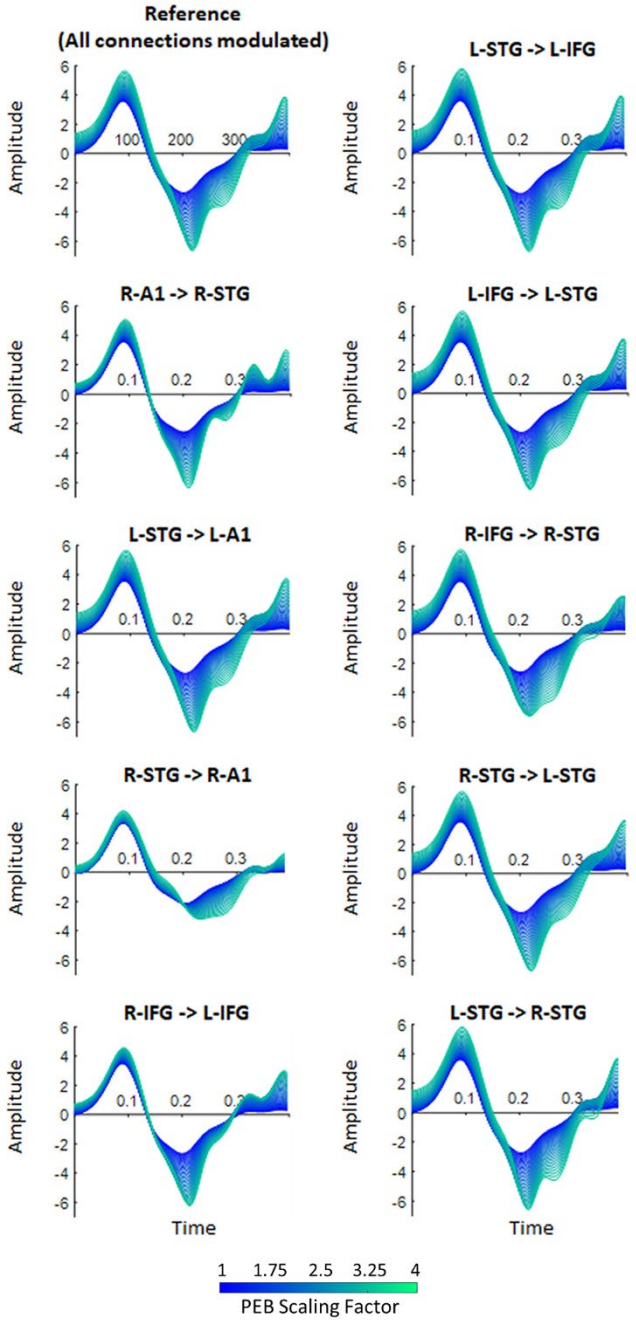

Supplementary Figure 2. Effect of fixed parameters on simulated ERPs. DCM generated simulated ERPs at electrode Cpz. The Reference plot shows how the ERP form changes when all 9 of the >95% confidence connections are modulated. More green colors indicates simulations where more extreme modulation was applied. Each of the plots (other than reference) show ERPs generated when all 8/9 parameters are modulated, but the labeled parameter was held constant. Changes in how the ERP scales with modulation relative to the reference can be used to make inferences about the role of each fixed parameter.

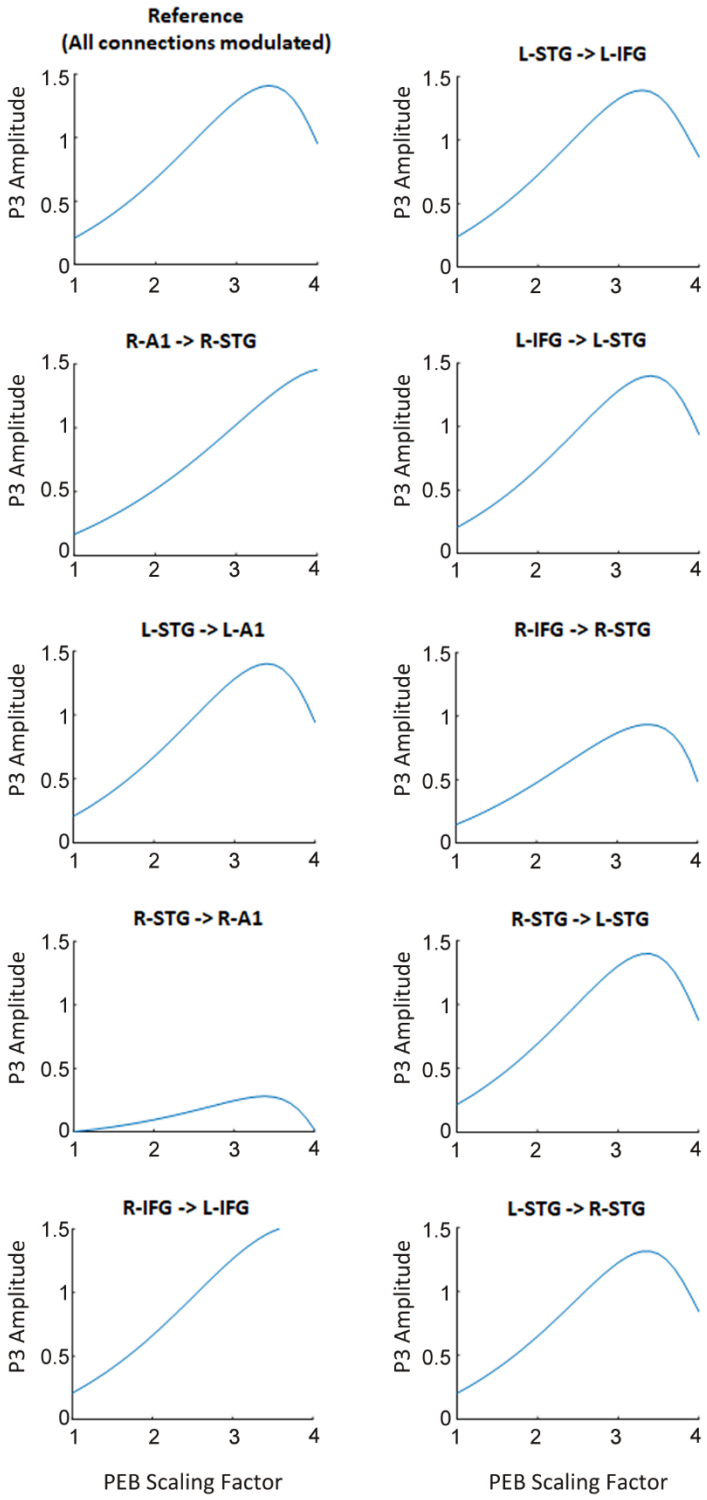

Supplementary Figure 3. Effect of fixed parameters on simulated ERP P3 component. DCM generated simulated ERPs at electrode Cpz. The Reference plot shows how the P3 changes when all 9 of the >95% confidence connections are modulated. Each of the plots (other than reference) show P3 scaling when all 8/9 parameters are modulated, but the labeled parameter was held constant. Changes in how the P3 scales with modulation relative to the reference can be used to make inferences about the role of each fixed parameter in P3 amplitude.

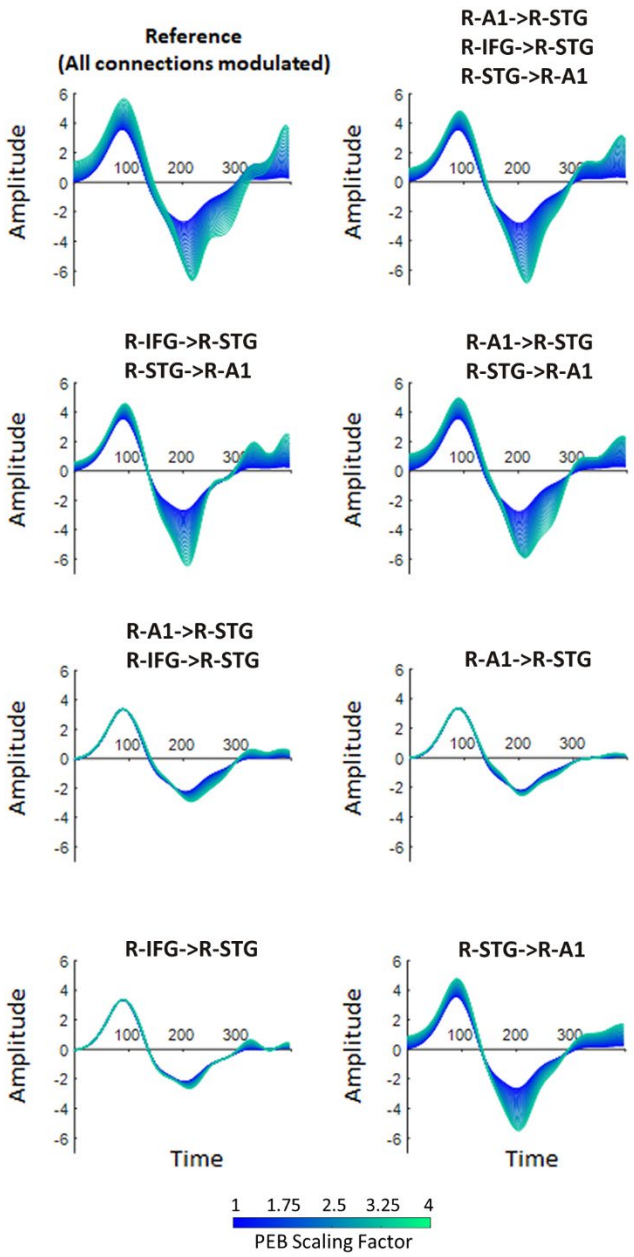

Supplementary Figure 4. Effect of modulating combinations of parameters on simulated ERPs. DCM generated simulated ERPs at electrode Cpz. The Reference plot shows how the ERP form changes when all 9 of the >95% confidence connections are modulated. More green colors indicates simulations where more extreme modulation was applied. Each of the plots (other than reference) show ERPs generated when only the labeled parameters are modulated and all others are held constant. Changes in how the ERP scales with modulation relative to the reference can be used to make inferences about the role of the modulated parameters.

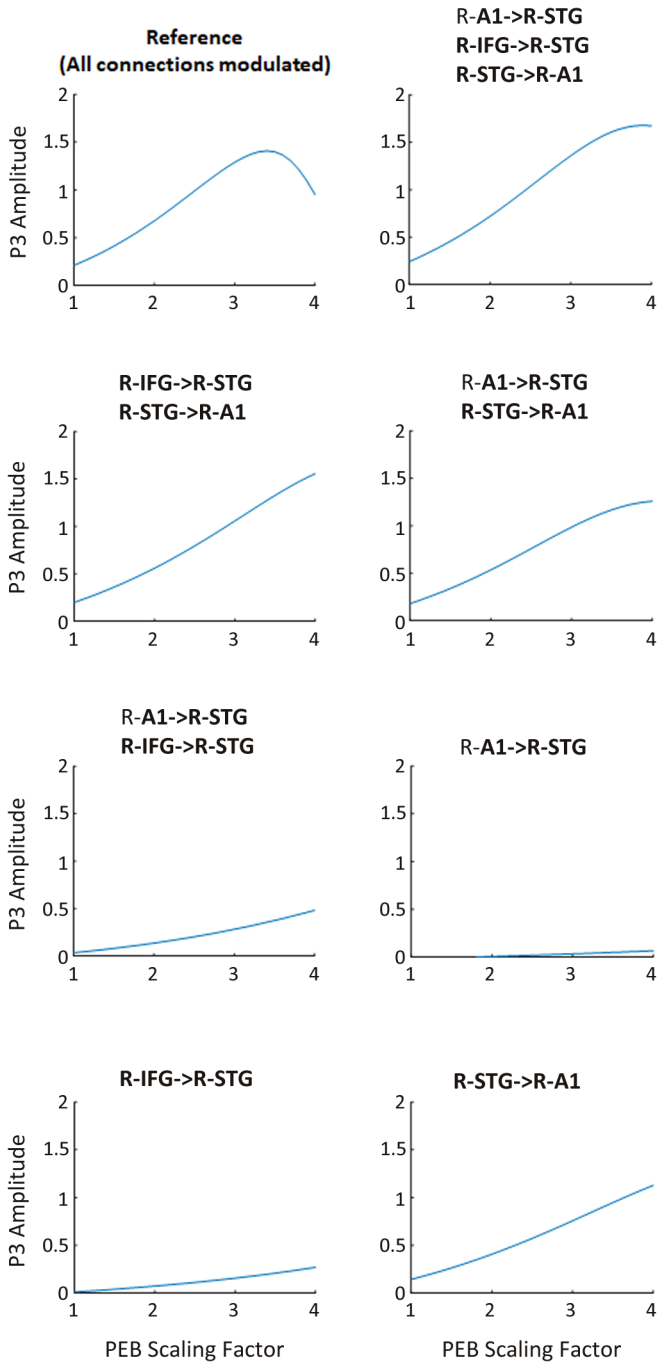

Supplementary Figure 5. Effect of modulating combinations of parameters on ERP P3 component. DCM generated simulated ERPs at electrode Cpz. The Reference plot shows how the P3 changes when all 9 of the >95% confidence connections are modulated. More green colors indicates simulations where more extreme modulation was applied. Each of the plots (other than reference) show P3 scaling when only the labeled parameters are modulated and all others are held constant. Changes in how the P3 scales with modulation relative to the reference can be used to make inferences about the role of the modulated parameters in P3 amplitude.

APPENDIX D: PEER REVIEWED PUBLICAITONS

The following is a list of peer reviewed publications I have authored while a member of the Neuroscience Training Program. Many of these publications extend beyond the range of my dissertation work but are noted here as an indication of my breadth of study. Though these papers are not all directly related to the study of connectedness and consciousness, in terms of content, each one has played an important role in my academic development. As such, these papers have all indirectly contributed to the skills and knowledge that this dissertation has been built upon.

I also include these works as another round of acknowledgements to the numerous phenomenal colleagues I have had while at the University of Wisconsin. Writing individual messages of thanks to each co-author in the opening acknowledgements proved to be rather daunting! However, each of them truly does deserve thanks. So here at the conclusion of my PhD studies, as well as the conclusion of this document, I say “thank you” to each and every person on this list.

-Cameron

H. Lindroth, V. A. Nair, C. Stanfield, **C. Casey**, R. Mohanty, D. Wayer, P. Rowley, R. Brown, V. Prabhakaran, R. D. Sanders, Examining the identification of age-related atrophy between T1 and T1 + T2-FLAIR cortical thickness measurements. *Sci. Rep.* **9**, 11288 (2019).

C. P. Casey, H. Lindroth, R. Mohanty, Z. Farahbakhsh, T. Ballweg, S. Twadell, S. Miller, B. Krause, V. Prabhakaran, K. Blennow, H. Zetterberg, R. D. Sanders, Postoperative delirium is associated with increased plasma neurofilament light. *Brain*. **143**, 47–54 (2019).

B. R. Barnett**, C. P. Casey**, M. Torres-Velázquez, P. A. Rowley, J.-P. J. Yu, Convergent brain microstructure across multiple genetic models of schizophrenia and autism spectrum disorder: A feasibility study. *Magn. Reson. Imaging*. **70**, 36–42 (2020).

S. Tanabe, R. Mohanty, H. Lindroth, **C. Casey**, T. Ballweg, Z. Farahbakhsh, B. Krause, V. Prabhakaran, M. I. Banks, R. D. Sanders, Cohort study into the neural correlates of postoperative delirium: the role of connectivity and slow-wave activity. *Br. J. Anaesth.* **125**, 55–66 (2020).

S. Tanabe, A. Bo, M. White, M. Parker, Z. Farahbakhsh, T. Ballweg, **C. Casey**, T. Betthauser, H. Zetterberg, K. Blennow, B. Christian, B. B. Bendlin, S. Johnson, R. D. Sanders, R. Sanders, Cohort study of electroencephalography markers of amyloid-tau-neurodegeneration pathology. *Brain Commun.* **2** (2020), doi:10.1093/BRAINCOMMS/FCAA099.

R. D. Sanders, L. Craigova, B. Schessler, **C. Casey**, M. White, M. Parker, D. Kunkel, K. Blennow, H. Zetterberg, R. A. Pearce, R. Lennertz, Postoperative troponin increases after noncardiac surgery are associated with raised neurofilament light: a prospective observational cohort study. *Br. J. Anaesth.* **126**, 791–798 (2021).

S. Mohanta, M. Afrasiabi, **C. P. Casey**, S. Tanabe, M. J. Redinbaugh, N. A. Kambi, J. M. Phillips, D. Polyakov, W. Filbey, J. L. Austerweil, R. D. Sanders, Y. B. Saalmann, Predictive Feedback, Early Sensory Representations, and Fast Responses to Predicted Stimuli Depend on NMDA Receptors. *J. Neurosci.* **41**, 10130–10147 (2021).

M. F. White, S. Tanabe, **C. Casey**, M. Parker, A. Bo, D. Kunkel, V. Nair, R. A. Pearce, R. Lennertz, V. Prabhakaran, H. Lindroth, R. D. Sanders, Relationships between preoperative cortical thickness, postoperative electroencephalogram slowing, and postoperative delirium. *Br. J. Anaesth.* (2021), doi:10.1016/j.bja.2021.02.028.

R. D. Sanders, **C. Casey**, Y. B. Saalmann, Predictive coding as a model of sensory disconnection: relevance to anaesthetic mechanisms. *Br. J. Anaesth.* **126**, 37–40 (2021).

T. Ballweg, M. White, M. Parker, **C. Casey**, A. Bo, Z. Farahbakhsh, A. Kayser, A. Blair, H. Lindroth, R. A. Pearce, K. Blennow, H. Zetterberg, R. Lennertz, R. D. Sanders, Association between plasma tau and postoperative delirium incidence and severity: a prospective observational study. *Br. J. Anaesth.* **126**, 458–466 (2021).

D. Kunkel, M. Parker, **C. Casey**, B. Krause, R. A. Pearce, R. Lennertz, R. D. Sanders, Impact of postoperative delirium on days alive and at home after surgery: a prospective cohort study. *Br. J. Anaesth.* **127**, e205–e207 (2021).

C. P. Casey, S. Tanabe, Z. Farahbakhsh, M. Parker, A. Bo, M. White, T. Ballweg, A. Mcintosh, W. Filbey, Y. Saalmann, R. A. Pearce, R. D. Sanders, Distinct EEG signatures differentiate unconsciousness and disconnection during anaesthesia and sleep. *Br. J. Anaesth.* (2022), doi:10.1016/J.BJA.2022.01.010.

M. Parker, M. White, **C. Casey**, D. Kunkel, A. Bo, K. Blennow, H. Zetterberg, R. A. Pearce, R. Lennertz, R. D. Sanders, Cohort Analysis of the Association of Delirium Severity With Cerebrospinal Fluid Amyloid-Tau-Neurodegeneration Pathologies. *Journals Gerontol. Ser. A*. **77**, 494–501 (2022).

D. Kunkel, M. Parker, **C. Casey**, B. Krause, J. Taylor, R. A. Pearce, R. Lennertz, R. D. Sanders, Impact of perioperative inflammation on days alive and at home after surgery. *BJA Open*. **2**, 100006 (2022).

J. Taylor, M. Parker, **C. P. Casey**, S. Tanabe, D. Kunkel, C. Rivera, H. Zetterberg, K. Blennow, R. A. Pearce, R. C. Lennertz, R. D. Sanders, Postoperative delirium and changes in the blood–brain barrier, neuroinflammation, and cerebrospinal fluid lactate: a prospective cohort study. *Br. J. Anaesth.* (2022), doi:10.1016/J.BJA.2022.01.005.

J. Taylor, T. Payne, **C. Casey**, D. Kunkel, M. Parker, C. Rivera, H. Zetterberg, K. Blennow, R. A. Pearce, R. C. Lennertz, T. McCulloch, A. Gaskell, R. D. Sanders, Sevoflurane dose and postoperative delirium: a prospective cohort analysis. *Br. J. Anaesth.* (2022), doi:10.1016/J.BJA.2022.08.022.

C. P. Casey, S. Tanabe, Z. Farahbakhsh, M. Parker, A. Bo, M. White, T. Ballweg, A. Mcintosh, W. Filbey, M. I. Banks, Y. B. Saalmann, R. A. Pearce, R. D. Sanders, Dynamic causal modelling of auditory surprise during disconnected consciousness: The role of feedback connectivity. *Neuroimage*. **263**, 119657 (2022).

K. Gjini, **C. Casey**, S. Tanabe, A. Bo, M. Parker, M. White, D. Kunkel, R. Lennertz, R. A. Pearce, T. Betthauser, B. T. Christian, S. C. Johnson, B. B. Bendlin, R. D. Sanders, Greater tau pathology is associated with altered predictive coding. *Brain Commun.* **4** (2022), doi:10.1093/BRAINCOMMS/FCAC209.